ISBN: 978-3-95450-240-0 ISSN: 2673-5539 doi:10.18429/JACoW-RuPAC2021-MOX02

# DEVELOPMENT AND IMPLEMENTATION OF BUNCH SHAPE INSTRUMENTATION FOR ION LINACS*

S. A. Gavrilov†, A. V. Feschenko, V. A. Gaidash,
Institute for Nuclear Research of the Russian Academy of Sciences, Moscow, Troitsk, Russia

*Abstract*

A longitudinal charge distribution in beam bunches, so-called bunch shape, is one of the most important and difficult to measure characteristics of a beam in ion linear accelerators. Despite the variety of approaches only the methods using low energy secondary electrons emitted, when the beam passes through a thin target, found practical application. The most common beam instrumentation, based on this method, became Bunch Shape Monitor (BSM) developed in INR RAS. The monitor provides direct measurements of bunch shape and bunch longitudinal halo, allows to carry out such complex diagnostic procedures as longitudinal emittance measurements, amplitude and phase setting of accelerating fields and observation of bunch shape evolution in time to check the overall quality of longitudinal tuning of the accelerator.

The principle of the monitor operation, design features, ultimate parameters and limitations are discussed. Several modifications of the monitor with implementation peculiarities are described as well as lots of measurement results at different ion linacs with a variety of beam parameters. New challenges for bunch shape instrumentation to satisfy demands of forthcoming linacs are also characterized.

## INTRODUCTION

The main requirement for bunch shape measurements is phase resolution. In ion linacs for typical bunch phase duration range from several degrees to several tens of degrees the resolution of 1° looks adequate. The corresponding temporal resolution, for example for 350 MHz, equals to ~8 ps.

In ion beams, as opposite to electron ones, an attempt to extract information on bunch shape through beam electromagnetic field results in aggravation of phase resolution due to large longitudinal extent of the particle field. The problem can be overcome if one localizes a longitudinal space passing through which the bunch transmits information on its shape.

This approach can be implemented if a longitudinally small target is inserted into the beam and some type of radiation due to interaction of the beam with this target is detected. Different types of radiation are used or proposed to be used [1-5], however low energy secondary electrons are used most extensively. The distinctive feature of these electrons is a weak dependence of their properties both on type and energy of primary particles, so the detectors can be used for almost any ion beam.

Among the characteristics of low energy secondary emission, influencing the parameters of the bunch shape monitor, one can point initial energy and angular distributions as well as time dispersion or delay of the emission. Time dispersion establishes a fundamental limitation on the resolution of the detector. The value of time dispersion for metals is estimated theoretically to be about $10^{-15}\div10^{-14}$ s [6], which is negligible from the point of view of bunch shape measurements. The experimental results of time dispersion measurements give not exact value but its upper limit. It was shown that the upper limit does not exceed $(4\pm2)\cdot10^{-12}$ s [7].

Operation of bunch shape monitors with low energy secondary electrons is based on coherent transformation of a time structure of the analyzed beam into a spatial distribution of secondary electrons through RF modulation. The first real detectors described in [8, 9] use RF modulation in energy or in other words a longitudinal modulation. Another possibility is using a transverse scanning [10]. The electrons are modulated in transverse direction and deflected depending on their phase. Spatial separation is obtained after a drift space.

## BUNCH SHAPE MONITOR OF INR RAS

### *Principle of Operation*

The first real BSM with transverse scanning of low energy secondary electrons, developed and fabricated in INR, has been described in [11, 12].

The operation principle of BSM with up-to-date design can be described briefly with the reference to Fig. 1.

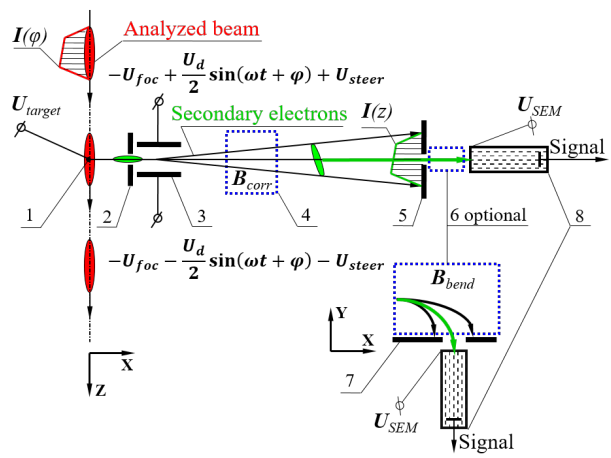


Figure 1: BSM scheme: 1 – tungsten wire target, 2 – inlet collimator, 3 – RF-deflector, 4 – correcting magnet, 5 – outlet collimator, 6 – optional bending magnet, 7 – registration collimator, 8 – electron detector.

* Work was awarded the Veksler Prize 2021 of RAS
† s.gavrilov@gmail.com

ISBN: 978-3-95450-240-0 ISSN: 2673-5539 doi:10.18429/JACoW-RuPAC2021-MOY01

# THE NICA COMPLEX INJECTION FACILITY

A. Butenko †, H. Khodzhibagiyan, S. Kostromin, I. Meshkov, A. Sidorin, E. Syresin, G. Trubnikov, A. Tuzikov, Joint Institute for Nuclear Research, Dubna, Russia

*Abstract*

The Nuclotron-based Ion Collider fAcility (NICA) is under construction in JINR. The NICA goals are providing of colliding beams for studies of hot and dense strongly interacting baryonic matter and spin physics. The NICA complex injection facility consists of following accelerators: Alvarez-type linac LU-20 of light ions up to 5 MeV/u; heavy ion linac HILAC with RFQ and IH DTL sections at energy 3.2 MeV/u; superconducting Booster synchrotron at energy up 578 MeV/u; superconducting synchrotron Nuclotron at gold ion energy 3.85 GeV/u. In the nearest future the old LU-20 will be substituted by a new light ion linac for acceleration of 2<A/z<3 ions up to 7 MeV/u with additional two acceleration sections for protons, first IH section for 13 MeV and the second one - superconducting for 20 MeV. The status of NICA injection facility is under discussion.

## NICA INJECTION COMPLEX

The NICA accelerator complex [1,2] is constructed and commissioned at JINR. NICA experiments shall be performed in search of the mixed phase of baryonic matter and nature of nucleon/particle spin. The new NICA accelerator complex will permit implementing experiments in the following modes: with the Nuclotron ion beams extracted at a fixed target; with colliding ion beams in the collider; with colliding ion-proton beams; with colliding beams of polarized protons and deuterons. The main elements of the NICA complex are an injection complex, which includes a set of ion sources and two linear accelerators, the superconducting acting Booster, the superconducting acting synchrotron Nuclotron, a Collider composed of two superconducting rings with two beam interaction points, a Multi-Purpose Detector (MPD) and a Spin Physics Detector (SPD) and beam transport channels.

The injection complex [1] is divided on two injection chains: one is used for heavy ions, other - for protons and light ions. The light ion injection chain includes laser ion source (LIS) and source of polarized ions (SPI), linear accelerator LU-20, Nuclotron and transfer line LU-20-Nuclotron. The heavy ion injection chain consists from electron string ion source (ESIS), laser ion source, plasma ion source, the acting Heavy Ion Linac (HILAC), transfer line HILAC-Booster, superconducting acting synchrotron Booster, transfer line Booster-Nuclotron and acting superconducting synchrotron Nuclotron.

## INJECTION CHAIN FOR LIGHT IONS

The linear accelerator LU-20, which is under operation since 1974, accelerates protons and ions from few sources: the laser source and the source of polarized ions - protons and deuterons. SPI was constructed by JINR-INR RAS collaboration. The beam current of polarized deuterons corresponds to 2 mA. During 2009 - 2018 years completely modernized all of the main systems of the Linac: RF power amplifiers (5MW/pulse), drift tubes power supply (PS), beam diagnostics, HV terminal, fore-injector, LLRF system, synchronization system, vacuum system, PS system of the injection line. At the LU-20 exit, the energy of ions is 5 MeV/n. At present time, the LU-20 beam is injected directly into the Nuclotron through transfer line Lu-20-Nuclotron. The HV injector of linac LU-20 has been replaced in 2016 by RFQ (Fig. 1) [1,3] with beam matching channels. The RFQ was constructed by JINR, ITEP of NRC "Kurchatov Institute", NRNU MEPHI, VNIITF collaboration. The new buncher constructed by ITEP of NRC "Kurchatov Institute" was installed between RFQ and LU-20 in 2017. Installation of new buncher permited to increase the heavy ion beam current by 5 times in Nuclotron 55 run in 2018.

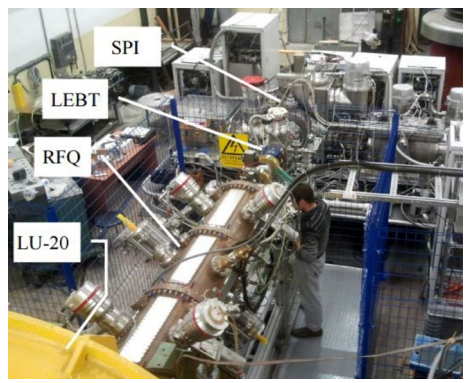

Figure 1: New fore-injector for LU-20.

The design of new Light Ion Linac (LILAc) was started in 2017 to replace the LU-20 in NICA injection complex. LILAc consists of three sections: warm injection section applied for acceleration of light ions and protons up to energy 7 MeV/n [4], warm medium energy section used for proton acceleration up to energy 13 MeV [4] and superconducting HWR sections [5], which provides proton acceleration up to energy 20 MeV. The LILAC should provide beam current of 5 emA. The construction of first light ion section [4] at ion energy 7 MeV/n was started in 2018 by Bevatech (Germany), it should be delivered in JINR in 2023. The next step of the LILAc project – design of a middle energy section and HWR superconducting sections.

The increased beam energy of LILAc is required for future researches with polarized proton beams. The operating frequency of the LILAc is equal to 162.5 MHz for first two sections and 325 MHz for HWR section. The two superconducting HWRs (Fig. 2) were constructed by Russian-Belarusian collaboration with participation of JINR, NRNU MEPhI, INP BSU and PTI NASB.

ISBN: 978-3-95450-240-0 ISSN: 2673-5539 doi:10.18429/JACoW-RuPAC2021-MOY02

# NICA ION COLLIDER AT JINR

E. Syresin, N. Agapov, A. Alfeev, V. Andreev, A. Baldin, A. Bazanov, O. Brovko, V. Bugaev, A. Butenko, A. Galimov, I. Gorelyshev, D. Donets, E.D. Donets, E.E. Donets, A. Eliseev, G. Filatov, V. Fimushkin, B. Golovenskiy, E. Gorbachev, A. Govorov, A. Grebentsov, E. Ivanov, V. Karpinsky, V. Kekelidze, A. Kirichenko, H. Khodzhibagiyan, A. Kobets, V. Kobets, A. Konstantinov, S. Korovkin, S. Kostromin, O. Kozlov, K. Levterov, D. Lyuosev, A. Malyshev, A. Martynov, S. Melnikov, I. Meshkov, V. Mikhailov, Yu. Mitrophanova, V. Monchinsky, A. Nesterov, A. Osipenkov, K. Osipov, R. Pivin, A. Philippov, D. Ponkin, S. Romanov, P. Rukojatkin, I. Shirikov, A. Shurygin, A. Sidorin, V. Slepnev, A. Slivin, G. Trubnikov, A. Tuzikov, B. Vasilishin, V.Volkov, Joint Institute for Nuclear Research, Dubna , Russia

*Abstract*

The Nuclotron-based Ion Collider fAcility (NICA) [1-5] is under construction in JINR. The NICA goals are providing of colliding beams for studies of hot and dense strongly interacting baryonic matter and spin physics. The accelerator facility of Collider NICA consists of following elements: acting Alvarez-type linac LU-20 of light ions at energy 5 MeV/u, constructed a new light ion linac of light ions at energy 7 MeV/u and protons at energy 13 MeV, new acting heavy ion linac HILAC with RFQ and IH DTL sections at energy 3.2 MeV/u, new acting superconducting Booster synchrotron at energy up 600 MeV/u, acting superconducting synchrotron Nuclotron at gold ion energy 4.5 GeV/n and two Collider storage rings with two interaction points. The status of acceleration complex NICA is under discussion.

## INJECTION ACCELERATOR COMPLEX NICA FOR HEAVY ION MODE

The injection accelerator complex NICA for heavy ion mode [2] involves following accelerators: a new heavy-ion linear accelerator (Heavy Ion Linac, HILAC) constructed by JINR-Bevatech collaboration is under exploitation since 2016. It will accelerate heavy ions such as $^{197}Au^{31+}$ and $^{209}Bi^{35+}$ injected from KRION-6T, a superconducting electron-string heavy ion source, constructed by JINR. At present time KRION-6T produces $8\cdot10^8$ $Au^{31+}$ ions and $9\cdot10^8$ $^{209}Bi^{35+}$ ions during three pulses of extracted beam. This ion source will be used at injection in Booster in 2022. Upgraded version of KRION-N with $^{197}Au^{31+}$ or $^{209}Bi^{35+}$ion intensity up $2.5\cdot10^9$ particles per pulse will be constructed in 2022 for Collider experiments. The energy of ions at the exit from HILAC is 3.2 MeV/n, while the beam intensity amounts to $2\times10^9$ particles per pulse or 10 emA, repetition rate is 10 Hz. The HILAC consists of three sections: RFQ and two IH sections. The RFQ is a 4-rod structure operating at 100.625 MHz. The RFQ and each IH section are powered by 140 kW and 340 kW solid state amplifiers. The acceleration of $^{12}C^{2+}$ ions with mass-charge ratio of A/Z=6, produced in laser ion source, was performed at first HILAC tests. Especially for the test run of the Booster the plasma source generating a single component $^4He^{1+}$ (A/Z = 4) beam was created. The maximal ion $^4He^{1+}$ beam current at HILAC entrance during first Booster runs corresponds to project value 10 mA, efficiency of beam transportation through second and third IH sections was 78.5%. During second Booster run the $^4He^{1+}$and $^{56}Fe^{14+}$ ions produced in plasma and laser ion sources were accelerated in HILAC and injected in Booster.

The transfer line from HILAC to Booster [*2*] (Fig. 1) consists of 2 dipole magnets, 7 quadrupole lenses, 6 steerers magnets, debuncher, collimator, vacuum and diagnostic equipment. The transfer line from HILAC to Booster was under operation since autumn 2020. The achieved efficiency of the beam transmission in HILAC – Booster transfer line was about 90% at the beam current of 4 mA.

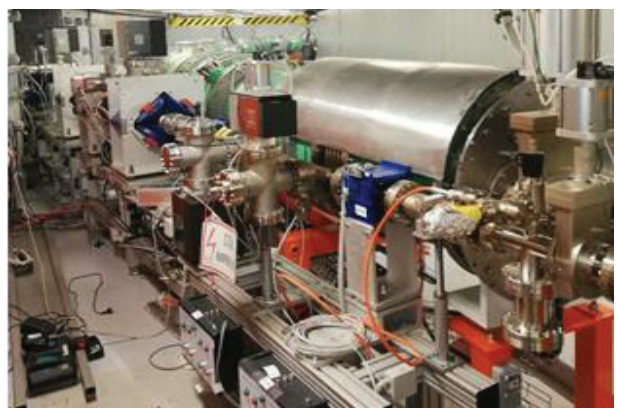

Figure 1: Transport channel HILAC-Booster.

The Booster [1-5] is a superconducting synchrotron intended for accelerating heavy ions up to energy of 578 MeV/u. The magnetic structure of the Booster with a 211 m - long circumference is mounted in tunnel inside the huge iron yoke of the Synchrophasotron magnet (Fig. 2). The main goals of the Booster are accumulation of $2\cdot10^9$ $^{197}Au^{31+}$ or $^{209}Bi^{35+}$ ions, acceleration of heavy ions up to the energy 578 MeV/u required for effective stripping, and forming of the required beam emittance with the electron cooling system.

ISBN: 978-3-95450-240-0 ISSN: 2673-5539 doi:10.18429/JACoW-RuPAC2021-MOY05

# LINEAR INDUCTION ACCELERATOR LIA-2 UPGRADE

D. Starostenko†, A. Akimov, P. Bak, D. Bolkhovityanov, V. Fedorov, Ya. Kulenko, G. Kuznetsov, P. Logachev, D. Nikiforov, A. Petrenko, O. Pavlov, A. Pavlenko, Budker Institute of Nuclear Physics SB RAS, Novosibirsk, Russia
A. Ahmetov, A. Chernitsa, O. Nikitin, A. Kargin, P. Kolesnikov, S. Khrenkov, D. Petrov, Russian Federal Nuclear Center – Zababakhin All-Russia Research Institute of Technical Physics, Snezhinsk, Russia

*Abstract*

X-ray facilities based on a linear induction accelerator are designed to study of high density objects. It requires the high-current electron beam to obtain a small spot and bright x-ray source using a conversion target. The electrons source in such facilities is injectors capable generate pulses with a duration from tens of nanoseconds to several microseconds and a current of several kA. The transportation and focusing of high-current beams into diameter about 1 mm is difficult due to the space charge phenomena. In the similar induction accelerators (AIRIX [1], DARHT [2], FXR, etc.), auto-emission cathodes are used to obtain high-current electron beams. The use of a thermionic cathode, in compared to auto-emission cathode, provides stable generation of several pulses with a time interval of several microseconds, but makes high requirements on the injector vacuum system: not less than $10^{-7}$ Torr [3].

## *Dispenser Cathode*

The cathode assembly is an integral part of any beam source system. Elements of the cathode assembly, such as a heater or internal components, not formally effects on the beam dynamics. However, the uniformity of heating of the cathode surface, is very important for the uniformity of emission. To develop of this issue, the thermal calculations of cathode heating system were performed in order to optimize the cathode assembly. In particular, the homogeneity of the temperature distribution along the surface of cathode core was studied. This is important for high quality beam forming.

3D-modeling was performed using COMSOL Multiphysics software platform. In simulation of heat exchange by radiation between solids in vacuum the module "Surface-to-surface radiation" was used. A 3D-model of the cathode assembly was used as the initial geometry. All calculations were made for a stationary thermal conditions. The appearance of the modified cathode assembly is shown in Fig. 1.

At power 2500 W, the heater temperature reaches 1500 °C, the cathode surface temperature is about 1000 °C. The asymmetrical shape of the heater (Fig. 2) leads to an increase in the local zone by 4 degrees, which is an acceptable value (Fig. 3).

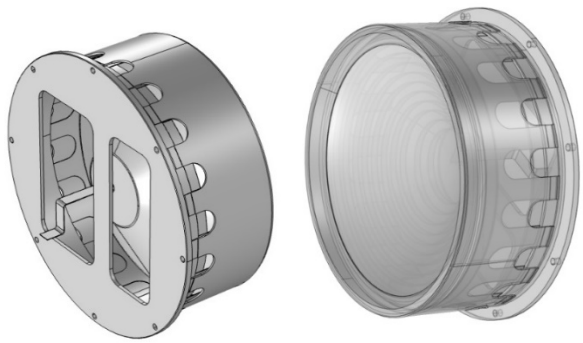

Figure 1: The cathode assembly.

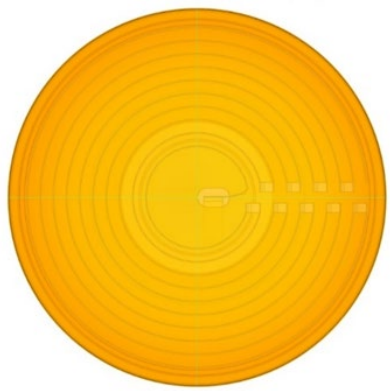

Figure 2: The cathode model for simulate heating process in COMSOL to estimate the temperature distribution along the surface.

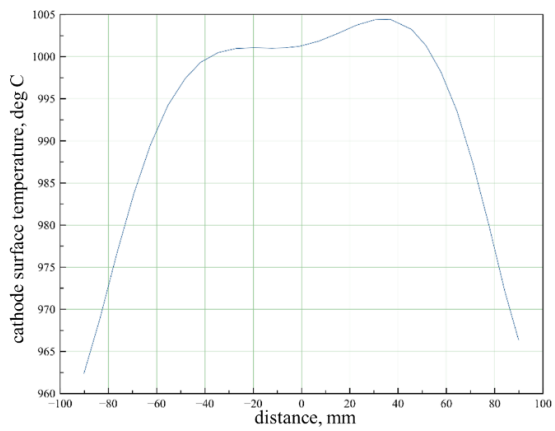


Figure 3: Cathode surface temperature distribution in horizontal section.

† d.a.starostenko@inp.nsk.su

ISBN: 978-3-95450-240-0 ISSN: 2673-5539 doi:10.18429/JACoW-RuPAC2021-MOB01

# STATUS OF U70

V. Kalinin†, Yu. Antipov, A. Afonin, N. Ignashin, S. Ivanov, V. Lapygin, O. Lebedev, A. Maksimov, Yu. Milichenko, A Soldatov, S. Strekalovskikh, S. Sytov, N. Tyurin, D. Vasiliev A. Zaitsev
NRC "Kurchatov Institute"– IHEP (Institute for High Energy Physics)
Protvino, Moscow Region, 142281, Russia

*Abstract*

The report overviews present status of the Accelerator Complex U-70 at IHEP of NRC "Kurchatov Institute" (Protvino). The emphasis is put on the recent activity and upgrades implemented since the previous conference RuPAC-2018, in a run-by-run chronological ordering.

History of the foregoing activity is recorded sequentially in [1].

## GENERALITIES

The entire Accelerator Complex U70 comprises four machines — 2 linear (I100, URAL30) and 2 circular (U1.5, U70) accelerators. Proton mode (default) employs a cascade of URAL30–U1.5–U70, while the light-ion (carbon) one — that of I100–U1.5–U70.

Since the previous conference RuPAC-2018, the U70 complex operated for five runs in total. Table 2 lists their calendar data. The second run of 2021 is being planned for October–December of 2021.

Details of the routine operation and upgrades through years 2018–21 are reported in what follows, run by run.

## RUN 2018-2

The run lasted from October 01 till December 12 2018 in the two modes and with four beam energies — proton (0.7 and 50 GeV) and carbon (250 and 456 MeV/u).

At the 1st half of proton mode, 50 GeV proton beam was directed to applied research at the radiographic facility.

To this end, the facility was fed with the fast-extracted bunched beam with equal bunches of $3–4\cdot10^{11}$ ppb.(see Fig. 1) To attain electric energy conserving operation, the flattop length was cut short to 0.6 sec.

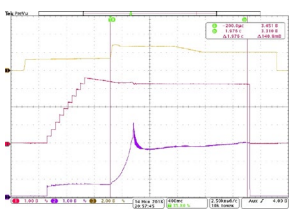

Figure 1: Fast extraction to radiographic facility. Traces from top to bottom: envelope of RF electric field, beam DC current; bunch peak current.

At the 2nd half of the proton mode, research activity was focus to expand the range of the working beam intermediate energy in U-70 (350÷1320 MeV for proton and 250÷455 MeV/u for carbon). The presence of extracted beams of intermediate energies opens up new possibilities for proton radiography, radiobiological studies, etc. To this end, the U70 magnet lattice was toggled to regulated power supply unit [2]. Magnetic cycle for slowing down (from 1320 to 700 MeV) proton beam was created. Proton bunch from U1.5 ($1.8\cdot10^{11}$ ppb) was injected in U-70 on the injection plateau (356 Gs) then, after adjustment RF and magnet field correction systems, was slowed down to 0.7 GeV and circulating at extraction plateau (230 Gs) ($1.2\cdot10^{11}$ ppb). All efforts to decrease extraction plateau field (less than 230 Gs) lead to rapid loss of all beam intensity. Same research was repeated in carbon mode. In this case, carbon beam was slowed down from 456 MeV/u to 250 MeV/u and circulating at extraction plateau (250 Gs).

Closer to end of the run the regulated power supply unit was switched to the DC mode at 455 MeV/u, the main ring being operated as beam storage and stretcher ring at flatbottom DC magnetic field. The beam was extracted slowly with a stochastic extraction scheme [3] capable of yielding 0.6 s long square-wave spills. The in-out transfer ratio amounted 55-57%, close the top expected value of around 68% The beam was used for applied radiobiological and biophysical research (see Fig. 2) by teams from four institutes listed in the 2nd row of Table 1.

Figure 2: Screenshot of the Radio-Biological Workbench work monitor.

## RUN 2019-1

It was an intermediate-energy ad hoc one-month long run dedicated to the several sequential tasks:

First, to provide more time for studies and finer tuning of deceleration regime (455÷180 MeV/u).

Second, obtain the regimes of deceleration, of circulation and slow extraction of a beam of carbon nuclei two different energies 300 and 200 MeV/u.

Third, testing new irradiation field-forming system based on electromagnetic wobbler magnets. Testing new

†vakalinin@ihep.ru

ISBN: 978-3-95450-240-0 ISSN: 2673-5539 doi:10.18429/JACoW-RuPAC2021-TUX01

# STATUS OF THE HIAF ACCELERATOR FACILITY IN CHINA*

L. J. Mao, J. C. Yang†, D. Q. Gao, Y. He, G. D. Shen, L. N. Sheng, L. T. Sun, Z. Xu, Y. Q. Yang, Y. J. Yuan and HIAF project team, IMP CAS, Lanzhou, China

*Abstract*

The High Intensity heavy-ion Accelerator Facility (HIAF) is under constructed at IMP in China. The HIAF main feature is to provide high intensity heavy ion beam pulse. A rapid acceleration in the booster synchrotron ring (BRing) with the ramping rate of 12 T/s is used. The challenges are related to the systems injector, RF cavities, power supplies, vacuum, magnets, etc. Works on key prototypes of the HIAF accelerator are ongoing at IMP. In this paper, an overview of the status and perspective of the HIAF project is reported.

## INTRODUCTION

The High Intensity heavy-ion Accelerator Facility (HIAF) is a new accelerator under construction at the Institute of Modern Physics (IMP) in China [1]. It is designed to provide intense primary heavy ion beams for nuclear and atomic physics. The facility consists mainly of a superconducting electron-cyclotron-resonance (SECR) ion source, a continuous wave (CW) superconducting ion linac (iLinac), a booster synchrotron (BRing) and a high precision spectrometer ring (SRing). A fragment separator (HFRS) is also used as a beam line to connect BRing and SRing. Six experimental terminals will be built in phase-I at HIAF. The layout of the HIAF accelerator was shown in Fig. 1. The main parameters are listed in Table 1.

The construction of the HIAF project was started officially in December 23rd, 2018. Up to now, roughly 50% of civil construction is finished. The first component of SECR is planned to equip in the tunnel in the middle of 2022. The first beam will be accelerated at BRing in the middle of 2025. A Day-one experiment is proposed before the end of 2025. A brief time schedule of HIAF construction is shown in Fig. 2.

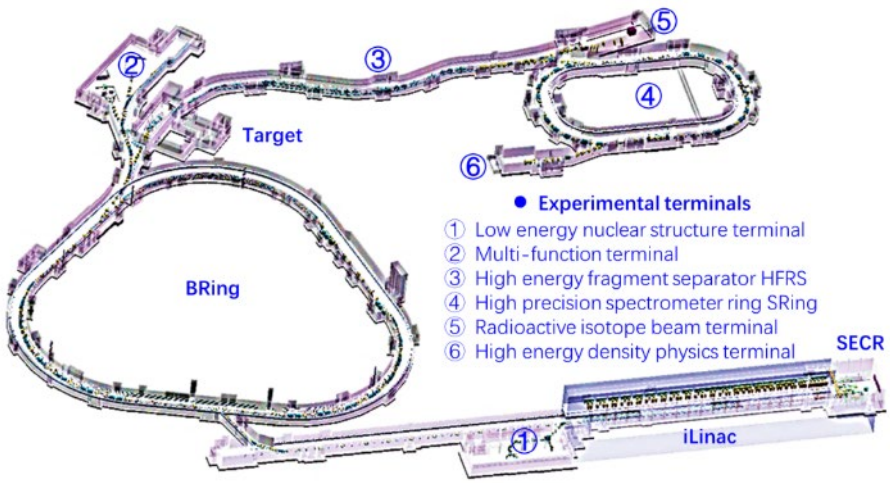


Figure 1: Layout of the HIAF project.

Table 1: Main Parameters of the HIAF Accelerators

| | SECR | iLinac | BRing | HFRS | SRing |
|---|---|---|---|---|---|
| Length / circumference (m) | --- | 114 | 569 | 192 | 277 |
| Final energy of U (MeV/u) | 0.014 ($U^{35+}$) | 17 ($U^{35+}$) | 835 ($U^{35+}$) | 800 ($U^{92+}$) | 800 ($U^{92+}$) |
| Max. magnetic rigidity (Tm) | --- | --- | 34 | 25 | 15 |
| Max. beam intensity of U | 50 pμA ($U^{35+}$) | 28 pμA ($U^{35+}$) | $10^{11}$ppp ($U^{35+}$) | | $10^{10}$ppp ($U^{92+}$) |
| Operation mode | DC | CW or pulse | fast ramping (12T/s, 3Hz) | Momentum-resolution 1100 | DC or deceleration |
| Emittance or Acceptance (H/V, π·mm·mrad, dp/p) | | 5 / 5 | 200/100, 0.5% | ±30mrad(H)/±15 mrad(V), ±2% | 40/40, 1.5%, normal mode |

Currently, most of the prototypes related to the HIAF technical challenges have being manufactured or tested. In this paper, the status and perspectives of the HIAF project are presented. The developments and test results of hardware are reported.

* Work supported by the National Development and Reform Commission, China
† yangjch@impcas.ac.cn.

ISBN: 978-3-95450-240-0 ISSN: 2673-5539 doi:10.18429/JACoW-RuPAC2021-TUY01

# VEPP-2000 COLLIDER OPERATION IN 2019–2021 RUNS: CHALLENGES AND RESULTS*

M. Timoshenko†, Yu. Aktershev, O. Belikov, D. Berkaev, D. Burenkov, V. Denisov, V. Druzhinin, K. Gorchakov, G. Karpov, A. Kasaev, A. Kirpotin, S. Kladov[1], I. Koop[1], A. Kupurzhanov, G. Kurkin, M. Lyalin[1], A. Lysenko, S. Motygin, A. Otboev, A. Pavlenko[1], E. Perevedentsev[1], V. Prosvetov, S. Rastigeev, Yu. Rogovsky, A. Semenov[1], A. Senchenko[1], L. Serdakov, D. Shatilov, P. Shatunov, Yu. Shatunov[1], D. Shwartz[1], V. Yudin, I. Zemlyansky, Yu. Zharinov
Budker Institute of Nuclear Physics, Novosibirsk, Russia
[1]also at Novosibirsk State University (NSU), Novosibirsk, Russia

*Abstract*

VEPP-2000 is the only electron-positron collider operating with a round beam that permits to increase the limit of beam-beam effects. VEPP-2000 is the compact collider with circumference of 24.39 m which has record design luminosity of $1 \times 10^{32}$ cm$^{-2}$ s$^{-1}$ per bunch at energy up to 1 GeV and record achieved luminosity of $5 \times 10^{31}$ cm$^{-2}$ s$^{-1}$ at energy of 500 MeV, magnetic fields in superconducting solenoids is 13 T and 2.4 T in the bending magnets. Collider complex experimental program of 2019–2021 was focused on several energy ranges. Energy range was (180–300) MeV in the second half of 2019, in the first half of 2020 we worked in (935–970) MeV, in the first half of 2021 that was (970–1003.5) MeV. Data taking was carried out by CMD-3 and SND detectors, the operation efficiency is compared with previous runs. Luminosity was limited by beam-beam effects. 2021 year was clouded by vacuum accident and subsequent intensive degassing using beam synchrotron radiation.

## INTRODUCTION

We present in this paper an overview of VEPP-2000 electron-positron collider, operation chronology and statistics. In spite of problems connected with some vacuum accident and also with Anti COVID measures, luminosity records at operation energy ranges have been achieved. Data taking was also successful comparable to previous years level. This factor was provided by using several instruments for increasing peak luminosity such as Beam-shaker and lattice optimization. The analysis of operation time for data taking by collider detectors have been done and some solution for increasing the rate of collecting integral luminosity are in plans and have already been implementing.

## VEPP-2000 OVERVIEW

VEPP-2000 is a compact electron-positron single rind collider [1] equipped with electron-positron booster ring [2] (Fig. 1) operating at bunch energy range (160–1000 MeV). Booster is feeded with particles by BINP Injection complex [3] at 430 MeV energy (until recently it was 390 MeV). Table 1 shows main parameters of the collider.

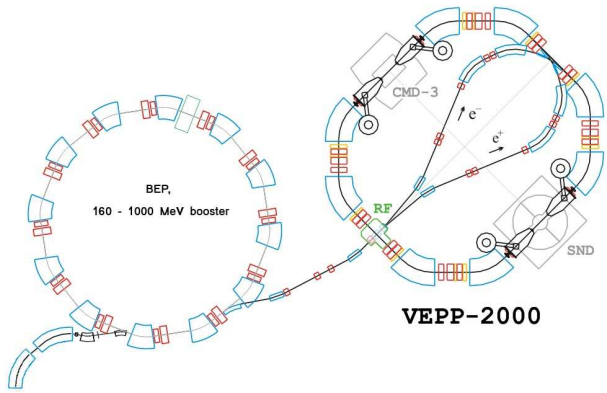


Figure 1: VEPP-2000 complex layout.

Table 1: VEPP-2000 Design Main Parameters at $E$= 1 GeV

| Parameter | Value |
|---|---|
| Circumference, $C$ | 24.39 m |
| Energy range, $E$ | 160–1000 MeV |
| Number of bunches | $1 \times 1$ |
| Number of particles per bunch, $N$ | $1 \times 10^{11}$ |
| Betatron functions at IP, $\beta^*_{x,y}$ | 8.5 cm |
| Betatron tunes, $\nu_{x,y}$ | 4.1; 2.1 |
| Beam emittance, $\varepsilon_{x,y}$ | $1.4 \times 10^{-7}$ m rad |
| Beam–beam parameters, $\xi_{x,z}$ | 0.1 |
| Luminosity, $L$ | $1 \times 10^{32}$ cm$^{-2}$ s$^{-1}$ |

### *Round Beam Concept*

Uniqueness and feature of VEPP-2000 collider is realization of Round Beam Concept [4, 5]. This factor allowed VEPP-2000 to have high luminosity and to make particles' dynamic one-dimensional although still non-linear. The concept applies several requirements to collider lattice:

- Head-on collisions (zero crossing angle)
- Small and equal $\beta$ functions at IP ( $\beta^*_x = \beta^*_y$ ).
- Equal beam emittances ( $\varepsilon_x = \varepsilon_y$ ).
- Equal fractional parts of betatron tunes ( $\nu_x = \nu_y$ ).

* The reported study was partly funded by RFBR, project number 20-32-90217
† tim94max@gmail.com

ISBN: 978-3-95450-240-0 ISSN: 2673-5539 doi:10.18429/JACoW-RuPAC2021-TUA01

# VEPP-4M COLLIDER OPERATION AT HIGH ENERGY

P. A. Piminov†, G. N. Baranov, A. V. Bogomyagkov, V. M. Borin, V. L. Dorokhov, S. E. Karnaev, K. Yu. Karyukina, V. A. Kiselev, E. B. Levichev, O. I. Meshkov, S. I. Mishnev, I. A. Morozov, I. B. Nikolaev, O. N. Okunev, E. A. Simonov, A. G. Shamov, S. V. Sinyatkin, E. V. Starostina, C. Yu. Todyshev, V. N. Zhilich, A. A. Zhukov, A. N. Zhuravlev,
Budker Institute of Nuclear Physics SB RAS, Novosibirsk, Russia

*Abstract*

From 2018 HEP experiments at the VEPP-4M collider with the KEDR detector were carried out in the high energy range (higher than 2 GeV). VEPP-4M is an electron positron collider in the beam energy range from 1 to 6 GeV. KEDR is the universal magnetic detector with 6 kGs longitudinal field and the particle tagging system for selection of gamma-gamma interaction. The paper discusses recent experimental activity of the VEPP-4M: the hadron cross section measurement from 2.3 to 3.5 GeV, ϒ(1S) meson searching, gamma-gamma physics luminosity run, synchrotron radiation, etc. Also the beam energy measurement by the resonance depolarization method using the laser polarimeter has been presented.

## INTRODUCTION

The multipurpose accelerator complex VEPP-4 [1] is used for high energy physics (HEP) experiments at electron positron collider VEPP-4M with KEDR detector [2], experiments with synchrotron radiation (SR) at VEPP-3 and VEPP-4M [3], nuclear physics experiments at Deuteron facility [4], experiments with extracted hard gamma beams (~ 0.1÷3 GeV) at Test Beam Facility for detector physics [5] and accelerator physics researches. The VEPP-4 facility is shown schematically on Fig. 1. On the figure SR is experimental halls for synchrotron radiation researches and ROKK-1M is an experimental hall for the Test Beam Facility and the laser polarimeter.

The VEPP-3 is storage ring with 74 m length and beam energy from 400 MeV to 2 GeV. It has its own experimental program and is used also for the particle acceleration and the particle polarization for VEPP-4M. The transport channel from VEPP-3 to VEPP-4M is pulse with 1.9 GeV maximum energy.

The VEPP-4M ring is a racetrack of 366 m length with single magnetic turn for electron and positron beams. The beam energy range is from 0.9 to 6.0 GeV. Four vertical bumps by 4 electrostatic plates in each allow circulating of 2 electron and 2 positron bunches. The beams are collided in main interaction point after the injection and the acceleration. For radiation beam control 2 Robinson gradient wigglers two dipole 3-pole wigglers at 2 T are used. The vertical digital feedback suppresses single-bunch instability and the analog RF feedback suppresses the multibunch longitudinal instability. All this allows increasing the beam currents and the beam lifetime at low energies and obtaining threshold currents for the beam-beam.

† piminov@inp.nsk.su

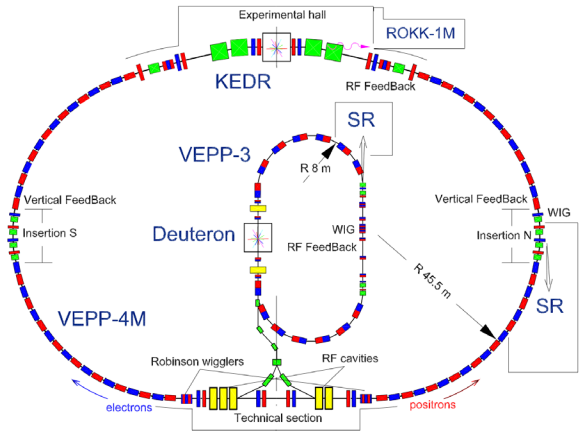


Figure 1: VEPP-4 layout.

The maximum acceleration rate is 20 MeV/s. RF system has 5 cavities and operates at 180 MHz frequency (222 harmonic number) and 4.5 MV maximal voltage.

Parameters of VEPP-4M for different energies are given in Table 1. The red colour marks out nearest goals.

Table 1: Parameters of VEPP-4M for Different Energies

| **Energy** | **2.3** | **3.5** | **4.75** | **GeV** |
|---|---|---|---|---|
| Betatron tunes | | 8.54/7.57 | | |
| Nat. chroms | | –14/–20 | | |
| Comp. factor | | 0.0168 | | |
| Hor. emit. | 42 | 100 | 180 | nm·rad |
| Energy spread | 3.7 | 6.5 | 7.5 | $\cdot 10^{-4}$ |
| Bunch length | | 4 | | cm |
| Beam | 2x2 | 2x2 | 1x1→2x2 | |
| Bunch current | 6 | 9→12 | 9→12 | mA |
| Luminosity | 0.5 | 1.2→2.0 | 0.5→1.4 | $\cdot 10^{31}$ cm$^{-2}$ s$^{-1}$ |

## HIGH ENERGY PHYSICS EXPERIMENT

Since 2018 KEDR experimental program in the high energy range of VEPP-4M was started. It requires the beam acceleration in the collider. The beam injection and the acceleration take during 30 minutes and the luminosity time is 2 hours.

### *Hadron Cross Section scan from 2.3 to 3.5 GeV*

The first goal of the KEDR physical program was measurement of the hadron cross section (R-scan) from 2.3 to 3.5 GeV in 17 points. The total luminosity integral is 13.7 pb$^{-1}$. The beam energy measurement is not required. The beam energy stability in each point is 5 MeV.

The R values are critical in various precision tests of the Standard Model. The energy region 4.6÷7 GeV, where KEDR data has been collected, gives small contribution

ISBN: 978-3-95450-240-0 ISSN: 2673-5539 doi:10.18429/JACoW-RuPAC2021-TUA02

# CURRENT STATUS OF VEPP-5 INJECTION COMPLEX

Yu.I. Maltseva*[1], A. Andrianov[1], K. Astrelina, V. Balakin[1], A. Barnyakov, A.M. Batrakov, O.V. Belikov, D.E. Berkaev, D. Bolkhovityanov, F.A. Emanov[1], A. Frolov, G. Karpov, A. Kasaev, A.A. Kondakov, N. Kot, E.S. Kotov[1], G. Ya. Kurkin, R. Lapik, N. Lebedev[1], A. Levichev[1], A. Yu. Martynovsky, P. Martyshkin, S. V. Motygin, A. Murasev, V. Muslivets, D. Nikiforov[1], A. Pavlenko[1], A. Pilan, Yu. Rogovsky[1], S. Samoylov, A.G. Tribendis[2], S. Vasiliev, V. Yudin,
Budker Institute of Nuclear Physics SB RAS, Novosibirsk, Russia
[1]also at Novosibirsk State University, Novosibirsk, Russia
[2]also at Novosibirsk State Technical University, Novosibirsk, Russia

*Abstract*

VEPP-5 Injection Complex (IC) supplies VEPP-2000 and VEPP-4 colliders at Budker Institute of Nuclear Physics (BINP, Russia) with high energy electron and positron beams. Since 2016 the IC has shown the ability to support operation of both colliders routinely with maximum positron storage rate of $1.7 \cdot 10^{10}$ e+/s. Stable operation at the energy of 430 MeV has been reached. Research on further improvements on the IC performance is carried out. In particular control system was improved, additional beam diagnostics systems were developed, monitoring of RF system was upgraded. In this paper, the latest achieved IC performance, operational results and prospects are presented.

## INTRODUCTION

Since 2016 the IC [1,2] has supplying the VEPP-2000 [3] and VEPP-4 [4] facilities with high energy electron and positron beams. The layout of BINP colliders together with IC is shown in Fig. 1.

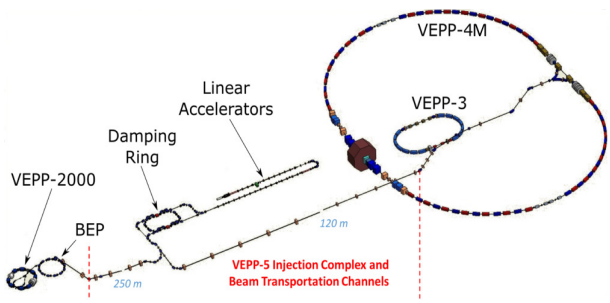


Figure 1: Layout of BINP accelerator facilities.

The IC consists of electron and positron S-band linacs with achieved energies of 280 MeV and 430 MeV, respectively, and the damping ring (DR) alternately storing both electron and positron beams. Then beams are transported to users via the set of K-500 beam transfer lines. Main IC parameters are presented in Table 1.

During the 2020/2021 run malfunction of positron solenoid reduced the positron storage rate, however by proper tuning the beam orbit and optimizing the regime-switching procedures positron storage rate of $0.9 \cdot 10^{10}$ e+/s was reached.

* yu.i.maltseva@inp.nsk.su

Table 1: Main IC Parameters

| Parameter | Value |
|---|---|
| Linac energy e-, e+ (reached) | 280, 430 MeV |
| Linac RF frequency | 2855.5 MHz |
| Energy spread e-, e+ | ±1%, ±3% |
| Linac repetition rate | up to 12.5 Hz |
| Extr. repetition rate | up to 1 Hz |
| Design horizontal emittance | $2.3 \cdot 10^{-6}$ rad·cm |
| Design vertical emittance | $0.5 \cdot 10^{-6}$ rad·cm |
| DR energy (design) | 510 MeV |
| DR RF frequency | 11.94 MHz |
| DR circumference | 27.4 m |
| DR design current | 30 mA |
| e+ storage rate (reached) | $1.7 \cdot 10^{10}$ /s |
| Damping time@510MeV(h/v/l) | 11/18/12 ms |

In terms of beam charge and injection repetition rate, VEPP-2000 collider imposes strict requirements on the IC performance. It requires constant beam injection due to small beam lifetime of 500 s. In order to achieve the desired luminosity a new portion of $10^{10}$ particles at least every 50 s has to be injected into the main ring. To meet these requirements switching between electron and positron beams in the IC was minimized up to 5 s by tuning both linacs to achieve equal energy for electron and positron beams, while keeping the DR operation mode to be constant. K-500 transfer line magnets and power supplies limit minimal switching time between the particle types to at least 30 s.

Due to small conversion efficiency for positron production, positron storage rate and extraction from the DR are the main concern. Considering achieved positron storage rate of $0.9 \cdot 10^{10}$ e+/s and transfer losses of up to 50-60 %, remaining time of 20 s to supply $10^{10}$ particles into VEPP-2000 main ring is sufficient. Thus, the IC meets the VEPP-2000 requirements. However, further improvement on the IC performance are essential for its reliable operation.

The IC has four operating modes: electron or positron production for VEPP-2000 or VEPP-4. The switching between these modes is automated with simple asynchronous state machine, 12 transitions between K-500 modes in order to reliably remagnetize its elements are utilized. Currently the IC is able to automatically supply the VEPP-2000 with all

ISBN: 978-3-95450-240-0 ISSN: 2673-5539 doi:10.18429/JACoW-RuPAC2021-TUB02

# NICA COLLIDER MAGNETIC FIELD CORRECTION SYSTEM

M. M. Shandov*, H. G. Khodzhibagiyan, S. A. Kostromin[1], O. S. Kozlov, I. Yu. Nikolaichuk, T. Parfylo, A. V. Phillippov, A. V. Tuzikov, Joint Institute for Nuclear Research, Dubna, Russia
[1]also at Saint Petersburg University, Saint-Petersburg, Russia

*Abstract*

The NICA Collider is a new superconducting facility that has two storage rings, each of about 503 m in circumference, which is under construction at the Joint Institute for Nuclear Research, Dubna, Russia. The influence of the fringe fields and misalignments of the lattice magnets, the field imperfections and natural chromaticity should be corrected by the magnetic field correction system. The layout and technical specification of the magnetic field correction system, the main parameters, arrangements and the field calculations and measurement results of the corrector magnets are presented. The results of dynamic aperture calculation at working energies are shown.

## INTRODUCTION

NICA (Nuclotron-based Ion Collider fAcility) is a new accelerator complex currently under construction at the Joint Institute for Nuclear Research, Dubna, Russia. One of the main goals of the NICA project is experimental studies of dense nuclear (baryonic) matter [1]. Two arcs and two straight sections with two interaction points compose the Collider lattice [2]. The FODO optics with 12 periods is chosen for the arc structure. The twin-aperture superconducting dipoles and quadrupoles with the distance between beams 320 mm [3] are used in FODO cells (see Fig. 1). The correction system includes 124 corrector magnets for each beam (46 in arcs and 16 in straight sections) and 8 corrector magnets combined for 2 beams (in interaction point regions), in total 132 corrector magnets.

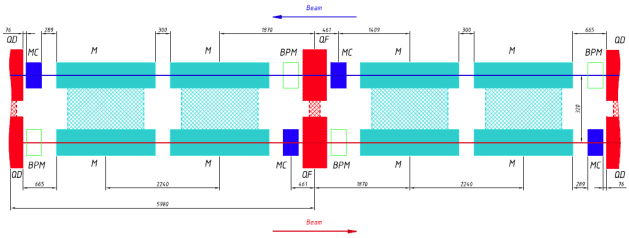


Figure 1: FODO-cell of the NICA Collider.

## MAGNETIC FIELD CORRECTION SYSTEM

Corrector magnets are installed in each module of the quadrupole magnet (see Fig. 1, MC) except for special corrector magnets in straight sections of the Collider. As it was shown in [4], the designed lattice structure and the magnetic field correction system of the NICA Collider are made it possible to reach the design parameters. In addition, a dynamic aperture (DA) 8 -9 $\sigma$ was reached. The main limitation of the dynamic aperture is the effect of the fringe fields (FF) of quadrupole magnets (see Fig. 2). At the present time, a tuning mode for compensation of the betatron tune coupling, ring chromaticity and fringe fields influence have been found. The current state of the results of calculating the beam dynamics for the NICA Collider was carried out in [5].

Random and systematic errors should be compensated by the correction system. The field imperfections, the deviation of magnetic field integrals, the influence of the FF and misalignments of lattice magnets are the sources of systematic errors. In addition, the natural chromaticity and betatron tune coupling are should be compensated too. The main aims for the magnetic field correction system are presented in Table 1. More details can be found in [6].

Table 1: Goals of the Correction System

| Field Type | Correction Goal | Field Strength |
|---|---|---|
| Normal dipole | Hor. orbit | 0.15 T |
| Skew dipole | Vert. orbit | 0.15 T |
| Normal quadrupole | Betatron tune | 3 T/m |
| Skew quadrupole | Motion coupl. | 3 T/m |
| Normal sextupole | Ring chrom. | 175 T/m$^2$ |
| Normal octupole | DA correction | 1300 T/m$^3$ |
| Normal dodecapole | DA correction | 125 000 T/m$^5$ |

## CORRECTOR MAGNETS

The design of the corrector magnets is based on the Nuclotron corrector magnets. In general, these are superconducting magnets with sector coils and an iron yoke (see Fig. 3). The cooling of the superconducting coils is carried out by an inner cooling cylinder (see Fig. 3, 1). The positioning and electrical insulation of the superconducting coils are carried out with spacer cylinders (see Fig. 3, 2). Structurally, the corrector magnets are separated in 10 groups according to the type of the installed coils. The design of the magnet, the main characteristics and the results of 2D FEM field calculation were presented in [6].

The DA value is reduced to 6 -7 $\sigma$ based on the results of 3D FEM field calculation of final focusing quadrupole magnets, in particular, by the integral value of the allowed harmonics $B_5$. For this reason, a special dodecapole corrector magnet has been developed. The superconducting coil with a cooling spacer is mounted directly on the surface of the beam pipe in the centre of the central final focusing

* shandov@jinr.ru

ISBN: 978-3-95450-240-0 ISSN: 2673-5539 doi:10.18429/JACoW-RuPAC2021-TUB03

# METHOD AND SYSTEMATIC ERRORS FOR SEARCHING FOR THE ELECTRIC DIPOLE MOMENT OF CHARGED PARTICLE USING A STORAGE RING

Y. Senichev, A. Aksentyev, A. Melnikov, Institute for Nuclear Research of Russian Academy of Sciences, Moscow 117312, Russia

*Abstract*

One of possible arguments for CP-invariant violation is the existence of non-vanishing electric dipole moments (EDM) of elementary particles [1]. To search for the EDM the BNL proposed to construct a special ring implementing the frozen spin mode in order to detect the EDM signal. Since systematic errors determine the sensitivity of a method, this article analyses some major methods proposed for searching for the EDM from the point of view of this problem. The frequency domain method (FDM) proposed by the authors does not require a special accelerator for deuterons and requires spin precession frequency measurements only. The method has four features: the total spin precession frequency due both to the electric and the magnetic dipole moments in an imperfect ring in the longitudinal-vertical plane is measured at an absolute statistic error value of ~$10^{-7}$ rad/sec in one ring filling; the ring elements position remain unchanged when changing the beam circulation direction from clockwise (CW) to counter-clockwise (CCW); calibration of the effective Lorentz factor by means of spin precession frequency measurements in the horizontal plane is carried out alternately in each CW and CCW procedure; the approximate relationship between the spin precession frequency components is set to exclude them from mixing to the expected EDM signal at a statistical sensitivity level approaching $10^{-29}$ e cm. The FDM solves the problem of systematic errors, and can be applied in the NICA facility.

## ORIGINAL IDEA

The idea of searching for electric dipole moment of the proton and deuteron using polarized beams in a storage ring is based on "the frozen spin" method and was originally proposed at Brookhaven National Laboratory (BNL) [2]. The concept of the "frozen spin" lattice consists of deflectors with electric and magnetic fields incorporated in one element, in which the spin vector of the reference particle is always orientated along the momentum. This is clearly evident from the Thomas–Bargmann–Michel–Telegdi equation:

$$\frac{d\vec{S}}{dt} = \vec{S} \times \left(\vec{\Omega}_{mdm} + \vec{\Omega}_{edm}\right),$$

$$\vec{\Omega}_{mdm} = \frac{e}{m\gamma}\left\{(\gamma G + 1) - \left(\gamma G + \frac{\gamma}{\gamma+1}\right)\frac{\vec{\beta}\times\vec{E}}{c}\right\}, \quad (1)$$

$$\vec{\Omega}_{edm} = \frac{e\eta}{2m}\left(\vec{\beta} \times \vec{B} + \frac{\vec{E}}{c}\right), \; G = \frac{g-2}{2} \quad ,$$

where $G$ is the anomalous magnetic moment, $g$ is the gyromagnetic ratio, $\Omega_{mdm}$ is the spin precession frequency due to the magnetic dipole moment (hereinafter referred to as MDM precession), $\Omega_{edm}$ is the spin precession frequency due to the electrical dipole moment (hereinafter referred to as EDM precession), and $\eta$ is the dimensionless coefficient defined in (1) by the relation $d = \eta e\hbar/4mc$. The advantages of purely electrostatic machines are especially evident at the "magic" energy, when:

$$G - 1/\left(\gamma_{mag}^2 - 1\right) = 0, \quad (2)$$

and the spin vector initially oriented in the longitudinal direction rotates in the horizontal plane with the same frequency as the momentum $\Omega_p$, i.e., $\Omega_{mdm} - \Omega_p = 0$.

In the case of deuterons with $G = -0.142$ the only possible method is a storage ring with both electric and magnetic fields [3]. This can be done by applying a radial electric field $E_r$ to balance the vertical magnetic field $B_v$ contribution to $\Omega_{mdm}^p$, as shown in Eq. (1):

$$E_r = \frac{GBc\beta\gamma^2}{1-G\beta^2\gamma^2} \approx GB_v c\beta\gamma^2. \quad (3)$$

Thus, for both protons and deuterons there is a general idea of how to construct a ring, but this is realized with the help of different types of deflectors.

## METODS OF EDM MEASUREMENT

for searching for the EDM are determined by the success of solving the problem of systematic errors. From this point of view, there are currently three promising methods of searching for the electric dipole moment of protons and deuterons: BNL "frozen spin" method [2], Koop's "spin wheel" method [3] and Frequency Domain method (FDM) [4]. Basically, their difference is delineated by how the problem of systematic errors is solved.

### *BNL "Frozen Spin" Metod*

First, we will consider the "frozen spin" method [2]. In common case the orientation of the spin in 3D space is determined by three frequency projections of spin precession due to magnetic dipole moment $\Omega_r, \Omega_y, \Omega_z$ and electric dipole moment $\Omega_{edm}$:

$$\Omega = \sqrt{(\Omega_{edm} + \Omega_r)^2 + \Omega_y^2 + \Omega_z^2}. \quad (4)$$

ISBN: 978-3-95450-240-0 ISSN: 2673-5539 doi:10.18429/JACoW-RuPAC2021-TUB04

# DEVELOPMENT OF THE ELECTRON COOLING SYSTEM FOR NICA COLLIDER

M. Bryzgunov, A. Bubley, A. Denisov, A. Goncharov, V. Gosteev, V. Panasyuk, V. Parkhomchuk, V. Reva[1], A. Batrakov, E. Bekhtenev[1], O. Belikov, V. Chekavinskiy, M. Fedotov, K. Gorchakov, I. Gusev, I. Ilyin, A. Ivanov[1], G. Karpov, M. Kondaurov, N. Kremnev[1], D. Pureskin, A. Putmakov, D. Senkov, K. Shtro, D. Skorobogatov, R. Vakhrushev, A. Zharikov
Budker Institute of Nuclear Physics, Novosibirsk, Russia
[1]also at Novosibirsk State University, Novosibirsk, Russia

*Abstract*

The high voltage electron cooling system for the NICA collider is now under development in the Budker Institute of Nuclear Physics (Russia). The aim of the cooler is to increase ion beams intensity during accumulation and to decrease both longitudinal and transverse emittances of colliding beams during experiment in order to increase luminosity. Status of its development and results of tests of the cooler elements are described in the article.

## INTRODUCTION

The NICA project is aimed to provide experiments with highly compressed baryonic matter with the help of colliding ion beams. In order to achieve project luminosity it is planned to use electron and stochastic cooling, which will help both during accumulation (to increase beam intensity) and during experiment (to compensate beam's emittance grow due to beam-beam effects, intra-beam scattering etc.).

Budker INP has big experience in production of electron cooling systems for different energies and now it develops project of high voltage electron cooling system (HV ECS) for the NICA. In Fig. 1 a 3-D model of the ECS is shown. Its design is based on design of HV electron cooler for COSY, produced by BINP [1]. The system consists of two almost independent coolers, which cool both colliding beams. Each cooler consists of high voltage system (which is placed in high pressure vessel, filled with $SF_6$, and which contains electron gun, electron collector, electrostatic tubes and HV power supplies), cooling section and transport channels (consisting of linear and bend magnets). Electron beam, emitted by cathode in electron gun, is accelerated by electrostatic tube to working energy. After that, it moves through transport cannel to the cooling section, where it interacts with ion beam. After the cooling section it moves back (through another transport channel) to high voltage system where it is decelerated and absorbed by collector surface. Such not standard scheme of ECS with whole high voltage system in one vessel is usual for high energy electron coolers and besides the COSY cooler it was realized on 4.3 MeV Fermilab electron cooler of the Recycler ring [2].

On whole trajectory from gun to collector electron beam moves in longitudinal magnetic field, which provides transverse focusing of the beam. In the cooling section longitudinal field provides, so-called, "fast" (or magnetized) electron cooling [3].

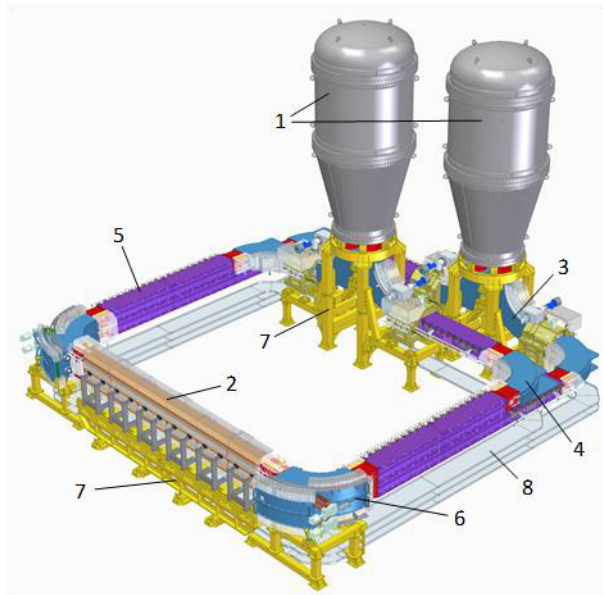


Figure 1: 3D model of the electron cooling system for NICA collider. 1 – high-voltage vessels, 2 – cooling section, 3 – vertical bend, 4 – horizontal bends, 5 – linear sections, 6 – toroid magnet, 7 – supports, 8 – cable channels.

## HIGH VOLTAGE SYSTEM

The HV system of the cooler (Fig. 2) generally consists of HV column and HV terminal on its top. The column consists of 42 identical sections (Fig. 3). Each section contains 2 HV power supplies (up to 30 kV), connected in series, magnetic coils for longitudinal field, power supplies for coils and control electronics. The sections are separated from each other with insulating (plastic) supports. Section height is 48 mm, period is 64 mm. Connection of every section with control computer is realized with the help of wireless interface ZigBee. All sections are powered with the help of cascade transformer [4]. For this purpose each section of the transformer has small winding.

Two electrostatic tubes are installed in magnetic coils for beam acceleration and deceleration.

ISBN: 978-3-95450-240-0 ISSN: 2673-5539 doi:10.18429/JACoW-RuPAC2021-TUB07

# THE CONCEPTUAL DESIGN OF THE 7.5 MeV/U LIGHT ION INJECTOR

S.M. Polozov, A.E. Aksentyev, M.M. Bulgacheva, O.A. Deryabochkin, M.S. Dmitriyev, V.V. Dmitriyeva, M.V. Dyakonov, V.S. Dyubkov, A.V. Gerasimenko, A.A. Gorchakov, M.A. Gusarova, M.A. Guzov, E.N. Indiushnii, O.A. Ivanov, A.M. Korshunov, K.I. Kozlovskiy, A.S. Krasnov, M.V. Lalayan, Y.Y. Lozeev, T.A. Lozeeva, A.I. Makarov, S.V. Matsievskiy, A.P. Melekhov, O.V. Murygin, R.E. Nemchenko, G.G. Novikov, A.E. Novozhilov, A.S. Panishev, V.N. Pashentsev, E.A. Plotnikov, A.G. Ponomarenko, A.V. Prokopenko, V.I. Rashchikov, A.V. Samoshin, A.A. Savchik, V.L. Shatokhin, A.E. Shikanov, K.D. Smirnov, G.A. Tsarev, S.A. Tumanov, I.A. Yurin, M.I. Zhigailova
National Research Nuclear University - Moscow Engineering Physics Institute, Moscow, Russia
N.V. Zavyalov, M.L. Smetanin, A.V. Telnov
RFNC-VNIIEF, Sarov, Nizhniy Novgorod region, Russia

*Abstract*

The new linac for light ion beam injection is under development at MEPhI. Such linac was proposed for acceleration of 7.5 MeV/nucleon ion beam with $A/Z$=1-3.5 and current up to 5 mA for proton and 0.4 pmA for light ions. The linac general layout will include two types of ion sources: ECR ion source for proton and He ions and laser ion source for ions form Li to O. Following the LEBT ions will be bunched and accelerated to the final energy using RFQ section and 14 IH-cavities. These IH-cavities will be identical (divided into two groups) and independently phased. All cavities will operate on 81.25 MHz. Results of the beam dynamics simulations and the cavities design will be presented in the report.

## INTRODUCTION

Starting 2018 the new ion synchrotron complex is under development at RFNC-VNIIEF, Sarov. New complex will include booster and storage rings, two injectors LU1 (protons and light ions) and LU2 (heavy ions, designing at NRC Kurchatov Institute - ITEP) and many experimental channels. MEPhI is duty for LU1 linac which will accelerate ions from protons to oxygen up to energy of 7.5 MeV/nucleon with mass-to charge ratio $A/Z$<3.5.

LU1 linac will include two types of ion sources: ECR for protons and He beam and laser ion source for ions from Li to O. Both types of ion sources will be doubled to growth the reliability of the linac operation. All accelerating and bunching cavities will operate on the same frequency of 81.25 MHz. The low energy beam transport channel (LEBT) will be complex to compose beams from four ion sources. LEBT also will include buncher B1 for beams pre-bunching before the RFQ and first beam diagnostics devices block. RFQ will bunch and accelerate beam up to 820 keV/nucleon and should to provide the beam capturing coefficient not less than 90 % for all types of ions. Following RFQ section and medium energy transport line MEBT1 two groups of short 5-gaps independently feeded IH-cavities will be placed. The geometric velocity $\beta_g$ will be constant for the group of cavities to reduce the linac cost. As it was shown due to the beam dynamics simulation it will be enough to have two groups of cavities with $\beta_g$=0.057 and 0.099 (six and eight cavities for the first and the second groups correspondently) to achieve the final beam energy of 7.5 MeV/nucleon. The second buncher B2 will be added to MEBT1 to control the bunch length and to chop the bunch tail. Two groups of cavities will also separated by short transport line MEBT2 includes one reserve buncher B3.

After acceleration the beam should be rotated at the angle ~40 degrees at the high-energy transport line (HEBT). After junction with the direct HEBT of LU2 the beam will start to prepare for injection into the storage ring. Note that it is planned to inject the continuous beam into the booster ring and we should to use a debuncher in HEBT for this aim

Finally, we will have 19 accelerating and bunching cavities for LU1 in total, they will operating on the same frequency of 81.25 MHz. The linac total length is about 40 m (without HEBT). All cavities will feed by solid state amplifiers.

## ION SOURCES

As it was noted above LU1 linac will include four ion sources: two ECR and two laser ion sources. The key difficulty for the ECR design is the aim to generate both protons and $He^{2+}$ ions in the same source and to have the necessary beam intensity. The operating frequency of 2450 MHz was choused for ECR due to availability of magnetrons and successful experience of its operation at MEPhI [1]. The magnet system for ECR was chosen basing on solid state magnets with mechanical motion of the sextupole trap and end rings. The simulation shows that the necessary $p^+$ and $He^{2+}$ beam intensity will be achieved.

New laser ion source will be also designed basing on the old prototype operation experience. The laser ion source operates at MEPhI more that 30 years. It is used to generate different ion beams having single chatge state- and it was used to test the proposed technical solutions and to verify our analytical estimations for multi-charged beams. Unfortunately, the ion source is now equipped by low power (<450 mJ) laser, that prevents to generate multi-charged ions because this energy is lower that the

ISBN: 978-3-95450-240-0 ISSN: 2673-5539 doi:10.18429/JACoW-RuPAC2021-TUC01

# STATUS OF THE KURCHATOV SYNCHROTRON RADIATION SOURCE

V. Korchuganov, A. Belkov, Y. Fomin, E. Kaportsev, Yu. Krylov, V. Moiseev, K. Moseev, N. Moseiko, D. Odintsov, S. Pesterev, A. Smygacheva, A. Stirin, V. Ushakov, A. Valentinov
NRC Kurchatov Institute, Akademika Kurchatova Sq., 1, Moscow, 123182 Russia

*Abstract*

The Kurchatov synchrotron radiation source goes on to operate in the range of synchrotron radiation from VUV up to hard X-ray. An electron current achieves 120 mA at 2.5 GeV, up to 12 experimental stations may function simultaneously. Improvement of the facility according Federal Program of KSRS modernization is in progress. Two 3 Tesla superconducting wigglers have been installed at main ring at 2019. They were tested with small electron beam current at 2020-2021. Wigglers' influence on beam parameters is much closed to calculated value. Vacuum system has been upgraded at 2020. In 2021 control system will be completely modified. Manufacturing of third 181 MHz RF generator, new preliminary amplification cascades and new waveguides for all three generators continues in Budker Institute (Novosibirsk). Preparation of great modernization of the whole facility according Federal Program for science infrastructure development has been started.

## INTRODUCTION

A 2.5 GeV electron storage ring Siberia-2 is a main source of synchrotron radiation (SR) at Kurchatov Synchrotron Radiation Source (KSRS) facility. A magnetic structure of Siberia-2 provides 98 nm·rad horizontal emittance of an electron beam, electron current achieves 150 mA. At present Federal KSRS modernization program (below – Program 1) is in progress, it was prolonged till 2022. Within the scope of Program 1 a third 181 MHz RF generator was manufactured in addition to two existing generators of Siberia-2. Besides 2 new identical superconducting wigglers (SCW) with 3 Tesla maximal magnetic field were put in operation during 2019 – 2021. They were tested with small electron beam. In 2019 – 2020 a modernization of vacuum system was completed, now control system modernization is close to completion.

At 2020 a preparing to deep KSRS modernization has been started according to Federal Program for Scientific Infrastructure Development (below – Program 2). As a result of Program 2 all KSRS accelerators must be replaced to new ones. New main 2.5 GeV KSRS ring should have horizontal emittance less than 3 nm·rad and top-up injection from booster synchrotron. Only RF system, SCWs and SR beamlines will be retained from old KSRS equipment. Because of Program 2 appearance some items were cancelled from Program1.

## OPERATIONAL STATISTICS

As a rule Siberia-2 operates for SR users during 9 months per year. It functions during 3 or 4 weeks in around-the-clock mode from Monday to Saturday. Then one week of preventive maintenance and machine tuning follows. Usually there is one beam storing per day. Storing of 150 mA takes approximately one hour, then energy ramping occurs for 3 minutes with 2 - 3 % loss of current. Then beam current slowly decreases down to 40 – 50 mA so new storing is needed. Beam lifetime at 2.5 GeV depends on vacuum level and beam integral accumulated from the moment of last vacuum chamber violation.

As a result of KSRS development a stable facility operation was achieved during last several years (see Table 1, values for 2021 correspond to first half of the year.). But prominent decrease of these values occurred in 2020. Mostly it was caused by coronavirus pandemic which lead to KSRS shutdown at April-May and December. A long summer break for vacuum system modernization was one more reason. Finally initial plan for duration of users' work was completed only by 55% (in comparison with 100 – 110% during previous 4 years). Activity of SR users also was lower for the same reasons. But in 2021 all values became close to normal ones.

Table 1: Statistics of Siberia-2 Operation for last 4 Years

| Parameter | 2018 | 2019 | 2020 | 2021 |
|---|---|---|---|---|
| Time for users, hours | 3035 | 2728 | 1202 | 1706 |
| Beam current integral, A·hours | 227.1 | 200.1 | 88.8 | 105.0 |
| Average number of stations in use | 7.4 | 7.4 | 5.6 | 10.6 |
| Average current, mA | 74.8 | 73.4 | 73.9 | 61.5 |

## FEDERAL KSRS MODERNIZATION PROGRAM (PROGRAM 1)

KSRS modernization according Program 1 should not change overall scheme of the facility, all magnetic elements are the same. The facility still consists of two storage rings (Siberia-1 and Siberia-2), linac and two

ISBN: 978-3-95450-240-0 ISSN: 2673-5539 doi:10.18429/JACoW-RuPAC2021-TUC03

# DEVELOPMENT OF POWERFUL LONG-PULSE THz-BAND FEL DRIVEN BY LINEAR INDUCTION ACCELERATOR*

N. Yu. Peskov†, V. I. Belousov, N. S. Ginzburg, D. I. Sobolev and V. Yu. Zaslavsky,
Institute of Applied Physics, Russian Academy of Sciences, Nizhny Novgorod, Russia
A. V. Arzhannikov, D. A. Nikiforov, E. S. Sandalov, S. L. Sinitsky,
D. I. Skovorodin, A. A. Starostenko, and K. I. Zhivankov
Budker Institute of Nuclear Physics, Russian Academy of Sciences, Novosibirsk, Russia

*Abstract*

Project of high-power long-pulse sub-THz to THz-band FEL is under development based on the linac "LIU" of the new generation forming 5 - 20 MeV / 2 kA / 200 ns electron beam. The aim of this project is to achieve a record sub-GW power level and pulse energy content up to 10 - 100 J at the specified frequency ranges. In the present paper, results of electron-optical experiments on the formation of an electron beam with parameters acceptable to drive the FEL are discussed. Helical pulse undulators were elaborated for pumping operating transverse oscillations of the beam electrons. As a key component of the electrodynamic system of the FEL-oscillator, the possibility of using advanced Bragg resonators based on the coupling of propagating and quasi-cutoff waves, which are capable to provide stable narrow-band generation under conditions of substantial oversize of the interaction space, is analyzed.

## INTRODUCTION

Project of free-electron laser (FEL) is under development in collaboration between BINP RAS (Novosibirsk) and IAP RAS (Nizhny Novgorod) based on a new generation of induction linac "LIU" 5 - 20 MeV / 2 kA / 200 ns implemented in recent years at BINP RAS [1]. The use of such beam makes it possible to realize ultra-high power long-pulse FEL operating from sub-THz to THz frequency range [2]. Principal problems in realization of this generator include: (a) formation of the relativistic electron beam (REB) with parameters acceptable for operation in the short-wavelength ranges, (b) development of undulator for pumping operating transverse oscillations in the beam, and (c) elaboration of electrodynamic system that can provide stable narrow-band oscillation regime in a strongly oversized interaction space.

Initial proof-of-principle experiments are planned to start at the "LIU-5" accelerator in the 0.3 THz frequency range, with prospects of transition to 0.6 THz range and higher frequencies after positive results would be demonstrated. In the paper, the design parameters of the FEL project are discussed. Results of electron-optical experiments on the beam formation are presented. Structural elements of the FEL magnetic system based on helical undulator and a guide solenoid that provides intense beam transportation were elaborated. An electrodynamic system was proposed exploiting a new modification of oversized Bragg structures, so-called advanced Bragg structures, which have significantly improved selective properties. Structures of such type were designed with the diameter of 20 and 40 wavelengths for operation in specified frequency ranges.

## RESULTS OF ELECTRON-OPTICAL EXPERIMENTS AT THE LINAC "LIU"

The experimental basis for realization of the novel FEL scheme is the "LIU-5" accelerator complex [1] comprising a 2 MeV thermionic injector and the induction accelerating sections (total number of 8 with the acceleration of ~ 0.4 MeV each), which finally provide formation of 5 MeV beam with the current of up to 2 kA, duration of 200 ns and diameter of ~ 4 cm at the output. Beam focusing between these sections is provided by the pulsed magnetic lenses of ~ 0.2 T.

To conduct experiments on sub-THz /THz generation in the FEL, it is necessary to perform a significant compression over the beam cross-section from the size given above to the required diameter $D_{beam}$ ~ 5 - 7 mm and further transportation of the beam along the interaction region of about 1 - 1.5 m without loss of current. Based on the existing electron-optical system of the "LIU-5", the beam injection into the undulator was designed using magnetic lens of the accelerator and focusing pulsed solenoid of ~ 0.4 T. Simulations of the beam dynamics in this magnetic system were carried out using WARP code (which takes into account the electric and magnetic fields of an intense REB) and demonstrated possibility to compress the beam with measured emittance to the diameter needed to drive the FEL (see Fig. 1).

Schematic of experiments on the injection of an electron beam formed by the linac "LIU-5" into the FEL electron-optical system and its further transportation is shown in Fig. 1. As a result of the experiments, the required beam compression was realized. Beam current transmission through the vacuum channel was obtained with an efficiency of about 90%, which, however, was accompanied by reduction in the beam pulse duration to 80 - 100 ns due to the cutting of its leading and trailing edges. Currently, additional tuning of the accelerator and the magnetic system is being carried out, which should allow transportation of the compressed beam through the FEL interaction space to be close to 100% without beam pulse shortening. In this case, according to the simulation, energy spread in the beam is expected to be less than 1%.

* Work supported by the Russian Science Foundation, grant 19-12-00212
† peskov@ipfran.ru

ISBN: 978-3-95450-240-0 ISSN: 2673-5539 doi:10.18429/JACoW-RuPAC2021-WEA01

# BEAM TRANSFER SYSTEMS OF NICA FACILITY: FROM HILAC TO BOOSTER

A. Tuzikov†, A. Bazanov, A. Butenko, D. Donets, A. Fateev, A. Galimov, B. Golovenskiy, E. Gorbachev, A. Govorov, S. Kolesnikov, A. Kozlov, K. Levterov, D. Lyuosev, I. Meshkov, H. Nazlev, A. Petukhov, D. Ponkin, G. Sedykh, V. Seleznev, I. Shirikov, V. Shvetsov, A. Sidorin, A. Sidorov, A. Svidetelev, E. Syresin, V. Tyulkin, Joint Institute for Nuclear Research, Dubna, Russia

*Abstract*

New accelerator complex is being constructed by Joint Institute for Nuclear Research (Dubna, Russia) in frame of Nuclotron-based Ion Collider fAcility (NICA) project. The NICA layout includes new Booster and existing Nuclotron synchrotrons as parts of the heavy ion injection chain of the NICA Collider as well as beam transport lines which are the important link for the whole accelerator facility. Designs and current status of beam transfer systems in the beginning part of the NICA complex, which are partially commissioned, are presented in this paper.

## INTRODUCTION

The Nuclotron-based Ion Collider fAcility (NICA) including new accelerator complex [1, 2] is constructed in Joint Institute for Nuclear Research (Dubna, Russia). In frame of the NICA project the existing superconducting synchrotron Nuclotron which is under operation since 1993 was modernized to match the project specifications [3, 4] and the new accelerators - the heavy ion linear accelerator (HILAC) and the superconducting Booster synchrotron [5] – as well as systems of beam transfer between these accelerators had been created and commissioned in 2016-2021 [6-9].

In the paper, design and current status of creation and commissioning of the first of connecting links of the heavy ion injection chain of the NICA Collider - beam transfer systems from the HILAC to the Booster - are given.

## BEAM TRANSFER FROM HILAC TO BOOSTER

The beam transfer of heavy ions ($Au^{31+}$ is chosen as reference ions) from the HILAC into the Booster ring at energy of 3.2 MeV/n is fulfilled by means of a beam transport channel and devices of a beam injection system of the synchrotron [10-13]. The ion-optical system of the beam transport channel and the beam injection system provide beam injection by several methods for accumulation of ions in the Booster with required intensity. Main methods of beam injection are single-turn, multi-turn (up to three turns) and multiple injections (twice or triple injection repetitions with rate of 10 Hz). Accumulation of ions is based on betatron stacking in the horizontal phase plane of the Booster synchrotron. To be able to inject beams by three given methods, the beam injection system of the Booster has a set of devices containing the electrostatic septum ESS and three electric kickers, or modules of inflector plates IP1 – IP3. The beam transport channel from HILAC to the Booster [14] contains 2 dipole and 7 quadrupole magnets, 6 steerers, a debuncher and extended set of beam diagnostics devices including Faraday cups, fast and AC current transformers, shoe-box and button pick-ups, a phase probe, multi-wire profile monitors (see Fig. 1). The ion-optical system of the channel provides beam debunching and betatron matching of ion beams of the target charge state with the Booster lattice functions as well as separation and collimation of neighbor parasitic charge states of ions. It is designed to be flexible enough to maintain required beam parameters at the channel exit for different working points of the Booster as well as for different initial beam parameters at the exit of the HILAC. The beam transfer systems also have options useful to fill more compact the phase space of the Booster by injected ions: rapid change of electric fields inside the kickers and variation of electric fields of the septum and magnetic fields of the channel's magnets in intervals between beam injections during multiple injection.

The HILAC-Booster beam transport channel is located in the median plane of the synchrotron and connected to the Booster at the entrance of the electrostatic septum ESS. The septum ESS and the kicker IP2 [15] are placed in the 1st straight section of the Booster ring (see Fig. 2) which is under room-temperature conditions. The kickers IP1 and IP3 are located in the vicinity of the 1st straight section and placed inside the Booster cryostat.

## EQUIPMENT

Dipole, quadrupole and steering magnets of the channel are room-temperature. Dipoles and quadrupoles are powered in pulsed mode. Pulsed power supplies developed and assembled at JINR provide twice-triple repetitions of pulses to maintain multiple injection and also allow to realize dynamical retuning of the channel. 2D steerers have DC power supplies. Optional DC power supply is also used for the dipoles to obtain high stability of magnetic fields.

The 4-gap debuncher was produced as a part of Bevatech (Germany) project on design and creation of the HILAC. The debuncher is integrated into the HILAC RF system.

The electrostatic septum with length of 1.9 m is a pair of curved anode and cathode with curvature radii of 11.535 m and 11.5 m correspondingly installed inside a vacuum box. High voltage up to 130 kV is applied to the cathode while the anode is grounded. HV power supply maintains capability to vary the voltage in intervals between beam injections during multiple injection in the range to 10 kV.

† tuzikov@jinr.ru

ISBN: 978-3-95450-240-0 ISSN: 2673-5539 doi:10.18429/JACoW-RuPAC2021-WEA02

# ACCELERATION THE BEAMS OF $He^{+}$ AND $Fe^{14+}$ IONS BY HILAC AND ITS INJECTION INTO NICA BOOSTER IN ITS SECOND RUN

V. Akimov, A. Bazanov, A. Butenko, A. Galimov, A. Govorov, B. Golovenskiy, D. Donets, D. Egorov, V. Kobets, A. Kovalenko, K. Levterov, D. Letkin, D. Leushin, D. Lyuosev, A. Martynov, V. Mialkovsky, V. Monchinskiy, D. Ponkin, A. Sidorin, E. Syresin, I. Shirikov, G. Trubnikov, A. Tuzikov, Joint Institute for Nuclear Research, Dubna, Moscow region, Russia
H. Höltermann, U. Ratzinger, A. Schempp, H. Podlech, BEVATECH GmbH, Frankfurt, Germany

*Abstract*

Injector of NICA accelerating facility based on the Heavy Ion Linear Accelerator (HILAC) is aimed to inject the heavy ions having atomic number A≈200 and ratio A/Z ≤ 6.25 produced by ESIS ion source accelerated up to the 3.2 MeV for the injection into superconducting synchrotron (SC) Booster. The project output energy of HILAC was verified on commissioning in 2018 using the beams of carbon ions produced with the Laser Ion Source and having ratio A/Z=6 that is close to the project one. Beams of $He^{1+}$ ions were injected into Booster in its first run and accelerated in 2020. In 2021 ions of $Fe^{14+}$ produced with the LIS were injected and accelerated up to 200 MeV/u. Beam formation of Fe ions and perspectives of using LIS for the production the ions with high atomic mass A and ratio A/Z matching to HILAC input parameters are described.

## HEAVY ION LINEAR INJECTOR

Heavy ion injector of the NICA project is based on the heavy ion linear accelerator (HILAC) and aimed to be injector of gold ions into SC Booster synchrotron of the NICA facility. The main features of it are presented in the Table 1.

Table 1: Main Features of HILAC

| | HILAC |
|---|---|
| Species of ions | $Au^{31+}$ |
| Z/A | ≥ 0.16 |
| Input energy | 17 keV/u |
| Output energy | 3.2 MeV/u |
| Beam current, mA | 10 |
| Operating frequency, MHz | 100.625 |
| Beam transmission rate, % | 98 |

The accelerator is based on 4-rod RFQ [1] and IH DTL cavities with the KONUS accelerating structure inside [2]. Output energy of the HILAC was verified on its commissioning in 2015-2018 [3,4]. The beams of carbon ions $C^{2+}$ having mass-to-charge ratio A/Z=6 that was close to the project value 6.25 were accelerated. Transverse strong focusing featured for KONUS was provided by two doublets and two triplets. RF power supply system is based on the solid state amplifiers: 140 kW for RFQ, two 340 kW amplifiers for IH1 and IH2 and two 4 kW for rebuncher and debuncher.

LLRF system designed and commissioned in collaboration with ITEP [2] provided five continuous sin input signals for RF amplifiers up to 1V amplitude. Output RF power of the amplifier is tuned by the amplitude of the input signals. Phase shifting between LLRF signals is tuned with accuracy 0.1°. Level of RF power inside each cavity was controlled by the pickups signals monitoring.

## HELIUM ION SOURCE

The beams of $He^{+}$ ions produced with the ion source developed in LHEP JINR were used for the first run of SC synchrotron Booster. For designing helium ion source the proton ion sources described in [3,4] were taken as a prototype. Ion source with cold magnetron cathode and magnetic plasma compression produced ~90% of $He^{+}$ ions (see Fig. 1). There are three basic space emay be attributed to plasma generator: space of auxiliary discharge between magnetron cathode and magnetron anode, space of the basic discharge between magnetron cathode and anode, and area of plasma expansion.

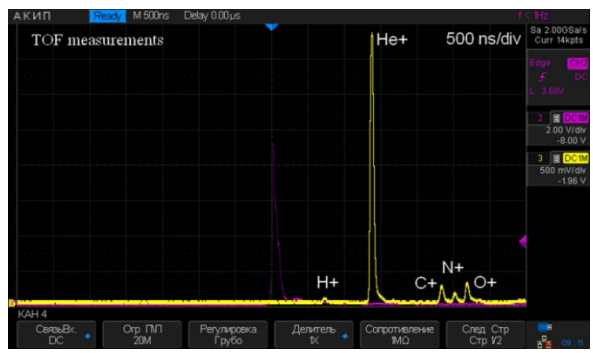


Figure 1: TOF spectrum of the ions at the output of the helium ion source.

## LASER ION SOURCE

Laser ion source, developed as the ion source for Alvarez linac LU-20 at the JINR Laboratory of High energy physics in 1983, is based on a $CO_2$ laser operating in Q-fixed mode. The radiation flux density at the target is estimated as ~$10^{10}$ W/cm² and is enough to produce light ions having mass-to-charge ratio A/Z≤ 3 that is the limit value for the acceleration in LU-20. Range of accelerated ions provided with LIS is various enough: $^{6}Li^{3+}$, $^{7}Li^{3+}$,

ISBN: 978-3-95450-240-0 ISSN: 2673-5539 doi:10.18429/JACoW-RuPAC2021-WEA03

# 200 MeV LINAC DEVELOPMENT FOR THE SKIF LIGHT SOURCE INJECTOR

A. Andrianov, M. Arsentyeva†, A. Barnyakov, D. Chekmenev, A. Levichev, O. Meshkov, D. Nikiforov, O. Pavlov, I. Pivovarov, S. Samoylov, V. Volkov
Budker Institute of Nuclear Physics SB RAS, Novosibirsk, Russia

*Abstract*

A new synchrotron light source SKIF of the 4th generation is construction at Budker institute of nuclear physics (Novosibirsk, Russia). It consists of the main ring, the booster ring and the linear accelerator. This paper presents design of the linear accelerator which is expected to provide electron beams with the energy of 200 MeV. Construction of the linear accelerator is discussed. Description of the linear accelerator main systems is presented.

## INTRODUCTION

The SKIF light source is designed for the top-up injection to the main ring from the booster ring at the electron energy of 3 GeV. The linear accelerator is designed based on the injector technical requirements and BINP experience at the linac development. Electron linac with the energy of 200 MeV is similar to that of the Injection complex VEPP-5 [1]. The booster synchrotron with the maximum energy of 3 GeV is a modification of the synchrotron designed by BINP for NSLS II [2].

In the main operation mode the SKIF storage ring will be supplied by approximately 500 bunches with the total current of 400 mA. There is also a possibility to work in other modes depending on the requirements of the light source users. Table 1 presents required parameters of the electron beam to be obtained at the linear accelerator.

Table 1: Requirements for the Electron Beam Parameters

| Parameter | Value |
|---|---|
| Operating energy | 200 MeV |
| Energy spread (RMS) | 1% |
| Injection rate | 1 Hz |
| Bunch period | 5.6 ns |
| Number of bunches | 55 |
| Single bunch charge | 0.3 nC |
| Horizontal emittance at 200 MeV | 150 nm |

Figure 1 presents layout of the linear accelerator. The injection rate is 1 Hz and the operating frequency of the RF gun is 178.5 MHz while the booster and storage rings operate at 357 MHz. Thus, it is supposed that a single linac beam consisting of 55 electron bunches fills every second separatrix and after the phase shift next bunch train fills other separatrices. After the gun the beam passes through the bunching channel which consists of the third harmonic cavity, the solenoids and the preaccelerator. Three klystrons Canon E3730A with the peak power of 50 MW are used as RF power sources for the preaccelerator and five regular accelerating structures. Linac ends by the diagnostic channel with the magnet spectrometer and the Faraday cup.

## ELECTRON GUN

RF gun which is an electron source for the linac has an operating frequency 178.5 MHz and is planned to be built on the cathode-grid assembly. Using this scheme allows one to perform modulation of the cathode current, providing variation of the bunch charge.

Parameters of the RF gun cavity are shown in Table 2. At the electric field amplitude on the axis of 13 MV/m it is possible to extract electron bunches with the charge up to 1.1 nC (Fig. 2, left) while the average particle energy is about 0.6-0.7 MeV.

Table 2: RF Gun Parameters

| Parameter | Value |
|---|---|
| Operating frequency | 178.5 MHz |
| Electric field amplitude | 13 MV/m |
| Injection rate | 1 Hz |
| Pulse power | 500 kW |
| Quality factor | 10300 |

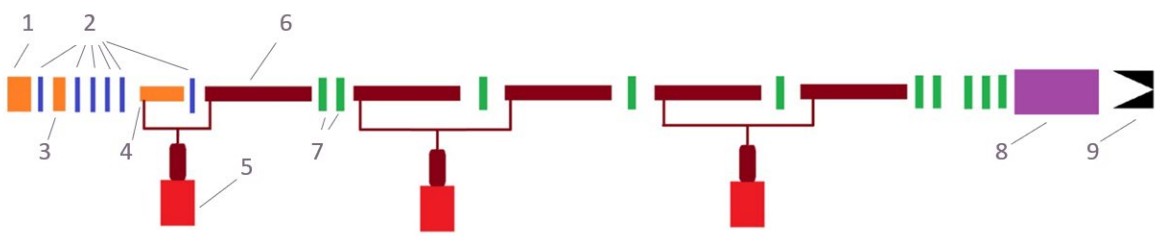


Figure 1: Layout of the linac. 1 – electron gun, 2 – solenoids, 3 – 535 MHz buncher, 4 – preaccelerator, 5 – klystrons, 6 – regular accelerating structures, 7 – quadruple lenses, 8 – spectrometer, 9 – Faraday cup.

† M.V.Arsentyeva@inp.nsk.su

ISBN: 978-3-95450-240-0 ISSN: 2673-5539 doi:10.18429/JACoW-RuPAC2021-WEB02

# MAGNETIC FIELD MEASUREMENTS FOR THE NICA COLLIDER MAGNETS AND FAIR QUADRUPOLE UNITS

A. V. Shemchuk†, V. V. Borisov, I. I. Donguzov, O. M. Golubitsky, H. G. Khodzhibagiyan, B. Kondratiev, S. A. Kostromin, D. I. Khramov, A. V. Kudashkin, T. Parfylo, M. M. Shandov, E. V. Zolotykh, D. A. Zolotykh,
JINR, Dubna, Moscow Region, Russia

*Abstract*

The magnetic system of the NICA collider includes 86 quadrupole and 80 dipole twin-aperture superconducting magnets. The serial production and testing of the dipole magnets was completed in the summer of 2021. The tests of the quadrupole magnets of the collider and the quadrupole units of the FAIR project have successfully entered the phase of serial assembly and testing at the Joint Institute for Nuclear Research (VBLHEP JINR). One of the important testing tasks is to measure the characteristics of the magnetic field of magnets. The article describes the state of magnetic measurements and the main results of magnetic measurements of NICA collider magnets, quadrupole units of the FAIR project, as well as plans for measuring the following types of magnets of the NICA project.

## INTRODUCTION

NICA (Nuclotron-based Ion Collider fAcility) is a new acceleration-storage complex[1]. It is under construction in JINR. In parallel with the NICA project, the FAIR project is being implemented in Darmstadt, Germany, of which the SIS100 accelerator is a part [2]. The SIS100 accelerator includes 166 quadrupole units of various configurations. For quadrupole units, it is necessary to measure these parameters of the magnetic field:

- Integral of the mainl field component (GL).
- Effective length ($L_{eff}$).
- Roll angle ($\alpha$).
- Position of magnetic axis (dz, dy).
- Relative harmonics up to $10^{th}$.

At the moment, 25 units have successfully passed cryogenic tests.

Collider includes 86 quadrupole and 80 dipole twin-aperture superconducting magnets. Manufacturing of 80 main and 6 reserve magnets is finished now. To carry out magnetic measurements, the method of rotating harmonic coils, described in articles [3], [4] was chosen. It is necessary to measure the parameters of the magnetic field such as:

- Field in the center of the dipole ($B_1(0)$).
- Effective length ($L_{eff}$).
- Magnetic field angle ($\alpha$).
- Relative harmonics up to $10^{th}$.

Dipoles were tested at the ambient and operating (4.5 K) temperatures. Maximal operating current at operating temperature is 10.44 kA for NICA collider and 11.5 kA for SIS100 quadrupole units.

## MAGNETIC MEASUREMENTS SYSTEMS (MMS)

Figure 1 shows the progress of magnetic measurements. For serial magnetic measurements, 4 stands are used, 3 for measurements at room temperature, 1 for measurements in cryogenic conditions. The total number of magnetometers is 15 pcs.

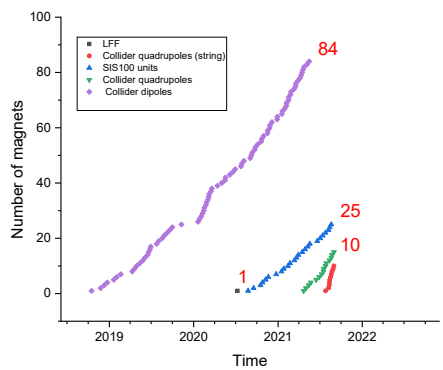


Figure 1: The progress of magnetic measurements.

For measurements of quadrupole magnets of both the NICA and FAIR projects, in addition to the method of rotating harmonic coils, the method of a vibrating string is used.

### *MMS for NICA Collider Dipoles*

During the measurements, 6 serial magnetometers (see Fig. 2) were created to measure the collider dipole magnets. 2 magnetometers are used in the area of warm magnetic measurements, and 4 magnetometers on the cryogenic stand. A detailed description of the measurement system and design of the magnetometer is presented in [5].

The statistics of parameters of magnetic field are presented in the results (see Fig. 7, Fig. 8, Fig. 9).

† shemchuk@jinr.ru

ISBN: 978-3-95450-240-0 ISSN: 2673-5539 doi:10.18429/JACoW-RuPAC2021-WEB03

# FIRST EXPERIENCE OF PRODUCTION AND TESTING THE SUPERCONDUCTING QUADRUPOLE AND CORRECTOR MAGNETS FOR THE SIS100 HEAVY ION ACCELERATOR OF FAIR

E. Fischer, H. Khodzhibagiyan, D. Nikiforov, V. Borisov, T. Parfylo, Y. Bespalov, D. Khramov, B. Kondratiev, M. Petrov, A. Shemchuk, JINR, Dubna, Russia
A. Waldt, A. Bleile, GSI, Darmstadt, Germany

*Abstract*

The fast-cycling superconducting SIS100 heavy ion accelerator is the designated working horse of the international Facility for Antiproton and Ion Research (FAIR) under construction at GSI in Darmstadt, Germany [1].

The main dipoles will ramp with 4 T/s and with a repetition frequency of 1 Hz up to a maximum magnetic field of 1.9 T. The field gradient of the main quadrupole will reach 27.77 T/m. The integral magnetic field length of the horizontal/vertical steerer and of the chromaticity sextupole corrector magnets will provide 0.403/0.41 m and 0.383 m, respectively. The series production of the high current quadrupoles and of the individually ramped low current corrector magnets was started in 2020 at the JINR in Dubna and is planned to be completed in 2023. We present the technological challenges that must be solved from production of the first magnets toward a stable and high-rate series production with reliably magnet quality as well as the first test results at operation conditions.

## INTRODUCTION

The international scientific center FAIR will provide high intensity beams of ions and antiprotons for experiments in nuclear, atomic and plasma physics 0. The operation modes of the FAIR facility will facilitate four experiments simultaneously. Beside the reference Uranium and proton beams, acceleration of all other ion species is foreseen. The SIS100 synchrotron has a magnetic rigidity of 100 T·m. The high repetition rate of its acceleration cycles up to 1 Hz requires fast-ramped superconducting magnets with high dynamic heat load which must be cooled steadily. The SIS100 dipole and quadrupole magnets as well as the magnets for the NICA project [2] were designed based on the fast-cycling super-ferric magnets for the Nuclotron synchrotron at JINR in Dubna [3-8]. The production and test facility [2] of SC magnets for the NICA and FAIR project at the Laboratory of High Energy Physics of JINR was commissioned by end of 2016. For production and testing of the superconducting magnets a detailed quality assurance system was introduced, various sets of geometrical and magnetic measurement equipment were developed, methodically optimized 0, 0 and the high-resolution data analysis processing was adjusted.

## THE CRYOMAGNETIC COMPONENTS

The synchrotron ring has a circumference of 1.1 km consists of six sections with cryomagnetic components, bypass lines and electrical supply systems, shown in Fig. 1. In each sector there are 9 quadrupole doubled modules (QDM) of the arc-section type, two QDM of the arc-termination type, 18 dipole modules (DPM) and 2 missing DPM. The basic ion optic cell is 12.9 m long and built of the dipole – dipole – defocusing quadrupole – focusing quadrupole structure (DP – DP – QD – QF). Besides the 108 main dipoles there are three families of quadrupoles, powered in their own electrical circuits – F1, F2, QD.

The operation modes of the accelerator are planned to vary in a wide parameter range of magnetic field amplitude, ramp rate and repetition frequency 0.

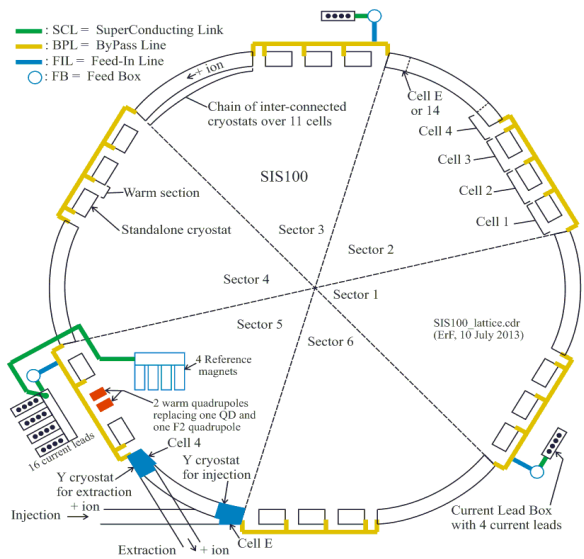


Figure 1: Scheme of the six sections of the synchrotron ring with Bypass Lines, the cryogenic and electrical supply systems.

The cryomagnetic modules have 11 different types of QDM, always containing two quadrupole units (QPU). Two QPU are mounted on a common girder system and combined with additional components of the vacuum system or a collimator. A QPU is a combination of a quadrupole magnet with different corrector magnets or also with a beam position monitor, mounted on the quadrupole as one cold mass. The detailed schema of the modules and units is given in Table 1. In this paper we present the results for the magnet parts of units VQD, SF2B and SF1B. The assembly with beam position monitors as well as their integration into a complete doublet configuration (here 2.5 or 1.7B) is not part of the working contract between JINR and the GSI/FAIR company and remains in the responsibility of the latter.

ISBN: 978-3-95450-240-0 ISSN: 2673-5539 doi:10.18429/JACoW-RuPAC2021-WED04

# PRECISE ANALYSIS OF BEAM OPTICS AT THE VEPP-4M BY TURN-BY-TURN BETATRON PHASE ADVANCE MEASUREMENT

I.A. Morozov*, P.A. Piminov, I.S. Yakimov, BINP SB RAS, Novosibirsk, Russia

*Abstract*

Turn-by-turn (TbT) beam centroid signals can be used to evaluate various relevant accelerator parameters including betatron frequencies and optical functions. Accurate estimation of parameters and corresponding variances are important to drive accelerator lattice correction. Signals acquired from beam position monitors (BPMs) are limited by beam decoherence and BPM resolution. Therefore, it is important to obtain accurate estimations from available data. Several methods based on harmonic analysis of TbT data are compared and applied to the VEPP-4M experimental signals. The accuracy of betatron frequency, amplitude, and phase measurements are investigated. Optical functions obtained from amplitudes and phases are compared.

## INTRODUCTION

The VEPP-4M is an electron-positron collider operating in 1 GeV to 6 GeV beam energy range [1]. The VEPP-4M storage ring is equipped with 54 dual-plane BPMs [2] capable of performing accurate TbT measurements. TbT data is acquired by excitation of the circulating beam with impulse kickers. In Fig. 1 the optical functions of the VEPP-4M ring are shown along with corresponding BPM positions.

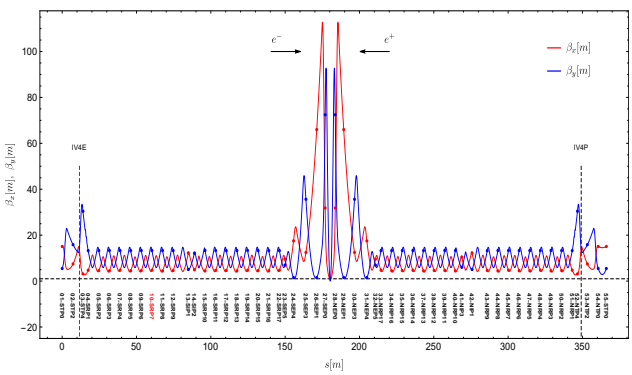


Figure 1: The VEPP-4M lattice functions.

Harmonic analysis [3] can be used to obtain frequency and optics from TbT data. Previously, optics measurements were based only on the computation of $\beta$ functions from amplitudes. In this paper, the extension of the optics measurement procedure is described. It includes the addition of TbT data processing, anomaly detection and BPM noise estimation. The frequency measurement algorithm has been tuned. Statistical error propagation has been added to the computation of BPM signal parameters. Optics measurement from phase has been performed for the first time at the VEPP-4M. This provides an additional tool to check optics measurement from amplitude and to study BPM calibrations. Both methods with statistical error propagation will allow more accurate lattice correction. Experimental results of optics measurement are reported.

* I.A.Morozov@inp.nsk.su

## VEPP-4M TBT PROCESSING LOOP

In Fig. 2 TbT analysis workflow at the VEPP-4M is shown. First, detection of anomalies in TbT signals is performed [4], and anomalies are flagged. After anomaly detection, TbT filtering is performed. Noise estimation using optimal SVD truncation [5] is performed for each BPM signal. The frequency for each BPM is computed from its interpolated spectrum maximum. For known frequencies, amplitudes and phases are computed for each BPM with statistical error propagation. Amplitudes and phases are then used to compute linear optics.

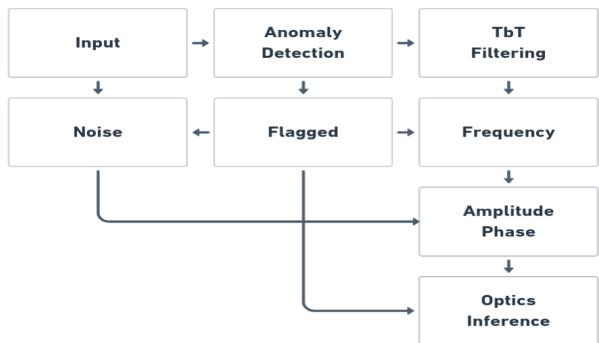


Figure 2: The VEPP-4M TbT processing loop.

We have tested several different techniques for TbT data noise cleaning. One of the common options is to used truncated SVD applied to the full TbT matrix. For the VEPP-4M case, the optimal rank of truncated representation was found to be eight. Another option is to apply Robust PCA [6] to the full TbT matrix. This method was found to introduce a bias for estimated amplitudes and phases, but no bias was observed in frequencies. Both SVD and Robust PCA can be applied to individual BPM signals. In this case each signal $x = [x_1\ x_2\ x_3\ x_4\ x_5\ x_6]$ is represented using Hankel matrix:

$$X = \begin{bmatrix} x_1 & x_2 & x_3 \\ x_2 & x_3 & x_4 \\ x_3 & x_4 & x_5 \\ x_4 & x_5 & x_6 \end{bmatrix}$$

Truncated SVD or Robust PCA can be applied to this signal representation. The filtered signal is then reconstructed as the mean of skew diagonals.

ISBN: 978-3-95450-240-0 ISSN: 2673-5539 doi:10.18429/JACoW-RuPAC2021-WED05

# NONDESTRUCTIVE DIAGNOSTICS OF ACCELERATED ION BEAMS WITH MCP-BASED DETECTORS AT THE ACCELERATOR COMPLEX NICA. EXPERIMENTAL RESULTS AND PROSPECTS

A. A. Baldin†, V. I. Astakhov, A. V. Beloborodov, D. N. Bogoslovsky, A. N. Fedorov, P. R. Kharyuzov, A. P. Kharyuzova, D. S. Korovkin, A. B. Safonov, Joint Institute for Nuclear Research, Dubna, Russia

*Abstract*

Non-destructive ion beam detectors based on microchannel plates are presented. The design of two-coordinate profilometer situated in the high vacuum volume of the Booster ring is discussed. Experimental data on registration of circulating beam of the Booster in the second run (September 2021) are presented. The possibility of adjustment of the electron cooling system with the help of this detector based on the obtained experimental data is discussed.

## INTRODUCTION

Obviously, development of nondestructive diagnostic systems for both circulating and extracted beams is one of the most important tasks at the acceleration complex NICA [1]. One can speak of nondestructive systems of two types: the first one registers electromagnetic radiation, and the second one registers interaction of beam ions with molecules of residual gas in the vacuum chamber of the accelerator.

This paper considers some first results of operation of the nondestructive diagnostic system implemented at the Booster put in operation at the end of 2020. This diagnostic system provides registration of the space-time beam structure directly inside the Booster vacuum chamber at the input point from HILAC.

A similar system is situated in the Nuclotron ring and at the extracted beam line of Nuclotron (see Fig. 1) [2, 3, 4, 5].

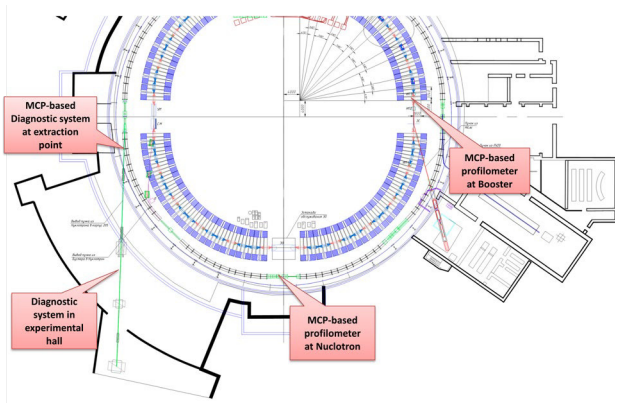


Figure 1: Schematic diagram of diagnostic system locations at the Booster and Nuclotron.

* This work was supported in part by the Russian Foundation for Basic Research, project no.18-02-40097.
† an.baldin@mail.ru

## NUMERICAL STUDY OF MCP-BASED DETECTOR

The drawing of the MCP-based profilometers mounted inside the chamber is shown in Fig. 2.

This detector geometry implemented in the Booster chamber was used in the software CST for simulation of the detector operation.

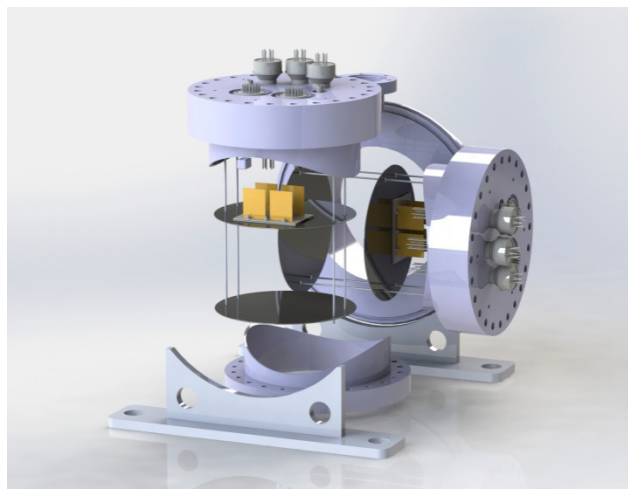

Figure 2: Assembly drawing of MCP-based profilometers mounted on vacuum flanges.

CST is designated for simulation of a wide range of electromagnetic interactions, including construction of electrostatic models and charged particle tracking in simulated fields. The study presented here used the solvers "E-Static" and "Particle Tracking" of the module "Statics and low frequency" CST. The real geometry of the existing detectors was input in the simulation.

The physics of the simulated processes is as follows. accelerated charged particles, passing the ion beam line, ionize residual gas. The number of ions produced in unit volume is proportional to the beam intensity, residual gas pressure, and squared ion charge. These ions are accelerated by electrostatic field toward the chevron assembly of the MCP detector and are registered by the detector to give the space-time parameters of the beam.

In the simulation, ionized particles were distributed uniformly over the whole detector volume and their trajectories were traced in the electrostatic system of the detector. It was found out that the electrostatic systems of the X and Y profilometers distort the electrostatic field and, as a consequence, ion trajectories inside the vacuum

ISBN: 978-3-95450-240-0 ISSN: 2673-5539 doi:10.18429/JACoW-RuPAC2021-THA01

# STATUS OF THE SC HWR CAVITIES PRODUCTION FOR NICA PROJECT

A. Butenko, E. Syresin, G. Trubnikov, D. Nikiforov, JINR, Dubna, Russia
M. Gusarova[1], M. Lalayan[1], S. Matsievskiy[1], R. Nemchenko, S. Polozov,
N. Sobenin, V. Shatokhin[1], NRNU MEPhI, Moscow, Russia
D. Bychanok[2], A. Sukhotski, S. Huseu, S. Maksimenko, INP BSU, Minsk, Belarus
A. Shvedov, S. Yurevich, V. Petrakovsky, A. Pokrovsky, I. Pobol, V. Zaleski, PTI NASB, Minsk, Belarus
[1]also at JINR, Dubna, Russia [2]also at TSU, Tomsk, Russia

*Abstract*

Since 2015 the superconducting (SC) linac-injector development for Nuclotron NICA (JINR, Dubna, Russia) is carried out by the collaboration of JINR, NRNU MEPhI, INP BSU, PTI NASB. This new SC linac is to accelerate protons up to 20 MeV and light ions to 7.5 MeV/u with possible energy upgrade up to 50 MeV for proton beam. This paper reports the current status of the development and manufacturing of superconducting accelerating cavities for a new linear accelerator of the injection complex of the Nuclotron-NICA project.

## INTRODUCTION

Nuclotron-based Ion Collider fAcility (NICA) is new accelerator complex under construction at JINR [1-5]. It was proposed for ion collision and high-density matter study. NICA facility will include the existing ion synchrotron Nuclotron together with new booster and two collider rings being under construction. The injection system of Nuclotron-NICA was upgraded in 2011-2016. The pulse DC linac forinjector of Alvarez-type DTL LU-20 was replaced by the new RFQ developed and commissioned by JINR, ITEP and MEPhI [6]. New RFQ linac can accelerate ions with charge-to-mass ratio Z/A>0.3. The first technical session of Nuclotron with new injector was ended on 2016 [7]. The LU-20 with new RFQ for-injector is used for p, p↑, d, d↑, He, C and Li ions acceleration till now. The other heavy ion linac for particles with Z/A=1/8-1/6 was developed by joint team of JINR, Frankfurt University and BEVATECH and commissioned in 2016.

It must be noted that LU-20 operation causes many technical issues because of its age: it was commissioned in 1972. The possibility of LU-20 replacement by the new linac of 20 MeV energy for protons [8-12] and 7.5 MeV/nucleon for deuterium beam is discussed now. Project also include an option of the proton beam energy upgrade up to 50 MeV by installing several cavities in additional section. New linac will include a number of superconducting (SC) cavities.

The general layout of new light ion linac (LILac) for the NICA collider is presented in Fig. 1 [13]. LILac consists of 5 cavities: RFQ, re-buncher, two Interdigital H-mode Drift-Tube-Linacs (IH-1 and IH-2) and a de- buncher [14]. The operating frequency is 162.5 MHz and the final energy at the IH-2 exit is 7 MeV/u. After IH-2 the beam is transported towards the Nuclotron (bending magnets shown in blue). SPI stands for Source of Polarized Ions [15]. In future the extension of LILac is expected with normal-conductive cavities up to 13 MeV/u (marked green) and followed by SC HWR 1 cavities (light blue at Fig. 1) up to 20 MeV for protons and to 7.5 MeV/u light ions and by SC HWR 2 cavities up to 50 MeV for protons [16].

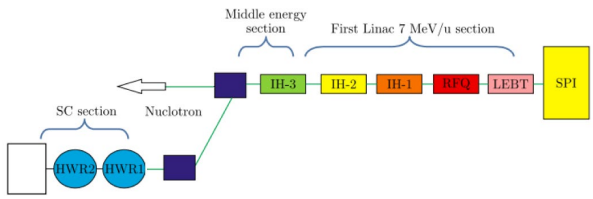


Figure 1: The Light Ion Linac.

The problem with SC cavities and SC linac construction for Nuclotron-NICA was the absence of SRF technology in Russia. The development of the SRF technologies is the key task of the new Russian - Belarusian collaboration launched in March 2015. For testing purposes, the test beamline is proposed with two HWR1 cavities installed. A test cryostat for two cavities HWR 1 is developing now by a joint team of JINR, GSI (Germany) and BEVATECH (Germany). Cryostat for 4 cavities HWR 1 is developing by JINR and IMP (China).

## BEAM DYNAMICS AND FR DESIGN

The beam dynamics simulation for superconducting part of the first linac layout was done using BEAMDULAC-SCL code designed at MEPhI [17-19]. According to the fourth version of SC linac design developed the accelerator is divided into two groups of cavities HWR 1 and HWR 2 with geometric velocities $\beta_G$ = 0.21 and 0.314. First group HWR 1 at $\beta_G$ = 0.21 accelerates protons to 20 MeV and light ions to 7.5 MeV/u. Second group HWR 2 at $\beta_G$ = 0.314 accelerates particles up to 50 MeV.

The beam dynamics of proton and deuterium ions beam was studied at [9]. Parameters of the first group of cavities (HWR 1) are shown in Table 1.

Considerations on the SC cavity types choice and their RF design done at MEPhI and JINR are presented in detail in [20]. HWR cavities were proposed because they could provide proper consent to electrodynamic parameters and beam dynamics [16, 20].

The operating frequency of SC sections is 325 MHz. Different concurring HWR cavity designs were considered one with ordinary cylinder-shaped central conductor and the second with cone-shaped one [21]. Geometric and electrodynamics parameters of the cavities are presented in Table 2.

ISBN: 978-3-95450-240-0 ISSN: 2673-5539 doi:10.18429/JACoW-RuPAC2021-THC03

# NUMERICAL SIMULATIONS OF SPACE CHARGE DOMINATED BEAM DYNAMICS IN EXPERIMENTALLY OPTIMIZED PITZ RF PHOTOGUN *

S.M. Polozov, V.I. Rashchikov†, NRNU(MEPhI) - NRC «Kurchatov Institute», Moscow, Russia

*Abstract*

Discrepancies between experimental data and computer simulation results of picosecond highly charged beam photoemission are discussed. New space charge limited emission numerical model with positively charged ions arising in the cathode region and dynamically changing during the emission is presented. Estimates on the time characteristics of the charge migrating process in the semiconductor region are given. The numerical results are compared with the results of other numerical models and with experimental observations at the Photo Injector Test facility at DESY in Zeuthen (PITZ).

## INTRODUCTION

High brightness electron sources are key components necessary for the successful operation of modern free electron lasers, new sources of synchrotron radiation and lepton colliders. For such facilities, it is required to have a rather high bunch charge (~nC), a very small transverse normalized emittance (< 1 mm×mrad), rather short bunches (~ 1÷20 ps), and a small energy spread (<1 %). For example, for the European X-ray Free Electron Laser (European XFEL) photo gun, electron bunches with a charge of 1 nC/bunch and a normalized transverse emittance < 0.9 mm×mrad should be generated by an RF gun operating with a $Cs_2Te$ photocathode at a high electric field on the cathode surface (~ 60 MV/m) and repetition rate up to 27,000 pulses per second. Detailed studies of the photoemission process are crucial for understanding the beam dynamics in space charge dominated photo injectors, without which it is difficult to achieve the high brightness.

## TEST FACILITY AND SIMULATION MODEL

The Photo Injector Test facility at DESY in Zeuthen (PITZ) develops and optimizes high brightness photo injectors for more than 20 years [1].

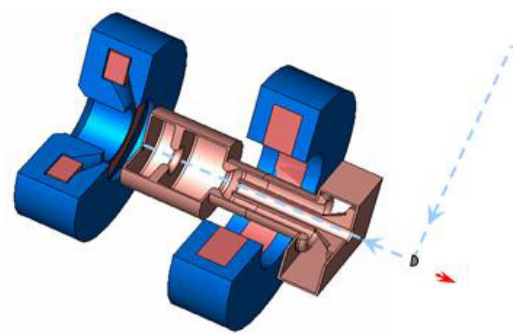

Figure 1: PITZ RF gun scheme.

The PITZ L-band 1.6-cell RF-gun (Fig. 1) consists of a 1.3 GHz copper cavity operated in π-mode fed by a coaxial RF power coupler and supplied with a pair of focusing solenoids. A molybdenum cathode plug with $Cs_2Te$ film is inserted in the cavity back wall using a load-lock vacuum system.

For precise description of the space charge dominated dynamics in the RF-photogun beam measurements and computer simulations have been performed. Discrepancies between experimental data and simulation results have been observed for these measurements [2-3]. The results of experimental studies on the bunch charge production and transverse emittance optimization revealed that the limiting current of the emitted beam obtained experimentally cannot be reproduced by ASTRA simulations [4] using the parameters of the experimental setup. The ASTRA code, used for these simulations, is one of the few in the world optimized to solve beam dynamics problems associated with photoemission and photoguns. In order to bring beam dynamics simulations closer to the experimental results the photoemission model for a space charge dominated regime has to be improved. A typical schematic of a semiconductor photocathode is illustrated by Fig. 2.

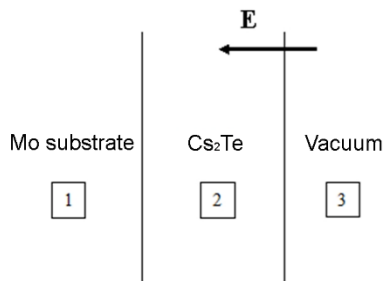


Figure 2: Photocathode model.

It consists of three regions: 1- molybdenum substrate, 2 - $Cs_2Te$ film (< 0.1μm), 3- vacuum. Since the photocathode is located in a strong electric field, the penetration of the field into the semiconductor film should be taken into account. With a field strength of $E \sim 10^7$ V/m on the cathode surface, it is necessary to create the following surface charge density $\sigma$ to compensate this field inside the film:

$$E = \frac{\sigma}{2\varepsilon\varepsilon_0} = \frac{qN}{2\varepsilon\varepsilon_0},$$

where $N$ is the surface charge density, $\varepsilon$ and $\varepsilon_0$ is the dielectric permittivity of the photocathode film and vacuum respectively, q is a particle charge. Hence, assuming ε ~10, we obtain the surface charge density at the cathode $N \sim 10^{11}$ cm$^{-2}$. If the average concentration of carriers in a semiconductor is $n \sim 10^{15}$ cm$^{-3}$ then the required number of charges is obtained at a thickness of $d = \frac{N}{n} \sim 1$μm. That is, the field penetrates to a depth that is significantly greater

* The reported study was partly funded by RFBR, project 19-29-12036
† VIRashchikov@mephi.ru

ISBN: 978-3-95450-240-0 ISSN: 2673-5539 doi:10.18429/JACoW-RuPAC2021-FRA01

# PECULIARITIES OF PRODUCING $^{48}$CA, $^{48}$TI, $^{52}$CR BEAMS AT THE DC-280 CYCLOTRON

K.B. Gikal†, S. L. Bogomolov, I. A. Ivanenko, N. Yu. Kazarinov, V. I. Lisov, A. A. Protasov, D.K. Pugachev, V.A. Semin, Joint Institute for Nuclear Research, Dubna, Russia

*Abstract*

The main task of the new accelerator is implementation of the long-term program of researches on the SHE Factory aimed on synthesis of new elements (Z≥119) and detailed studying of nuclear- physical and chemical properties of earlier opened 112-118 ones. The first beam of $^{84}Kr^{14+}$ ions was accelerated in the DC-280 on December 26, 2018 and extracted to the ion transport channel on January 17, 2019. In March 2019, beams of accelerated $^{84}Kr^{+14}$ ions with intensity of 1.36 pμA and $^{12}C^{+2}$ ions with and intensity of 10 pμA were extracted from the DC-280 to the beam transport channel with energy about 5.8 MeV/nucleon. In 2020-2021 years, beams of $^{48}Ca^{7+,10+}$ ions with intensity up to 10,6 pμA were accelerated and 7,1 pμA were extracted from the DC-280 to the beam transport channel with energy in range 4,51 - 5,29 MeV/nucleon. In 2021 year, beams of accelerated $^{52}Cr^{10+}$ ions with intensity up to 2,6 pμA were extracted from the DC-280 to the beam transport channel with energy 5,05 MeV/nucleon and beams of $^{48}Ti^{7+,10+}$ with intensity up to 1 pμA with energy 4,94 MeV/nucleon.

## DC-280 DESCRIPTION

DC-280 is the accelerated ions source for experiments on synthesis of super heavy elements [1]. It is part of Super Heavy Element (SHE) Factory which was created in FLNR in JINR. It is isochronous cyclotron designed for acceleration of ion with mass to charge ratio from 4.5 to 8 to energy from 4 to 8 MeV/n. Main parameters design and achieved present in Table 1.

Table 1: Main Parametrs of DC-280 Cyclotron

| parameters | design | achieved |
|---|---|---|
| Injecting beam energy | Up to 80 keV/Z | 38,04 – 72,89 keV/Z |
| A/Z | 4÷7.5 | 4,4($^{40}Ar^{+7}$) ÷6,9($^{48}Ca^{+7}$) |
| Energy | 4÷8 MeV/n | 4,01 – 7 MeV/n |
| Ion (for DECRIS-PM) | 4-136 | 12 ($^{12}C^{+2}$) – 84 ($^{84}Kr^{+14}$) |
| Intensity (A~50) | >10 pμA | 10,4 pμA ($^{40}Ar^{+7}$); |
| Magnetic field level | 0.6÷1.3 T | 0.8÷1.23 T |
| K factor | | 280 |
| Dee voltage | 2x130 kV | 130 kV |
| Power of RF generator | 2x30 kW | |
| Accelerator efficiency | >50% | 51,9 % ($^{48}Ca^{+10}$ 5 pμA) |

Electron Cyclotron Resonance (ECR) source DECRIS-PM is used for production of ions [2, 3]. It has magnetic structure from permanent magnets. It placed on high voltage platform with work voltage up 70 kV for increasing efficiency of initial beam transport and capture to acceleration [4].

In the DC-280 cyclotron, a spiral inflector is used to rotate the beam from the vertical direction of axial injection into the median plane. Both the cyclotron magnetic field and own electrostatic field of inflector rote the ion beam by spiral. To ensure optimal injection conditions for all range of accelerated ions, two versions of the inflector type A and type B with two magnetic radii of 7.5 and 9.2 cm are used.

Inflectors with magnetic radii of 7.5 cm and 9.2 cm for the range of accelerated ions with A / Z from 4 to 7 is shown in Fig. 1.

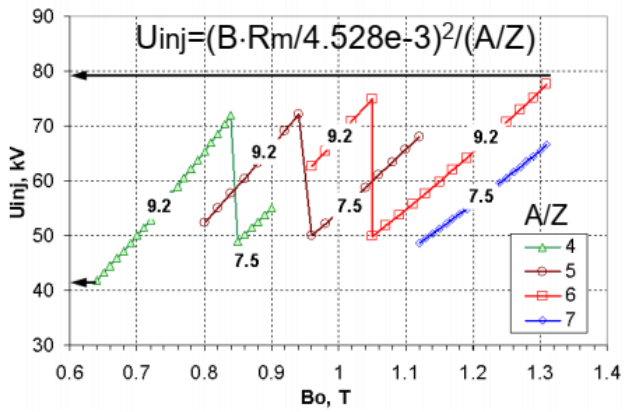


Figure 1: Dependence of the magnetic field on the injection voltage for the inflector A and B.

During experiments both of them were successful tested. There is electrostatic quadrupole lens in central part of cyclotron. Polyharmonic buncher is used for increasing of ions capture to acceleration [4].

Accelerated beam is extracted from cyclotron by electrostatic deflector. It works in conjunction with magnetic channel. Deflector length is 1.3 meters. The work electric field strength in gap between electrodes is up 90 kV/cm [1].

Extracted beam is delivered by transport channel to experimental setups [5]. There are 5 channels connected with 3 isolated halls.

On 26 December 2018, the first accelerated beam was got inside of DC-280 cyclotron [1, 6]. On January 2019, accelerated beam was extracted from cyclotron to transport channel. On September, the new experimental facility Dubna Gas Filled Separator 2 was mounted, and test with accelerator beam was started [7]. On December of 2019, work with beam of $^{48}$Ca was initiated. On November 2020, the first experiment on production of $^{115}$Mc was started.

† kbgikal@jinr.ru

ISBN: 978-3-95450-240-0 ISSN: 2673-5539 doi:10.18429/JACoW-RuPAC2021-FRA02

# CYCLOTRON OF MULTICHARGED IONS

Yu.K. Osina†, A.A. Akimova, Yu.N. Gavrish, A.V. Galchuck, S.V. Grigorenko, V.I. Grigoriev, M.L. Klopenkov, R.M. Klopenkov, L.E Korolev., K.A. Kravchuck, A.N. Kuzhlev, I.I. Mezhov, V.G. Mudrolyubov, K.E Smirnov., Yu.I. Stogov, S.S. Tsygankov, M.V. Usanova,
JSC «NIIEFA», 196641, St. Petersburg, Russia

*Abstract*

The JSC "NIIEFA" is designing a cyclotron system intended to accelerate ions with a mass-to-charge ratio of 3-7 in the energy range of 7.5-15 MeV per nucleon. The variety of ions, the range of changes in their energy, and the intensity of the beams provide conditions for a wide range of basic and applied research, including for solving a number of technological tasks.

The cyclotron electromagnet has an H-shaped design with a pole diameter of 4 meters and a four-sector magnetic structure. In the basic mode, the dependence of the induction on the radius corresponding to the isochronous motion is realized by turning on the main coil only through the shape of the central plugs, sector side plates, and sector chamfers. For other modes of isochronous acceleration, the current in the main coil is changed and correction coils are tuned. The resonance system consists of two resonators with an operating frequency adjustable from 13 to 20 MHz. The final stage of the RF generator is installed close to the resonator and is connected to it by a conductive power input device.

The external injection system generates and separates ions with a given A/z ratio. The injection energy is chosen such that the Larmor radius is constant, which allows using an inflector of unchanged geometry for the entire list of ions.

The transportation system forms beams of accelerated ions with specified parameters and delivers them to sample irradiation devices. Computer control of the cyclotron is provided.

## MAIN TECHNICAL FEATURES

A distinctive feature of heavy ions' interaction with a substance is high specific energy loss and, as a consequence, more localized dependence of the penetration depth on energy compared to light ions.

This property of heavy ions allows a broad range of applications from fundamental research in nuclear physics and sold- state physics to applied technological tasks, namely, deep layer-to-layer implantation, simulation of radiation damages of different materials, etc.

A cyclotron system producing multicharged ions is under designing in the JSC "NIIEFA". The system includes a cyclotron with an external injection system, a system to form and transport beams of accelerated ions, a sample irradiation system and utilities.

This cyclotron system is intended to generate and accelerate ions with a mass-to-charge ratio (A/z) of 3 - 7 in the energy range of 7.5-15 MeV per nucleon as well as to use this set of ions in practical applications.

Table 1 presents the calculation results of boundary accelerating modes of C, O, Ne, Si, Ar, Fe, Kr, Ag, Xe and Bi ions. For light ions, higher energies are possible.

Table 1: Boundary Modes Of Ions' Acceleration

| Element | Charge | Induction in the center of the magnet, T | Energy, MeV per nucleon |
|---|---|---|---|
| $Bi_{209}$ | 35 | 1.29 | 7.28 |
| | 43 | 1.6 | 16.94 |
| $Xe_{136}$ | 23 | 1.29 | 7.43 |
| | 28 | 1.56 | 16.12 |
| $Ag_{107}$ | 18 | 1.29 | 7.35 |
| | 21 | 1.6 | 15.41 |
| $Kr_{84}$ | 14 | 1.29 | 7.21 |
| | 18 | 1.5 | 16.5 |
| $Fe_{56}$ | 9 | 1.41 | 7.53 |
| | 11 | 1.6 | 15.44 |
| $Ar_{40}$ | 6 | 1.46 | 7.5 |
| | 10 | 1.29 | 16.2 |
| $Si_{28}$ | 4 | 1.5 | 7.18 |
| | 6 | 1.49 | 15.93 |
| | 9 | 1.42 | 32.1 |
| $Ne_{20}$ | 3 | 1.43 | 7.19 |
| | 4 | 1.56 | 15.22 |
| | 6 | 1.43 | 27.9 |
| $O_{18}$ | 3 | 1.33 | 7.11 |
| | 4 | 1.46 | 15.44 |
| $O_{16}$ | 3 | 1.29 | 9 |
| | 3 | 1.6 | 13 |
| | 5 | 1.42 | 32.1 |
| $C_{12}$ | 2 | 1.29 | 7.21 |
| | 3 | 1.29 | 16.23 |
| | 4 | 1.42 | 34.4 |

The variety of ions, range of their energy and intensity variation allow us to adjust a so-called coefficient of the linear energy transfer over a broad range, which is especially important for applied researches.

## ELECTROMAGNET

The iron core of the electromagnet is of an H-shaped design and of a four-sector magnetic structure. The pole diameter equals 4m. The magnet is equipped with the main coils and a set of additional radial and azimuthal coils.The induction in the center of the magnet varies in the limits of 1.29-1.6T for different types of ions. The mode with the

† npkluts@luts.niiefa.spb.su

ISBN: 978-3-95450-240-0 ISSN: 2673-5539 doi:10.18429/JACoW-RuPAC2021-FRA03

# SIMULATION AND DESIGN OF THE PERMANENT MAGNET MULTIPOLE FOR DC140 CYCLOTRON

V. Kukhtin†, A. Firsov, M. Kaparkova, E. Lamzin, M. Larionov, A. Makarov,
A. Nezhentzev, I. Rodin, N. Shatil, JSC "NIIEFA", St. Petersburg, Russia,
G. Gulbekyan, I. Ivanenko, N. Kazarinov, I. Kalagin, N. Osipov, JINR, Dubna, Russia,
N. Edamenko, D. Ovsyannikov, S. Sytchevsky, St.Petersburg State University, Russia

*Abstract*

Permanent magnet (PM) multipoles are very attractive for beam transportation and focusing in accelerators. The primary advantages over electromagnets are no power supply and no cooling systems, better maintainability.

A PM quadrupole is supposed to be utilized in the DC140 cyclotron destined for acceleration of heavy ions which is under construction in JINR, Dubna. The extracted ion beam passes through a region where the stray field reduces sharply. Horizontal focusing of the beam line will be provided with a passive magnetic channel (MC1) and a PM quad (PMQ) in the strong and low field regions, respectively.

## REQUIRED PMQ PARAMETERS

Table 1 lists design parameters of the quad.

Table 1: PMQ Design Parameters

| | |
|---|---|
| Field gradient ($G_0$) | 8.1 T/m |
| Working region (hor. × vert.) | 64 mm × 25 mm |
| Aperture (hor. × vert.) | 80 mm × 32 mm |
| Overall sizes (hor. × vert.) | 170 mm × 106 mm |
| Effective lenght* ($L_{eff0}$) | 299.26 mm |
| Error in working region** ($\Delta_{x,y}$) | ±1% |

*The effective length of the quad is calculated as:

$$L_{eff\,0} = \frac{1}{G_0}\int_{-L/2}^{L/2} \frac{\partial B_y(0,0,z(s))}{\partial x} dz(s)$$

**A linear approximation error in the horizontal and vertical directions is evaluated as:

$$L_{eff\,0}\Delta_x = \frac{1}{G_0 x}\int_{-L/2}^{L/2}\left[B_y(x,y,z) - \frac{\partial B_y(0,0,z)}{\partial x}x\right]dz = L_{effx} - L_{eff\,0}$$

$$L_{eff\,0}\Delta_y = \frac{1}{G_0 y}\int_{-L/2}^{L/2}\left[B_x(x,y,z) - \frac{\partial B_x(0,0,z)}{\partial y}y\right]dz = L_{effy} - L_{eff\,0}$$

Also, additional criteria should be considered together with the above magnetic specification, see Table 2.

Table 2: PMQ Operating Conditions

| | |
|---|---|
| External field | 0.35 T |
| Vacuum | $10^{-7}$ Torr |
| Operating temperature | 30-40 °C |
| Temperature range | 20-70 °C |
| Life time | 10-15 years |

† kukhtin-sci@yandex.ru

The DC140 quad will be located near the dees and designed as a set of identical PMs rigidly fixed in a non-magnetic housing encircling the aperture.

Additional aspects of the quad specification include:

- simple PM shape, preferably cuboidal bricks,
- minimized number of PM in assembly,
- minimized nomenclature,
- commercial availability of PM

## STAGES OF PMQ DESIGN

The initial quad design is selected from an analytical study with the use of a simplified 2D model [1]. At this stage the number and positions of PMs are determined. Then the chosen configuration is optimized in iterative 2D and 3D parametric simulations with realistic PM shape and magnetic characteristics in mind. Simulated data are used to select candidate magnet materials, number, dimensions, and tolerated mechanical and magnetic errors of PM blocks. As a result, the quad design is finalized, and an assembly procedure is proposed. Additional adjustment may be required on the basis of measurements of supplied PM. The assembled quad is magnetically inspected to make sure the desired field requirements are reached.

## SIMPLIFIED 2D MODEL OF PMQ

An initial configuration has been generated with the use of 2D analytical models [1] based on the mathematically strict reasoning:

- In the absence of degaussing (the magnetization **M** = const), a field integral of PM with a finite length $L_{PM}$ is equal to a two-dimensional field $\mathbf{B}_{2D}$ generated by an infinite PM multiplied by $L_{PM}$:
$$\int_{-\infty}^{+\infty} \boldsymbol{B}_{3D}(x,y,z)\,dz = \boldsymbol{B}_{2D}(x,y)\cdot L_{PM}$$
So, the 2D approximation is quite suitable to determine the initial PM quad configuration which then will be corrected with respect to the demagnetization.
- With distance, the field generated by an infinite PM of an arbitrary shape is approaching the field of an infinite PM cylinder with the same dipole magnetic moment. Thus, the cylindrical representation is applicable for the initial study of magnetic performance. At the next stage, modifications are introduced reasoning from practical implementation.

ISBN: 978-3-95450-240-0 ISSN: 2673-5539 doi:10.18429/JACoW-RuPAC2021-FRA04

# THE EXPERIMENTAL RESEARCH OF CYCLOTRON DC-280 BEAM PARAMETER

V.A. Semin†, S.L. Bogomolov, K. Gikal, G.G. Gulbekyan, I.A. Ivanenko, I.V. Kalagin, N.Yu. Kazarinov, V.I. Mironov, L. Pavlov, A.A. Protasov, K.B. Gikal,
Joint Institute for Nuclear Research, Dubna, Russia

*Abstract*

The DC-280 is the high intensity cyclotron for Super Heavy Elements Factory in FLNR JINR. It was successful commissioned in 2018 [1] and the design parameters were obtained [2,3]. It was designed for production of accelerated ions beam with intensity up 10 pμA to energy in range 4 - 8 MeV/n. The beam power is up 3,5 kW. The diagnostics elements shall be capable of withstanding this power. Moreover such intensity beam required continuous control for avoid of equipment damage. Special diagnostic equipment were designed, manufactured and commissioning. During the design the calculation of thermal loads was made. Some of them were tested before installation on cyclotron. Diagnostic elements used on DC-280 cyclotron are described in this paper.

The special Faraday cup was designed for beam current measurement. The moving inner probe and multylamellar probe are inside the cyclotron. The Scanning two-dimension ionization profile monitor was produced for space distribution analysis of accelerated high intensity beam. Inner Pickup electrode system with special electronic was created for beam phase moving analysis. Time of flight system based on two pick-up electrodes for energy measured was placed in transport channel. These and over diagnostic system were commissioned and tested. The results present in report.

## THE TEST OF THERMAL LOADS RESISTANCE

The DC-280 is the high intensive accelerator with beam power up 3,5 kW. For predicting the damage from hitting of the beam on elements, the modeling [4] and testing of prototypes of elements with the electron gun were carried out. It was collaboration of Flerov laboratory of nuclear reaction (JINR) and the Faculty of Mechanical Engineering of the Brno University of Technology (FME BUT During this work the Faraday cup was tested [4].

We heated the sample by electron beam with energy 100 keV. The power was concentrated in the spot with size Ø8 mm. Vacuum level was $10^{-6}$ Torr. In the process of experiments the temperature in different point of the cup were controlled. The visual monitoring of the beams hitting points was provide. The test results were compared with model ones.

We provide test of the normal work mode, the emergency modes: the hitting of the high intensity beam on the element and work without the water cooling. Series of repeating of high intensity beam and cooling for testing of construction resistance to repeating loads were produced.

† seminva@jinr.ru

The tests show, that this construction of the Faraday cup head from Al is able to withstand power 3500 W without of the damage in area Ø8 mm. The surface of Faraday cup was started destroyed only under beam with power 4200 W. Furthermore the test show the efficiency of cooling with half of cooling water flow. The construction does not damage after series of periodic thermal loads. Thus the construction correspond to requirements.

## FARADAY CUP CONSTRUCTION

The design of Faraday cup was presented in [4] in frame of DC-72 project was updated for DC-280. The cup was changed for reduce of distance between the inner surface of cup and water cooling channel. The design was optimization for decreasing of mistakes of current measuring by secondary electron emission on the edge of cup. The magnet system on permanent magnets, part of the design, was moved closer to entry. The magnet system on permanent magnets, part of the design, was moved closer to entry diaphragm. The diaphragm size was reduced, the taper angle was enlarge up to $80^0$. The design was optimized by FLNR constructors. The sketch of Faraday cup present on Fig. 1. The new construction was successfully tested and is used on DC-280.

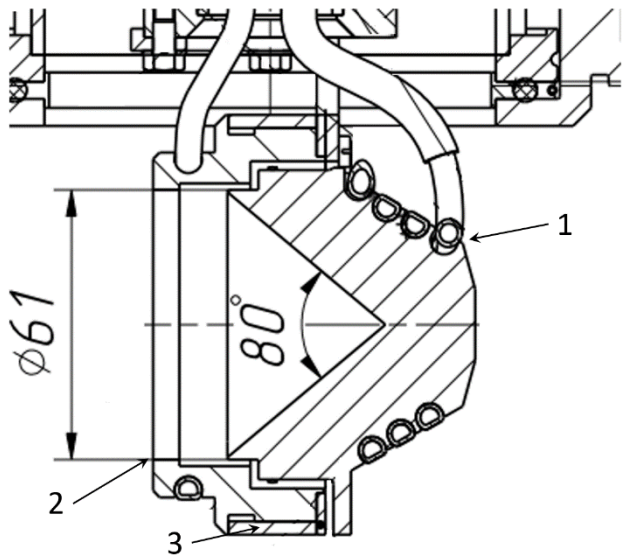


Figure 1: Sketch of the Faraday cup: 1- Water cooling channel; 2- diaphragm; 3- magnet system.

## INNER CYCLOTRON PTOBES

For measuring of ions beam current inside the cyclotron two moving probe are used. One is placed before the entry to deflector second is diametrically opposite. They

ISBN: 978-3-95450-240-0 ISSN: 2673-5539 doi:10.18429/JACoW-RuPAC2021-FRA05

# CYCLOTRON SYSTEM C-250

K.E. Smirnov†, Yu.N. Gavrish, A.V. Galchuck, S.V. Grigorenko, V.I. Grigoriev, R.M. Klopenkov, L.E. Korolev, K.A. Kravchuck, A.N. Kuzhlev, I.I. Mezhov, V.G. Mudrolyubov, Yu.K. Osina, Yu.I. Stogov, M.V. Usanova,
JSC «NIIEFA», 196641, St. Petersburg, Russia

*Abstract*

JSC "NIIEFA" is designing a cyclotron system that generates intensive proton beams with final energy in the range of 30-250 MeV. We have adopted a non-standard technical solution: at the energy of less than 125 MeV negative hydrogen ions are accelerated with the extraction of protons by the stripping device; at higher energies protons are accelerated, and the beam is extracted by a deflector and a magnetic channel. The isochronous dependence of the magnetic field on the radius for different final energies is provided by changing the current in the main coil and tuning the correction coils.

The cyclotron electromagnet has an H-shaped design with a pole diameter of 4 meters, a four-sector magnetic structure, and high spirality sectors. The dees of the resonance system are formed by delta electrodes and placed in the opposite valleys; stems are brought outwards through holes in the valleys. The operating frequency range is 24-33.2 MHz. The power of the RF generator is 60 kW.

The cyclotron complex is equipped with a branched beam transport system and target devices for applied research on the radiation resistance of materials. Computer control of the cyclotron and its associated systems is provided.

## MAIN TECHNICAL FEATURES

The JSC "NIIEFA" is designing a cyclotron system comprising a proton cyclotron, a developed system of beamlines, samples' irradiation system and utilities. The most complicated problem of this project is construction of a unique cyclotron generating proton beams with an energy varied in the range of 30-250 MeV. Cyclotrons with the energy variation over such a wide range are not available nowadays.

The method of negative ions' acceleration with the extraction of protons with a stripping device, which is standard for low-energy cyclotrons, cannot be applied as the binding energy of an additional electron is lower than 0,8 eV. With an increase in the energy of a negative ion when it is moving in a strong magnetic field, rapidly grows the probability of this electron detachment, and, consequently, a decrease in the beam intensity.

To reduce losses, it is necessary to lower significantly the induction of the electromagnet, which will result in a corresponding increase in the diameter of magnet poles. Therefore, at energies higher than 100 MeV, protons are used as accelerated particles. To provide the isochronous motion of protons with different final energy, it is necessary to change the magnetic field induction and its dependence on the radius over wide limits corresponding to the relativistic increase in the proton mass.

To make less stringent requirements to the magnetic field forming, a non-standard decision was adopted. We decided to use negative hydrogen ions as particles to be accelerated in the final energy range of 30-125 MeV; at energies of 125-250 MeV, protons are used.

The ion source is an inner radial Penning-type cold-cathode source.

## ELECTROMAGNET

The iron core of the electromagnet is of an H-shaped design, a four-sector magnetic structure and high helicity sectors. The mode with the 1.08 T induction in the center of the magnet and 1.35 T at the final acceleration radius corresponding to the final energy of 250 MeV was chosen as the basic mode. In this mode, the induction dependence on the radius corresponding to the isochronous motion is realized by turning on the main coil only through the shape of the central plugs, sector side plates, and sector chamfers.

To vary the final energy over the range of 250-125 MeV, the isochronous dependence of the magnetic field on the radius is provided by decreasing the current in the main coil and turn on of correction coils located on sectors. The beam is extracted from a fixed final radius by means of a deflector and magnetic channel.

At lower final energies, we used the magnetic field formed for an proton´s energy of 125 MeV (with reversal of the polarity). A beam of required energy is extracted by moving the stripping device with a thin carbon foil.

The electromagnet is shown in Fig. 1 and its parameters are given in Table 1.

Figure 2 shows trajectories of extracted beams. Green color shows protons after passing the deflector; in red are shown negative hydrogen ions and in blue are given protons at the output of the stripping device foil. The deflector is located in the upper left valley; the stripping device foil can be moved over the gap between left sectors.

† npkluts@luts.niiefa.spb.su

ISBN: 978-3-95450-240-0 ISSN: 2673-5539 doi:10.18429/JACoW-RuPAC2021-FRB01

# ADVANCES IN THE DEVELOPMENT OF A VACUUM INSULATED TANDEM ACCELERATOR AND ITS APPLICATIONS*

S.Yu. Taskaev†, T.A. Bykov, A.A. Ivanov, D.A. Kasatov, Ia.A. Kolesnikov, A.M. Koshkarev, A.N. Makarov, G.M. Ostreinov, I.M. Schudlo, E.O. Sokolova, I.N. Sorokin
Budker Institute of Nuclear Physics, 630090 Novosibirsk, Russia
Novosibirsk State University, Novosibirsk, Russia

*Abstract*

A compact accelerator-based neutron source has been proposed and created at the Budker Institute of Nuclear Physics in Novosibirsk, Russia. An original vacuum insulated tandem accelerator (VITA) is used to provide a proton/deuteron beam. As a result of scientific research and modernization, the power of the ion beam was increased, an operation mode without high-voltage breakdowns was achieved, and the operation of the accelerator in a wide range of changes in the energy and current of ions was ensured. The proton/deuteron beam energy can be varied within a range of 0.6 – 2.3 MeV, keeping a high-energy stability of 0.1%. The beam current can also be varied in a wide range (from 0.3 mA to 10 mA) with high current stability (0.4%). VITA is used to obtain epithermal neutrons for the development of boron neutron capture therapy, thermal neutrons for the determination of impurities in ITER materials by activation analysis method; fast neutrons for radiation testing of materials; 478 keV photons to measure the $^{7}$Li(p,p'γ)$^{7}$Li reaction cross section, etc. VITA is planned to be used for boron imaging with monoenergetic neutron beam, for characterizing of neutron detectors designed for fusion studies, for in-depth investigation of the promising $^{11}$B(p,α)αα neutronless fusion reaction, for studying the crystal structure of materials by neutron diffraction, etc.

## INTRODUCTION

To develop a promising procedure for treating tumors (boron-neutron capture therapy, BNCT [1]), an accelerator-based epithermal neutron source has been prepared and designed in the BINP [2]. Neutrons are generated as a result of the $^{7}$Li(p,n)$^{7}$Be threshold reaction by directing a proton beam, which is produced in an original design tandem accelerator, onto the lithium target.

Significant progress in the development of the accelerator and a significant expansion of its applications have been achieved recently. The report provides a description of the accelerator and its operating parameters, highlights the features of the accelerator, gives the examples of its application and declares plans.

## EXPERIMENTAL FACILITY

The neutron source comprises an original design tandem accelerator, solid lithium target, a neutron beam shaping assembly, and is placed in two bunkers as shown in Fig. 1. The facility has the ability to place a lithium target in 5 positions; they are marked as positions *A*, *B*, *C*, *D*, *E*.

The original design tandem accelerator, which was named as Vacuum Insulated Tandem Accelerator (VITA), has a specific design that does not involve accelerating tubes, unlike conventional tandem accelerators. Instead of those, the nested intermediate electrodes (*1b*) fixed at single feedthrough insulator (*1d*) is used, as shown in Fig. 1. The advantage of such an arrangement is moving ceramic parts of the feedthrough insulator far enough from the ion beam, thus increasing the high-voltage strength of the accelerating gaps given high ion beam current. A consequence of this design was also a fast rate of ion acceleration—up to 25 keV/cm.

## RESULTS AND DISCUSSION

The potential is supplied for the high-voltage electrode and five intermediate electrodes of the accelerator from a sectioned rectifier (*1e*) through a feedthrough insulator (*1d*) in which a resistive voltage divider is mounted. For the compactness of the accelerator, the average electric field strength on the insulator was chosen to be 14 kV/cm, which is 1.5 times higher than the recommended one. This led to breakdowns along the surface of smooth ceramic insulators with a height of 73 mm, from which the feedthrough insulator was assembled. Such breakdowns occurred approximately once every 10 – 20 min; they did not lead to a decrease in the electric strength of the accelerator, but required 15 s to restore the parameters of the ion beam. To eliminate breakdowns along the vacuum surface of insulators, smooth ceramic insulators were replaced with corrugated insulators of the same height.

A beam of negative hydrogen ions with an energy of 20 – 30 keV is injected into the tandem accelerator. Since VITA is characterized by a fast ion acceleration rate, the entrance electrostatic lens is strong. For this reason, the injected ion beam must be refocused to the entrance to the accelerator. To focus the ion beam at the entrance of the accelerator, we used a magnetic lens. Since the transport and focusing of a relatively low energy ion beam is accompanied by a spatial charge, a wire scanner OWS-30 (D-Pace, Canada) is used to control the position and size of the ion beam at the entrance to the accelerator.

The position and size of the ion beam in the accelerator are controlled by two pairs of video cameras overseeing the input and output diaphragms of the external accelerating electrode. Cameras register visible radiation caused by interaction of ions with residual and stripping gases, and heating of diaphragms.

* Work supported by Russian Science Foundation, grant No. 19-72-30005
† taskaev@inp.nsk.su

ISBN: 978-3-95450-240-0 ISSN: 2673-5539 doi:10.18429/JACoW-RuPAC2021-FRB02

# ACCELERATORS OF ELV SERIES: CURRENT STATUS AND FURTHER DEVELOPMENT

D.S. Vorobev, E.V. Domarov, M.G. Golkovskii, Y.I. Golubenko, A.I. Korchagin, D.A. Kogut. N.K. Kuksanov, R.A. Salimov, A.V. Semenov, S.N. Fadeev, A.V. Lavrukhin, P.I. Nemytov,
The Budker Institute of Nuclear Physics (BINP), Novosibirsk, 630090, Russia

*Abstract*

For many years, Budker Institute of Nuclear Physics produces medium-energy industrial electron beam accelerators. Flexible (due to the possibility of completing with different systems) and reliable accelerators cover the energy range from 0.3 to 3 MeV, and up to 130 mA of beam current, with power up to 100 kW.

New accelerators of the ELV type are also being developed. Namely ELV-15 with energy range up to 3.0 MeV and power up to 100 kW. At present time accelerator was assembled and tested in Novosibirsk.

In addition, an accelerator was developed and tested with a new model of extraction device of a focused electron beam into the atmosphere. At present, various experiments are run using the installation with a new device for the extraction of the concentrated electron beam into the atmosphere for the production of nanopowders, surfacing of powder materials for metals, etc.

## ELV ACCELERATORS

The ELV industrial accelerators [1] are widely used due to a number of advantages:

- High electron beam power in wide energy range
- High efficiency of electron beam (70-80%), which important for long term operation
- High stability of electron beam parameters
- Extra-long lifetime and high reliability: 24/7 mode of operation
- Wide set of underbeam equipment: for the film, and cables irradiation, nanopowders manufacturing, liquids, and gases treatment and crosslinking

Table 1 represent parameters of the most popular ELV accelerators. As you can see, a new accelerator appears here: ELV-15 with max energy 3 MeV. Also, the current range for the ELV-8 accelerator was increased up to 60 mA. The common view of the ELV type accelerators is shown on Fig. 1. Actually, the ELV accelerators are well described in [2].

### *Deliveries of last years*

More than 200 accelerators were delivered and installed by now. Even for the last three years, under the significant influence of COVID-19, we had delivered 17 accelerators to our customers. For 2022 is about 15 accelerators now in the queue.

Two accelerators, ELV-8 and ELV-4 were delivered to Russia in 2020. One of them (ELV-8) is installed into a new foam film plant. The plant is located in the Kotovsk city, Tambov region, and is currently reaching production parameters. It should be noted that the delivery of this accelerator was carried out jointly with our partner, the Chinese company “Shanxi Yuridi”. The electron beam crosslinking underbeam technology line was supplied by this company.

Table 1: Models of the ELV Accelerators

| Name | Energy, MeV | Max current, mA | Power, kWt |
|---|---|---|---|
| **ELV-0.5-130** | 0.3-0.5 | 130 | 65 |
| **ELV-0.5-70** | 0.4-0.8 | 70 | 50 |
| **ELV-4-1** | 0.7-1.0 | 100 | 100 |
| **ELV-4-1.5** | 1.0-1.5 | 67 | 100 |
| **ELV-8** | 1.0-2.5 | 60 | 100 |
| **ELV-15** | 1.5-3.0 | 50 | 100 |

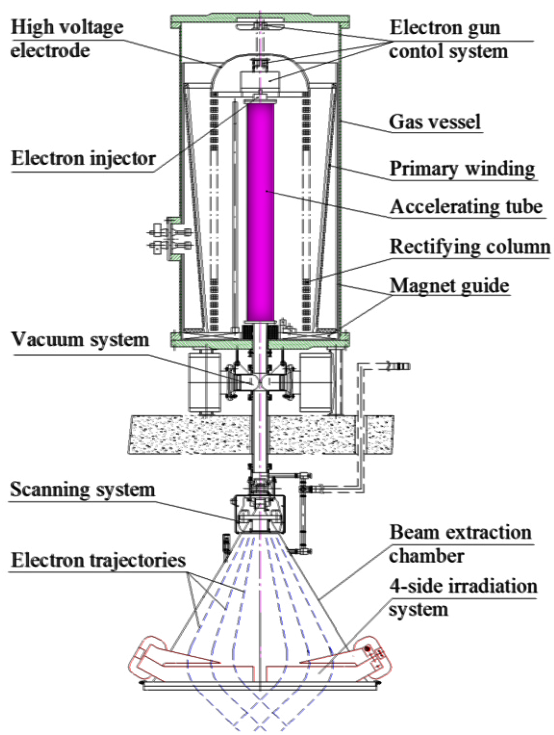


Figure 1: The ELV type accelerator view.

ISBN: 978-3-95450-240-0 ISSN: 2673-5539 doi:10.18429/JACoW-RuPAC2021-FRB03

# UPGRATED THE EXTRACTION DEVICE OF FOCUSED ELECTRON BEAM INTO THE ATMOSPHERE

E. V. Domarov, N. K. Kuksanov, R. A. Salimov, A. I. Korchagin, S. N. Fadeev, A. V. Lavrukhin, V. G. Cherepkov, Y. I. Golubenko, I. K. Chakin, M. G. Golkovsky, A,V, Semenov P. I. Nemytov,
Budker Institute of Nuclear Physics SB RAS, Lavrentyev av. 11 Novosibirsk, 630090 Russia

*Abstract*

This article deals the factors affecting the diameter and angle of divergence of the electron beam at the exit from the accelerator tube of an industrial ELV series accelerator. Measurements of the parameters of a high-power electron beam were carried out up to a power of 100 kW. On the basis of the data obtained, a new type of gas-dynamic extraction device was designed and pre-tested, which can efficiently output a focused electron beam to the atmosphere.

## INTRODUCTION

For more than 30 years at the Institute of Nuclear Physics (INP SB RAS), on ELV-6 accelerator has been successfully operating a multi-stage gas-dynamic extraction device through which a focused electron beam is released into the atmosphere. It uses an accelerating tube with permanent magnets. The design and manufacture of such accelerating tubes are rather complicated. At present, ELV accelerators use simpler and more reliable accelerating tubes without magnetic accompaniment. They have a large aperture of 100 mm and are mass-produced [1]. Since the reliability of serial accelerating tubes is high, and the technology for manufacturing tubes with permanent magnets has been lost. The task was posed of a possible replacement of the accelerating tube with permanent magnets with an accelerating tube with a large aperture without permanent magnets for the ELV-6 accelerators.

## BEAM MOTION ANALYSIS

The beam size and its angular divergence at the exit of the accelerating tube are influenced by the following main factors:

1. Longitudinal electric field: carries out the main focusing of the beam;
2. Influence of the magnetic field of heating coil ( the beam acquires an azimuthal momentum Pφ0);
3. The space charge of the beam;
4. The ripples of the accelerating voltage;
5. Aberrations of electromagnetic lenses. They also affect the optimal hole size in the outlet diaphragms;
6. Transverse component of the magnetic field of the primary and secondary windings, which leads to oscillations of the beam, and leads to increase the holes in the diaphragms

The calculations were carried out using the SAM program developed at the BINP SB RAS [2]: the effect of the intrinsic magnetic field of the incandescence was taken into account, the influence of the potential of electrodes with an aperture of 20 mm on the parameters of the beam, embedding of the LaB6 pellet and the shape of the cathode electrode was checked.

The potential distribution along the accelerating tube is shown in Fig. 1. A so-called "electric-gate" is formed near the high-voltage edge of the tube; a minimum of potential is created, which prevents the acceleration of secondary particles appearing as a result of ion bombardment of electrode with an aperture of 20 mm.

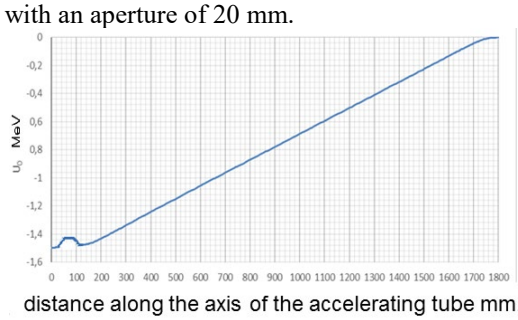


Figure 1: Distribution of potential along the axis of the accelerating tube.

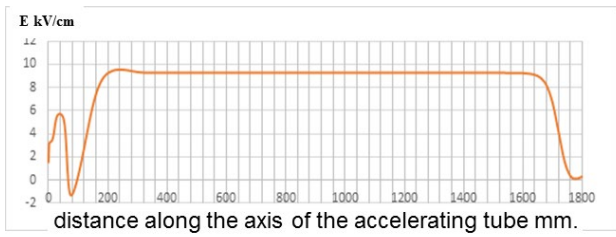


Figure 2: Distribution electric field along the axis of the accelerating tube.

The distribution of the electric field on the tube axis is uneven (see Fig. 2). With an increase the electric field, the beam is focused, and with a decrease the field, the beam is defocused. Three characteristic areas can be distinguished. The cathode is located at point 0. The first section is from 0 to 200 mm. In this section, the beam successively undergoes focusing, defocusing, and focusing. Integrally, this section is strongly focusing and has the greatest effect on the beam parameters at the tube exit. In the second section (200-1700 mm), the electric field is uniform and there is no focusing. In the third section - the tube exit - the electric field decreases to 0 and a defocusing lens is formed with a focal length of about 4 Ltr (where Ltr is the tube length), i.e. about 7 meters. Figure 3 shows the calculated beam envelopes for the optimal geometry of the electric field.

ISBN: 978-3-95450-240-0 ISSN: 2673-5539 doi:10.18429/JACoW-RuPAC2021-FRB04

# A LINEAR ACCELERATOR FOR PROTON THERAPY

V.V. Paramonov†, A.P. Durkin, A.A. Kolomiets
Institute for Nuclear Research of the RAS, 117312,Moscow, Russia

*Abstract*

For applications in Proton Therapy (PT), linear accelerators can provide beam performances not achievable with cyclic facilities. The results of the development of a proposal for a linac, operating in a pulsed mode, with the maximal proton energy of 230 MeV, are presented. Possibilities of fast, from pulse to pulse, adjustment of the output energy in the range from 60 MeV to 230 MeV, formation and acceleration to the output energy of a 'pencil-like' beam are shown. Optimized solutions, proposed for both the accelerating-focusing channel and the technical systems of the linac make it possible to create a facility with high both functional, economic and operational features. Special attention, due to the selection of proven in long-term operation parameters of the systems, is paid to ensuring the reliability of the linac operation. The feasibility of linac is substantiated on the basis of mastered, or modified with a guarantee, industrial equipment.

## INTRODUCTION

Advantages of linacs for PT are known and one can see it in reviews [1,2]. Now the mostly advanced, in the stage of construction, is the LIGHT project [3]. To meet the high requirements for such linacs for applied purpose, sometimes system parameters are set that are more suitable in record-breaking linacs for research purposes. In this report we present the physical justification for the proton linac with wide functional possibilities but conservative, well mastered systems parameters.

## RATIONALITY AND FEASIBILITY

The cornerstones of this linac proposal are:

- - wide functionality for both practical and research proton medicine;
- - operational reliability through conservative systems parameters, proven in long-term operation;
- - cost reduction, size reduction;
- - deep mutual optimization, balance and feasibility of proposals for beam dynamics, accelerating and focusing elements;
- - focus on well mastered level of technologies and elements parameters confidently mastered in high-tech industry (or with guaranteed parameters upgrade);
- - to be placed in regional PT centres.

To meet all requirements, everyone will come to the concept of high-frequency, multi-cavity, low-current, pulsed proton linac with pencil-like proton beam. The main solutions and features are briefly discussed below.

† paramono@inr.ru

## SCHEME AND PARTICULARITIES

The linac is built according to classical scheme for proton linear accelerators at medium, up to 200 MeV, proton energies, Fig. 1.

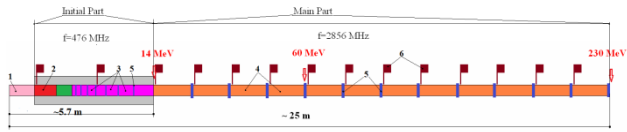


Figure 1: Linac scheme. 1 - proton source, 2 – RFQ, 3 – IH DTL structure, 4 – TW structure, 5 – focusing elements, 6 – RF sources.

The proton source provides 60 keV continuous proton beam with transverse emittance ~0.1 π mm mrad. Such beam can not be formatted, but confidently can be collimated from more powerful beam.

Further accelerator is in two parts. The initial part, operating with frequency 476 MHz, includes RFQ cavity, matching section and accelerating cavities. RFQ cavity provides pre-acceleration and formation of bunches with the small longitudinal emittance. Subsequent elements provide beam matching, allowing beam collimation at energies < 7 MeV, acceleration to energy ~14 MeV and preservation of emittance growth, both in transverse and in longitudinal directions. Operating frequency is selected as a compromise between beam dynamics requirements, parameters of accelerating elements and RF sources, taking into account further acceleration in the main part. As the result, at output of initial part we expect pencil beam with envelope of ~1 mm and extremely small, for such proton energies, phase length of bunches, ~4 degrees, see Fig. 2. In more details initial part of the linac is considered in [4].

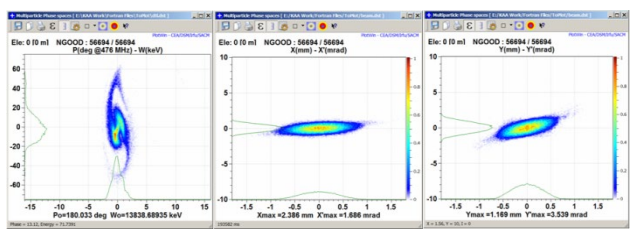

Figure 2: The phase space bunch portraits at the output of linac initial part.

In the main part, operating at frequency of 2856 MHz, protons will be accelerated for the maximal energy of 230 MeV. The value of operating frequency is selected both from commercial availability of RF hardware and parameters of accelerating strictures. In the main part the output proton energy can be changed fast in the range from 60 MeV to 230 MeV.

ISBN: 978-3-95450-240-0 ISSN: 2673-5539 doi:10.18429/JACoW-RuPAC2021-FRB05

# UPDATED STATUS OF PROTOM SYNCHROTRONS FOR RADIATION THERAPY

V.E. Balakin[1], A.I. Bazhan[1], V.A. Alexandrov[1], V.I. Chashurin[1], P.A. Lunev[1], A. A. Pryanichnikov[†1], A. E. Shemyakov[1], M. A. Belikhin[1], A.I. Shestopalov[1]
Lebedev Physical Institute RAS, Physical-Technical Center, Protvino, Russian Federation
[1]also at Protom Ltd., Protvino, Russian Federation

*Abstract*

Physical-Technical Center of P.N. Lebedev Physical Institute of RAS and Protom Ltd. are engaged in development and implantation of synchrotrons for proton therapy into clinical practice. There are two proton therapy complexes “Prometheus” in Russia. That are fully developed and manufactured at Physical-Technical Center and Protom. Every day patients with head and neck cancer get treatment using "Prometheus" at the A. Tsyb Medical Radiological Research Center. At the moment these facilities together have accumulated more than 5 years of clinical experience. Two facilities are based on the Protom synchrotrons in the USA. One operates at the McLaren Hospital PT Center, it started to treat patients in 2018. Another one is as a part of the single-room proton therapy system “Radiance330” in Massachusetts General Hospital that went into clinical operations in 2020. The first Israel proton therapy complex based on Protom synchrotron was launched in 2019. Protom facilities provide full stack of modern proton therapy technologies such as IMPT and pencil beam scanning. Key features of Protom synchrotron: low weight, compact size and low power consumption allow it to be placed in conventional hospitals without construction of any special infrastructure.

This report presents current data on accelerator researches and developments of Physical-Technical Center and Protom Ltd. In addition, it provides data on the use of Protom based proton therapy complexes under the clinical conditions.

## INTRODUCTION

Proton therapy (PT) is one of the most accurate and modern methods of radiotherapy and radiosurgery. [1, 2]. Protons can reduce the radiation load on surrounding tissues up to 30-50% in comparison with gamma rays. The use of a proton beam for tumors located near critical organs, such as the brain stem, optic nerves, etc. are particularly effective. Therefore, in cases of head and neck cancer, proton therapy is the most advantageous of the available types of treatment for many patients. Given the advantages of this type of treatment over radiation therapy, using gamma radiation and electron beams, proton therapy is increasingly being used in the treatment of cancer. There is an increase of PT centers around the world.

In the world, active work is being carried out aimed at increasing the accuracy of dose delivery to the tumor, reducing the time that patients stay under the influence of radiation and increasing the availability of this method for a larger range of patients. New proton accelerators, as well as more cost-effective and accurate immobilization systems for patients are being developed for these purposes [3].

Protom Ltd. is a manufacturer of the equipment for Proton Therapy (PT). Protom can provide full range of the technologies for PT including the accelerator complex based on the compact synchrotron, pencil beam scanning beam delivery system, patient positioning and immobilization system, treatment planning system and all needed software. The Protom synchrotron [4,5] – one of the most advanced medical accelerators in the world. It is the most compact synchrotron, the outer diameter is 5 m and the weight is 15 tons. This kind of accelerator does not use absorbers for proton range correction. That fact makes Protom synchrotron is radiation clean accelerator (radiation is produced only during patient irradiation session). Protom synchrotron is energy efficient facility. The average power consumption of all accelerator complex during treatment is 30 kW. The maximum energy of 330 MeV makes proton tomography of full patient body available [6].

Figure 1: Protom Synchrotron-based Accelerator Complex “Prometheus” in MRRC, Obninisk, Russia.

The first technical run of the prototype of Proton Synchrotron was in 2003. The technical runs of facilities based the synchrotron were performed in 2010 in Protvino City Hospital, Protvino, Russia and Central Military Hospital, Ruzhomberok. In 2011 the technical facility in McLaren Hospital, Flint, MI, USA was successfully performed too. Nowadays proton therapy facilities based on Protom Syn-

† pryanichnikov@protom.ru

ISBN: 978-3-95450-240-0 ISSN: 2673-5539 doi:10.18429/JACoW-RuPAC2021-FRB06

# THE RESULTS OBTAINED ON "RADIOBIOLOGICAL STAND" FACILITY, WORKING WITH THE EXTRACTED CARBON ION BEAM OF THE U-70 ACCELERATOR

V.A Pikalov, Y.M. Antipov, A.V. Maximov, V.A. Kalinin, A. Koshelev, A.P. Soldatov, M.K. Polkovnikov, M.P. Ovsienko and A.G. Alexeev,
NRC "Kurchatov Institute" – IHEP, Protvino, Russia

*Abstract*

This report provides an information of present status of the «Radiobiological stand» facility at the extracted carbon ions beam of the U-70 accelerator. The results of the development of the RBS facility are presented. A plans for development an experimental medical center for carbon ion therapy on the basis of the U-70 accelerator complex are also reported.

## INTRODUCTION

The experimental facility «Radiobiological Stand» (RBS) is in operation on the extracted from the U-70 accelerator complex beam of carbon nuclei since 2014 [1]. The installation is to conduct physics and radiobiological experiments at the ion energies up to 450 MeV/u. Development of the oncology treatment technology and training of domestic experts are the main goals of these radiobiological studies. The first cancer treatments with the beam of carbon nuclei can be the another primary goal of these studies. The RBS installation has been certified as a Center of Collective Use [2] in 2017 under the number 507813 with the following reference: http://www.ihep.ru/pages/main/6580/8769/index.shtml. The RBS installation [3] is in the continuous process of run-to-run development: beam parameters and beam control systems are being improved, systems of active and passive modification of the carbon beam are being developed. This report presents today's RBS and describes its nearest perspectives.

## RBS STATUS

The slow extraction of the carbon beam from U-70 into the channel No. 25 is being done with use of the scheme proposed by O. Piccioni and B.T. Wright in 1954–1955 [4]. The scheme is based on the beam energy moderation passing through a solid target. Currently 6 fixed energies are available for RBS: 450, 400, 350, 300, 250 and 200MeV/u. The channel No. 25 consists of septum magnet SM34, three dipoles BM1-BM3, two sets of quadrupoles: Q1-Q4 with the aperture of 75 mm and Q5-Q7 with the aperture of 100 mm, horizontal corrector and the beam stop. It is instrumented by three TV-boxes with remotely operated scintillation screens. The channel vacuum of $10^{-2}$ bar (not worse) starts from SM34 and ends up after Q7. The target station (see Fig. 1) consists of two target blocks with four Beryllium targets each.

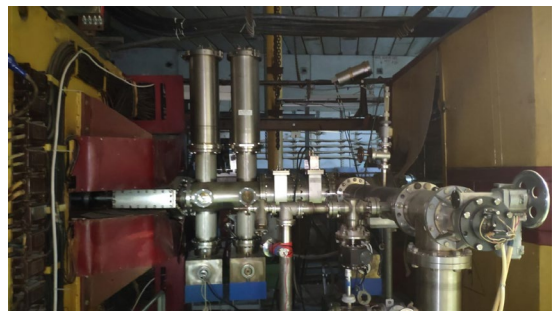

Figure 1: Target station of the channel No. 25.

Figure 2 presents the measured by RBS Bragg peaks in water.

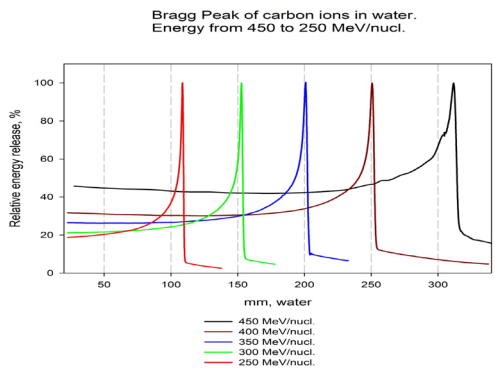


Figure 2: Bragg peaks for different energies of extracted carbon beam.

The shielded area of RBS consists of two zones: experimental and medical, as it can be seen in Fig. 3, with the common system of access control. These zones are separated from each other by a concrete wall with the intermediate collimator. The collimator aperture can be varied manually from 50x50 to 150x150 mm with use of special inserts.

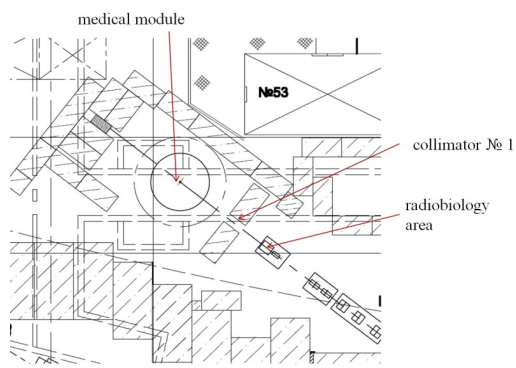


Figure 3: The schematic top view of the RBS installation.

ISBN: 978-3-95450-240-0 ISSN: 2673-5539 doi:10.18429/JACoW-RuPAC2021-FRB07

# TRANSMISSION STUDIES WITH ION BEAMS WITHIN FAMA*

Z. Jovanović†, N. Nešković, I. Telečki, M. Ćosić, and R. Balvanović
Laboratory of Physics, Vinča Institute of Nuclear Sciences, University of Belgrade, Serbia

*Abstract*

FAMA is a user facility for materials science with low-energy ion beams in the Vinča Institute of Nuclear Sciences, Belgrade, Serbia. It includes a heavy ion source, a light ion source, two channels for modification of materials, and two channels for analysis of materials. Recently, the designing of a channel for transmission studies within FAMA has begun. The initial studies to be undertaken in this channel are related to the rainbow effects with very thin electrostatic lenses and two-dimensional materials.

## INTRODUCTION

FAMA is a facility for materials science with low energy ion beams. It is the low energy part of the TESLA Accelerator Installation, a large user infrastructure for production, acceleration and use of ion beams in science, technology, medicine and education. Currently, FAMA includes a heavy ion source, a light ion source, and a small proton cyclotron complex. The heavy ion source delivers multiply-charged heavy ions of energies of 10–20 keV per charge unit, while the light ion source produces positive or negative light ions of energies of 10–30 keV. These beams are used in two channels for modification of materials. The cyclotron complex delivers protons of energies between 1 and 3 MeV, and they are employed in two channels for analysis of materials. Recently, the designing of the channel for transmission studies (C3) of FAMA has begun, in which the ion beams from the heavy and light ion sources will be used.

## INITIAL TRANSMISSION STUDIES

The first planned series of experiments in the C3 channel is related to ion transmission through very thin electrostatic multipolar and rainbow lenses (VTELs) [1–3]. The focusing properties of these lenses are fully determined by the rainbow effect. In the first measurements, the projectiles will be $H^+$ ions of energy of 15 keV from the light ion source and $^{40}Ar^{12+}$ ions of energy of 180 keV from the heavy ion source while the targets will be the quadrupole and square rainbow lenses [2, 3]. The beams should come on the targets closely parallel with the diameters of about 15 mm. The experiments will be performed in the high vacuum conditions.

The second planned series of measurements in the C3 channel is based on using the rainbow effect for specific characterization of 2D materials – by ion transmission [4–6]. In the first experiments, the projectiles will be 10 keV $H^+$ ions from the light ion source and 20 keV $^4He^{2+}$ ions from the heavy ion source. The ion beams should come on the targets closely parallel with the diameters of about 10 μm. The targets will be the flakes of graphene. The measurements require the ultra-high vacuum conditions.

## CHANNEL FOR TRANSMISSION STUDIES

A scheme of the C3 channel is depicted in Fig. 1. It is connected to the mass analyser of one of the channels for modification of materials (C2). The transport elements of the channel are: two steering magnets, to be used to correct the ion beam direction toward the target if needed, and three magnetic quadrupole lenses, making a quadrupole triplet, to finally shape the beam impinging on the target. The characteristics of the magnetic quadrupole triplet have been determined on the basis of the transport calculations for the above specified ion beams, to be used in the first experiments. The transport line of the C3 channel, extending down to its interaction chamber, contains two diagnostic boxes, both being high vacuum cylindrical chambers made of stainless steel, each including a variable circular ion beam collimator, to be used to generate a closely parallel beam. The standard diameters of the collimators are 5 mm in experiments with VTELs and 2 mm in the experiments with 2D materials. In the measurements with 2D materials, the differential pumping apertures with the standard diameters of 2 mm are placed at the entrance and exit of the interaction chamber.

The transport calculations have been conducted using the first-order matrix formalism and the Ion Beam Simulator computer code. As a result, we have adopted 2.0 T/m as the maximal magnetic field gradients on the axes of the magnetic quadrupole lenses. Besides, we have adopted 14 mT as the maximal horizontal and vertical components of the magnetic induction on the axes of the steering magnets.

The interaction chamber of the C3 channel is an ultra-high vacuum cylindrical chamber made of stainless steel. There are two target holder assemblies in the interaction chamber – for VTELs and 2D materials. The former assembly includes a three-axis manipulator while the letter assembly comprises a five-axis goniometer and a sample acceptor stage, enabling one to remove the irradiated target from the interaction chamber for analysis. An electrostatic deflector is placed immediately after the target holder assembly for 2D materials, to be able to move away from the axis of the channel the ions that remained charged upon the interaction with the crystal, and thus record the angular distribution of neutralized ions. The deflector will also enable one to measure the charge state distribution of transmitted ions. The crystal structure of the chosen 2D material will be determined using a reflection high energy electron diffraction (RHEED) system, attached to the interaction chamber.

* Work supported by the Ministry of Education, Science and Technological Development of the Republic of Serbia
† zjovanovic@vinca.rs

ISBN: 978-3-95450-240-0 ISSN: 2673-5539 doi:10.18429/JACoW-RuPAC2021-FRC01

# NEUTRON FIELD MEASUREMENTS BY GFPC BASED MONITORS AT THE CARBON BEAM OF IHEP U-70 PROTON SYNCHROTRON

I.L.Azhgirey, I.S. Bayshev, V.A. Pikalov and O.V. Sumaneev, NRC "Kurchatov Institute" – IHEP, Protvino, Russia

*Abstract*

Neutron monitors with gas filled proportional counter (GFPC) as a sensitive element were presented at RuPAC-2018. These monitors have been used recently to measure fast neutron fluxes near the carbon beam based experimental facility at IHEP. The experimental facility "Radiobiological test setup at the U-70 accelerator" was built at NRC "Kurchatov Institute" - IHEP, Protvino, to carry out radiobiological and physical experiments with the extracted beam of carbon nuclei with an energy up to 450 MeV/nucleon. The measurements were compared with the CERN FLUKA code simulations.

## INTRODUCTION

Neutron detection by GFPC monitors [1] is based on thermal neutron capture reaction by a 10B nucleus with emission of α particle. Incident neutrons are moderated to thermal energies by a moderator layer surrounding a corona counter SNM-14. The internal surface of the counter is covered with amorphous boron, with the 10B isotope content enriched up to 80-85%. The counter is filled with argon at atmospheric pressure. A signal is formed mainly after ionization of argon by ions of 4He or 7Li ions. The SNM-14 corona counter in these monitors is operated in proportional mode.

A pair of monitors can be more efficient for detecting high-energy neutrons, provided the response curve of the complementary (light) monitor is close to the response curve of the main (heavy) monitor below 100 keV and much lower at high energies. Each of the types of monitors can work independently as a neutron flux counter. Efficiency of the separate monitor will be determined by its response function and neutron spectrum in the monitor location. Pair of monitors works as a simplest spectrometer dividing the neutron spectrum in two groups.

The monitors are intended to work without intervention for a long period of time. They are controlled via a single coaxial cable (for both data and power supply) and are relatively small. The monitors themselves and their front-end electronics are radiation hard, and their operation is not affected by the magnetic field.

The main goal of these measurements was testing of the recently developed neutron monitors in a typical high energy neutron field at the Radiobiological Stand (RBS) facility [2]. The RBS layout is shown in Fig. 1, where big letters C point to the carbon beam axis at the entrance to and at the exit from the RBS area. The height of the beam axis with respect to the concrete floor is 215 cm.

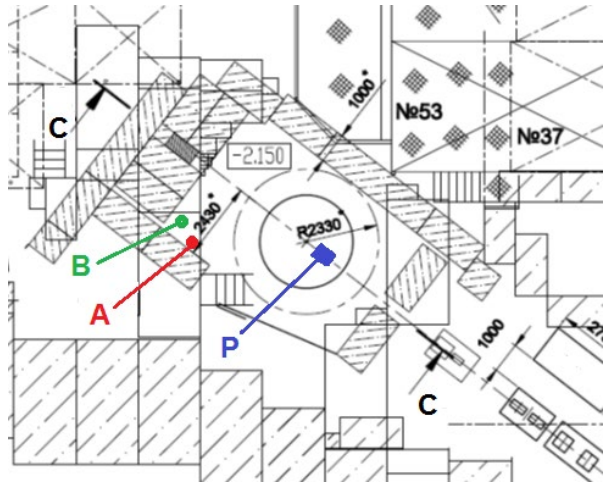


Figure 1: Schematic top view of the RBS facility. A and B – pair of the neutron monitors, C – ion beam, P – water phantom.

The wide beam passes through the collimator opening of 5×5 cm and approximately 50% of the beam hits the water phantom installed on the top of the medical bench. The main source of neutrons is the beam interaction with phantom and interactions with collimator material produce background source.

Passed beam is monitored by a flat air-filled ionization chamber of 20×20 cm area. The beam energy is 434 MeV/nucleon. Irradiation was done with 236 cycles, consisting of 0.6 s long pulses with 8 s spacing between them. The RBS area is surrounded by concrete shielding blocks and the monitors were placed inside shielding but not too close to the beam axis. Monitor coordinates are given in the Table 1.

Table 1: Transverse X, Vertical Y and Longitudinal Z Coordinates of the Monitor Centers With Respect to the Phantom Center

| Monitor | X, cm | Y, cm | Z, cm |
|---|---|---|---|
| A | 196 | -103 | 332 |
| B | 167 | -103 | 361 |

The main (heavy) monitor (monitor A through this report and in Fig.1) measured the fluence of fast neutrons (with energy greater 100 keV). The complementary (light) monitor (B through this report and in Fig.1) was used for the correction of the monitor A readings.

ISBN: 978-3-95450-240-0 ISSN: 2673-5539 doi:10.18429/JACoW-RuPAC2021-MOPSA02

# EXPERIMENTAL TESTS OF CW RESONANCE ACCELERATOR WITH 7.5 MeV HIGH INTENSITY ELECTRON BEAM

L.E. Polyakov, N.V. Zavyalov, Ya.V. Bodryashkin, M.A. Guzov, A.I. Zhukov, I.V. Zhukov, I.A. Konyshev, V.V. Kuznetsov, N.N. Kurapov, I.A. Mashin, V.R. Nikolaev, A.M. Opekunov, G.P. Pospelov, S.A. Putevskoj, M.L. Smetanin, A.V. Telnov, A.N. Shein, I.V. Shorikov, RFNC-VNIIEF, Sarov, Russia

*Abstract*

CW resonance accelerator with high average power electron beam is developed at RFNC-VNIIEF. Electron energy range is varied from 1.5 to 7.5 MeV and average beam current is up to 40 mA.

In this paper we present the results of electron beam dynamics simulation. The operating parameters of RF system, beam optics and bending magnets are determined. These parameters permit to obtain output beam with minimal current losses on each accelerating stage.

As a result of carried out tests 7.5 MeV electron beam was obtained after five passes of accelerating cavity. The electron energy spectrum, average beam current, transverse beam dimensions were determined on each accelerating stage. Common beam current loss is under 10 %.

## INTRODUCTION

CW electron accelerator is aimed to obtain beams with the electron energies – 1.5, 3, 4.5, 6 и 7.5 MeV [1]. The accelerator is based on coaxial half-wave cavity (type of oscillations $T_1$). The electron energy gain up to 1.5 MeV per one pass of the accelerating gap. If it's necessary electrons is returned to the cavity for the subsequent energy gain by bending magnets.

Average beam power at the maximum of energy (7.5 MeV) achieves 300 kW. It becomes possible because of grid-controlled RF gun, which allows to obtain quasicontinuous electron beams with the average current 40 mA and energy 100 keV. RF system of accelerator consists of three independent amplifying cascades and RF power summator. It permits to obtain output RF signal with the average power up to 560 kW at frequency 100 MHz. Main characteristics of CW electron accelerator are shown in Table 1.

Table 1: Characteristics of CW Electron Accelerator

| Parameter | Value |
|---|---|
| Electron energy, MeV | 1.5, 3, 4.5, 6, 7.5 |
| Average beam current, mA | 40 |
| Operating frequency, MHz | 100 |
| Average beam power, kW | 300 |
| Average power loss, kW | 165 |
| RF system power кВт | 560 |

## OPTIMIZATION OF OPERATING MODES

At present accelerator has the ability to product 7.5 MeV electron beams with the average current up to 100 μA. RF system consists of single amplifying cascade with 180 kW of output power. Current scheme of accelerator is shown in Fig. 1.

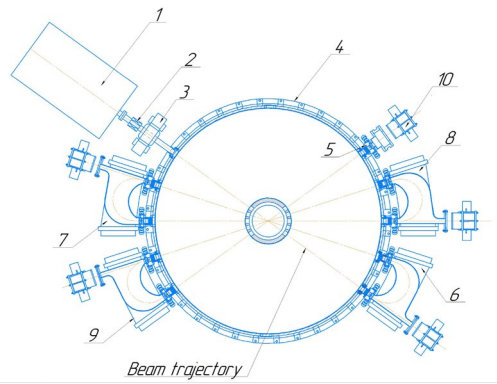


Figure 1: Accelerator scheme (1 – RF injector; 2 – focusing solenoid; 3 – quadrupole lens; 4 – accelerating cavity; 5 – corrector; 6 – 9 – bending magnets; 10 – Faraday cup).

Electron beam dynamics simulation was performed using program code ASTRA (A Space Charge Tracking Algorithm) [2]. Subsequent tests show that optimal beam injection phase into the accelerating cavity vary from - 20 to - 5 degree. Optimal magnetic field in the centre of focusing solenoid (2) is 12 mT. Magnetic quadrupole lens (3) installed in the injection channel is intended to compensate the various effect of transverse components of electric field in the cavity cross-section. Magnetic rigidity of lens is 20 mT [3]. Maximum of electric field inside the cavity is 185 kV/cm.

Calculated electron energy characteristic after each pass of accelerating cavity is shown in Fig. 2. Calculated values of average beam energies and energy spreads is shown in Table 2.

Table 2: Calculated Electron Energies znd Energy Spread

| Number of pass | Average energy, MeV | Energy spread, MeV |
|---|---|---|
| 1 | 1.5 | 0.074 (4.9%) |
| 2 | 3.05 | 0.098 (3.2% |
| 3 | 4.51 | 0.195 (4.3%) |
| 4 | 6.042 | 0.311 (5.15%) |
| 5 | 7.507 | 0.407 (5.43%) |

ISBN: 978-3-95450-240-0 ISSN: 2673-5539 doi:10.18429/JACoW-RuPAC2021-MOPSA03

# CALCULATIONS OF ION DYNAMICS AND ELECTRODYNAMIC CHARACTERISTICS OF 800 keV/NUCLON RFQ

M.A.Guzov, N.V. Zavyalov, A.V. Telnov, M.L. Smetanin, A.M. Opekunov, L.E. Polyakov,
Russian Federal Nuclear Center – All-Russia Research Institute of Experimental Physics (RFNC-VNIIEF), Sarov
S.M. Polozov, Yu.Yu. Lozeev, A.I. Makarov, E.N. Indushniy, NRNU MEPhI, Moscow

*Abstract*

An accelerating structure with radio frequency quadrupole (RFQ) [1] focusing is considered. The RFQ is capable of providing bunching and acceleration of ion beams from H+ to O5+ to energies of the order of 1 MeV/nucleon, with an A/Z ratio from 1 to 3.2. The proton current reaches 2 mA, and the ion current reaches 1 mA.

The calculation of the dynamics of ions has been carried out. An electrodynamic model of a four-vane RFQ with magnetic coupling windows has been created. The dependence of the operating frequency of the cavity on its geometric parameters is found. The geometry of the magnetic coupling windows, which provides the optimal mode separation, is determined. Various types of cavity shells are considered and the corresponding electrodynamic characteristics (EDC) are obtained. The influence of additional frequency tuning elements (plungers and "spacers" of frequency tuning) on the EDC is investigated. As a result, an optimized electrodynamic model of the accelerating structure is obtained.

## RESULTS OF CALCULATING THE ION DYNAMICS IN AN ACCELERATING STRUCTURE

The purpose of calculating the dynamics of ions in an accelerating structure is to obtain conditions for accelerating the beam with minimal losses [2]. There are two types of losses: transverse and longitudinal (phase). Transverse losses are eliminated by changing the modulation parameter. Longitudinal losses disappear due to a change in the phase of a synchronous particle, which in turn also depends on modulation. Therefore, the problem of finding the optimal parameters of the accelerating structure, which are interconnected, was solved.

The range of accelerated particles from H+ to O5+ is considered. Particle dynamics were simulated in three stages:

1) preliminary modeling in order to identify the main parameters of the accelerating structure;

2) dividing the structure into periods;

3) modeling the dynamics in the structure, divided into periods.

The initial data for calculating the dynamics of ions are presented in Table 1. The emittance for protons and O5+ ions were obtained (Figs. 1,2). The values of energy, particle velocity, particle current and particle loss are calculated (Table 2). The calculations of the dynamics of ions were carried out with a preliminary bunching device ("buncher") and without it.

Table 1: Parameters for Modeling the Dynamics of a Proton Beam

| Ions | $p^+$ | $O^{5+}$ |
|---|---|---|
| Length of structure, cm | 450,0 | |
| Length of buncher , cm | 280,0 | |
| Emittance, π×cm×mrad | 0,03 | |
| Transverse beam size (*x*,*y*), cm | 0,1 | 0,2 |
| Voltage, kV | 40,0 | 140,0 |
| Frequency, MHz | 81,25 | |
| Particle current, мА | 2,0 | 1,0 |

The calculation was carried out for the phase length of the beam 2π and 1.4π (pre-bunched beam).

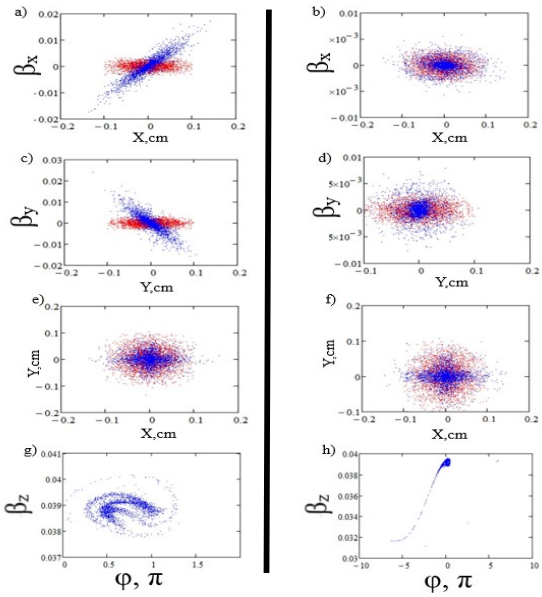


Figure 1: Results of calculations of the dynamics of protons :in RFQ (particles are indicated in red at the beginning of the structure, blue at the end), a - transverse emittance (X), without buncher; b - transverse emittance (X), with a buncher; c - transverse emittance (Y), without buncher; d - transverse emittance (Y), with a buncher; e - cross-section of the beam, without a buncher; f - cross-section of the beam, with a buncher; g - longitudinal emittance, without a buncher; h - longitudinal emittance, with a buncher.

ISBN: 978-3-95450-240-0 ISSN: 2673-5539 doi:10.18429/JACoW-RuPAC2021-MOPSA04

# THE TUNING RF PARAMETERS OF 40 MHz RFQ

A. Sitnikov, D. Seleznev, G. Kropachev[1], A. Semennikov, T. Kulevoy,
ITEP – NRC Kurchatov institute, Moscow, Russia
[1]also at JINR/FLNR, Moscow region, Russia

*Abstract*

The new linac for ions with mass(A)-to-charge(Z) ratio 8 (A/Z=8), output energy 4 MeV/u and 10 mA current is under development at NRC "Kurchatov Institute"-ITEP. The linac consists of Radio-Frequency Quadrupole (RFQ) and two sections of Drift Tube Linac (DTL).

The 40 MHz 11 meters long RFQ is based on a 4-vane structure with magnetic coupling windows [1]. The paper presents results of tuning radio-frequency (RF) RFQ parameters.

## INTRODUCTION

The cavity with Radio-Frequency Quadrupole is wide used as an initial part of ion linac [2, 3].

The RFQ accelerating structure is based on H-cavity with four electrodes with modulated tips. Each electrode has one or few coupling windows. In order to minimize field non-uniformity the coupling windows shifted in vertical electrodes line related to horizontal electrodes line (or vice versa) [1]. Thus, the RFQ linac could be divided on odd number separated identical sections with similar RF parameters (front/end sections have an input/output gaps).

The results of RF tuning of the RFQ linac which is under development in NRC "Kurchatov Institute"-ITEP are presented in this paper.

## THE RFQ LINAC

According to particles dynamics simulation the RFQ should has vanes length equals to ~11 m, average aperture radius $R_0$ = 12.5 mm, vane tip radius $R_e$=0.8* $R_0$ = 10 mm and operates at $f_0$ = 40.625 MHz. The RFQ cavity consists of 1000 mm long 11 identical sections and input/output flanges. The shifted windows structure was chosen for RFQ linac. The windows` areas were chosen as bigger as possible in order to minimize the cavity`s inner diameter [4]. The regular RFQ section is shown on Fig. 1. The main dimensions and RF parameters are presented at Tables 1 and 2, correspondently.

## THE RFQ LINAC RF PARAMETERS TUNING

It should be mentioned that:

1. All further explanation was done for ideal model;
2. All describing methods of RF tuning have an influence to resonant frequency as well as field distribution.

### *The RFQ Linac RF Parameters Tuning Under Manufacturing Stage*

The simulated RF parameters and measured one could be different to each other because of various reasons such as manufacturing or simulating errors. Thus, in RFQ linac design the special elements which could be modified at manufacturing stage should be provided.

The coupling window (area of coupling window) is the simplest element to be modified at manufacturing stages. It was tried out in [5]. The face of coupling window which could be modified is shown on Fig. 1.

The simulation has shown that resonant frequency has a linear relationship at coupling window`s height as it is shown at Fig. 2. The gradient is equal to $\Delta f / \Delta h =$ -45 kHz/mm. The same simulation was done for coupling window`s length. In this case the gradient is equal to $\Delta f / \Delta l =$ -90 kHz/mm.

Changing the coupling window`s height seems more simple and more precisely compared to changing coupling window`s length.

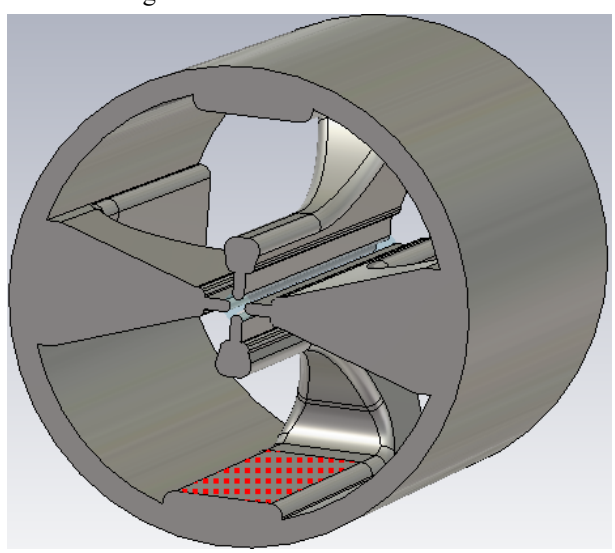

Figure 1: The regular RFQ section (the area for modification is highlighted with red).

Table 1: The Main Dimensions of RFQ Sections

| Parameter | Value (mm) |
|---|---|
| Cavity inner diameter | 860 |
| Cavity length | 1000 |
| Vane base width | 250 |
| Vane base height | 37.5 |
| Vane top width | 60 |
| Vane window length | 770 |
| Vane window height | 290 |
| Vane tip height | 30 |

ISBN: 978-3-95450-240-0 ISSN: 2673-5539 doi:10.18429/JACoW-RuPAC2021-MOPSA06

# PARAMETERS OF THE NORMAL CONDUCTING ACCELERATING STRUCTURE FOR THE UP TO 1 GeV HADRON LINACS

I.V. Rybakov†, A.V. Feschenko, L.V. Kravchuk, V.V. Paramonov, V.L. Serov, Institute for nuclear research of the Russian academy of sciences, Moscow, Russia

*Abstract*

Compensated bi-periodic accelerating structure Cut Disk Structure (CDS) was developed for accelerating particle beams at β~1. In the papers dedicated to the development of this structure, a significant decrease in Ze was shown for medium energies range, β~0.4-0.5. For high-intensity hadron linacs, this energy range, in which particles are captured to acceleration from the drift tube structure, is of the greatest interest. In this paper, a set of CDS parameters was obtained, which provides a Ze value not lower in the comparison to the proven structures in the medium energy range. By the comparison of the electrodynamic and technological parameters of CDS with these structures, the advantages of its application in multi-section cavities for the up to 1 GeV linacs are shown. The selection of optimal cells manufacturing tolerances, the method of its tuning before brazing and frequency parameters control, and the selection of the method for multipactor discharge suppression are determined. The results of the sketch project of the CDS cavity numerical simulation as a non-uniform coupled system and optimization of the transition part of sections and bridge devices are presented.

## INTRODUCTION

Compensated biperiodic structure CDS was proposed for high energy area, β~1 [1,2]. For particle velocities β>0,5 CDS is superior to known analogues in effective shunt impedance $Z_e$. But in lower energy area, β<0.5, it was difficult to implement internal cooling channels, required for CDS application in hadron linacs with intense beam [3,4]. In recent investigations the cells dimensions were optimized to equalize CDS with analogues in Ze value simultaneously placing internal cooling channels. Also, the techniques for multipacting discharge damping in CDS coupling cells [5], and combining of CDS sections into accelerating cavity [6], were developed. For application in hadron linacs with intense beams and energies up to 1 GeV in the total set of RF and technological parameters CDS surpass [7], known analogues.

## CDS STRUCTURE FOR β>0,5

The CDS structure has shown competitive electromagnetic parameters for hadron linacs at comparatively high velocity range 0.4≤ β≤0.8, as it is shown in Fig. 1 [4].

The advantage of CDS in $Z_e$ over proven strictures such as ACS, SCS and DAW decreases with high internal wall thickness at β<0.5. At the same time, it is necessary to place internal cooling channels in them. In high intensity linacs the RF heat load is about 3 kW/m. The RF loss density and temperature distribution is shown in Fig. 2.

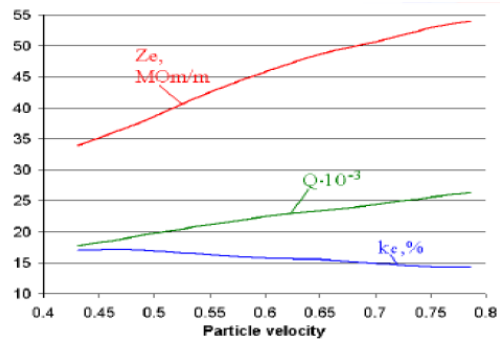


Figure 1: Comparison of the accelerating structures at 991MHz operating frequency.

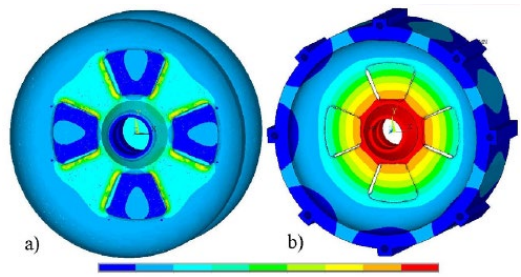


Figure 2: RF loss density (a) and temperature (b) distributions in CDS.

In case of only external cooling channels implemented the drift tube is overheated which causes thermal-stress deformations leading shift of operating frequency.

Calculating a combination of CDS parameters to implement internal cooling channels with maintaining high $Z_e$ value has become the main problem for its application at β<0.5.

## CDS OPTIMIZATION FOR β~0,4

To implement internal cooling channels a set of CDS geometrical parameters was calculated, providing both high $Z_e$ value and sufficient internal wall thickness. Comparison of CDS electrodynamic parameters with proven accelerating structures (Fig. 3) at β=0.4313 is shown in Table 1.

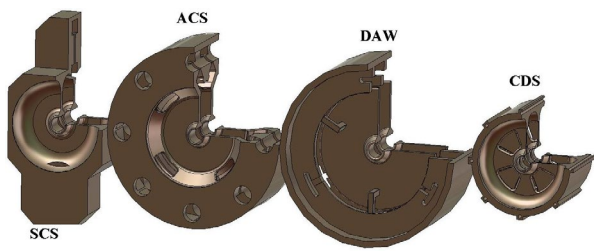


Figure 3: Comparison of the accelerating structures at 991MHz operating frequency.

† irybakov@inr.ru

ISBN: 978-3-95450-240-0 ISSN: 2673-5539 doi:10.18429/JACoW-RuPAC2021-MOPSA07

# 200 MeV LINEAR ELECTRON ACCELERATOR – PRE-INJECTOR FOR A NEW KURCHATOV SYNCHROTRON RADIATION SOURCE

I. A. Ashanin[1,2], S. M. Polozov[1,2] A. I. Pronikov[1,2] , V. I. Rashchikov[1,2],
V. N. Korchuganov[2], V. A. Ushakov[2]
[1]National Research Nuclear University MEPhI, Moscow, Russia
[2] National Research Center "Kurchatov Institute" Moscow, Russia

*Abstract*

New linear electron accelerator (linac) with an energy of about 200 MeV (or 300 MeV in a high-energy version) is being proposed for injection into the booster synchrotron, which is being developed for the reconstruction of the SIBERIA-2 accelerator complex with the aim of upgrade to 3rd generation source at the NRC «Kurchatov Institute». A modernized linac and its specific elements layout will described in the report. The modeling of accelerating structure and optimization of electrodynamics characteristics and fields distribution and geometric in order to reduce the beam spectrum at the output of the linac was done. A step-by-step front-to-end beam dynamics simulation results will discuss.

## INTRODUCTION

Kurchatov synchrotron radiation source (KSRS) today consists of 80 MeV linac, 450 MeV small booster ring Siberia-1 and 2.5 GeV main ring Siberia-2 [1]. Compact booster ring Siberia-1 uses for intermediate acceleration of electrons from 80 to 450 MeV and injection into the main ring, also a source of synchrotron radiation in the field of vacuum ultraviolet and soft X-ray. At the moment, a 40 keV diode gun and ~ 4 A in a pulse with a duration of ~ 18 ns is used as an injector. The energy spread at the output is about 7%. From the gun electron beam drives to the input of the linear accelerator. Disk-and-washer type accelerating structure has 112 accelerating gaps. After acceleration to 80 MeV, the beam pulse consists of about 50 microbunches following each other at a frequency of 2.8 GHz.

In the version for reconstruction (see Fig. 1), it is proposed to use a classic three-electrode gun with a heated oxide cathode (powered by a single modulator) as an electron source. The linear accelerator will include 4 or 6 sections, each about 2.14 m long, operating on a standing wave (biperiodical accelerating system, BAS) (see Fig. 2). Consequently, after acceleration beam energy will be 200 MeV.

Two bunchers – one short klystron type and one adiabatic – will be placed in front-end of linac, which will include several (4-7) irregular accelerating cells with increasing phase wave velocity and accelerating field amplitude for longitudinal beam bunching.

To increase the current transmission coefficient and to reduce the beam energy spectrum, in addition to the adiabatic buncher, a one- or two-gap buncher can be placed in front of the adiabatic buncher operating at a frequency that is two or four times lower than the operating frequency of the sections [2].

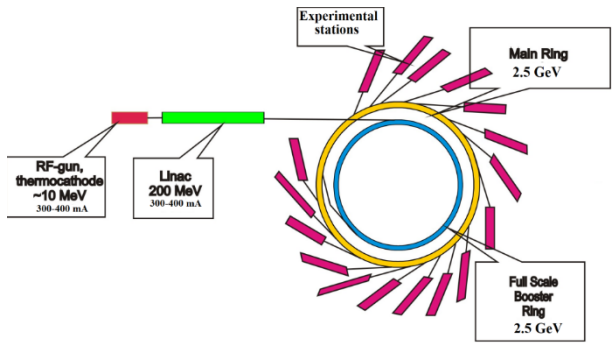


Figure 1: Planned scheme of the accelerator complex.

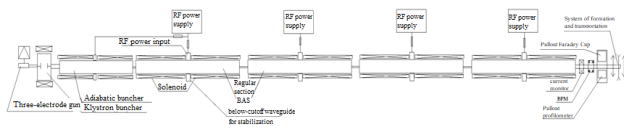


Figure 2: Possible scheme of the linac layout.

All results of the beam dynamics simulation were carried out using the BEAMDULAC-BL code developed at the Department of Electrophysical Facilities of NRNU MEPhI [3-5]. Numerical simulation was carried out in stages, with control of parameters after buncher, after the second, fourth and sixth regular sections.

## BEAM DYNAMICS SIMULATION IN THERMIONIC GUN

Simulation shows that the optimal injection energy will be 100–120 keV. The beam current at these parameters was 1.03 A, energy spread 0.76%, beam radius 3.6 mm, transverse emittance 6.5 π (cm-mrad), micropervance 0.03 mkA/B$^{3/2}$ [6]. Transverse beam focusing is carried out using magnetic solenoids on all sections of the linear accelerator and triplets of quadrupole lenses at higher energies.

## BEAM DYNAMICS SIMULATION IN ADIABATIC BUNCHER

Linac front-end with a thermionic cathode should provide an energy of ~ 10 MeV. The operating frequency is 2800 MHz. The number of periods is 26.

The adiabatic buncher includes four periods with increasing phase velocity and RF field amplitude. At the

ISBN: 978-3-95450-240-0 ISSN: 2673-5539 doi:10.18429/JACoW-RuPAC2021-MOPSA08

# BEAM DYNAMICS SIMULATION IN A LINEAR ELECTRON ACCELERATOR – INJECTOR FOR THE 4TH GENERATION SPECIALIZED SYNCHROTRON RADIATION SOURCE USSR

I. A. Ashanin[1], S. M. Polozov[1] A. I. Pronikov[1] , Yu.D. Kliuchevskaia
National Research Nuclear University MEPhI, Moscow, Russia
[1]also at National Research Center "Kurchatov Institute" Moscow, Russia

*Abstract*

USSR project (Ultimate Source of Synchrotron Radiation, 4th generation synchrotron light source) is being developed in the NRC «Kurchatov Institute». This Light Source will include both storage ring and soft FEL (Free Electron Laser) and one linac with an energyof 6 GeV, which is planned to be used both for beam injection into storage ring (top-up injection) and as a high-brightness bunch driver for FEL. It is suggested to use two front-ends in this linac: RF-gun with thermionic cathode with adiabatic buncher for injection into storage ring and RF-gun with photocathode will use to generate a bunch train for FEL. The purpose of this work was to development a general layout of the top-up linac with the aim of minimize of the beam energy spread and transverse emittance at the exit and analysis the front-to-end beam dynamics in this linear accelerator.

## INTRODUCTION

The 4th generation synchrotron light source called Ultimate Source of Synchrotron Radiation (USSR-4) is under construction at the moment in Russia [1-2]. New 4th generation source design will require the innovations and evolution in the domestic technologies of magnetic and vacuum systems, the solution of new problems in materials science and instrument engineering. New facilities will become one of the biggest world scientific centres conducted researches in a variety of disciplines spanning physics, chemistry, materials science, biology and nanotechnology.

General facility layout includes 6 GeV main storage ring and top-up injection linac. The top-up injection scheme into USSR main storage synchrotron is preferable. Thus it is proposed to use the same linac with two RF-guns. First of them will RF photogun and can be used to generate the drive beam for FEL. The second one will RF-gun with thermionic cathode can be used for injection into storage ring. Such layout leads to two linacs operation modes: 6 GeV beams for injection and 6-7 GeV high-brilliance bunches for FEL. It leads to the same for-injection scheme as it was used for SuperKEK-B and MAX-IV and is proposed for FCC-ee [3-4]. Both injectors will operate with the same regular part of the linac which consists of 80-90 identical sections (see Fig. 1). The planning transverse emittance is 70-100 pm·rad. The length of the circumference of the main storage ring is about 1300 m, it will consist of 40 super periods, including two asymmetric magnetic arches and a gap of about 5 m for the placement of plugg-in devices between them.

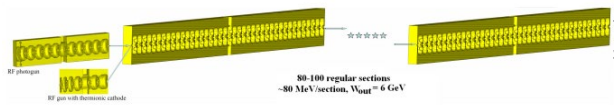


Figure 1: Expected scheme of the 6 GeV top-up injection linac.

The "front-to-end" beam dynamics simulation results in this linear accelerator will discuss in the paper.

All results of the beam dynamics simulation carried out using the BEAMDULAC package developed at the Department of Electrophysical Facilities of NRNU MEPhI [5]. The BEAMDULAC-BL code version was designed to study the beam dynamics in high-intensity electron linacs, it is discussed in detail in [6] and it was tested for a number of e-linac designs [7-8].

## RF-GUN'S PARAMETERS COMPARISON

The beam dynamics simulation was done both for RF-guns with photocathode and thermionic cathode (see Table 1) [9]. The beam dynamics simulation in the RF-photogun shows that 250 pC and 10 ps bunch can be easily accelerated by 5.5-cell accelerating structure with comparatively low accelerating gradient of 600 kV/cm [10]. RF-gun with thermionic cathode is a classic adiabatic buncher consists of 26 accelerating cells and 25 coupling cells. First 4 cells are the bunching cells and the phase velocity and the RF field amplitude growth here cell-to-cell. In the other 22 cells this parameters are constant.

Table 1: Comparison of the RF-gun's Parameters

| Parameter | Photogun | Thermogun |
|---|---|---|
| $W_{inj}$, keV | 100 | 100-120 |
| $E_{acc}$, kV/cm | 450-600 | 150 |
| $W_{out}$, MeV | 10.5 | 10.3 |
| Transmission coeff., % | 100 | 85-90 |
| FWHM, % | ±1 | ±2 % |
| $B$, T | 0.1 | 0.035 |

As the regular section, it is proposed to use a biperiodical accelerating structure (BAS) on a standing wave with a high coupling coefficient in the magnetic field, comparison

ISBN: 978-3-95450-240-0 ISSN: 2673-5539 doi:10.18429/JACoW-RuPAC2021-MOPSA11

# ROOM TEMPERATURE FOLDING SEGMENT FOR A TRANSFER OF MULTIPLE CHARGE STATES URANIUM IONS BETWEEN SECTIONS OF LINAC-100

V. S. Dyubkov, National Research Nuclear University MEPhI, Moscow, Russia

*Abstract*

Beam dynamics simulations results of multiple charge states uranium ions ($_{238}U^{59+,60+,61+}$) in a transfer line between two LINAC-100 superconducting sections of DERICA project (JINR, Dubna, Russia) are presented. Transfer line is an advanced magnetic optical system and provides beams bending on 180 degrees. Transfer line options are proposed. Parameters of its optic element are chosen so that dispersion function has zero value at the start and end of the channel for transporting the 35.7 MeV/nucleon ion beams.

## INTRODUCTION

Fundamental problems such as studies of neutron matter, searching the borderline of nuclear stability in the major part of the nuclear char, studies of nuclei structure far from "stability valley" requires studies of unstable isotopes synthesized in a laboratory. For this reason a construction of radioactive isotope beam "factories" is the mainstream of the low-energy nuclear physics development. One of the mega science facilities for direct radioactive isotopes studies in electron-ion collisions is a rare isotope beam "factory" of FLNR (JINR) called "Dubna Electron-Radioactive Ion Collider fAcility" (DERICA) [1]. DERICA will consist of a number accelerators. The main of them is quasi-CW superconducting driver LINAC-100 [2, 3] that will accelerate heavy ions and will be used for secondary radioactive ion production. Two-step stripper approach is proposed for LINAC-100 [4]. Numerical simulations of uranium beam stripping shows that only 22% of initial beam intensity for one charge state of uranium ions can be obtained. In order to reach world record of beam current on the target it needs to accelerate charge states of uranium ions closed to central one that is considered to be 60. $_{238}U^{59+}$ and $_{238}U^{61+}$ ions appear in stripping the beam. Doing so one can obtain the three charge states uranium ion beam with intensity is about 60% and total beam current of about 0.6 mA under 1.1 π·mm·mrad normalized transverse beam emittance. A similar technique was used in [5].

There are two options of LINAC 100 layout nowadays. One of them the so called "serial" option, when the second LINAC-100 section is placed straight after the first one. Another one is the so called "parallel" option, when the second LINAC-100 section is placed in parallel to the first one. Diagram of the international accelerator-storage complex DERICA in the case of the "parallel" option is shown in Fig. 1. In this case folding segment (marked by I in Fig. 1) for a transfer of multiple charge states uranium ions between sections of LINAC-100 is required. One of the main restrictions for a transfer line is a demand of a zero dispersion function at the end of it. In this paper folding segment for a transfer of three charge states uranium ions between sections of LINAC-100 is presented.

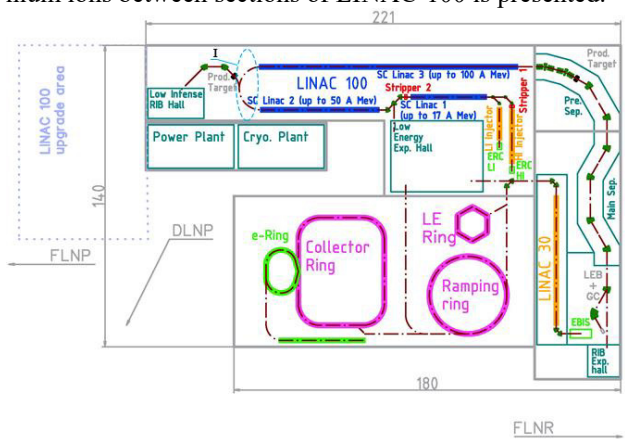


Figure 1: "Parallel" layout option of LINAC-100 for DERICA.

## TRANSFER LINE DESIGN

One of a designs for DERICA folding segment was already suggested in [6]. One more option of DERICA folding segment that is called as "current mirror" is presented here. The concept of "current mirror" is widely spread in electron optics. The discussed transfer line layout is presented in Fig. 2.

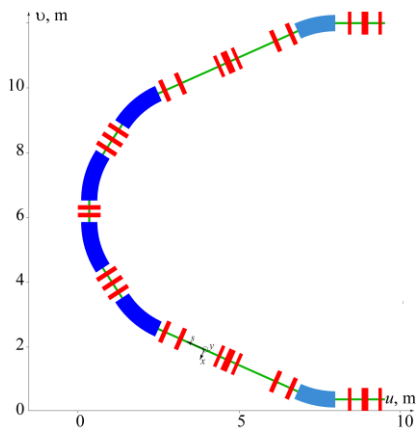


Figure 2: View of the folding segment for heavy ion transfer between sections of LINAC-100.

There are 3 families of quadrupoles and two (33° and 24°) bending magnet families in the transfer line that is a linear achromat. Main magnets parameters are presented in Table 1. Parameters were defined in order to transfer 35.7 MeV/nucleon $_{238}U^{60+}$ ions without transverse size increase and zero dispersion function at the beam exit.

ISBN: 978-3-95450-240-0 ISSN: 2673-5539 doi:10.18429/JACoW-RuPAC2021-MOPSA13

# COMPUTER SIMULATION OF THE MECHANICAL BEHAVIOR OF THE FFS SUPERCONDUCTING QUADRUPOLE COIL*

Y. Altukhov, A. Ageev, I. Bogdanov, S. Kozub, T. Ryabova, L. Tkachenko, A. Riabchikova,
NRC "Kurchatov Institute" – Institute for High Energy Physics, Protvino, Russia

*Abstract*

In the frame of the work, carried out at the Research Center of the Kurchatov Institute - IHEP on the development of four wide-aperture superconducting quadrupoles, a mathematical study of the mechanical behavior of the coil block of these magnets was carried out. The quadrupoles are intended for use in the magnetic final focusing system (FFS) of the ion beam in the experiments of the HED@FAIR collaboration [1, 2]. At the design stage of superconducting magnets, it is necessary to perform mathematical modeling to analyze the deformation of coil blocks during the assembly stages, cooling to operating temperature and the influence of ponderomotive forces. The results of computer simulation of changes in the geometry and distribution of forces in the coil block at all these stages are necessary to determine the value of the preliminary mechanical stress in the superconducting coil. The main results of numerical simulation of the mechanics of these magnets are presented in the article.

## INTRODUCTION

An international accelerator complex for ions and antiprotons is currently being created (FAIR, Germany, Darmstadt). The HED @ FAIR collaboration will conduct new experiments to study the fundamental properties of high energy density states in matter, generated by intense beams of heavy ions. To carry out these experiments NRC "Kurchatov Institute" - IHEP creates 4 superconducting (SC) quadrupole magnets for the final focusing system (FFS) of the ion beam.

To provide a focal spot of the order of 1 mm, these magnets must have a unique combination of a high magnetic field gradient of 38 T/m and a large inner diameter of the superconducting coil of 260 mm, the operating temperature of the magnets is 4.5 K.

Significant ponderomotive forces arise in the coil of such a magnet, which can transfer it to its normal state. To prevent this transition, the coil is compressed by the bandage with a force sufficient to compensate for the ponderomotive forces. To determine this effort, it is necessary to carry out mathematical modeling of the stress-strain state of the SC coil - bandage system during manufacture and operation.

The main steps taking place with the quadrupole coil block are:

1. Creation of a pre-stressed state under pressure in the coil-bandage system.
2. Fixing the position of the bandage with a key and relieving the press load.
3. Cooling from room to operating temperature.
4. Action on the coil of ponderomotive forces when current is injected into it.

## GEOMETRY QUADRUPOLE FFS

Figure 1 shows the cross section of the quadrupole FFS.

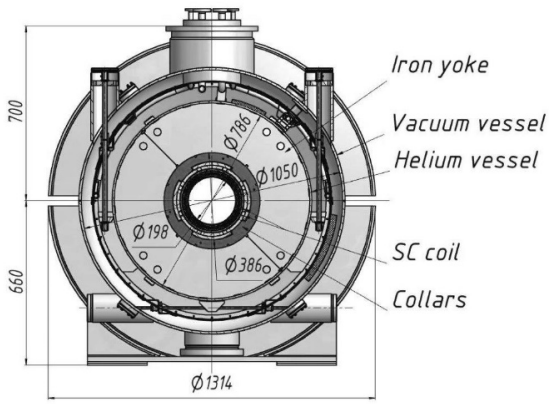


Figure 1: Cross section of the quadrupole FFS.

The main parameters of the quadrupole FFS are presented in Table 1.

Table 1: The Main Parameters of the Quadrupole FFS

| Parameter | Value |
|---|---|
| Operating mode | DC |
| Inner diameter of the coil | 260 mm |
| Central field gradient | 37.6 T/m |
| Nominal current | 5.73 kA |
| Magnetic field in the coil | 5.87 T |
| Stored energy | 1079 kJ |
| Vacuum vessel length | 2400 mm |
| Vacuum vessel diameter | 1400 mm |
| Cold mass of the quadrupole | ~6.5 t |
| Mass of quadrupole | ~10 t |

The cold mass inside the helium vessel, with the help of a two-layer superconducting coil, creates a magnetic field, while significant forces arise in the coil, which are compensated by the stainless steel collars (bandage) compressing the coil. Around the collars there is an iron yoke (magnetic shield) made of electrical steel plates. A helium vessel with a cold mass is attached to a vacuum vessel by means of a suspension system; between the walls of the vacuum vessel and the walls of the helium vessel there is a heat shield cooled by a helium flow having a pressure of 13 bar and an inlet temperature of 50 K.

* Work supported by the contract between FAIR and IHEP from 19.12.2016.

ISBN: 978-3-95450-240-0 ISSN: 2673-5539 doi:10.18429/JACoW-RuPAC2021-MOPSA14

# THE TECHNOLOGY BEHIND THE PRODUCTION OF DIFFERENT NICA COLLIDER MAGNETS

S. A. Korovkin†, H.G. Khodzhibagiyan, S.A. Kostromin, D.N. Nikiforov,
A.V. Merkurev, V.V. Borisov, M.V. Petrov, Y.G. Bespalov,
JINR, Dubna, Moscow Region, Russia

*Abstract*

The NICA collider magnetic system includes 70 quadrupole and 80 dipole superconducting (SC) magnets. The serial production and testing of these magnets are near to completion at the Veksler and Baldin Laboratory of High Energy Physics of the Joint Institute for Nuclear Research (VBLHEP, JINR). Manufacturing and assembly technology directly affects the quality of the magnetic field. The article describes the technology behind the production of different type of the NICA collider magnets.

## INTRODUCTION

NICA (Nuclotron-based Ion Collider fAcility) is a new acceleration-storage complex. It is under construction in JINR. Collider includes 80 dipole and 70 quadrupole twin-aperture superconducting magnets [1]. The collider is designed to work with operating energies 1.0, 3.0, and 4.5 GeV / nucleon, which correspond to the operating fields of dipole magnets 0.4, 1.2 and 1.8 T, respectively. Serial Production of these magnets started at JINR in 2013 [2]. The magnet includes a cold (4.5K) window frame iron yoke and a SC winding made of a hollow NbTi composite SC cable cooled with a two-phase helium flow.

## SC MAGNET PRODUCTION STAGES

The magnet production begins from the fabrication of the SC cable, which show in Fig. 1.

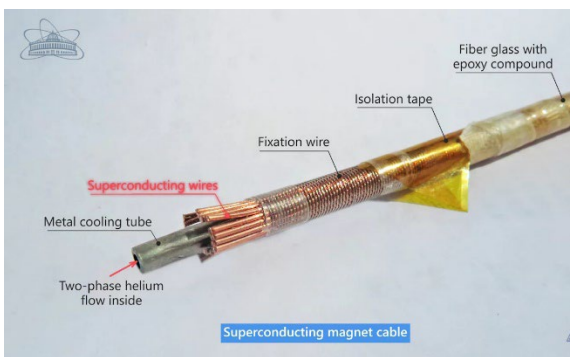


Figure 1: View of the hollow SC cable.

Superconducting wires are wrapped on a cooper- nickel tube and have with cooling tube reliable thermal contact provided by means of fixation wire. The cable is electrically insulated with Kapton tape and fiberglass tape impregnated with epoxy compound. Each SC wire contains 12600 Nb-Ti filaments of 8 microns in a copper matrix. This wire is made in Joint Stock Company "Chepetsk Mechanical Plant". The production of SC cable takes place in LHEP on a special cabling machine (see Fig. 2) when, in one pass, all SC cable components are wind.

Figure 2: Cabling machine for the manufacture of a hollow composite SC cable.

The wet cable is coil on a bobbin and is ready for SC winding production. The wet SC cable on a special rotary table is manually placed in the coil structure and wrapped with prepreg show in Fig. 3.

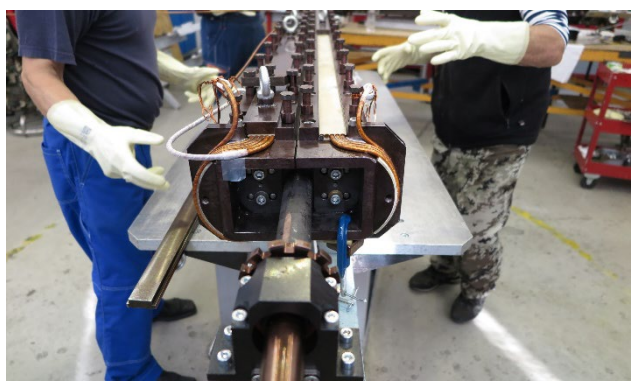

Figure 3: Equipment for baking the SC winding for the NICA collider dipole magnet.

The entire assembly is sent to an oven for baking at a specific temperature regime so that the epoxy compound polymerizes. After baking, the winding is ready for further tests, namely checking the electrical parameters and checking the geometric dimensions.

The iron yoke of the magnet consists of three parts that are bolted together. The yoke is fabricated of the laminated isotropic 0.65 mm thick electrical steel M 530. The laminations are compressed with specific pressure of 5 MPa and clamped together with stainless steel side plates 10 mm thick. The side plates are welded with laminations and 20 mm thick stainless steel end plates. After assembly and welding, yoke is processed on a high-precision machine,

† korovkins@jinr.ru

ISBN: 978-3-95450-240-0 ISSN: 2673-5539 doi:10.18429/JACoW-RuPAC2021-MOPSA15

# THERMODYNAMIC CHARACTERISTICS OF THE SUPERCONDUCTING QUADRUPOLE MAGNETS OF THE NICA BOOSTER SYNCHROTRON

A.A. Bortsova, H.G. Khodzhibagiyan, D.N. Nikiforov,
Joint Institute for Nuclear Research, Dubna, Russia

*Abstract*

The Booster synchrotron of the NICA accelerator complex in Dubna is designed for acceleration of heavy ions before injection into the Nuclotron. The first run of the Booster synchrotron was carried out in the end of 2020. This work presents calculated and experimental data of static heat leak and dynamic heat releases for quadrupole magnets of the Booster synchrotron with different configuration of the corrector magnets. Obtained results will be taken into account for development of new superconducting magnets and cryogenic installations.

## INTRODUCTION

The magnetic system of the booster synchrotron includes 40 dipole magnets, 16 doublets of quadrupole magnets with dipole corrector magnet (DCM) and 8 doublets of quadrupole magnets with multipole corrector magnet (MCM), a reference dipole and a reference doublet of quadrupole magnets.

Correction magnets are designed to correct the orbit and focus the beam. DCM consists of two dipole coils: horizontal and vertical. MCM has 4 coils: sextupole normal, octupole normal, sextupole skew and quadrupole skew.

The magnets produced at JINR are subjected to cryogenic tests, one of the main stages of which is the measurement of static heat leak and dynamic heat releases.

## STATIC HEAT LEAK

The calculated total static heat input to the SC magnet is determined as the sum of the heat input by thermal radiation, thermal conductivity of residual gases and along thermal bridges.

### *Thermal Radiation*

For the considered SC magnets, the heat leak includes radiation from the inner surface of the thermal shield at 80 K to the magnet yoke at 4.6 K and the vacuum shell at 300 K to the magnet yoke through the technological holes in the thermal shield for the magnet suspension system and the vacuum system. The heat transmitted by thermal radiation is calculated using the Stefan-Boltzmann Eq. (1) [1]:

$$Q_l = \varepsilon_n C (T_2^4 - T_1^4) A, \qquad (1)$$

where $\varepsilon_n$ – emissivity; $C$ – Stefan-Boltzmann constant,$\mathrm{W/m^2K}$; $T_2$, $T_1$ – temperature of warm and cold surfaces; $A$– surface area of the thermal radiation, $\mathrm{m^2}$.

### *Heat Leak by Thermal Conductivity of Residual Gases*

The heat leak by thermal conductivity of residual gases for vessels can be calculated using the Eq. (2) [1]:

$$Q_g = 1.82 \cdot 10^5 A_1 \frac{\alpha_1 \alpha_2}{\alpha_2 + \frac{A_1}{A_2}(1-\alpha_2)\alpha_1} \frac{k+1}{k-1} \frac{p(T_2 - T_1)}{\sqrt{MT}}, \qquad (2)$$

where $A_1$, $A_2$– surface area of the inner and outer vessel, $\mathrm{m^2}$; $\alpha_1$, $\alpha_2$– accommodation coefficient for the first and second gas in the vessel; $k$ – adiabatic exponent; $p$ – vessel pressure, Pa; $M$ – molecular weight of gas mixture; $T$- pressure gauge temperature, K. The mixture of nitrogen and helium is taken as the residual gas in the insulating volume of the vacuum shell.

The calculated value of the heat input by the thermal conductivity of the residual gases is 0.02 W.

### *Heat Along the Thermal Bridges*

Static heat leak through thermal bridges is determined from the heat transfer equation:

$$Q_t = \lambda \Delta T \frac{S}{l}, \qquad (3)$$

where $\lambda$ – thermal conductivity coefficient, $\mathrm{W\,m^{-1}\,K^{-1}}$; $S$ – thermal bridge cross-sectional area, $\mathrm{m^2}$; $\Delta T$ – temperature difference, K; $l$ – thermal bridge length, m.

The SC magnets of the NICA accelerator complex are fixed in the cryostat using eight rods. After the magnet cools down to operating temperature, a large temperature gradient from 293 K to 4.5 K appears in the rods. Then the calculated static heat leak to the magnet by eight rods is 2.9 W. To reduce this value, thermal bridge to the thermal shield is provided in the design of the SC magnet (see Fig. 1), due to which the temperature gradient in the rods decreases from 82 K to 4.5 K. This reduces static heat leak to the SC magnet from 2.9 to 1 W.

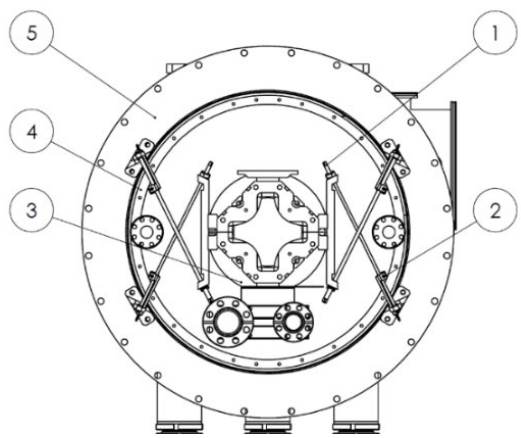


Figure 1: Quadrupole magnet of the booster synchrotron in the cryostat: 1 – rod; 2 – thermal bridge to the thermal shield; 3 – yoke of the SC magnet (4.5 K); 4 – thermal shield (82 K); 5 – vacuum chamber (293 K).

ISBN: 978-3-95450-240-0 ISSN: 2673-5539 doi:10.18429/JACoW-RuPAC2021-MOPSA16

# DESIGN AND CHARACTERISTICS OF CRYOSTAT FOR TESTING OF LOW-BETA 325 MHz HALF-WAVE RESONATORS

D. Bychanok[1]*, S. Huseu, E.Vasilevich, A. Sukhotski, V. Bayev, S. Maksimenko,
Research Institute for Nuclear Problems of Belarusian State University, Minsk, Belarus
M. Gusarova, M. Lalayan, S. Polozov,
National Research Nuclear University MEPhI, Moscow, Russia
A. Shvedov, S. Yurevich, V. Petrakovsky, A. Pokrovsky,
Physical-Technical Institute, Minsk, 220141, Belarus
D. Nikiforov, A. Butenko, E. Syresin, Joint Institute for Nuclear Research, Dubna, Russia
[1]also at Tomsk State University, Tomsk, Russia

*Abstract*

Design of the cryomodule prototype for testing low-beta 325 MHz half-wave cavities is currently in the process at INP BSU. The cryomodule allows performing intermediate vacuum-, temperature-, and rf-tests during the fabrication of half-wave resonators. The first experimental results of cryomodule cooling down to liquid nitrogen temperatures are presented and discussed. The pressure and temperature control allows us to estimate the main cooling/heating characteristics of the cryostat at different operation stages. The presented test cryomodule will be used for further development and production of superconductive niobium cavities for the Nuclotron-based Ion Collider fAcility (NICA) injector.

## INTRODUCTION

The first stages of the fabrication process and properties control of superconductive cavities for high energy particle acceleration are performed at room temperature. The intermediate rf-measurements allow to control of the resonant frequency during initial "warm" tests [1]. Since the niobium-based cavities operate at liquid helium temperatures their resonant frequency significantly differs from intermediate room temperature measurements. The complexity of the half-wave resonators(HWR) geometry and a large number of welds make it difficult to estimate the shrinkage and frequency shift when the resonators are cooled to cryogenic temperatures.

The difference between the cavity's resonant frequency at room and at cryogenic temperatures is one of the most important experimental parameters related to the fabrication of resonators. To determine this parameter, it is necessary to develop a test cryostat that provides temperature and vacuum conditions close to the operational characteristics in the particle accelerator.

The test cryostats are widely used for research purposes in the manufacture of resonators [2, 3]. The present communication is devoted to the cryostat design for testing of low-beta 325 MHz half-wave resonators. In the next sections, we will discuss the main features of the cryostat design and the most important results obtained from a preliminary experiment on cooling to liquid nitrogen temperature.

* dzmitrybychanok@yandex.by

## TEST CRYOSTAT DESIGN

The test cryomodule should be designed to effectively perform intermediate vacuum-, temperature- and rf-tests of HWR. Additionally, the geometrical parameters of the cryostat should provide enough space to test different types of frequency tuning systems and other support devices like power coupler, field probe antenna, etc.

The proposed concept of test cryostat consists of standard cryogenic parts [4, 5] including stainless vacuum chamber, liquid nitrogen ($LN_2$) inputs, liquid helium (LHe) inputs, rf inputs for cavity electromagnetic response measurements, $LN_2$ shield, etc. The model of the cryostat with a cavity inside is presented in Fig.1 (a-b).

In Fig.1(b) the vacuum chamber providing a protective vacuum (residual pressure ~ $10^{-6}$ bar) around the resonator. The main heat flux from the environment is screened by a $LN_2$ shield. It is cooled by a liquid nitrogen subsystem (blue pipes in Fig.1(b)). The integrated helium vessel of HWR is connected to the liquid helium subsystem (yellow pipes in Fig.1(b)). The cavity is mounted inside the cryomodule using two thin stainless steel spokes that are attached to the top cover of the cryostat. The spokes pass through the nitrogen shield and have good thermal contact with it.

The proposed system has an inner length $L = 830$ mm and an inner diameter of $D = 890$ mm. The peripheral devices (power coupler, frequency tuning system, etc.) can also be partially located in the additional volume of the side pipes.

In Fig.2 (a,b) are presented fabricated cryostat and thermal $LN_2$ shield inside them.

$LN_2$ shield was fabricated from 3mm thick aluminium type AMc. The copper pipe of the $LN_2$ system was brazed to the cylindrical part of the $LN_2$ shield to provide good thermal contact. The outer surface of the $LN_2$ shield was covered by multilayered thermal isolation. The shape of the copper pipe of the $LN_2$ system provides gaseous nitrogen to the area of cryogenic inputs on the top of the cryomodule. Vacuum, rf, and electrical inputs are located on the right side of the cryostat.

In the next section, we present the first experimental results of cryostat temperature and pressure tests.

ISBN: 978-3-95450-240-0 ISSN: 2673-5539 doi:10.18429/JACoW-RuPAC2021-MOPSA17

# AUTOMATED SYSTEM FOR HEATING ULTRA-HIGH VACUUM ELEMENTS OF SUPERCONDUCTING SYNCHROTRONS OF THE NICA COMPLEX

A.Sergeev, A.Butenko, A.Svidetelev, JINR, Dubna

*Abstract*

The Nuclotron-based Ion Collider fAcility that is under construction and commissioning in the Veksler - Baldin Laboratory for High Energy Physics of JINR contains three superconducting synchrotrons, three detectors and several beam transfer lines. All these installations and devices are equipment of high and ultra-high vacuum that requires standard procedure of preparation: preliminarily degassing the "warm" sections of the vacuum systems of the synchrotrons by prolonged heating to remove water vapor from the inner surface of the walls of the beam chamber. The heating system for the "warm" sections of the beam chambers allows one to heat up individual sections of the accelerators with minimal time spent and maximum efficiency. Due to the fact that the Booster and Collider are experimental facilities of original design, they consist of many "warm" areas. Each such element is an experimental, which has an peculiar exterior form and is made of specific composition of materials.

## INTRODUCTION

The system being created allows heating elements with an unknown heat capacity and thermal conductivity, which is a very urgent task, since some of the installations are delivered without their own heating system and heating is carried out by the specialists of VBLHEP JINR directly at the place where installation is mounted.

A new method has been developed for correcting the parameters of the power supplied to the heating elements, depending on the temperature of the surface of the heated element. Since in such systems (installations) it is impossible to use high-speed proportional-integral-differentiating controllers (hereinafter PID) due to possible overheating and, consequently, destruction of installation elements due to different coefficients of thermal expansion of different interconnected elements, the algorithm is additionally used correction, which prevents overheating of individual components of the system.

## FEATURES OF THE DEVELOPED SYSTEM

- Temperature control of critical elements of the heated system.
- Control of the heating process by introducing feedbacks from temperature sensors, which allows automatically, according to the set parameters of the heating process, to control the speed and intensity of heating of accelerator elements.
- The temperature control of the installation is carried out along the heated surface, which allows evenly heating parts of various shapes and lengths.
- Optimization of the heating process due to the implementation of the connection between the cabinets of different devices, which allows combining several cabinets into a single system that heats up one complex installation as a whole.
- Flexibility of controllability of system parameters, directly in the process of work (warm-up).
- The ability to exclude individual elements from the heating zones, which allows you to concentrate power on certain areas of the heated equipment.
- Automated operational control of a non-staff set of heaters or other equipment (vacuum pumps, gates, etc.).
- Automatic processing of the progress of the heating process and its results, which makes it possible to generate the final product heating certificate.

Within the framework of the NICA project, the following elements of the Booster were heated: numerous high-vacuum posts, RF stations, beam pipe, Septum.

ISBN: 978-3-95450-240-0 ISSN: 2673-5539 doi:10.18429/JACoW-RuPAC2021-MOPSA23

# MACHINE LEARNING FOR THE STORAGE RING OPTIMIZATION

Ye. Fomin†, NRC "Kurchatov Institute", Moscow, Russia

*Abstract*

The design and optimization of new lattices for modern synchrotron radiation sources are for the most part art and highly dependent on the researcher's skills. Since both modern existing and designing storage rings is a very complex nonlinear system the researchers spend a lot of effort to solve their problems. In this work, the use of machine learning technics to improve the efficiency of solving nonlinear systems optimization problems is considered.

## INTRODUCTION

There are many methods of optimization. All of them can be divided into three groups: determinate, random (stochastic), and combined. It is advisable to use algorithms from each group to solve their group of problems. Different task solving optimization efficiency using different algorithms is presented in Fig. 1.

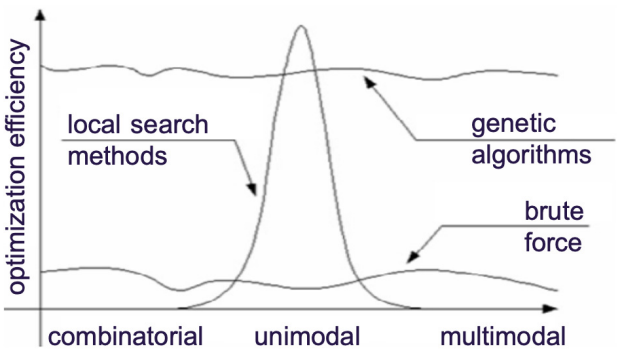


Figure 1: Different task solving optimization efficiency.

Most accelerators and synchrotron radiation sources optimization problems can be attributed to islands of combinatorial problems with many different quality solutions inside an island and between them. An exhaustive search of all solutions or an only subset of solutions is the main feature of combinatorial algorithms. To find the best solution directed, random, and combined an exhaustive search of all possible problem variables is used. Therefore, the search for proper solutions often becomes art. Because very often if you want to optimize nonlinear problem with many variable parameters and restrictions you will face serious difficulties (most rapid and effective optimization methods can't be used, there are many local minima solutions, solving time is directly related to the number of variable parameters, etc.).

So, as you can see in Fig. 1 one of the effective ways to solve multimodal and combinatorial problems within a reasonable time is the use of genetic algorithms. Genetic algorithms are heuristic search algorithms used to solve optimization problems by random selection, combining, and modification of desired parameters using a process like biological evolution. Evolution, as in nature, is an iterative process. The new population from each iteration is referred to as a "generation." The process generally starts with a population that is randomly generated and the fitness of the individuals is evaluated. Individuals with greater/smaller fitness are randomly selected, and their genomes are modified to form the next generation. The average fitness of each generation, therefore, increases/decreases with each iteration of the algorithm. Commonly, the algorithm terminates when either a maximum number of generations has been reached, or a satisfactory fitness level has been achieved for the population.

A genetic algorithm can be used to solve both constrained and unconstrained optimization problems. It likes any other optimization algorithms have their advantages and disadvantages. Their most important advantages may be said to be:

- Any information about the fitness function behavior is not required.
- Discontinuities of the fitness function don't have a significant effect on optimization.
- Methods are relatively stable to fall into local minima.

Their most important disadvantages may be said to be:

- Methods are inefficient for optimizing fitness functions that have a long calculation time.
- A large number of parameters often turns «work with genetic algorithm» to «play with genetic algorithms».
- In the case of simple fitness functions, genetic algorithms are slower than specialized optimization algorithms.

Nowadays, genetic algorithms are powerful computing tools to solve different multidimensional optimization problems. So, the use of genetic algorithms for accelerator and light source optimization allows simplifying and speeds up the search of proper solutions. That's why they have become popular in the accelerator physicist community. The common block diagram for the optimization process using genetic algorithms is shown in Fig. 2.

The long computation time of the fitness function, constraints, and discontinuities are the main features of optimization problems of modern synchrotron radiation sources. When solving this class of problems, any optimization algorithms begin to lose their effectiveness, the time to find satisfactory solutions increases dramatically, and the task of becoming practically unsolvable. To overcome these difficulties, it is necessary to simplify the original problem, divide it into subproblems, reduce the number of variables and the scope of their definition, etc. As a result, the optimization problem becomes solvable but the search time for satisfactory solutions is mainly not reduced.

† yafomin@gmail.com

ISBN: 978-3-95450-240-0 ISSN: 2673-5539 doi:10.18429/JACoW-RuPAC2021-MOPSA29

# APPLIED RESEARCH STATIONS AND NEW BEAM TRANSFER LINES AT THE NICA ACCELERATOR COMPLEX*

A. Slivin†, A. Agapov, A. Baldin, A. Butenko, G. Filatov, A. Galimov, S. Kolesnikov, K. Shipulin, E. Syresin, A. Tikhomirov, G. Timoshenko, A. Tuzikov, V. Tyulkin, A. Vorozhtsov, Joint Institute for Nuclear Research, Dubna, Russia
T. Kulevoy, Y. Titarenko, Institute for Theoretical and Experimental Physics of National Research Centre "Kurchatov Institute", Moscow, Russia
D. Bobrovskiy, A. Chumakov, S. Soloviev, Specialized Electronic Systems (SPELS) and National Research Nuclear University (NRNU) "MEPHI", Moscow, Russia
A. Kubankin, Belgorod State University, Belgorod, Russia
P. Chernykh, S. Osipov, E. Serenkov, Ostec Enterprise Ltd, Moscow, Russia
S. Antoine, W. Beeckman, X. Guy Duveau, J. Guerra-Phillips, P. Jehanno, A. Lancelot, SIGMAPHI S.A., Vannes, France
I. Glebov, V. Luzanov, LLC "GIRO-PROM" (GIRO-PROM), Dubna, Russia

*Abstract*

Applied research at the NICA accelerator complex include the following areas that are under construction: single event effects testing on capsulated microchips (energy range of 150-500 MeV/n) at the Irradiation Setup for Components of Radioelectronic Apparature (ISCRA) and on decapsulated microchips (ion energy up to 3,2 MeV/n) at the Station of CHip Irradiation (SOCHI), space radiobiological research and modelling of influence of heavy charged particles on cognitive functions of the brain of small laboratory animals and primates (energy range 500-1000 MeV/n) at the Setup for Investigation of Medical Biological Objects (SIMBO). Description of main systems and beam parameters at the ISCRA, SOCHI and SIMBO applied research stations is presented. The new beam transfer lines from the Nuclotron to ISCRA and SIMBO stations, and from HILAC to SOCHI station are being constructed. Description of the transfer lines layout, the magnets and diagnostic detectors, results of the beam dynamics simulations are described given.

## INTRODUCTION

NICA (Nuclotron-based Ion Collider fAcility) is a new accelerator complex being constructed at the Laboratory of High Energy Physics of the Joint Institute for Nuclear Research [1]. Within the framework of the NICA project, it is planned to create three experimental stations for conducting of applied research with long-range ion beams extracted from the Nuclotron, and short-range ion beams extracted from the heavy ion linear accelerator (HILAC) [2].

## NEW BEAM LINES IN MEASUREMENT HALL OF VBLHEP JINR

Two new areas are organized within the framework of the NICA applied research program.

Special area 1 includes beam channel (Fig. 1) to SOCHI station.

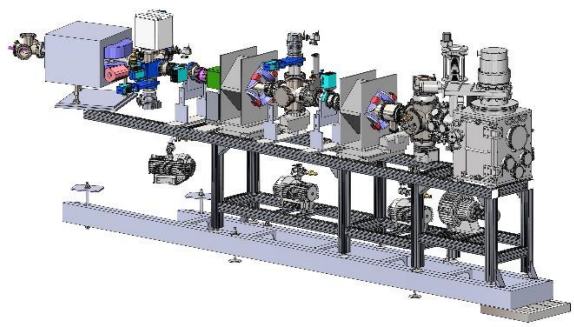

Figure 1: SOCHI beam channel design.

Special area 2 includes two beam channels to SIMBO and ISCRA stations. Beam channels are being developed as part of the JINR-SIGMAPHI collaboration. These channels will be integrated into the existing Nuclotron-to-VP-1 extraction beam line (Fig. 2).

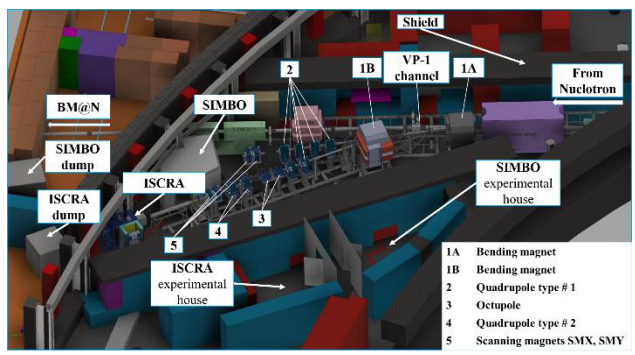


Figure 2: Area 2 infrastructure layout.

## BEAM DYNAMICS SIMULATIONS

One of the main conditions required for irradiation of samples is the beam distribution homogeneity at the target area.

* Work supported by grant for young scientists. Unique id 21-102-09
† slivin@jinr.ru

ISBN: 978-3-95450-240-0 ISSN: 2673-5539 doi:10.18429/JACoW-RuPAC2021-MOPSA39



# APPLICATION OF A SCINTILLATION DETECTOR FOR PERIODIC MONITORING OF BEAM PARAMETERS AT MEDICAL PROTON THERAPY COMPLEX «PROMETHEUS»

A.E. Shemyakov†[1], M.A. Belikhin[1,2], A.A. Pryanichnikov[1,2]
Lebedev Physical Institute RAS, Physical-Technical Center, Protvino, Russian Federation
A.I. Shestopalov, Protom Ltd., Protvino, Russian Federation
[1]also at Protom Ltd., Protvino, Russian Federation
[2]also at Lomonosov Moscow State University, Accelerator Physics and Radiation Medicine Department, Moscow, Russian Federation

*Abstract*

In November 2015 the first domestic complex of proton therapy "Prometheus" start to treat oncology patients. This complex uses a modern technique for irradiation of tumours by scanning with a pencil beam. This technique requires continuous monitoring and regular verification of main beam parameters such as range in water, focusing and lateral dimension. To control these parameters, we developed a waterproof detector for measurements in air and in a water phantom.

The detector system consists of a luminescent screen 5 cm in diameter, a mirror and a CCD camera. When the beam goes through the screen, a glow appears, the reflected image of which is perceived by the camera and analysed. This design is waterproof, which makes it possible to perform measurements in water. To measure the range of protons in water, this detector was fixed on a special positioner, which allows to move the sensor with an accuracy of 0.2 mm. We measured the beams also in comparison with EBT3 dosimetry film for energies from 60 to 250 MeV with a step of 10 MeV. Same measurements of the ranges were carried out using a standard PTW Bragg Peak ionization chamber.

It was shown that this system is a simple and inexpensive tool for conducting regular quality assurance of beam parameters. Unlike the EBT3 dosimetry film, this detector gives an immediate response, which makes it possible to use it when debugging the accelerator and adjusting the beam.

## INTRODUCTION

Proton therapy is receiving close attention from radiation oncologists around the world [1]. The research beams of large physics scientific centers adapted for medical purposes have been replaced by specialized medical proton facilities. In November 2015 the first domestic complex of proton therapy "Prometheus" start to treat oncology patients. It is the first specialized medical proton facility put into clinical operation in Russia (Fig. 1). «Prometheus» based on an original synchrotron with a diameter of 5 meters, which makes it possible to obtain proton beams with energy smoothly varying in the range of 30-330 MeV. The active scanning beam of the «Prometheus» synchrotron provides high conformity of the irradiation. This small spots can be used to build intensity modulated proton therapy treatment plans. But this benefit requires accurate tuning and quality assurance procedures of main beam parameters such as range in water, focusing and lateral dimension. For these purposes, a number of special equipment is used in radiation therapy. There are devices for determining the exact range of the particles, such as variable water column “Peakfinder” (PTW) or multi-layer ionisation chamber “Giraffe” (IBA Dosimetry). To assess the size of the beam and its symmetry, film dosimetry or scintillation screen detectors are mainly used [2-7]. All this devices have some limitations. For example, it requires scanning and processing of film dosimetry, which significantly increases the time of the study.

We developed a waterproof detector for measurements in air and in a water phantom that can be used in routine practice.The purpose of this work was to investigate the performances of own development scintillator detector with comparison of PTW Bragg Peak ionisation chamber and EBT3 film dosimetry.

Figure 1: Proton therapy facility «Prometheus».

## MATERIALS AND METHODS

For calibration procedures we developed a detection system for measuring the geometric parameters of the beam spot in the energy 50-330 MeV. It consists of 50 mm diameter scintillation screen based on gadolinium oxysulfide, installed perpendicular to the proton beam, a mirror and a CCD camera (Fig. 2). The distance between the camera and the mirror is large enough to minimize the distortion of the

† alshemyakov@yandex.ru

ISBN: 978-3-95450-240-0 ISSN: 2673-5539 doi:10.18429/JACoW-RuPAC2021-MOPSA40

# THE PIPLAN PROTON-CARBON ION RADIATION THERAPY PLANNING SYSTEM

A. A. Pryanichnikov†[1,2], A. S. Simakov[1],
Lebedev Physical Institute RAS, Physical-Technical Center, Protvino, Russian Federation
I. I. Degtyarev, F. N. Novoskoltsev, O. A. Liashenko, E. V. Altukhova, R.Y. Sinyukov
Institute for High Energy Physics named by A.A. Logunov of NRC "Kurchatov Institute", Protvino, Russian Federation
[1]also at Protom Ltd., Protvino, Russian Federation
[2]also at Lomonosov Moscow State University,
Accelerator Physics and Radiation Medicine Department, Moscow, Russian Federation

*Abstract*

This paper describes the main features of newest version of the Proton-Carbon Ion Radiation Therapy Planning System (PIPLAN). The PIPLAN 2021 code was assigned for precise Monte Carlo treatment planning for heterogeneous areas, including lung, head and neck location. Two various computer methods are used to modeling the interactions between the proton and carbon ion beam and the patient's anatomy to determine the spatial distribution of the radiation physical and biological dose. The first algorithm is based on the use of the RTS&T 2021 high precision radiation transport code system. The second algorithm is based on the original Ulmer's method for primary proton beam and adapted Ulmer's algorithm designed for primary carbon ion beam with energy in the range 100-450 MeV/u.

## INTRODUCTION

Today in Russia there are no heavy ion accelerators used in cancer therapy [1]. On the basis of SRC IHEP of NRC "Kurchatov institute" Accelerator Complex U-70 it is planned to create a Ion Beam Therapy Center using the 200-450 MeV/u $^{12}C^{6+}$ ion beams. Currently, a Radiobiological Workbench (RBC) U-70 was created and successfully operated It is shown in Fig. 1.

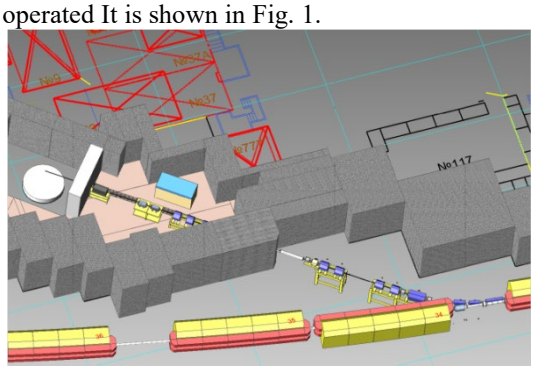


Figure 1: Layout of equipment in the RBC beam transfer line of the U-70 Accelerator Complex.

One of the important areas is the creation of a Radiotherapy Treatment Planning system. The purpose of Radiotherapy Treatment Planning systems is to estimate the dose absorbed by a patient in a radiotherapy session, so that tumors can be irradiated with the strictly necessary dose. Many publications have proved Monte Carlo techniques as a highly accurate dose calculation tool, having the only limitation of computing time cost. Several Monte Carlo based treatment planning systems have been developed and tested at the IHEP U-70 facility for carbon ion therapy. The irradiation of the water phantom has been simulated with the RTS&T and PIPLAN codes.

† pryanichnikov@protom.ru

## ION BEAM TREATMENT PLANNING SYSTEM (PIPLAN 2021)

The PIPLAN 2021 Treatment Planning System consist 2 independent methods to Monte Carlo simulation the spatial distribution of the radiation physical and biological dose.

### *The RTS&T 2021 Precision Simulation Algorithm*

The RTS&T [2] code (Radiation Transport Simulation and Isotopes Transmutation Calculation) was assigned for detailed Monte Carlo simulation of many particle types (γ, $e^{\pm}$, p, n, $\pi^{\pm}$, $K^{\pm}$, $K_L^0$,, antinucleons, muons, ions and etc.) transport in a complex 3D geometry's with composite materials in the energy range from a fraction eV to 20 TeV and calculation of particle fluences, radiation field functionals and isotopes transmutation problem as well. A direct using of evaluated nuclear data libraries (data-driven model) (ENDF/B, JENDL, ROSFOND, BROND, TENDL etc. - total 14 libraries) to N, d, t, $^3$He,$^4$He particles transport and isotopes transmutation modeling in low and intermediate (E<200 MeV) energy regions is the idea of the RTS&T code construction. In general, this approach is limited by the available evaluated data to particle kinetic energies up to 20 MeV, with extensions up to 30 MeV or 200 MeV.

### *Adapted Ulmer's Fast Simulation Algorithm*

The original Ulmer's method that is designed for incident proton beam up to 400 MeV [3] was adapted for primary carbon ion beam up to 450 MeV/u. We have developed a model for carbon ion depth dose and lateral distributions based on Monte Carlo highly accurate calculations (RTS&T 2021 code). The model accounts for the transport of primary particles, the creation of recoil pro-

ISBN: 978-3-95450-240-0 ISSN: 2673-5539 doi:10.18429/JACoW-RuPAC2021-MOPSA41

# EFFECT OF A PROTON BEAM FROM A LINEAR ACCELERATOR FOR RADIATION THERAPY

L. Ovchinnikova*[1], S. Akulinichev, A. Durkin, A. Kolomiets, V. Paramonov
INR RAS, Moscow, Russia
A. Kurilik, Moscow, Russia
[1]also at Ferrite Domen Co., St. Petersburg, Russia

*Abstract*

Linear accelerators can provide beam characteristics that cannot be achieved by circular accelerators. We refer to the concept of a compact linac for creating a proton accelerator with a maximum energy of 230 MeV, operating in a pulsed mode. The linac is designed to accelerate up to $10^{13}$ particles per 10 to 200 seconds irradiation cycle and is capable of fast adjustment the output energy in the range from 60 to 230 MeV, forming a pencil-like beam with a diameter of ~2 mm. Simulation of dose distribution from a proton beam in a water phantom has been performed. The radiological effect of the linac beam during fast energy scanning is considered, and the features for providing the high dose rate FLASH radiation therapy are specified. The possibility of a magnetic system for increasing the transverse dimensions of the beam-affected region is discussed.

## INTRODUCTION

### *Cancer*

Cancer is the second leading cause of death worldwide, as noted by the World Health Organization [1]. The probability of cancer in general population is dependent on genetic predisposition, gender, age, environmental factors, lifestyle and past illnesses [2, 3]. Various preventive strategies, early diagnosis, efficiency and accessibility of applicable types of treatment contribute to the odds of a favorable outcome.

### *Proton Therapy*

Radiation therapy is one one of the most widely used non-surgical methods of malignant tumor treatment. External beam radiation therapy is the method of choice when dealing with deep pathological foci. Gamma rays from various radiation sources, bremsstrahlung photons and electrons produced by electron accelerators, and protons, neutrons and ions originating from hadron accelerators provide the required penetration into body tissue. Proton beams allow to achieve good localization of therapeutic dose delivery while minimizing collateral damage to healthy tissue [4].

### *Linac Advantages*

Linear accelerators provide numerous advantages over circular accelerators. Combination with gantry is possible [5]. This type of accelerator enables precise beam energy modulation while eliminating the necessity for auxiliary energy changes. It also eliminates the losses, parasitic material activation and elevated background radiation levels associated with beam extraction from circular orbits. In this work, we focus on the linear proton accelerator concept, as described in [6].

## DOSE DELIVERY

There are several methods of dose distribution forming in patient's body, used throughout the long-standing history of proton therapy, passive scattering being the most traditional one, and involving the use of collimation and compensation equipment. This method causes excessive patient irradiation by nuclear reaction products and necessitates safe storage of single-use collimators and compensators before disposing or recycling.

Beam scanning method eradicates these inconveniences and allows to apply almost arbitrary dose distribution [7, 8]. Also, proton arc therapy is promising [9, 10].

## BEAM MANIPULATION

Most of the units put in operation over the past five years in the USA make use of gantries and Pencil Beam Scanning [11]. In this work, we focus on Pencil Beam Scanning with energy up to 250 MeV. Consequently, beam transportation and dose distribution forming are the most important research objectives.

Non-linear magnetic systems are often used to achieve uniform lateral dose distribution. A single non-linear magnet can be used for uniform dose distribution in a single plane [12]. Such magnets are designed for specific mean-square beam radius, [13] describing an auxiliary mechanical device for additional field tuning. Such device allows a beam be stretched into a line in a single plane, e.g. horizontal. This way, scanning can be used in a vertical plane, facilitating strip scanning, similarly minibeam [14, 15].

We also consider the use of dual scanning magnets in vertical and horizontal planes [16], this type of installation providing the most simple and versatile irradiation method. We also take into account that additional simulation is necessary when choosing the best method to achieve the desired distribution when dealing with distant tumor patches. A magnetic multipole combination [17–20] should be used when uniform distribution is desired. Such combination allows for wide beam energy range, facilitating beam width modulation. One can also use permanent magnets when designing achromatic turn only beam transportation system [21].

* lub.ovch@yandex.ru

ISBN: 978-3-95450-240-0 ISSN: 2673-5539 doi:10.18429/JACoW-RuPAC2021-MOPSA42

# COMPACT S-BAND ACCELERATING STRUCTURE FOR MEDICAL APPLICATIONS

A.A. Batov, R.A. Zbruev, M.A. Gusarova, M.V. Lalayan, S.M. Polozov,
National Research Nuclear University MEPhI, Moscow, Russia

*Abstract*

This paper describes electromagnetic design results for the compact 6.3 MeV electron linac for the radiation therapy facility. Linac is based on S-band biperiodic accelerating structure with inner coupling cells with an increased coupling coefficient.

## INTRODUCTION

Biperiodic accelerating structures with on-axis coupling cells with high cell-to-cell coupling coefficients have been developed in NRNU MEPhI since 2010 [1-5]. The joint team of CORAD and MEPhI has constructed a linear electron accelerator for industrial applications based on the developed structures [6, 7]. That accelerator was successfully launched, tested and put into operation in 2015 [8]. Linac has high electrical efficiency, narrow beam energy spectrum, provides energy regulation, and low accelerated beam losses. It is based on 2856 MHz biperiodic accelerating structure for the energy range from 7.5 to 10 MeV and beam power up to 20 kW. The klystron TH2173F (Thales Electron Devices) was used for linac RF feed. It provides up to 5 MW of pulse power for 17 μs RF pulses duration and up to γ 6 kW of averaged power. Another two accelerators have been manufactured, installed at EB-Tech Company site in Daejeon, Republic of Korea, and at "Rodniki" Industrial Park, Ivanovo Region, Russia, and successfully tested [8].

This paper presents biperiodic accelerating structure with inner coupling cells with an increased coupling coefficient. It was developed for compact 6.3 MeV electron linac for radiation therapy facility. The power source that is planned to use is 3 MW magnetron MI456B or E2Vmg7095. The operating frequency of these sources are 2997.8 MHz. Since the accelerating structures should be tuned to the source frequency, the operating frequency of the linac should be set at 2997.8±1.0 MHz.

The structure was based on the MEPhI and CORAD designed S-band linac operated at 2856 MHz design with relatively large cell-to-cell coupling coefficient [3]. Structures operating at frequency of 2856 MHz have one more advantage: the production technology was earlier developed and is ready [8]. However, the 2856 MHz structures cannot be used in the facility under development due to the fact that operating frequency does not correspond to power source one. For this reason, the accelerating structure geometry was scaled in order to reach the 2997.8 MHz RF frequency, while keeping the coupling coefficient of at least 8% and reach the highest possible shunt impedance.

The optimization of the structure in order to increase the shunt impedance is necessary because of power source limitations and necessary beam parameters to be met.

Accelerating section of this linac has been designed under the strict limitations on the facility length and ratio of electromagnetic fields values in bunching cells. Linac technical requirements are summarized below in the Table 1.

The geometry of the structure is developed according to the beam dynamics simulation results and the electrodynamic parameters requirements. The longitudinal dimensions were calculated from beam dynamics. The angle and depth of the drift tube cones and the diaphragm thickness were selected on the basis of the original structure and were kept unchanged due to the fact that the overvoltage factor value in the base structure was low enough for fast conditioning and stable operation.

Table 1: Technical Requirements for Accelerating Structures of the Compact 6.3 MeV Electron Linac for Radiation Therapy Facility

| Parameter | Value | Unit |
|---|---|---|
| Total length | 400< | mm |
| Number of bunching cells | 3 | |
| Number of regular cells | 5 | |
| Operating frequency | 2997.8 | MHz |
| Coupling coefficient | 8…10 | % |
| Shunt impedance | 65…90 | MΩ/m |
| Total Loss | 1.6< | MW |
| Ratio of EM field values in buncher | 0.4…1 | |
| RF Power source | 3 | MW |

## REGULAR CELLS

Dimensions of regular cells were adjusted by scaling [5] the original structure [3] in order to achieve the required values of the cell operating frequency, shunt impedance and the coupling coefficient. Then the particular dimensions were adjusted to make the result more precise. Fine tune was done using electromagnetic field simulation software CST Studio Suite [9]. The cell tuning was considered successful when the value of the accelerating field in the coupling cells turned out to be zero upon reaching the above parameters.

The coupling coefficient and the shunt impedance values were adjusted using the position and the area of the coupling slots. The obtained electrodynamic characteristics are presented in Table 2.

The geometry of the regular cell, electric field topography and the accelerating field distribution along the tuned cavity axis for 1 J of stored energy respectively are presented on the Fig. 1.

ISBN: 978-3-95450-240-0 ISSN: 2673-5539 doi:10.18429/JACoW-RuPAC2021-MOPSA44

# CONCEPTUAL PROJECT OF THE PROTON BEAM LINES IN THE NUCLEAR MEDICINE PROJECT OF THE "KURCHATOV INSTITUTE" - PNPI

D.A. Amerkanov, S.A. Artamonov, E.M. Ivanov, V.I. Maximov, G.A. Riabov, V.A. Tonkikh†, NRC KI-PNPI, Gatchina, Russia

*Abstract*

The paper presents the calculation and layout of the beam transport lines to the target stations, the operation mode of the magnetic elements and beam envelopes. The method of the proton beam formation for ophthalmology and its parameters are described.

## INTRODUCTION

The project of a nuclear medicine complex based on the isochronous cyclotron of negative hydrogen ions C-80 is being developed at the National Research Centre "Kurchatov Institute"-PNPI. The project provides for the design of a building, the creation of stations for the development of methods for obtaining new popular radionuclides and radiopharmaceuticals based on them. The commercial component is not excluded. The project also provides for the creation of a complex of proton therapy of the eyesight. For these purposes, the modernization of the beam extraction system of the cyclotron C-80 is planned: a project for the simultaneously two beams extraction systems is being developed. The one for the production of isotopes with an intensity up to 100 mkA and an energy of 40-80 MeV and the second - for ophthalmology with an energy of 70 MeV and intensity up to 10 mkA.

The initial conditions for both beams at the output window from the accelerator were obtained using the Orbita-1 program [1].

A blueprint of the project and beam transfer lines is shown in Fig. 1.

## BEAM TRANSPORT LINES

### *Radio Isotope Complex*

The isotope complex (direction A, Fig. 1) includes four target stations. Target stations will be equipped with special devices for removing highly radioactive targets, loading them into protective containers for safe transportation to storage sites or to hot chambers for further processing.

When designing the line for the production of radionuclides for each energy of the proton beam in the range of 40-80 MeV, the optimal parameters of the magnetic elements of the beam were found under conditions of minimal losses of particles in the transportation path, and so that the beam size on the target was at least 20 mm.

The optimization of the beam transfer lines was carried out using the PROTON_MC program created at the NRC KI-PNPI [2]. The calculation algorithm consists in tracing the proton beam trajectories along the transport channel from the source to hitting the experimenter's target or the aperture of the magnetic elements. The initial conditions of the particles are chosen random within normal distribution. The beam from the accelerator is presented in the form of a multidimensional Gaussian distribution in x, x', z, z', Δp/p phase spice. In the case when an absorber is installed in the transport channel the beam parameters after the absorber are calculated using the GEANT4 program [3].

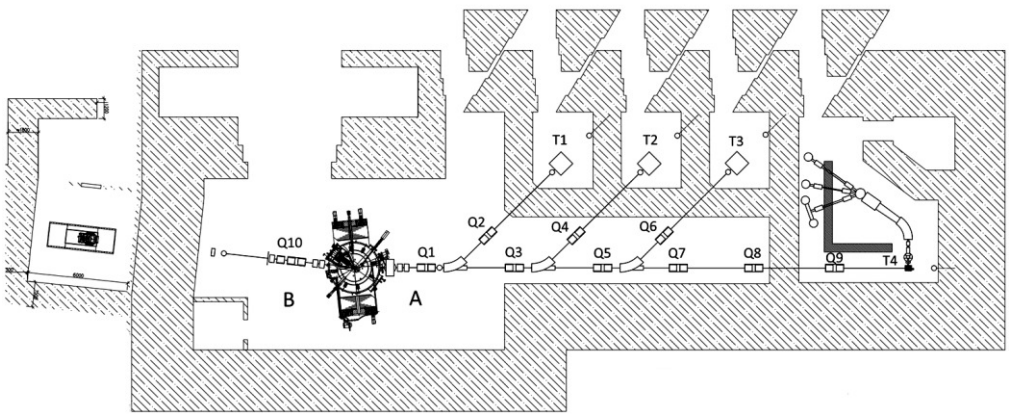


Figure 1: Blueprint of the project and beam transfer lines: (Right) A - beam line for radioisotope part, Q1-Q9 - lens doublets, T1-T4 - target stations. (Left) B - beam line for the ocular oncology complex, Q10 - triplet lenses.

† tonkikh_va@pnpi.nrcki.ru

ISBN: 978-3-95450-240-0 ISSN: 2673-5539 doi:10.18429/JACoW-RuPAC2021-MOPSA45



# EXPERIMENTAL SIMULATION OF VOLUME REPAINTING TECHNIQUE AT PROTON SYNCHROTRON IN CONTEXT OF SPOT SCANNING PROTON THERAPY

M. A. Belikhin†[1], A.A. Pryanichnikov[1], A. E. Shemyakov,
Lebedev Physical Institute RAS, Physical-Technical Center, Protvino, Russian Federation
A.P. Chernyaev, Lomonosov Moscow State University, Accelerator Physics and Radiation Medicine Department, Moscow, Russian Federation
[1]also at Lomonosov Moscow State University, Accelerator Physics and Radiation Medicine Department, Moscow, Russian Federation

*Abstract*

Reduction the influence of respiration-induced intrafractional motion is one of the main tasks of modern Spot Scanning Proton Therapy (SSPT). Repainting is one of the techniques of motion compensation. It consists in multiple repeated irradiations of the entire volume or individual iso-energy layers with the dose that is a multiple of the prescribed dose. As a result, the dose is averaged which leads to an increase in the homogeneity of the dose field.

The purpose of this study is experimental simulation of volume repainting and dosimetric estimation of its capabilities in the context of SSPT.

Simulation of respiration-like translational motion is performed using a non-anthropomorphic water dynamic phantom. Target of this phantom is compatible with EBT3 films and ion chamber. Estimation of repainting technique is based on the analysis of dose field shape, average dose and dose homogeneity in the Region of Interest (ROI) located within Planning Target Volume (PTV), and dose gradients along the direction of motion. Repainting technique was used for motion with amplitudes of 2, 5, 10 mm with 2, 4, 6, 8 and 10 iterations at the prescribed dose of 6 Gy. For each case values of the average dose, dose homogeneity and dose gradient were calculated and compared with corresponding values in case of no motion.

Repainting removes hot and cold spots and increases the homogeneity in the ROI from 85.9% to 96.0% at amplitude of 10 mm and 10 iterations. The dose gradient is inversely proportional to the motion amplitude and was not improved by repainting. Optimization of the irradiation time, PTV dose and dose field margins is necessary for clinical using of repainting.

## INTRODUCTION

Today proton therapy is the most precision and effective method of modern radiation oncology. These advantages are based on the presence of sharp Bragg peak at the end of the path, low lateral scattering and dependence of the beam penetration depth on its energy [1, 2].

However, these advantages can be fully realized only in case of complete immobility of the tumor, for example, in case of head and neck tumors. Respiration-induced intrafractional motion [3] leads to significant distortions of dose distribution and conformity degradation in case of other localizations such as lungs, liver, prostate, breast and etc. Interplay effect between tumor motion and beam delivery dynamic causes hot and cold spots in the target volume, and irradiation of healthy tissues and organs at risk. These factors significantly decrease efficiency of SSPT [4].

Conventional photon radiation therapy has a lot of solution [5] for monitoring, compensation and mitigation of intrafractional motion. However, direct transfer of these techniques to SSPT is difficult and requires additional research [4, 5]. In the main, the difficulties are caused by differences in the interaction principles of proton and photon beams with matter.

Repainting [3] is a specific method of tumor motion compensation used in SSPT. This one increases homogeneity of dose field and eliminates hot and cold spots. Repainting consists in multiple repeated irradiations of the entire volume or individual iso-energy layers with a dose that is a multiple of the prescribed dose. Intensity of the beam for repainting can be calculated as:

$$I = {}^{I_0}/_{N}$$

where $I$ – intensity of the repainting beam, $I_0$ – total intensity, $N$ – number of scanning iterations. Prescribed dose in the target volume are delivered as a result of the summation of doses from individual rescans. There are several repainting strategies: uniform, random, level, time delay and breath sampling repainting [3]. These methods differ from each other in the sequence of scanning the target volume and optimization of the irradiation time.

## MATERIALS AND METHODS

### *Proton Therapy Complex*

The current experiment was carried out on proton therapy complex «Prometheus» [6, 7]. This one is a specialized serial medical installation for particle therapy manufactured by Protom Ltd. This complex consists of proton synchrotron, patient immobilization system in sitting position and X-ray system. Irradiation of tumor is performed by a thin scanning proton beam with energy in the range of 30-330 MeV and with intensity about $10^9$ particles per second in spot scanning mode. Also the complex

† mikhailbelikhin@yandex.ru

ISBN: 978-3-95450-240-0 ISSN: 2673-5539 doi:10.18429/JACoW-RuPAC2021-MOPSA46

# PRELIMINARY STUDY OF THE GANTRY DESIGN FOR THE CENTER OF PROTON RADIATION THERAPY OF THE NRC "KURCHATOV INSTITUTE"

A. N. Chernykh, M. S. Bulatov, G. I. Klenov, V. S. Khoroshkov, NRC “Kurchatov institute”, Moscow, Russia

*Abstract*

NRC "Kurchatov Institute" is creating a center for proton radiation therapy (PRT), which will include a synchrotron with an energy of 250 MeV, gantry beam installations with a 360° rotation angle and a stationary channel installation. This article presents a block diagram of a gantry beamline installation and a project of a magneto-optical channel of a gantry beam installation with the main magnetic elements. In addition, a turning frame will be presented to accommodate the magnetic elements of the considered project of the gantry beamline installation.

## INTRODUCTION

NRC "Kurchatov Institute" is developing a PRT center, which will become part of the Kurchatov Scientific and Educational Medical Center of Nuclear Medicine. In the future, this facility will be used for long-term development of equipment and technologies for new generation PRT and training of personnel (medical physicists and clinicians).

The second purpose of the project and the first product to be introduced into the Russia practical healthcare is a modular clinical center PRT.

A center of PRT will include a synchrotron, two treatment rooms with a 360-degree gantry and a fixed channel. This article presents the main design considerations for the turning frame of the 360-degree gantry and its beamline, which include layout of the beamline with physical and technical characteristics main elements, design and layout of the turning frame.

The main characteristics of the gantry beamline are shown in Table 1.

Table 1: Main Specification of the Gantry Beamline

| Parameter | Specification |
|---|---|
| Energy range from ESS | 70 - 250 MeV |
| Gantry type | ±185 degrees |
| Nozzle type | Combined (Downstream scanning/passive beam) |
| Virtual SAD | 3 m |
| Max. dose rate | 3 Gy/min |
| Field size | 250 mm x 250 mm |

Basic requirements for the turning frame: (1) Overall dimensions length no more than 10 m, diameter no more than 13 m; (2) Angle of rotation of the gantry is not less than ± 185° (overlap in the down position); (3) Accuracy of gantry rotation + 0.3°; (4) Isocentricity of gantry rotation <0.5 mm.

## IMAGE OPTICS DESIGN FOR THE GANTRY BEAMLINE

Based on the results of modeling various options for the arrangement of the gantry beamline, it is proposed to consider the arrangement made according to the "barrel" type scheme (- 60, + 60, +90 degrees) as a working option. Fig. 1 shows a diagram of a beamline for transporting a proton beam of the gantry facility. MDH 60-1 and MDH 60-2 are two 60-degree dipoles, and MDH 90-1 is a 90-degree dipole with zero angular bevels in the inlet and outlet sections. To focus the proton beam, seven MQ 50-1 - MQ 50-7 quadrupole lenses and three CHV-1 - CHV-3 correctors are installed between the dipole magnets. Five lenses and two correctors on the drift section between 60-degree dipole magnets and two lenses and a corrector on the drift section between 60- and 90-degree dipole magnets, respectively. The longitudinal size of the gantry is 8.2 m, the diameter (along the axis of the proton duct) is 10.24 m.

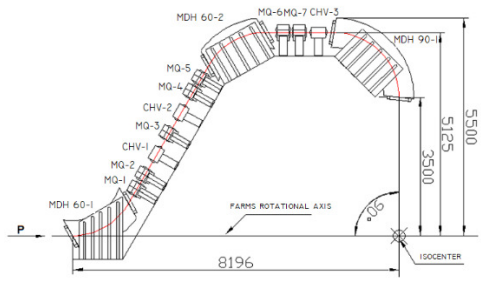


Figure 1: Diagram of the gantry beamline.

The main considerations when choosing the scheme of the gantry beamline are: (1) when an active system for generating a dose field is placed after the MDH 90-1 rotary dipole magnet, large field sizes in the isocenter can be achieved: 250 mm x 250 mm; (2) The arrangement with two 60-degree and one 90-degree dipole magnets reduces the longitudinal dimension of the gantry turning frame and avoids the more complex design of the last dipole.

The diameter of the gantry beamline is largely due to the need to ensure the maximum perpendicularity of the dose distribution entrance into the patient's body, both in the passive and in the active method of its formation. In the case of active method at small distances from the last scanning magnet to the patient's body, the non-parallelism of the beams leads to an increase in the dose on the patient's body surface. To compensate for this effect, a longer SAD L ~ 3.0 m is incorporated in the gantry design. For this

ISBN: 978-3-95450-240-0 ISSN: 2673-5539 doi:10.18429/JACoW-RuPAC2021-MOPSA47

# VERIFICATION OF A BEAM OF EPITHERMAL NEUTRONS FOR BORON-NEUTRON CAPTURE THERAPY*

G. D. Verkhovod†, D. A. Kasatov, Ia. A. Kolesnikov, A. Koshkarev, A. N. Makarov, I. M. Shchudlo, T. V. Sycheva, S. S. Savinov, S. Yu. Taskaev
Budker Institute of Nuclear Physics, 630090 Novosibirsk, Russia
Novosibirsk State University, Novosibirsk, Russia

*Abstract*

A promising method of treatment of many malignant tumors is the boron neutron capture therapy (BNCT). It provides a selective destruction of tumor cells by prior accumulation of a stable boron-10 isotope inside them and subsequent irradiation with epithermal neutrons. As a result of absorption of a neutron by boron, a nuclear reaction occurs with the release of energy in a cell containing boron. To measure the "boron" dose, a small-size neutron detector based on a boron-enriched cast polystyrene scintillator was proposed and developed at the BINP. The paper presents the results of changing the boron dose and the dose of gamma radiation in a water phantom and the comparison of these results with the calculated ones. The obtained result is important for irradiation of small laboratory animals with grafted tumors, large domestic animals with spontaneous tumors, and the planned clinical trials of the technique.

## INTRODUCTION

A promising method of treatment of many malignant tumors is the boron neutron capture therapy (BNCT) [1]. It provides a selective destruction of tumor cells by prior accumulation of a stable boron-10 isotope inside them and subsequent irradiation with epithermal neutrons. As a result of absorption of a neutron by boron, a nuclear reaction occurs with the release of energy in a cell containing boron. To measure the "boron" dose, a small-size neutron detector based on a boron-enriched cast polystyrene scintillator was proposed and developed [2]. The paper presents the results of measuring the boron dose and the dose of γ-radiation in a water phantom and the comparison of these results with the calculated ones.

In BNCT, it is customary to distinguish four components of the absorbed dose: 1) Boron dose due to α-particles and atomic nuclei of lithium – products of the nuclear reaction $^{10}B(n,\alpha\gamma)^{7}Li$. In the BNCT technique, when boron is accumulated predominantly in tumor cells, the boron dose is therapeutic. 2) The dose of thermal neutrons due to recoil nuclei, mainly protons, of the nuclear reaction of neutron absorption by the atomic nucleus of chlorine $^{35}Cl(n,p)^{35}S$ and nitrogen $^{14}N(n,p)^{14}C$. 3) The dose of fast neutrons due to recoil nuclei during elastic scattering of neutrons on the nuclei of matter. 4) The dose of γ-radiation due to the ionization of atoms of a substance under the influence of γ-radiation. Sources of γ-quantum are a charged particle accelerator, a neutron-generating target, a beam shaping assembly, and an irradiated object (patient).

In the book on neutron capture therapy [1] on page 279 it is written that “the first two components of the dose cannot be measured in principle”. However, for the measurement of the boron dose, a small-sized neutron detector with a cast polystyrene scintillator enriched with boron has been developed [2].

## DESIGN OF THE ACCELERATOR

The studies were carried out at the accelerating neutron source of the BINP, constructed for the development of boron neutron capture therapy for malignant tumors [3] (Fig. 1). The neutron source consists of three main units: 1) an electrostatic tandem proton accelerator of an original design (a tandem accelerator with vacuum insulation) to obtain a stationary proton beam with an energy of up to 2.3 MeV and a current of up to 10 mA; 2) a lithium target for generating neutrons in the threshold reaction $^{7}Li(p,n)^{7}Be$; and 3) a system for generating a therapeutic neutron beam for forming an epithermal neutron beam for therapy or a thermal neutron beam for research on cell cultures or small laboratory animals.

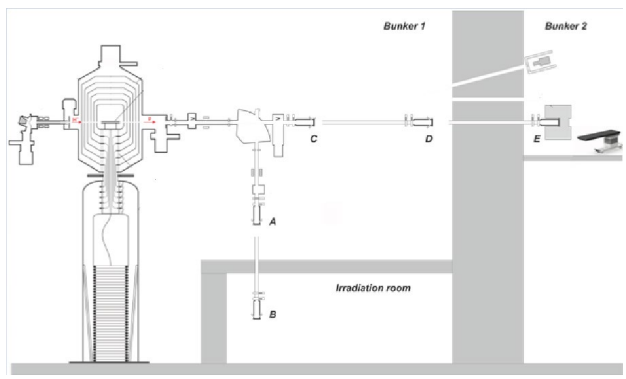


Figure 1: Layout of the experimental facility.

As seen in Fig. 1, the lithium target is placed both in the vertical path (position A) and in the horizontal path (position C) and is planned to be placed in position B for radiation testing of materials with fast neutrons, in position D for boron imaging by the method of instantaneous γ-spectroscopy with a beam monoenergetic neutrons and in position E for clinical trials of the BNCT technique.

In carrying out these studies, preliminary experiments were carried out with the target in position A, the main ones – in position C.

* Work supported by Russian Science Foundation, grant No. 19-72-30005
† g.verkhovod@alumni.nsu.ru

ISBN: 978-3-95450-240-0 ISSN: 2673-5539 doi:10.18429/JACoW-RuPAC2021-MOPSA48

# SIMULATION OF THE ELECTROSTATIC DEFLECTOR OF DC140 CYCLOTRON

A. Zabanov†, K. Gikal, G. Gulbekyan, I. Kalagin, N. Kazarinov, V. Lisov, S. Mitrofanov, V. Semin,
JINR, 141980, Dubna, Russia

*Abstract*

The main activities of Flerov Laboratory of Nuclear Reactions, following its name - are related to fundamental science, but in parallel a lot of efforts are paid for practical applications. Currently, work is underway to create an irradiation facility based on the DC140 cyclotron for applied research at FLNR. The beam transport system will have three experimental beam lines for testing of electronic components (avionics and space electronics) for radiation hardness, for ion-implantation nanotechnology and for radiation materials science. The DC140 cyclotron is intended to accelerate heavy ions with mass-to-charge ratio A/Z within interval from 5 to 8.25 up to two fixed energies 2.124 and 4.8 MeV per unit mass. The intensity of the accelerated ions will be about 1 pμA for light ions (A<86) and about 0.1 pμA for heavier ions (A>132). The extraction system based on four main elements - electrostatic deflector (ESD), focusing magnetic channel, Permanent Magnet Quadrupole lens and steering magnet. The results of numerical simulation of the ESD of DC140 cyclotron are presented in this this paper.

## INTRODUCTION

Flerov Laboratory of Nuclear Reaction of Joint Institute for Nuclear Research carries out the works under the creating of Irradiation Facility based on the DC140 cyclotron [1]. The DC140 will be a reconstruction of the DC72 cyclotron [2, 3].

The ion beam extraction process from the DC140 cyclotron is implemented using the ESD. The azimuthal extension of the ESD is 40° (70° - 110°). Due to the low power of the accelerated ion beams, it was decided that the potential electrode will not have an active cooling system.

The main criteria in the design of the ESD are the absence of electrical breakdowns between the electrodes and the minimum possible particle loss on the surface of the ESD.

This report presents the simulation and comparative analysis of various modifications of the ESD: with a constant gap and variable gap.

## THE DETERMINATION OF CURVATURE RADIUS OF THE SEPTUM

The first step of the designing the ESD is determination of curvature radius of the septum. The extraction orbits of ion beams $^{40}Ar^{8+}$, $^{209}Bi^{38+}$ ($W = 4.8$ MeV/u), $^{197}Au^{26+}$, $^{132}Xe^{16+}$ ($W = 2.124$ MeV/u) were used to determine of curvature radius of the septum. The listed ion beams correspond to the corners of the working diagram of DC140 cyclotron (see Fig. 1).

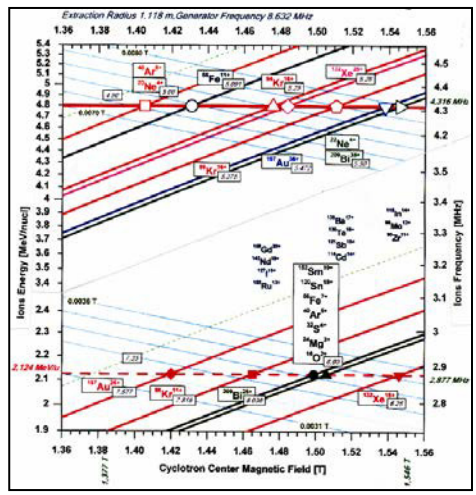


Figure 1: Working diagram of DC140 cyclotron.

The extraction orbit of ion beam in ESD can be represented as circular arc with center coordinates ($x_s$; $y_s$). The optimization task is to find the curvature radius of the septum $R_s$ and coordinates of the center ($x_s$; $y_s$), which ensure the minimum value of the functional (Eq. 1).

$$\frac{1}{n}\sum_{i=1}^{n}(R_s - R_i)^2 \longrightarrow 0 \qquad (1)$$

where $R_i = \sqrt{(r_i \cdot \cos(\varphi_i) - x_s)^2 + (r_i \cdot \sin(\varphi_i) - y_s)^2}$ is distance from the center coordinates ($x_s$; $y_s$) to the $i$ point of the extraction orbit of the ion beam, ($r_i$, $\varphi_i$) are the coordinates of point $i$ of the extraction orbit of the ion beam in cylindrical coordinate system with origin in the cyclotron center.

The optimization results are presented in Table 1.

Table 1: the Optimization Results of the Determination of Curvature Radius of the Septum

| Ion | $W$, MeV/u | $x_s$, cm | $y_s$, cm | $R_s$, cm |
|---|---|---|---|---|
| $^{40}Ar^{8+}$ | 4.8 | 20.87 | -200.26 | 309.28 |
| $^{209}Bi^{38+}$ | 4.8 | 19.01 | -176.31 | 285.68 |
| $^{197}Au^{26+}$ | 2.124 | 20.6 | -198.67 | 307.68 |
| $^{132}Xe^{16+}$ | 2.124 | 19.16 | -177.33 | 286.71 |

The optimal values of curvature radii of the septum for the ion beams are very different from each other. It is necessary to find the value of curvature radius, which ensures the minimum beam losses. The curvature radius of the septum was chosen $R_s = 301.9$ cm. This value was chosen from geometric and design considerations.

† zabanov@jinr.ru

ISBN: 978-3-95450-240-0 ISSN: 2673-5539 doi:10.18429/JACoW-RuPAC2021-MOPSA49

# DC140 CYCLOTRON, TRAJECTORY ANALYSIS OF BEAM ACCELERATION AND EXTRACTION

I.A. Ivanenko†, N.Yu. Kazarinov, V.I. Lisov, JINR, Dubna, Russia

*Abstract*

At the present time, the activities on creation of the new heavy-ion isochronous cyclotron DC140 are carried out at Joint Institute for Nuclear Research. DC140 facility is intended for SEE testing of microchip, for production of track membranes and for solving of applied physics problems. Cyclotron will produce accelerated beams of ions A/Z= 5 – 5.5 and 7. 5 – 8.25 with a fixed beam energy 4.8 MeV/n and 2.124 MeV/n respectively. The variation of operation modes is provided by changing of magnetic field in the range 1.4T – 1.55T with fixed generator frequency 8.632MHz. In this report, the results of design and simulation of the beam acceleration and extraction are presented.

## INTRODUCTION

DC140 cyclotron will accelerate the beams from O till Bi in two main operational modes, (see Fig. 1). First mode - for SEE testing of microchips, based on ions with A/Z =5.0 – 5.5 and fixed extraction energy 4.8 MeV/nucl. Second mode - for research works on radiation physics and production of track membranes, based on ions with A/Z= 7.5 – 8.0 and fixed extraction energy 2.1 MeV/nucl. [1].

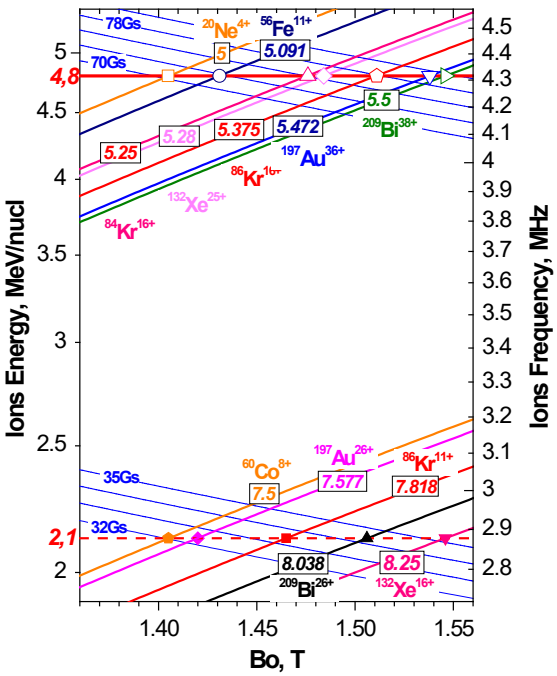


Figure 1: DC140 operational modes diagram.

DC140 cyclotron will be created as a deep reconstruction of DC72 cyclotron. The main parameters of new DC140 cyclotron are presented at Table 1. DC72 main magnet cover the new cyclotron magnetic field range 1.4T – 1.55T and stays without changing. Two 42-degree dees are placed at opposite valleys and provides acceleration voltage up to 60kV. DC140 RF generator works at fixed frequency 8.632 MHz. Acceleration modes operates at 2 and 3 RF harmonics, 4.316 MHz, and 2.877 MHz respectively. The usage of fixed frequency gives the extremely decreases of the time for switching between operation modes that very important in applied physics tasks, especially for SEE testing method.

Table 1: Main Parameters of DC140 Cyclotron

| | |
|---|---|
| Magnet size, m | 5,6x2,7x3,1 |
| Diameter of the pole, m | 1.6 |
| Number of sector pairs | 4 |
| Number of radial trim coils | 10 |
| Number of azimuthal trim coils | 4 |
| Magnetic field range, T | 1.4 – 1.55 |
| Number of dees | 2 |
| RF voltage, kV | 60 |
| RF frequency, MHz | 8.632 |
| RF harmonic | 2 – 3 |
| Ion injection method | axial |
| Ion source | ECR |
| Ion extraction method | electrostatic |
| Deflector voltage, kV | 75 |

## CYCLOTRON MAGNETIC FIELD

DC140 is a compact type isochronous cyclotron based on DC72 magnet [2]. Main magnet has H-shape form with 1.6 meter pole diameter.

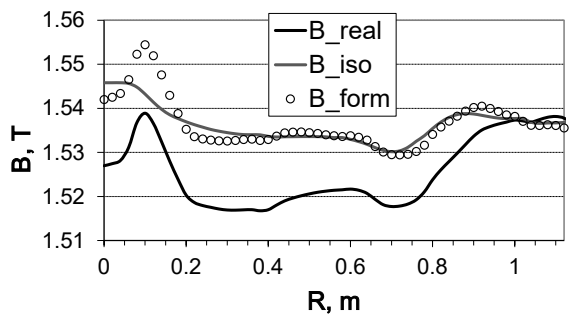


Figure 2: Operational formation of the magnetic field for 209Bi38+ acceleration mode.

Figure 2 demonstrates the usage of 10 radial trim coils for operational formation of isochronous magnetic field for 209Bi38+ acceleration mode. B_real presents base magnetic field, without trim coils. B_iso presents calculated isochronous field for 209Bi38+ acceleration mode. B_form presents final magnetic field, operationally formed with radial trim coils. Formed magnetic field keeps betatron frequencies in the ranges 1.005<Qr<1.05 and

† ivan@jimr.ru

ISBN: 978-3-95450-240-0 ISSN: 2673-5539 doi:10.18429/JACoW-RuPAC2021-MOPSA50

# AXIAL INJECTION SYSTEM OF DC140 CYCLOTRON OF FLNR JINR

N.Yu. Kazarinov†, G.G. Gulbekyan, V.V. Bekhterev, I.A. Ivanenko, I.V. Kalagin, V.I. Lisov, S.V. Mitrofanov, N.F. Osipov, V.A. Semin, JINR, 141980, Dubna, Russia

*Abstract*

Flerov Laboratory of Nuclear Reaction of Joint Institute for Nuclear Research continues the works under creating of FLNR JINR Irradiation Facility based on the cyclotron DC140. The facility will have three experimental beam lines for SEE testing of microchips, for production of track membranes and for solving of applied physics problems. The injection into cyclotron will be realized from the external room temperature 18 GHz ECR ion source. The systems of DC140 cyclotron – axial injection, main magnet, RF- and extraction systems and beam lines are the reconstruction of the DC72 cyclotron ones. The acceleration in DC140 cyclotron is carried out for two values of harmonic number h = 2,3 of heavy ions with mass-to-charge ratio A/Z within two intervals 5 – 5.5 and 7.5 – 8.25 up to two fixed energies 2.124 and 4.8 MeV per unit mass, correspondingly. The intensity of the accelerated ions will be about 1 pmcA for light ions (A≤86) and about 0.1 pmcA for heavier ions (A≥132). The design of the axial injection system of the DC140 cyclotron is presented in this report.

## INTRODUCTION

Flerov Laboratory of Nuclear Reaction of Joint Institute for Nuclear Research carries out the works under the creating of Irradiation Facility based on the DC140 cyclotron [1]. The DC140 will be a reconstruction of the DC72 cyclotron [2, 3]. Table 1 presents the main parameters of DC140 cyclotron.

Table 1: Main Parameters of DC140 Cyclotron

| | | |
|---|---|---|
| Pole (Extraction) Radius, m | 1.3 (1.18) | |
| Magnetic field, T | 1.415÷1.546 | |
| Number of sectors | 4 | |
| RF frequency, MHz | 8.632 | |
| Harmonic number | 2 | 3 |
| Energy, MeV/u | 4.8 | 2.124 |
| A/Z range | 5.0÷5.5 | 7.57÷8.25 |
| RF voltage, kV | 60 | |
| Number of Dees | 2 | |
| Ion extraction method | electrostatic deflector | |
| Deflector voltage, kV | 73.5 | |

The irradiation facility will be used for Single Event Effect (SEE) testing of microchips by means of ion beams ($^{16}$O, $^{20}$Ne, $^{40}$Ar, $^{56}$Fe, $^{84,86}$Kr, $^{132}$Xe, $^{197}$Au and $^{209}$Bi) with energy of 4.8 MeV per unit mass and having mass-to-charge ratio A/Z in the range from 5.0 to 5.5.

Besides the research works on radiation physics, radiation resistance of materials and the production of track membranes will be carrying out by using the ion beams with energy of about 2.124 MeV per unit mass and A/Z ratio in the range from 7.577 to 8.25.

The working diagram of DC140 cyclotron is shown in Fig. 1. The acceleration of ion beam in the cyclotron will be performed at constant frequency f = 8.632 MHz of the RF-accelerating system for two different harmonic numbers h. The harmonic number h = 2 corresponds to the maximal and value h = 3 – to minimal ion beam energy. The intensity of the accelerated ions will be 1 pμA for light ions (A≤86) and 0.1 pμA for heavier ions (A≥132).

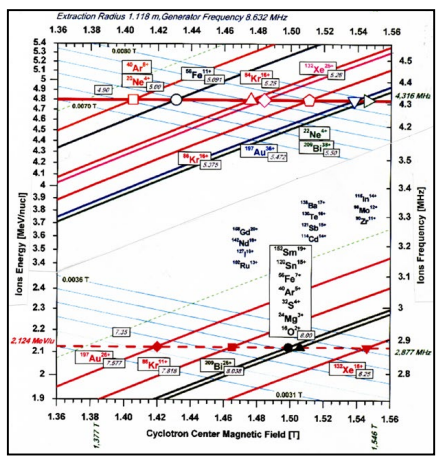


Figure 1: Working diagram of DC140 cyclotron.

The axial injection system of DC140 cyclotron will be adapted from the existing DC72 cyclotron one [4].

This report presents the design and simulation of the beam dynamic in the axial injection beam line of DC140 cyclotron. The simulation was carried out by means of MCIB04 program code [5].

## ECR ION SOURCE

The ion beams are produced in room temperature ECR ion source DECRIS-5 designed in Flerov Lab of JINR [6]. The working frequency DECRIS-5 is equal to 18 GHz. It is able to produce the beams of ion from $^{22}$Ne to $^{209}$Bi.

## BEAM LINE ELEMENTS

The scheme of the beam line is shown in Fig. 2. The length of the beam line is equal to 5.065 m. The 90-degree analyzing magnet **M90** separates the injected beam. The solenoidal lenses **S1-4** focus and match beam with the acceptance of the spiral inflector **I** for all level of the cyclotron magnetic field. Two movable diaphragms **CL1, 2** are

† nyk@jinr.ru

ISBN: 978-3-95450-240-0 ISSN: 2673-5539 doi:10.18429/JACoW-RuPAC2021-MOPSA51

# THE EXTRACTION SYSTEM OF DC140 CYCLOTRON

V. Lisov†, K. Gikal, G. Gulbekyan, I. Ivanenko, G. Ivanov, I. Kalagin, N. Kazarinov, S. Mitrofanov, N. Osipov, A. Protasov, V. Semin, A. Zabanov
JINR, 141980, Dubna, Russia

*Abstract*

The main activities of Flerov Laboratory of Nuclear Reactions, following its name - are related to fundamental science, but, in parallel, plenty of efforts are paid for practical applications. For the moment continues the works under creating irradiation facility based on the cyclotron DC140 which will be dedicated machine for applied researches in FLNR. The beam transport system will have three experimental beam lines for testing of electronic components (avionics and space electronics) for radiation hardness, for ion-implantation nanotechnology and for radiation materials science. The DC140 cyclotron is intended for acceleration of heavy ions with mass-to-charge ratio A/Z within interval from 5 to 8.25 up to two fixed energies 2.124 and 4.8 MeV per unit mass. The intensity of the accelerated ions will be about 1 pμA for light ions (A<86) and about 0.1 pμA for heavier ions (A>132). The following elements are used to extract the beam from the cyclotron: electrostatic deflector, focusing magnetic channel, Permanent Magnet Quadrupole lens and steering magnet. The design of the beam extraction system of DC140 cyclotron are presented in this report.

## INTRODUCTION

The DC140 is a sector cyclotron is intended for acceleration of heavy ions [1]. It will be a reconstruction of the DC72 cyclotron [2, 3]. In DC72 beam was extracted by stripping method. In DC140 the extraction will be carried out using an electrostatic deflector.

For beams extraction from the cyclotron is used the electrostatic deflector. The extraction system of the DC140 cyclotron consist a next elements (see Fig. 1):

1. Electrostatic deflector (ESD);
2. Focusing magnetic channel (MC);
3. Permanent Magnet Quadrupole lens (PMQ).

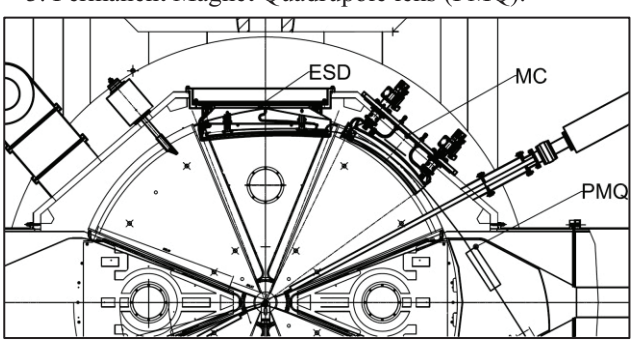


Figure 1: Layout of the elements of extraction system.

The main parameters of DC140 cyclotron are given in Table 1.

Table 1: DC140 Cyclotron Main Parameters

| Parameter | Value | |
|---|---|---|
| Magnetic field [T] | 1.415÷1.546 | |
| Pole (extraction) radius [m] | 1.3(1.18) | |
| Number of sectors | 4 | |
| RF frequency [MHz] | 8.632 | |
| Harmonic number | 2 | 3 |
| Energy [MeV/u] | 4.8 | 2.124 |
| A/Z range | 5.0÷5.5 | 7.57÷8.25 |
| RF voltage [kV] | 60 | |
| Number of Dees | 2 | |
| Ion extraction method | electrostatic deflector | |
| Deflector voltage [kV] | 73.5 | |

## NUMERICAL SIMULATION OF THE BEAM EXTRACTION

For numerical simulation the test ion in accordance with working diagram are used [see Fig. 2, 3, 4, 5]. The parameters of this ion are given in Table 2.

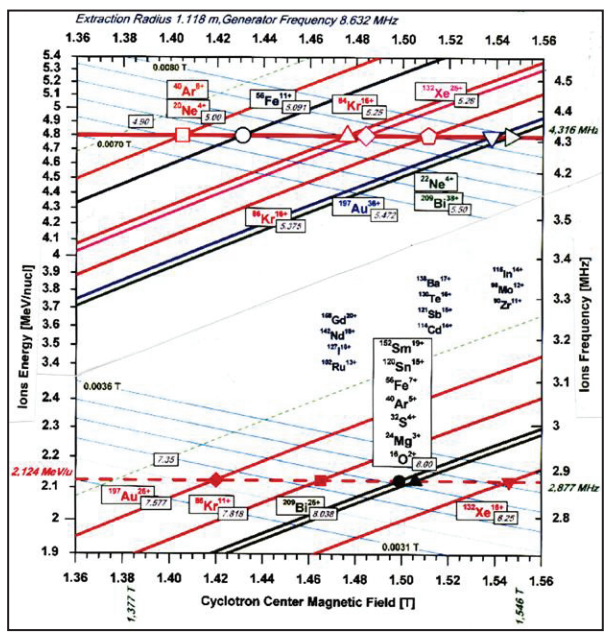


Figure 2: Working diagram of DC140 cyclotron.

† lisov@jinr.ru

ISBN: 978-3-95450-240-0 ISSN: 2673-5539 doi:10.18429/JACoW-RuPAC2021-MOPSA52

# MODELING OF THE MAGNETIC SYSTEM OF THE CYCLOTRON OF MULTICHARGED IONS

Yu.K. Osina†, Yu. N. Gavrish, A.V. Galchuck, Yu.I. Stogov,
JSC «NIIEFA», 196641, St. Petersburg, Russia

*Abstract*

This paper presents the results of the calculation of the magnetic system of the cyclotron for accelerating of multicharged ions developed at NIIEFA JSC. The cyclotron complex is designed to generate ions with a mass-to-charge ratio in the range A/Z= 3÷7, accelerate them to energies in the range of 7.5-15 MeV per nucleon. The cyclotron electromagnet has a four-sector structure, with a pole diameter of 4 m. Radial coils placed on the poles under the sectors are designed to adjust the magnetic field for providing isochronous acceleration conditions for different ions. A group of azimuthal coils designed to correct the first harmonic of the magnetic field and to center the orbits of the accelerated ion, as well as to adjust the position of the axial symmetry plane of the magnetic field is located on the sectors. The required magnetic field topology for ion acceleration was formed in the induction range of 1.29-1.6 T. Calculations were performed for the 1/8 part of the electromagnet. A mode was chosen in which the dependence of induction on the radius, which provides isochronism, is realized due to the shape of "iron". For this mode with an induction in the center of 1.44 T, the shape of side plates, plugs, and sector chamfers was determined. The currents in radial coils and the main dynamic characteristics of the cyclotron magnetic field for ion acceleration in the energy control range were calculated using the obtained magnetic field maps.

## INTRODUCTION

According to the design data, the cyclotron of multicharged ions is designed to accelerate ions having a mass-to-charge ratio A/Z=3÷7 ($C_{12}^{+3}$, $O_{16}^{+4}$, $O_{18}^{+3}$, $Ne_{20}^{+5}$, $Si_{28}^{+6}$, $Ar_{40}^{+10}$, $Fe_{56}^{+14}$, $Kr_{84}^{+18}$, $Ag_{107}^{+22}$, $Xe_{136}^{+28}$, $Bi_{209}^{+43}$). The electromagnet of the cyclotron will provide the isochronous motion of a wide range of ions in the process of acceleration to energy regulated in the range of 7.5 - 15 MeV/nucleon [1]. Taking into account the significant dimensions of the electromagnet, the H-shaped version of the magnetic circuit with a four-sector magnetic structure was chosen. The diameter of the pole of the electromagnet is 4 m. The air gaps in the "hill" and in the "valley" are 80 mm and 370 mm, respectively. This structure makes it possible to place resonators in the valleys of the electromagnet with the horizontal placement of rods and tanks. The electromagnet is equipped with a set of correcting coils.

Correcting coils are designed for: adjusting the shape of the distribution of the magnetic field over the radius to ensure isochronous conditions for the acceleration of specific ions; adjusting the position of the plane of symmetry of the magnetic field; correcting the first harmonic of the magnetic field and centering the orbits of the accelerated ions.

† npkluts@luts.niiefa.spb.su

## MAGNETIC SYSTEM OF THE CYCLOTRON

The magnetic field for the cyclotron of multicharged ions was simulated using the Ansys Maxwell software package [2, 3]. Magnet type is H-shaped. The structure of the magnetic field is four-sector, the angular length of the sectors is $51^0$. The formation of the magnetic field was carried out by changing the shape of the boundaries of the sector side plates and correcting coils. As a result of numerical simulation, the magnetic circuit of the multicharged ion cyclotron and the shape of the sector side plates was determined, provided the required ion acceleration mode for A/Z = 4.66. 3D calculation model of 1/8 part of the magnet is shown in Fig. 1.

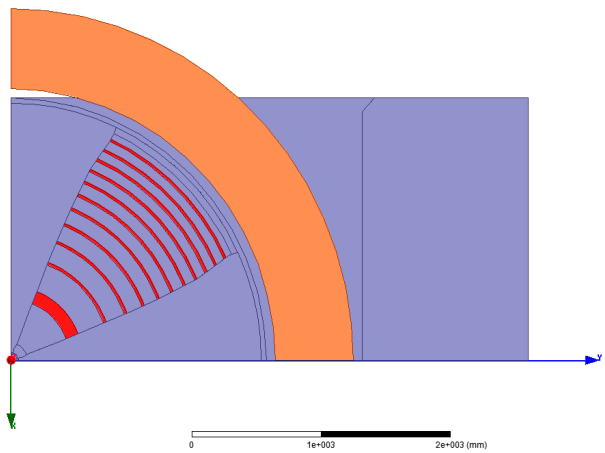


Figure 1: 3D calculation model of 1/8 part of the magnet.

The required maximum of the magnetic field rigidity at the final orbit (Rf.o. = 1.8 m) should reach 2.73 T·m [1].

During the magnetic field formation in the center, there were difficulties due to the effects of the saturation of steel and the complex shape of the surface of the sectors. As a result of numerical modeling, the shape of the sector side plates and the cyclotron central plug was determined, providing an isochronous mode of acceleration for particles with A/Z = 4.66.

Figure 2 shows the calculated magnetic fields for ions with A/Z=3÷7.

ISBN: 978-3-95450-240-0 ISSN: 2673-5539 doi:10.18429/JACoW-RuPAC2021-MOPSA53

# FOCUSING PROPERTIES OF THE MAGNETIC STRUCTURE OF ISOCHRONOUS CYCLOTRONS WITH LARGE SPIRALITY ANGLE OF POLE TIPS

D.A. Amerkanov, S.A. Artamonov†, E.M. Ivanov, G.A. Riabov, V.A. Tonkikh,
NRC "Kurchatov Institute" - PNPI, Gatchina, Leningrad district, 188300, Russia

*Abstract*

Magnetic structures with a large spirality angle of pole tips have been investigated in a number of works and are used in superconducting cyclotrons, $H^-$ ion cyclotrons, etc. With the design and construction of an 80 MeV isochronous $H^-$ cyclotron, such studies were continued and extended. In this work, a relatively simple approach for analyzing the spiral structure is proposed.

## INTRODUCTION

The magnetic structure with a large spirality angle of the pole tips is used in cases when vertical focusing from the flutter (field difference in the valley and the sector) is insufficient and it is necessary to add the angle focusing. This situation is typical for superconducting cyclotrons and for cyclotrons that accelerate negative hydrogen ions. Moreover, at JINR in Dubna, such structures have been investigated and a cyclotron and a synchrocyclotron with sectors in the form of an Archimedes spiral with a maximum spirality angle of up to 70 degrees were built. Numerical calculations of the magnetic field for an isochronous superconducting cyclotron with spiral sectors in the approximation of their uniform magnetization were carried out [1].

Two effects were noted: a decrease in the flutter in the central region with the introduction of spirality and a mismatch between the spirality of the sector Irion and the magnetic field. However, calculations made for a specific geometry are not applicable in the case of a different design. With the construction of an isochronous cyclotron for accelerating H-ions up to 40-80 MeV [2, 3], studies of the focusing properties of spiral structures were continued and expanded. Modern 3D software codes simplify the design of the magnetic field of any configuration by using trial- and- error method. However, to speed up the procedure and reduce the number of options for 3D analysis, it is useful to first perform a simplified and visual analysis of the system and estimate the importance of various parameters in the framework of a simpler 2D approximation.

## OPTIMIZATION OF THE MAGNET GAPS

As a first approximation, the hill and the valley gaps have been chosen using the 2D POISCR code calculations with the fill factor method. In this method, a 3D problem is reduced to a 2D one. The iron rings or the so-called shims mounted on the magnet poles and providing an isochronous rise in the field are calculated using a 2D program with a reduced value of the magnetic permeability $\mu_{new}(B) = \mu(B) \cdot C$. The permeability is reduced by a factor $C$ – so-called filling factor equal to the ratio of the azimuthal length of the sector to the length of the periodicity element at a radius r. The gap of the magnet obtained in this way corresponds to the gap of the hill, and there is no additional shim in the valley. Thus, two variants of the gaps of the main magnet and the gaps of the hills and the valleys were analyzed. The parameters of these variants are presented in the caption to Fig. 1.

## FLUTTER

The azimuthal variation of the magnetic field [1] is determined by the so-called flutter $F(r)$:

$$F(r) = <(B - <B>)^2> / <B>^2, \quad <...> = (2\pi)^{-1} \int_0^{2\pi} ... d\theta$$

Flutter can be represented as a Fourier harmonics expansion of the azimuthal variation of the magnetic field. The fundamental contribution to the expansion is made by the general focusing harmonic associated with the number of sectors and periodicity elements (in our case, $N = 4$). If we denote the value of the fundamental focusing harmonic $f = B_N / <B>$, then $F = f^2/2$.

Analytical calculation of flutter is a complex problem and therefore approximate methods have been used. In particular, in [4], an expression was obtained for the general harmonic of the magnetic field variation in an isochronous cyclotron in the approximation of uniform magnetization of the sectors of a magnet

$$B_N = 8M \sin(\frac{2\pi a}{d}) \exp(-\frac{2\pi g_h}{d}),$$

where $2a$ is the length of the sector along the azimuth for a given radius $r$, $2g_h$ is the gap in the hill, $d$ is the period of the structure, equal to the total length of the hill and valley, $4\pi M$ = 21kG. It follows from this expression that for an isochronous cyclotron with a period of the magnetic field structure equal to $d = 2\pi r / N$, where $N$ is the number of sectors, the flutter grows with increasing radius according to the law

$$F \sim B_N^2 / 2 \sim \exp(-2/x), \quad x = r / N \cdot g_h \qquad (1)$$

Although this approximation is insufficient for obtaining accurate quantitative estimates, it allows, in a unified manner, to get an idea of the relationship between the different parameters of the magnetic structure. Moreover, the introduction of the dimensionless parameter $x$ enables the comparison of different variants of structures. In particular, flutter rises as the gap in the hill decreases and falls as the number of sectors increases.

†artamonov_sa@pnpi.nrcki.ru

ISBN: 978-3-95450-240-0 ISSN: 2673-5539 doi:10.18429/JACoW-RuPAC2021-MOPSA54



# CALCULATION OF DOSE FIELDS AND ENERGY SPECTRA OF SECONDARY RADIATION IN THE EXTRACTION ZONE OF A SYNCHROTRON ACCELERATOR FOR PROTONS WITH ENERGIES UP TO 700 MeV

R.P. Truntseva, N.V. Zavyalov, A.V. Telnov, A.M. Opekunov, N.N. Kurapov,
FSUE "RFNC-VNIIEF", Sarov, Russian Federation

*Abstract*

The possibility of using a multipurpose synchrotron accelerator for studying the processes of interaction of heavy charged particles with various materials is considered. The accelerator provides proton energies up to 700 MeV. At the design stage of the experimental room, it is necessary to evaluate the emerging dose fields. In this case, it is important to evaluate the dose environment, energies and types of secondary radiation that may enter the adjacent rooms.

This paper presents the results of the radiation environment evaluation in the radiation extraction zone of the synchrotron accelerator. Simulation results of secondary radiation energy spectra near the walls, which separate the irradiation zone from adjacent rooms, are presented. Proton energies are equal to 60, 85, 110 and 700 MeV are considered. Simulation was performed by the Monte Carlo method in a program developed using Geant4 libraries.

## INTRODUCTION

Dose distribution estimation can be performed in different ways: experiment; simulation; comparison. At experimental rooms development stage estimation of arising dose fields is performed in simulation method. The extraction zone of a synchrotron accelerator which provide proton energies up to 700 MeV for studying the processes of heavy charged particles interaction with matter is considered. Apart from dose field estimation it is necessary to define type and energy of radiation which may enter the adjacent rooms. Against this characteristics can be adjust such parameters as: time spent in adjacent rooms, working hours in additional rooms, biological shielding thickness at the border of two rooms.

Simulation results of dose distribution estimation and energy spectra in experimental room by Monte-Carlo method in Geant4 [1] based software are presented. Primary particles energies are 60, 85, 110 and 700 MeV.

## SIMULATION DESCRIPTION

The major mechanisms of proton interaction with the target material are: elastic scattering, excitation and ionization of atoms in the medium and nuclear reactions. Other interaction mechanisms have minor contribution [2, 3]. The package of physical processes "FTFP_BERT" [4] was used. This package includes the functions of the FRITIOF [5] model, the compound-nucleus model and the Bertini intranuclear cascade model [6]. The major nuclear reactions are: (*p*, *MpNn*), where *M* and *N* are integers; (*p, xα*); (*p*, *xd*); (*p*, *xt*); (*p*, γ) [2, 7]. Reactions of type (*p*, *MpNn*) and in a less degree (*p, xα*); (*p*, *xd*); (*p*, *xt*); (*p*, γ) are expected in simulation with protons energy up to 110 MeV. Also arising of muons and different ions is expected in simulation with proton energy equal to 700 MeV.

Simulation geometry is shown in Fig. 1. The air volume 495×600×810 cm is divided to cells 45x45x50 cm. Concrete walls (ρ = 2.3 g/cm$^3$) 50 cm wide are set around the air volume. At h = 150 cm height from the floor and distance d = 70 cm from the wall iron cylinder with 10 cm diameter and length is located. At 10 cm distance from cylinder the monodirectional proton source with 3 cm diameter is placed (energy distribution - Gaussian).

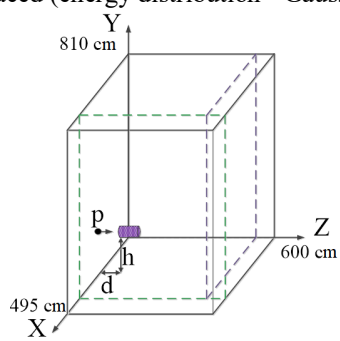


Figure 1: Simulation geometry.

Simulation results were: absorbed dose distribution in volume elements per one primary particle and secondary radiation energy spectra in areas specified by green and purple dotted lines in Fig. 1 (layers of air with 10 cm thickness). Further, coordinate denomination (according to Geant4 geometry): *x* – room width, *y* – height a, *z* – length.

In energy spectra calculation were registered: *p*, γ, *n*, $e^-$ и $e^+$, μ–mesons, α and other types of secondary radiation ("other"). Width of energy bin for all cases is equal to 100 keV.

## DOSE FIELD CALCULATION

The resulting dose field was divided into key sections. The following describes the simulation result for one of these sections (Fig. 2, near the side wall).

Maximum absorbed dose (90-180 cm in height and 0-50 cm in length) is: 60 MeV - 3 158 · $10^{-18}$ Gy; 85 MeV - 4.934 · $10^{-18}$ Gy; 110 MeV - 7 284 · $10^{-18}$ Gy per one primary proton. Minimum values (720-810 cm

ISBN: 978-3-95450-240-0 ISSN: 2673-5539 doi:10.18429/JACoW-RuPAC2021-MOPSA55

# BEAM-INDUCED BACKGROUND SIMULATIONS FOR THE CMS EXPERIMENT AT THE LHC

I. Azhgirey, I. Bayshev, I. Kurochkin, A. Riabchikova*, NRC "Kurchatov Institute" - IHEP, Protvino, Russia
A. Dabrowski, CERN, Geneva, Switzerland
S. Mallows, KIT, Karlsruhe, Germany

*Abstract*

Beam-induced background (BIB) comes from interactions of the beam and beam halo particles with either the residual gas in the vacuum chamber of accelerator or the collimators that define the beam aperture. Beam-induced processes can potentially be a significant source of background for physics analyses at the Large Hadron Collider (LHC).

This contribution describes the simulation software environment used for this part of the Compact Muon Solenoid (CMS) experiment activity and recent beam-induced background simulation results for the Phase-2 CMS operation design.

## INTRODUCTION

The LHC [1] will be upgraded to enable baseline operation for the High Luminosity LHC (HL-LHC) [2] period (Phase-2) at an instantaneous luminosity of $5 \times 10^{34}$ cm$^{-2}$ s$^{-1}$. The accelerator will operate at energy of 7 TeV per beam and a distance between bunches of 25 ns. This will allow to the CMS experiment [3] to collect integrated luminosity order 300 fb$^{-1}$ per year and up to 3000 fb$^{-1}$ during the HL-LHC projected lifetime of ten years, assuming machine efficiency is around 50%. The consideration of the radiation effects is a key to the overall success of the CMS experiment.

The Beam Radiation Instrumentation and Luminosity (BRIL) Project is responsible for the simulation and monitoring of the BIB in the CMS. The collaboration needs to understand and take into account all sources of the BIB and kinematic parameters of BIB particles entering the experimental cavern from the LHC tunnel.

## BIB FORMATION ANF EFFECT

BIB comes from interactions of the beam or beam halo particles either with the residual gas in the beam pipe or with the collimators that define the beam aperture. We can divide BIB into three different types based on their origin.

The first one is the local inelastic beam-gas interactions (LBG). This is the dominant source of BIB in the CMS near-beam region. The main locations of inelastic beam gas collisions are the superconducting parts of the beam pipe in the Long Straight Section 5 (LSS5). Cold sections have a relatively high rate of the residual gas pressure compared to warm ones. The most important is the final focus triplet cryostat just upstream of the CMS hall.

The second source is the distant Beam Halo (BH). BH particles are produced when off-orbit components of the beam scrape one of the collimators in the cleaning sections of the LHC, and the resulting collision products are absorbed downstream by the tertiary collimators (TCT), which are about 150 m upstream of the interaction point 5 (IP5). The products of hadronic and electromagnetic showers started in the TCT can reach the CMS cavern.

The third source is the distant elastic beam gas interactions (DBG) that occur anywhere around the ring. Elastically scattered particles can make several turns before they hit a collimator. When they interact with the TCT, they can produce particle showers similar to those produced by the BH.

In the HL-LHC time the BIB will differ in several aspects from what is currently experienced at the LHC. The cold section of the final focus triplet will be extended and thus a longer degraded vacuum section is expected there. The higher luminosity and the beam current will also amplify the degradation of the vacuum in the beam pipe in the forward regions of the CMS. In addition, the aperture of the final focus triplet and the Target Absorber Secondaries collimator (TAS) will be larger, and this will allow more BIB particles to enter the CMS cavern at a low radius. Most of the BIB particles that enters the CMS inner tracker volume is originating from interactions of the previous generations of the BIB particles with the beam pipe material. Thus, compared to the current conditions, where the beam pipe in the CMS is partially sheltered from background particles by the TAS, highly energetic BIB particles will be able to travel through the TAS aperture and interact with the beam pipe in the central part of the detector, resulting in a higher level of background.

Low-radius BIB mainly affects pixel and strip trackers in CMS, where it induces spurious hits in detectors, increasing dead time and adversely affecting track reconstruction. The main impact arises when a muon produced in a decay of mesons created by the interaction of the beam or beam halo particles upstream of the detector interacts with the CMS detector and produces an energy deposition that can mimic the signatures of particles originating from central collisions in the IP5, also introducing a large imbalance in the measured total transverse momentum.

The rate of BIB events was typically a few Hz during Phase-1 Run 2 data taking.

* Anastasiia.Riabchikova@cern.ch

ISBN: 978-3-95450-240-0 ISSN: 2673-5539 doi:10.18429/JACoW-RuPAC2021-MOPSA56

# UPGRADES OF A VACCUM INSULATED TANDEM ACCELERATOR FOR OBTAINING REQUIRED VOLTAGE WITHOUT BREAKDOWNS

I. Sorokin†, Ia. Kolesnikov, A. Makarov, I. Schudlo, S. Taskaev,
Budker Institute of Nuclear Physics, 630090 Novosibirsk, Russia and
Novosibirsk State University, Novosibirsk, Russia

*Abstract*

Epithermal neutron source based on an electrostatic tandem accelerator of a new type - Vacuum Insulation Tandem Accelerator, and lithium neutron target has been proposed and developed at BINP for Boron Neutron Capture Therapy - promising method for treatment of tumors. 2 MeV proton beam was obtained in the accelerator, the neutron generation carried out with bombardment of lithium target by protons, successful experiments on irradiation of cell cultures incubated in boron medium have been carried out, human glioblastoma grafted mice were cured. It is necessary to increase proton energy from 2 to 2.3 MeV to form a neutron beam suitable for the treatment of deep-seated tumors and to provide the high-voltage strength of the accelerator at a potential of 1.2 MV in order to suppress dark currents to an acceptably small value. Two upgrades to obtain the required potential were consistently implemented. At first, the glass rings of the feedthrough insulator were replaced by smooth ceramic ones doubled in height which made it possible to refuse placing the resistive divider inside. Then the smooth ceramic rings were replaced by the new ceramic rings with a ribbed outer surface. Modernization made it possible to obtain the required voltage of 1.15 MV in the accelerator without breakdowns. The report describes in detail the modernizations carried out, presents the results of the studies.

## INTRODUCTION

The source of epithermal neutrons based on a tandem accelerator with vacuum isolation and a lithium target [1] for the development of boron neutron capture therapy [2] of malignant tumors was proposed and created at the BINP. A stationary proton beam with energy of 2 MeV was obtained, neutrons were generated, and the effect of neutron radiation on cell cultures [3] and laboratory animals [4] was studied. An increase in proton energy up to 2.3 MeV [5] is required for a neutron beam suitable for the treatment of deep-seated tumors. The purpose of this work was to modernize a feedthrough insulator to increase a high-voltage strength of the accelerator when receiving a voltage of 1.2 MV.

## ACCELERATOR DESIGN

Figure 1 shows a vacuum-insulated tandem accelerator. A beam of negative hydrogen ions is injected into the accelerator and accelerated to 1 MeV. In the gas (argon) stripping target 7, which has installed inside the high-voltage electrode 1, negative hydrogen ions are converted into protons. Then, protons are accelerated to energy of 2 MeV by the same potential of 1 MV [5]. Gas is pumped by a turbomolecular pump 10 installed at the output of the accelerator and a cryogenic pump 4 through a jalousies 3 in the electrodes.

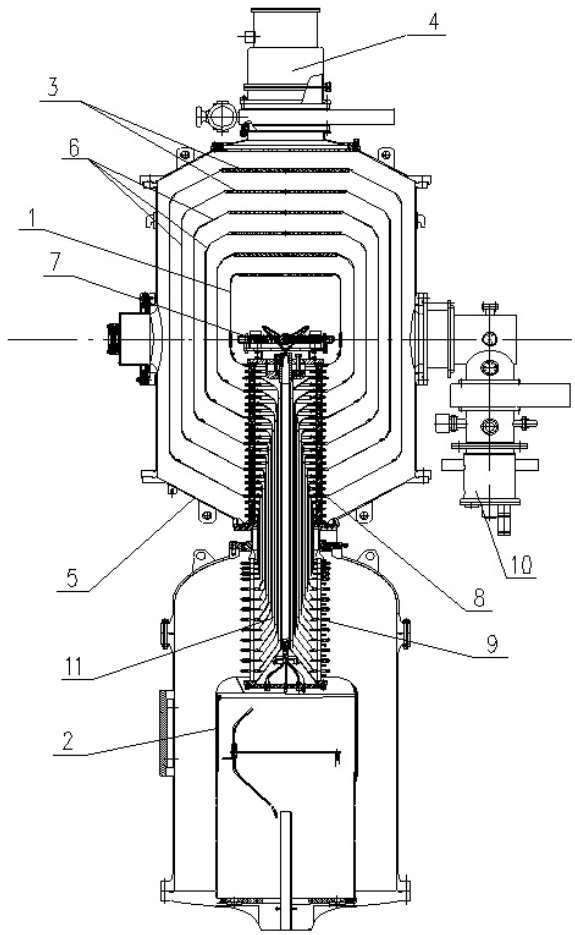


Figure 1: General cross-section view of the electrostatic 6-gap accelerator-tandem with vacuum insulation: 1 - high-voltage electrode of the accelerator-tandem; 2 - high-voltage electrode of high-voltage rectifier; 3 - jalousies of electrodes; 4 - cryogenic pump; 5 - vacuum tank of the accelerator; 6 - intermediate electrodes of the tandem-accelerator; 7 - gas stripping target; 8 - vacuum part of feedthrough insulator; 9 - gas part of feedthrough insulator; 10 - turbomolecular pump; 11 - internal coaxial cylinders.

One of the basic elements of the vacuum-insulated tandem accelerator is a sectionalized disassemble feedthrough insulator through which the voltage from the high-voltage rectifier 2 is fed to the central electrode of accelerator 1.

† I.N.Sorokin@inp.nsk.su

ISBN: 978-3-95450-240-0 ISSN: 2673-5539 doi:10.18429/JACoW-RuPAC2021-MOPSA57

# EXPERIMENTAL INVESTIGATION THE SYNTHETIC CRYSTAL DIAMOND PLATES OF METHODS OF POSITRON ANNIHILATION SPECTROSCOPY

M.K. Eseev, I.V. Kuziv, Northern (Arctic) Federal University named after M.V. Lomonosov, Arkhangelsk, Russia
A.G. Kobets[1], I.N. Meshkov, O.S. Orlov, A.A. Sidorin, K. Siemek[2], Joint Institute for Nuclear Research, Dubna, Moscow Region, Russia
[1]also at Institute of Electrophysics and Radiation Technologies, NAS of Ukraine, Kharkov, Ukraine
[2]also at Institute of Nuclear Physics Polish Academy of Sciences, Krakow, Poland

*Abstract*

Nowadays positron annihilation spectroscopy is a powerful technique of microstructure investigations of crystalline materials. Doped diamonds were studied by Positron annihilation spectroscopy and Infrared spectroscopy. As a result of the experiments, data show the effect of nitrogen doping of diamonds on the occurrence of defects in a doped diamonds.

## INTRODUCTION

Synthetic crystal diamond plates are used in scientific and technical fields and in new materials. Various defects and types of defects in diamond plates can changed its properties. Investigation the defects of diamond plated is very important for use diamond plates for fully solving applied problems in roentgen-optical systems and quantum sensorics. The investigation included three different spectroscopy types. First type is Positron annihilation spectroscopy (PAS). PAS is unique non-destructive instrument to detect open-volume defects, such as vacancies, vacancy clusters, microvoids or dislocations. PAS can define defects in the near-surface layer of materials with thickness up to 10…100 nm. It can be used in cases where other popular methods such as scanning electron microscopy (SEM) or X-ray diffraction are not applicable [1,2]. The second type of spectroscopy which used in this investigation is Infrared spectroscopy. This technique allows to define types of diamond defects such as A type and C type. The third type is Raman spectroscopy. It is valuable method because it provides readily distinguishable signatures of each of the different forms of carbon.

## MATERIALS AND METHODS

Generation of the synthetic crystal diamond plates was conducted by HTHP method with addition of nitrogen in different concentrations (12,5 ppm, 75 ppm, 88 ppm). Defects in the atomic structure of diamond plates are responsible for this colour. Transparent sample contained 12 ppm, yellow - 7 ppm, pink - 88 ppm. Then diamonds were cut by laser. Several series of paired samples of the diamond plates with 0,8 mm in height and different side size were studied (Fig. 1).

One sample from each group was cut along and across and left for investigation by Infrared and PAS spectroscopy methods.

Simultaneously one sample from each group was left for investigation by Raman spectroscopy method. Pink sample contained $NV^0$ (575 nm) and $NV^-$ (637 nm) defects.

Figure 1: Synthetic crystal diamond plates.

First part of experiment consisted in measurement the positron annihilation lifetime spectroscopy (PALS). PALS measurements were conducted using digital spectrometer APU-8702RU and the $BaF_2$-based scintillator (Fig. 2).

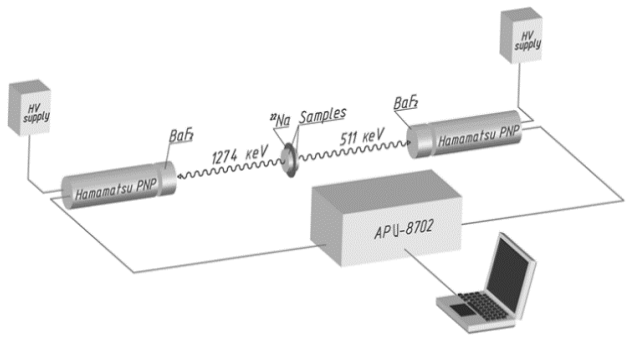


Figure 2: PALS instruments.

The timing resolution equaled 250 ps. The typical sandwich geometry was used, where the positron source located between two identical samples. The $^{22}Na$ isotope with an activity of 850 kBq was used as a positron source. It was placed between two identical samples. The positron source consisted of $^{22}NaCl$ salt between two titanium foils (10 μm).The measurements were carried out at room temperature.

This method shows average lifetime of the positron in diamond plates. The positron lifetime gives information

ISBN: 978-3-95450-240-0 ISSN: 2673-5539 doi:10.18429/JACoW-RuPAC2021-MOPSA58

# SOURCES OF ULTRASHORT X-RAY PULSES IN THE INVESTIGATION OF THE STRUCTURE AND DYNAMICS OF NANOSYSTEMS

M. K. Eseev†, D. N. Makarov, Northern Arctic Federal University, Arkhangelsk, Russia

*Abstract*

Free electron lasers are today one of the main sources of ultrashort X-ray pulses. The installations used in the world today are presented and the results of experiments and calculations with various nanosystems are presented.

## INTRODUCTION

Free Electron Lasers (FELs) were invented by Madey [1] and then experimentally demonstrated by his group at Stanford University in the 1970s. These lasers use relativistic electrons propagating through a periodic system of magnets (undulator) to generate and amplify coherent electromagnetic radiation.

Initially, the operation of such lasers was demonstrated in infrared mode. After that, work continued on expanding the FEL in the direction of EUV and X-ray modes. To solve this problem, the radiation was additionally amplified using the spontaneous emission self-amplification (SASE) mode. In the SASE mode, the particles of the electron beam are grouped into microbunches when they pass through the undulator and interact in it with the radiation of the beam itself. It is these FELs that are currently actively used in SAR and have great prospects for further improvement.

FELs have the widest frequency setting range and can generate very high peak and average laser powers. The formation of attosecond X-ray pulses on XFELs is currently being reported [2]. The possibility of creating zeptosecond pulses has been reported [3]. The extremely high power, coupled with the excellent lateral coherence of these XFELs, provides a dramatic increase in peak brightness.

The advent of XFELs has ushered in a new era in X-ray and X-ray studies. A large number of such lasers have been built in the last 15 years.

FLACH is the first XFEL facility for photons with energy in the extreme ultraviolet (EUV) region and was built in 2005 at DESY, Hamburg. LCLS is the first hard X-ray FEL built in 2009 at the SLAC National Accelerator Laboratory, USA. The SACLA plant in Japan and the FERMI plant in Trieste represent the first generation of XFELs, which have demonstrated tremendous scientific potential and influence in broad fields of science. XFEL installations are currently expanding worldwide: PAL-XFEL in South Korea, SwissFEL in Switzerland, European XFEL (EuXFEL) in Germany, etc.

## DIFFRACTION ANALYSIS USING X-RAY USP

One of the most common approaches that can be used to observe an object in four dimensions x, y, z, t is time-dependent femtosecond crystallography (TR-SFX).

Measuring the temporal dynamics of such processes includes 2 stages, see Fig.1. The first is the launch of the studied dynamic process, and the second is the collection of diffraction patterns with different time delays by irradiating the ultrashort pulses of the studied system. To study such processes, ultrashort pulses of high brightness are used, since a pulse of even shorter duration $\tau$ is required to study dynamic processes with characteristic times $\tau_T$, i.e., the condition $\tau << \tau_T$ must be satisfied. A very bright USP source is necessary because in the short time $\tau$ of interaction of the pulse with the system under study, a sufficient amount of radiation has been scattered so that it can be detected. To implement this concept, difficulties arise due to the destruction of the sample under study due to the high brightness of the ultrashort pulses. Despite this, in 2000 Janos Hajdu and his colleagues showed how this difficulty can be overcome [4]. They calculated that a molecule exposed to an X-ray pulse would begin to explode on a time scale of about 10 femtoseconds. Thus, shorter light pulses can pass through the molecule, capturing information about the virtually unperturbed structure. And pulses bright enough will give rise to continuous diffraction patterns strong enough to be measured.

The first stage can be implemented in several ways. The most common method is the so-called *pump-probe*. This method, suitable for studying quantitatively reproducible dynamics, is based on the creation of a time-delayed sequence of two short pulses: a "pump" pulse (usually an optical laser or the first XFEL pulse) unbalances the substance, and a "probe" X-ray pulse is used to create or taking "snapshots" of the structure of a substance at a specific point in time during the dynamic response of the substance. The structural response of the system can then be traced as a function of time by repeatedly applying these two impulses to the substance with different relative delays.

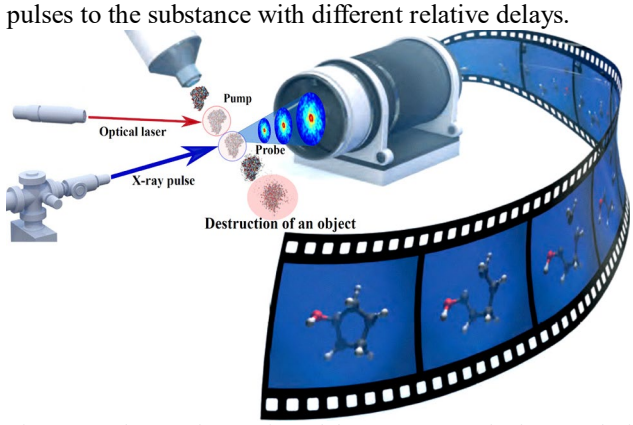


Figure 1: Scheme of operation of the TR-SFX method. Instead of an optical laser (Pump), there can be an X-ray pulse (the first pulse is Pump, and the second is Probe) [5].

† m.eseev@narfu.ru

ISBN: 978-3-95450-240-0 ISSN: 2673-5539 doi:10.18429/JACoW-RuPAC2021-TUPSB04

# FEATURES OF THE ELECTRON COOLING SYSTEM OF THE NICA BOOSTER

S.A. Melnikov†, E.V. Ahmanova, A.V. Butenko, A.G. Kobets, I.N. Meshkov, O.S. Orlov, K.G. Osipov, S.V. Semenov, A.S. Sergeev, A.A. Sidorin, A.O. Sidorin, E.M. Syresin,
Joint Institute for Nuclear Research, Dubna, Russia
A.V. Ivanov, The Budker Institute of Nuclear Physics, Novosibirsk, Russia

*Abstract*

The report presents the results obtained during the commissioning the Electron Cooling System (ECS) of the Booster (Fig. 1), the first in the chain of three synchrotrons of the NICA accelerator complex. The work was performed without an ion beam and with a circulating ion beam $He^{1+}$ and $^{56}Fe^{14+}$. In the work with a circulating ion beam $He^{1+}$, the effect of reducing the lifetime of the circulating ions was observed when the velocities of the cooling electrons and the cooled ions coincide. The dependences of the electron beam current on the ECS parameters for different electron energy values were experimentally obtained. The specific features of operation of electron gun of the NICA Booster are hollow beam formation and the phenomenon of virtual cathode creation confirmed both experiments and by numerical simulation. In conclusion section the results of first experiments on electron cooling of $^{56}Fe^{14+}$ ion electron cooling are presented.

## INTRODUCTION

The main tasks of the Booster synchrotron of heavy ions are the accumulation of $2 \cdot 10^9$ gold ions $^{197}Au^{31+}$ or other low-charged heavy ions and their acceleration to the maximum energy (578 MeV/u for $^{197}Au^{31+}$), which is sufficient for their subsequent stripping to the state of bare nuclei. The use of electron cooling in a Booster at ion energy of 65 MeV/u makes it possible to significantly reduce the 6D emittance of the beam.

## SCHEME OF THE ELECTRON COOLING SYSTEM OF THE NICA BOOSTER

The ECS is constructed according to the classical scheme proposed and implemented in the early 1970s in the Institute of Nuclear Physics of SB of USSR Academy of Science [1].

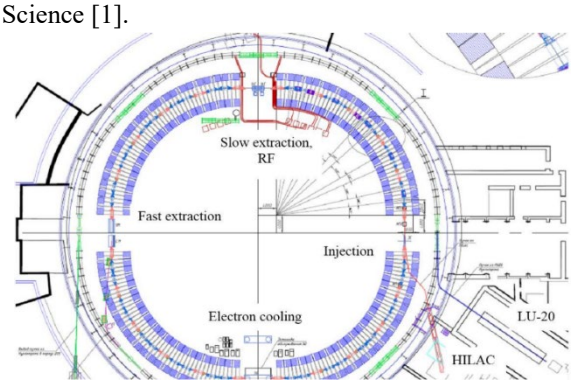


Figure 1: Booster Scheme with Built-in ECS.

In electron cooling set-up (Fig. 2), an electron beam passes from the cathode of the electron gun to the collector in a uniform longitudinal magnetic field. A short rectilinear solenoid allows one to form an electron beam with the necessary parameters in a gun with special optics. The toroidal sections of the Cooler magnetic system are used to transport the beam to straight solenoid – the cooling section.

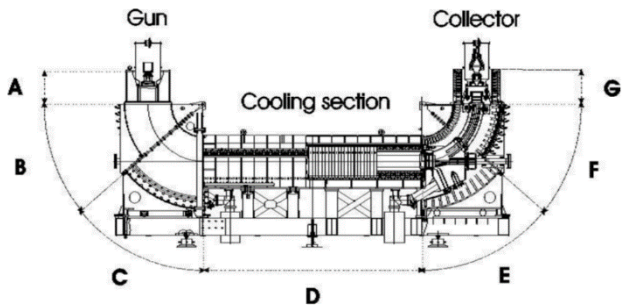


Figure 2: A, G–the solenoids of the gun and the collector, B, C, E, F - the sections of the toroidal solenoids, D-the cooling section solenoid.

In the ECS of the NICA Booster (Table 1), the homogeneity of the magnetic field of this solenoid is made at the level of $3 \cdot 10^{-5}$ (straightness of the magnetic field line) that provides the design value of the cooling time. The energy of the ECS electrons variates in this range of 1.0 – 50.0 keV.

Table 1: Parameters of the Booster ECS

| Electron energy E, keV | 1.5 – 50 |
|---|---|
| Electron beam current I, A | $\leq 1$ |
| Accuracy of energy adjustment and its stability, $\Delta E/E$ | $\leq 1 \cdot 10^{-5}$ |
| Beam current stability, $\Delta I/I$ | $\leq 1 \cdot 10^{-4}$ |
| Electron beam loss current, $\delta I/I$ | $\leq 3 \cdot 10^{-5}$ |
| The strength of the ECS longitudinal magnetic field, kGs | 1 – 2 |
| Permissible inhomogeneity of the longitudinal magnetic field in the cooling area, $\Delta B/B$ | $\leq 3 \cdot 10^{-5}$ on the length 15 cm. |
| Transverse temperature of electrons in the cooling section (in the particle system), eV | $\leq 0.3$ |
| Correction of the ion orbit at the input and output of ECS | offset, mm $\leq 1{,}0$<br>angular deviation, mrad $\leq 1{,}0$ |

† smelnikov@jinr.ru

ISBN: 978-3-95450-240-0 ISSN: 2673-5539 doi:10.18429/JACoW-RuPAC2021-TUPSB05

# LONGITUDINAL IMPEDANCE OF THE NICA COLLIDER RING AND ION BEAM STABILITY

S. Melnikov†, E. Ahmanova, M. Korobitsina, I. Meshkov, K. Osipov,
Joint Institute for Nuclear Research, Dubna, Russia

*Abstract*

The report presents the results of optimization of the longitudinal coupling impedance of the NICA collider ring using numerical simulation of its individual elements by the CST Studio. Based on the obtained results, analytical estimates of the stability of the ion beam in the ring are obtained for one value of the ion mode energy – 3 GeV/u.

## INTRODUCTION

The project of the Nuclotron-based Ion Collider fAcility (NICA) accelerator complex [1] is being developed at JINR. The ion Collider, which is the main part of it, will allow us to study the collision processes of gold ions with a kinetic energy of 1 – 4.5 GeV/u ($\sqrt{s} \leq 11$ GeV/u) and polarized protons with energy of 2 – 12.6 GeV ($\sqrt{s} \leq 27$ GeV). One of the criteria determining the stability of the motion of charged particles inside the beam chamber is the value of its impedance, which is most important for high-intensity beams.

The interaction of the charged particle beam with the accelerator beam chamber leads to the appearance of electromagnetic fields induced in the chamber (wake-fields) and their reverse effect on the beam, leading to coherent instabilities in the longitudinal and transverse directions. The value $W_{||}(r_1, s) = \frac{1}{q_1}\int_{-\infty}^{\infty} E(r_1, z, t)_{t=(s+z)/c} dz$is called the longitudinal Wake potential. Its transverse component can be found according to the Panofsky-Wenzel theorem: $W_{\perp}(r_1, s) = -\nabla_{\perp}\int_{-\infty}^{s} W_{||}(r_1, s')ds'$. The coupling impedance is the Fourier image of the Wake potential

$$Z_{\parallel}(\omega) = \frac{\int_{-\infty}^{\infty} W_{\parallel}(s)e^{-i\omega s}ds}{\int_{-\infty}^{\infty} \lambda(s)e^{-i\omega s}ds}$$
$$Z_{\perp}(\omega) = i\frac{\int_{-\infty}^{\infty} W_{\perp}(s)e^{-i\omega s}ds'}{\int_{-\infty}^{\infty} \lambda(s)e^{-i\omega s}ds} \quad (1)$$

where λ (s) is the charge distribution normalized by $q_1$.

The longitudinal and transverse impedances can excite instabilities of the beam particle motion in the Collider. In addition, the real part of the longitudinal impedance determines the contribution to the growth of energy dissipation in the walls of the vacuum chamber, which, with a high-intensity beam, can cause significant heating of individual elements of the superconducting Collider.

Each of the Collider rings (Fig. 1) is a racetrack type accelerator and consists of two rotary arches and two long straight sections. The perimeter of the Collider 503.04 m is equal to two perimeters of the Nuclotron.

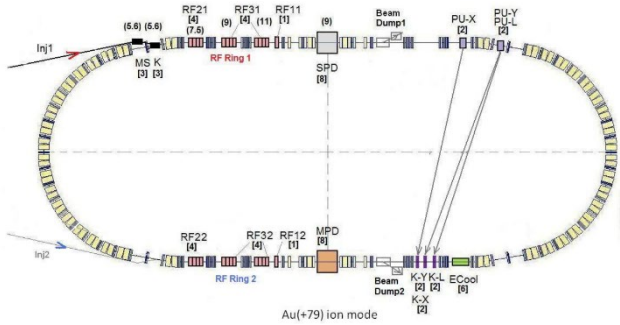


Figure 1: Scheme of the Collider ring. Here Inj1, 2 – injection channels; RFij – RF-stations with i – number of station, j – number of the ring; SPD – spin physics detector, MPD – multipurpose detector, PU-X,Y,L and K-X,Y,L – pick-up stations and kickers for stochastic cooling; ECool – electron cooling system; MS – septum magnet; K – injection kicker.

## CALCULATION OF IMPEDANCE

After the initial calculation, changes were made to its design for each element to minimize the value of $Z_{||}/n$, where n is the circulation frequency harmonic.

In this work, the calculation of Wake-potentials was performed in the CST Studio program. To minimize the contribution of the impedance to the particle dynamics, it is possible to change the design of the element to reduce the amplitude of low-frequency resonances, or to shift them up in frequency. In other words, changes were made to minimize the value of $Z_{||}/n$. The choice of a design change is helped by the wakefield picture calculated by CST Studio, which displays the excitation of the electromagnetic field in various cavities of the chamber elements.

The biggest changes were made to the collimator unit, kicker of feedback system and pick-up stations in Collider arches (Beam Position Monitor – BPM).

### *Collimator Unit*

The collimator unit consists of scraper and absorber, having a similar design, so we will limit ourselves to considering changes in the design only on the example of a scraper (Fig. 2).

†smelnikov@jinr.ru

ISBN: 978-3-95450-240-0 ISSN: 2673-5539 doi:10.18429/JACoW-RuPAC2021-TUPSB07

# PARTICLE COLLIMATION IN THE NICA COLLIDER

O.Kozlov, Yu.Gusakov, I.Meshkov, I.Semenova, E.Syresin, JINR, Dubna, Russia

*Abstract*

The system of particles collimation developed for the NICA collider is considered. The main collimation goal is the beam halo cleaning to minimize the background for experiment. The main mechanisms of particle losses, including the ion recombination in electron cooler, are also reviewed.

## INTRODUCTION

The Nuclotron-based Ion Collider fAcility (NICA) [1] is a new accelerator complex being constructed at JINR. Two collider rings are designed to achieve the required luminosity up to $10^{27}$ $cm^{-2}s^{-1}$ at two interaction points (IP). The first IP is connected with Multipurpose detector (MPD) for the ion-ion ($Au^{+79}$) collider experiments in the energy range of 1÷4.5 GeV/u. The second IP is aimed for the polarized proton-proton and deuteron-deuteron collisions. The collider must obtain the required luminosity taking into account the certain conditions: luminosity lifetime limitation by intrabeam scattering in a bunch (IBS), space charge tune shift, threshold of microwave instability, slippage factor optimization for efficient stochastic cooling, maximum required RF voltage amplitude. This article considers the $^{197}Au^{+79}$ ion mode of the facility operation.

## LATTICE OF THE RINGS

Collider lattice was developed and optimized [2] with some constraints: ring circumference, a number of the dipole magnets in an arc, convenience of the beam injection into the ring. The rings are vertically separated (32 cm between beam axes) and use two-aperture superconducting magnets (dipoles and quadrupoles). Rings have the racetrack shape with the bending arcs and long straight section. Bending arc comprises 12 FODO cells. The cells with empty dipoles are used for horizontal dispersion suppression and convenient beam injection and extraction (dumping) schemes. The long straight sections matched to the arcs contain the RF stations, electron and stochastic cooling devices, BPMs, superconducting quadrupole blocks and collimation elements as well. The optics in these sections produces the betatron tune variation, vertical beam separation in the rings and conditions for colliding beams in interaction points (IP). The project parameters of the collider ring are presented in Table 1. The placement of collimation system elements in both collider rings is possible only in the western superperiod (Fig. 1). The eastern part of the collider is designed to accommodate the modules of the acceleration system.

Table 1: Main Parameters of the Collider Rings

| | | |
|---|---|---|
| Ring circumference | 503.04 m | |
| Number of bunches | 22 | |
| Rms bunch length | 0.6 m | |
| β-function in the IP | 0.35 m | |
| Betatron tunes, $Q_x/Q_y$ | 9.44/9.44 | |
| Chromaticity, $Q'_{x,0}/Q'_{y,0}$ | -33/-28 | |
| Acceptance | 40 π·mm·mrad | |
| Long. acceptance, Δp/p | ±0.010 | |
| Gamma-transition, $\gamma_{tr}$ | 7.088 | |
| | Dipole | Quadrupole |
| Number of magnets | 80+8(vert.) | 86+12(fin.foc) |
| Max. magnetic field | 1.8 T | 23 T/m |
| Effective length | 1.94 m | 0.47 m |
| Beam pipe (h/v) | 120mm/70mm | |

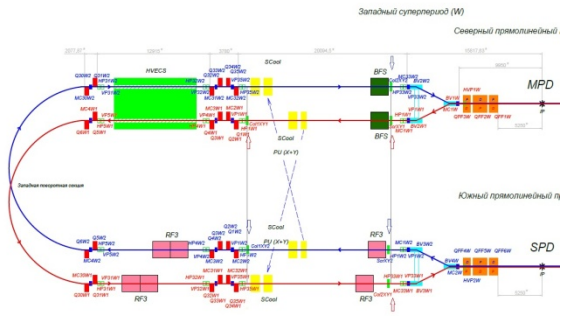


Figure 1: Positioning of the collimation elements in the collider lattice (shown by thick arrows).

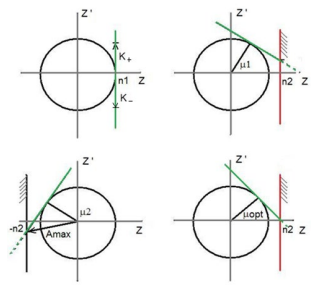


Figure 2: Principle of two-stage collimation in transversal phase space.

## STATUS OF THE SYSTEM OF PARTICLE COLLIMATION

The collimation system is designed to clean the beam halo [3], the particles that have get maximum amplitudes (comparable to acceptance) due to intrabeam scattering or nonlinearities of the magnetic field, to reduce it interaction with the walls of the vacuum chamber and, especially, to protect the detector from additional background.

ISBN: 978-3-95450-240-0 ISSN: 2673-5539 doi:10.18429/JACoW-RuPAC2021-TUPSB08

# MAGNETO-OPTICAL STRUCTURE OF THE NICA COLLIDER WITH HIGH CRITICAL ENERGY

S. Kolokolchikov, Yu. Senichev, INR RAS, Moscow, Russia
E. Syresin, JINR, Dubna, Russia

*Abstract*

For proton option of NICA collider, it is necessary to cross the transition energy ($\gamma_{tr} = 7{,}1$). For this reason, a magneto-optical structure with a high critical energy ($\gamma_{tr} = 15$) is considered. In this case, methods of increasing the critical energy for the proton option of the NICA collider are investigated. The method of superperiodic modulation of quadrupole gradients is applied. The selection of sextupoles is carried out to suppress the natural chromaticity and compensate the sextupole component. The Twiss parameters for the proposed structures are given, as well as the dynamic apertures and working points are investigated.

## SUPERPERIODIC MODULATION

The momentum compaction factor is defined in general as

$$\alpha = \frac{1}{\gamma_{\mathrm{tr}}} = \frac{1}{C}\int_0^C \frac{D(s)}{\rho(s)}\,ds \qquad (1)$$

where $C$ – the length of a closed equilibrium orbit, $D(s)$ – horizontal dispersion function, $\rho(s)$ – radius of curvature of the equilibrium orbit. And taking into account equation for dispersion function with biperiodic focusing:

$$\frac{d^2D}{ds^2} + [K(s) + \varepsilon k(s)]D = \frac{1}{\rho(s)} \qquad (2)$$

where $K(s) = \frac{e}{p}G(s)$, $\varepsilon k(s) = \frac{e}{p}\Delta G(s)$, $G(s)$ – gradient of magneto-optical lenses, $\Delta G(s)$ – superperiodic gradient modulation. Thus, MCF depend on the functions: the curvature of the orbit $\rho(s)$, gradient and modulation of quadrupole lenses respectively $G(s)$, $\Delta G(s)$.

In the NICA structure, the regular arrangement of dipole magnets eliminates the possibility of modulating the curvature of the orbit. Therefore, to change transition energy use only the modulation of dispersion function by modulating the strength of quadrupole lenses over the superperiod. For one superperiod, the MCF is determined [1]:

$$\alpha_s = \frac{1}{\nu_{x,\mathrm{arc}}^2}\left\{1 + \frac{1}{4}\left(\frac{\bar{R}_{\mathrm{arc}}}{\nu_{x,\mathrm{apk}}}\right)^4 \sum_{k=-\infty}^{\infty} \frac{{g_k}^2}{\left(1-\frac{kS}{\nu_{x,\mathrm{arc}}}\right)\left[1-\left(1-\frac{kS}{\nu_{x,\mathrm{arc}}}\right)^2\right]^2} \ldots\right\} \qquad (3)$$

where $\overline{R}_{arc}$ – the average value of the curvature, $\nu_{x,arc}$ – the number of horizontal betatron oscillations on the length of the arc, S – number of superperiods per arc length, $g_k$ – $k$-th harmonic of the gradient modulation in the Fourier series expansion of the function $\varepsilon k(s) = \sum_{k=0}^{\infty} g_k\, cos(k\phi)$. First harmonic $k = 1$ has a dominant influence and for 12 FODO cells, the condition is implemented $S = 4$, $\nu_{x,\mathrm{apk}} = 3$, where 3 FODO cells are combined into one superperiod as shown on Fig. 1. Thus, due to the tune of betatron oscillations of a multiple of 2π, the arc has the properties of a first-order achromat [2].

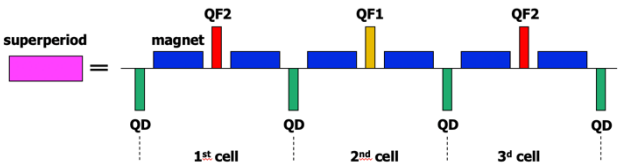


Figure 1: Superperiod contains 3 FODO cells.

## DISPERSION SUPPRESSION

An important requirement in the design of a magneto-optical structure is to ensure zero dispersion in straight sections to ensure the movement of particles along the equilibrium orbit in these sections. This requirement is easily implemented in the case of creating regular arcs composed of identical superperiods. In this case, by providing a zero dispersion value $D = 0$ (as well as the derivative of the dispersion $D' = 0$) at the entrance to the arc, due to the regularity, the output of the arc will also have zero values of the dispersion and its derivative, and therefore on the entire straight section. However, the peculiarity of the given structure of the NICA collider, the presence of missing magnets on the two extreme cells does not make it possible to create a completely regular arc of 4 identical superperiods. Thus, it is necessary to ensure the suppression of dispersion at the edges of the arc.

Two possible cases of dispersion suppression are considered and shown on Fig. 2.

- Dispersion suppression is carried out by using two edge FODO cells located symmetrically on both sides.
- Dispersion suppression by arc, by selecting the gradients of the quadrupoles of the two families.

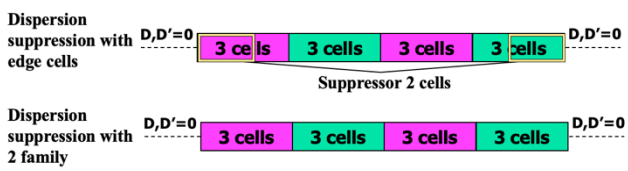


Figure 2: Principal scheme of arc for different dispersion suppression.

**Edge suppressor**. The edge superperiod has a missing magnet in 2 cells, thus making the collider arcs not regular and there is a need to suppress the dispersion in straight sections using 2 additional families of QFE1 and QFE2 quadrupoles on the edge of the arc. The scheme of arc with $\beta$-function and dispersion function of all entire ring are shown on Fig. 3.

ISBN: 978-3-95450-240-0 ISSN: 2673-5539 doi:10.18429/JACoW-RuPAC2021-TUPSB09

# RESONANCE SLOW EXTRACTION FROM ION SYNCHROTRON FOR TECHNOLOGICAL APPLICATION

M. F. Blinov, I.A. Koop, V. A. Vostrikov, Budker Institute of Nuclear Physics, Novosibirsk, Russia

*Abstract*

Third-order resonance slow extraction from synchrotron is the most common use extraction method for external target experiments nuclear physics, proton and heavy ion therapy, since it can provide relatively stable beams in long time. The principle of third-order resonant slow extraction is intentionally exciting the third-order resonance by controlling detuning and sextupole strength to gradually release particles from inside to outside stable separatrix. BINP develop the ion synchrotron for wide range of technological application. The present paper describes slow extraction method with exiting betatron oscillations by the transverse RF-field. Such extraction technique provides stable current extraction for entire extraction time. The paper present simulation of slow extraction driving RF-knockout.

## INTRODUCTION

The synchrotron will produce beams of protons accelerated up to 4 GeV and wide range of ion species including $^{209}Bi^{41+}$ up to 36 MeV/n respectively (see Table 1).

Table 1: Synchrotron Specifications

| Characteristics | Value |
|---|---|
| Circumference, m | 168.37 |
| Beam injection energy proton/$^{209}Bi^{41+}$, MeV/n | 700 / 36 |
| Maximum energy proton/$^{209}Bi^{41+}$, MeV/n | 4000 / 400 |
| Magnetic rigidity, T·m | 16.2 |
| Max dipole field, T | 1.6 |
| Critical γ | 6.39 |
| Tune, $Q_x/Q_z$ | 6.65 / 4.61 |
| Natural chromaticity, $\xi_x/\xi_z$ | -10.2 / -10.1 |
| Acceptance hor/ver, π cm·mrad | 7.5 / 1.9 |
| Beam intensity, protons/$^{209}Bi^{41+}$ | $10^{12}$ / $10^{8}$ |
| Momentum compaction factor | 0.024 |
| Proton beam emittance under injection, π cm·mrad | 0.52 |
| Frequency revolution proton/$^{209}Bi^{41+}$, MHz | 1.46 ÷ 1.75 / 0.48 ÷ 1.27 |

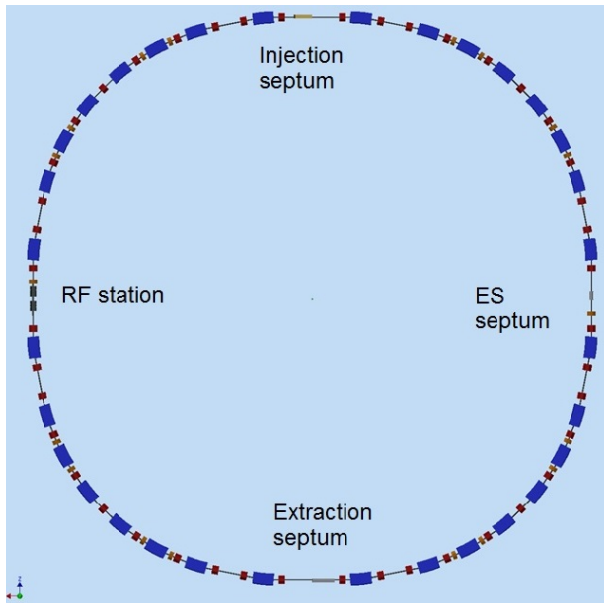


Figure 1: General layout of synchrotron.

The general layout of synchrotron is presented in Fig.1. The synchrotron optics is characterized by four super periods and four closed dispersion bumps (see Fig. 2). The injection and extraction septum magnets, RF-cavity and electrostatic septum located in free dispersion drifts. One resonance sextupole used for extraction is located close to RF-cavity. For slow extraction convenience the synchrotron operates below critical energy in the entire range of energy.

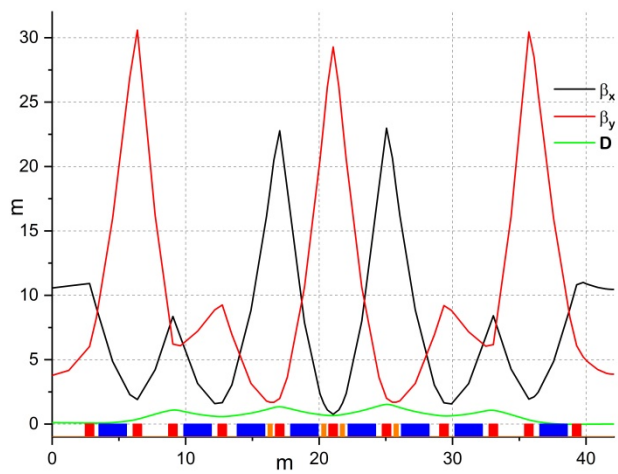


Figure 2: Lattice function of synchrotron quarter.

## SLOW EXTRACTION

The slow extraction from synchrotron based on the third order horizontal resonance. The sextupole magnet excites resonance harmonics. When the excitation achieves a cer-

ISBN: 978-3-95450-240-0 ISSN: 2673-5539 doi:10.18429/JACoW-RuPAC2021-TUPSB10

# MODELING OF THE SPIN-NAVIGATOR METHOD FOR MANIPULATING THE BEAM POLARIZATION IN A SPIN-TRANSPARENT STORAGE RING

A. E. Aksentev[1]*, A. A. Melnikov, Y. V. Senichev,
Institute for Nuclear Research of the Russian Academy of Sciences, Moscow, Russia
V. P. Ladygin, Joint Institute for Nuclear Research (JINR), Dubna, Russia
[1]also at National Research Nuclear University "MEPhI," Moscow, Russia

*Abstract*

A method for manipulating the orientation of the beam polarization axis based on using the so-called "spin-navigator" technique in a storage ring operating in the spin-transparent regime has been modelled. The beam particles' spin- and orbital dynamics have been numerically investigated with the purpose of determining the method's feasibility; the latter's effect on spin-decoherence has been studied also.

## INTRODUCTION

In the projected method for the manipulation of the beam polarization, the spin-transparent (ST) regime is effected by means of "Siberian snakes" which set the beam particles' spin precession frequencies close to zero (in the beam rest frame). Practically, this means that the spin-vector of a particle on the closed orbit (CO) coincides with itself after passing the accelerator lattice sequence (see Fig. 1). The additionally used "spin-navigating" solenoids (Fig. 2) have a two-fold purpose: not only to orientate the polarization axis, but also to stabilize this orientation by slowly turning the beam particles' spin-vectors about it, thus offsetting the "zero spin precession frequency" condition [1].

However, the finiteness of the beam phase space volume prevents the simultaneous satisfaction of the "zero precession frequency" condition by all beam particles. Due to the differences in their spin-orbit motion the particles' spin-vectors diverge (which phenomenon is termed "spin-decoherence"), which causes depolarization of the beam. One must meet certain conditions, homogenizing the distribution of the spin-precession axis over the beam phase space, in order to preserve the polarization.

The purpose of the present work was to study the beam particles' spin-orbital dynamics in the neighborhood of the zero spin resonance and the determination of whether the spin-navigator method for manipulating the orientation of the beam polarization axis is a feasible option. To that end, the COSY INFINITY modeling environment was used [2]. Depolarization mechanisms, in particular those specific to the proposed polarization manipulation method, have been considered.

## MODELLING RESULTS

Numerical modeling has been done using the COSY INFINITY [2] modelling environment. We used three bunches

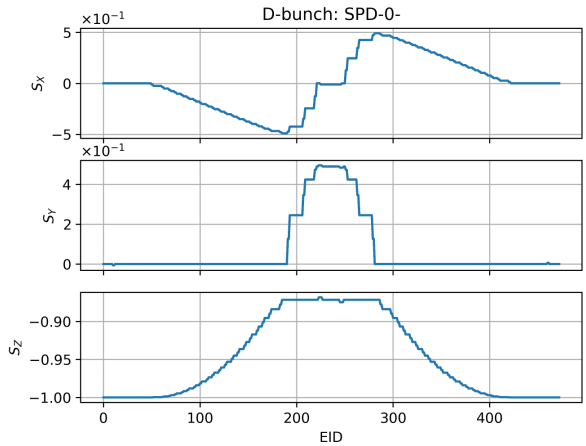


Figure 1: Transformation of the reference particle's spin-vector coordinates during one revolution in the accelerator lattice. The ordinal numbers (EID) on the horizontal axis indicate the element just passed. The particles whose spin-vector coordinates are represented in the figure have only energy deviation $\delta = {}^{\Delta K}/_{K}$ from the reference particle at injection, which is indicated by the words "D-bunch"; the words "SPD-0-" indicate that the spin-vectors of all particles pointed backwards along the reference particle's momentum vector.

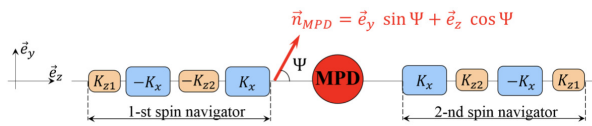


Figure 2: Spin-navigator placement scheme in the MPD-detector section [1].

of $N = 300$ particles each for a sufficiently precise beam polarization estimate

$$\boldsymbol{P} = \frac{1}{N}\sum_{j=1}^{N} \boldsymbol{s}^{(j)}.$$

Particles were uniformly distributed in phase space at injection:

1. X- and Y- bunches: $x, y = \pm 2$ mm respectively (the other phase-space coordinates set to zero);
2. D-bunch: $\delta = {}^{\Delta K}/_{K} = \pm 2 \cdot 10^{-4}$ (same as above).

* a.aksentyev@inr.ru

ISBN: 978-3-95450-240-0 ISSN: 2673-5539 doi:10.18429/JACoW-RuPAC2021-TUPSB11

# NUMERICAL INVESTIGATION OF THE ROBUSTNESS OF SPIN-NAVIGATOR POLARIZATION CONTROL METHOD IN A SPIN-TRANSPARENT STORAGE RING

A. Melnikov[1†], A. Aksentyev[1,2], Y. Senichev[1], V. Ladygin[3]
[1]Institute for Nuclear Research of the Russian Academy of Sciences, Troitsk, Moscow, Russia
[2]National Research Nuclear University "MEPhI," Moscow, Russia
[3]Joint Institute for Nuclear Research, Dubna, Moscow region, Russia

*Abstract*

The robustness of spin-navigator based method for manipulating the beam polarization axis has been investigated with respect to bend magnet installation errors. Toward that end, variation of the invariant spin axis components along the beamline of an imperfect storage ring operating in the spin-transparent mode has been estimated. The beam polarization vector behavior in the given lattice has been investigated. Conclusions are made regarding the feasibility of using "spin navigator" solenoids for defining the beam polarization axis in the detector region.

## INTRODUCTION

In the proposed method of polarization control in a spin-transparent (ST) mode spin precession frequency is set close to zero with the help of "siberian snakes". Since particles are in the vicinity of an integer resonance, "navigator" solenoids with weak fields are used for stabilization of polarization direction (Fig. 1) [1]. They consist of solenoids with longitudinal field and magnets with radial field rotating spin-vectors of particles by small angles. In ST method one can obtain any polarization direction at any point of an orbit for arbitrary beam energy.

This method of polarization control is highly sensitive to errors. That is why it is necessary to investigate its robustness in the numerical simulation. The stabilizing influence of navigator solenoids in the vicinity of an integer resonance should be larger than the influence of effects arising from lattice imperfections. Spin-orbit dynamics simulations using NICA lattice were made below to estimate the influence of magnet tilts on the ability to guide polarization direction with navigator solenoids in the detector.

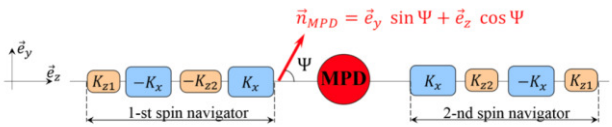


Figure 1: The scheme of navigator solenoids location close to MPD detector [1].

† alexei.a.melnikov@gmail.com

## METHOD "SPIN-KICK"

When the bending magnets are rotated around the optical axis it is necessary to compensate the vertical component of the guiding field to preserve the closed orbit. The latter will not be flat if the radial components of magnetic field are present. In the simulation a simplifying assumption was used that orbital dynamics does not change with magnet tilts but spin transfer matrix of an element is rotated by an angle depending on a tilt. All the results obtained with this assumption can be interpreted without the loss of generality in the frame of estimation of ST method robustness and feasibility.

Spin dynamics of particles in a laboratory frame is described by T-BMT equation:

$$\frac{d\vec{S}}{dt} = \vec{S} \times (\vec{\Omega}_{MDM} + \vec{\Omega}_{EDM}),$$

$$\vec{\Omega}_{MDM} = \frac{q}{m\gamma}\left[(\gamma G + 1)\vec{B}_{\perp} + (1+G)\vec{B}_{\parallel} - \gamma\left(G + \frac{1}{\gamma+1}\right)\frac{\vec{\beta}\times\vec{E}}{c}\right],$$

$$\vec{\Omega}_{EDM} = \frac{q\eta}{2m}\left[\vec{\beta}\times\vec{B} + \frac{\vec{E}}{c}\right],$$

where $\vec{\Omega}_{MDM}$ and $\vec{\Omega}_{EDM}$ are spin-vector $\vec{S}$ precession frequencies, caused by the presence of magnetic and electric dipole moment of particles – MDM and EDM respectively. $G$ is the anomalous magnetic moment, $\gamma$ – Lorentz factor. $\vec{B} = \vec{B}_{\parallel} + \vec{B}_{\perp}$, $\vec{B}_{\parallel} = \frac{\vec{v}\cdot\vec{B}}{v^2}\vec{v}$.

In the case of a purely magnetic lattice ($E = 0$) and taking into account that $\Omega_{EDM} \ll \Omega_{MDM}$, in the rest frame:

$$\vec{\Omega}_{MDM} = \frac{q}{m\gamma}[\gamma G\,\vec{B}_{\perp} + (1+G)\vec{B}_{\parallel}].$$

In the case of bend magnet tilts around the optical axis of the accelerator $B_{\parallel} = 0$. In linear approximation the vertical precession frequency does not change. The radial component $\Delta\Omega_{MDM}$ emerges that is equivalent to spin-vector rotation around the radial axis by an angle $\psi$:

ISBN: 978-3-95450-240-0 ISSN: 2673-5539 doi:10.18429/JACoW-RuPAC2021-TUPSB12

# DEVELOPMENT OF A PROGRAM CODE FOR CALCULATION OF CHARGED PARTICLE DYNAMICS IN RFQ

A.S. Boriskov, N.V. Zavyalov, A.V. Telnov, M.L. Smetanin, A.M. Opekunov, L.E. Polyakov,
RFNC-VNIIEF, Sarov, Russia

*Annotation*

The code for the beam dynamics simulation in radio-frequency quadrupole (RFQ) accelerating structure was written in the C++ programming language. Charged particle beam dynamics was simulated in RFQ structure aimed to accelerate ion beams up to energies of 1.25 MeV / nucleon.

The characteristics of the beam at the exit of the structure (velocity, particle capture coefficient, beam profile, transverse emittances, longitudinal phase portrait) were determined.

## INTRODUCTION

The considered accelerating structure is intended for the initial acceleration of ions with an A/Z ratio from 1 to 3.2 (A is the mass number, Z is the charge of the ion). Particles from H to O fall within the specified range.

In order for the capture coefficient in the acceleration mode to be high, it is necessary to use systems that are effective at a low initial particle velocity. These requirements are met by accelerating structures in which acceleration, grouping and focusing of charged particles by a radio-frequency (RF) electromagnetic field occur simultaneously.

## RFQ ACCELERATOR

Focusing systems use conventional electrostatic or magnetic quadrupole lenses. To focus the beam in two transverse directions, it is necessary to change the polarity of the poles. When using an alternating RF field, it is possible to use a quadrupole system of electrodes, which is uniform along the axis of the accelerator [1]. Such a system is shown in Fig. 1.

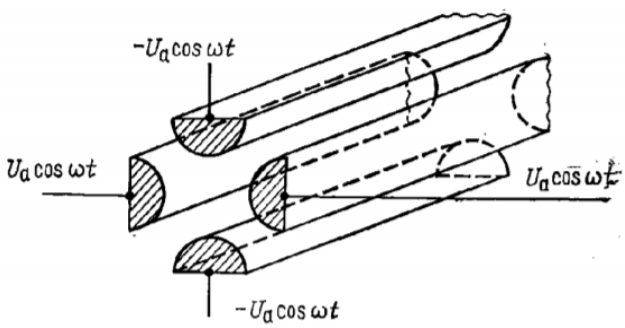


Figure 1: Quadrupole symmetric four-wire line.

The value $2U_a$ is the amplitude value of the voltage between adjacent electrodes. Since an RF voltage is applied to the electrodes, the particles, when moving along the axis, successively experience the action of fields with an alternating sign of the gradient.

The longitudinal accelerating component of the electric field in a four-wire line is created if the distance between opposite electrodes of the same polarity changes periodically along the axis [2]. The spatial period of the change in the distance between the electrodes should be equal to the path that the equilibrium particle travels during the RF period, and the phases of the change in the distances in the perpendicular planes are shifted by half a period.

## PROTON AND LIGHT ION BEAM DYNAMICS SIMULATION

The selection of the parameters of any accelerating structure for calculating the particle dynamics begins with the selection of the operating frequency. It is selected based on the condition of the minimum length of an accelerator with a RFQ.

The closest to the optimal value is the widely used frequency of 81.25 MHz from the range of frequencies from 40.625 to 972 MHz.

Taking into account the literature data on the recommended field strength on the surface of the electrodes [3], the value of the Kilpatrick criterion was chosen 1.85.

A pre-buncher is usually placed between the ion source and the accelerating structure. Taking into account the buncher, the phase length of the beam at the entrance to the structure with the RFQ is set equal to 1.4 π.

## EQUATION OF MOTION IN THE APPROXIMATION OF ANALYTICALLY GIVEN FIELDS

To simulate the action of an electromagnetic field on accelerated particles in the equation of motion, it is sufficient to take into account only the electric component of the RF field:

$$\frac{d\vec{p}}{dt} = e\vec{E}(r,t)\,. \qquad (1)$$

In the Cartesian coordinate system, the expression for the accelerating potential in the RFQ structure on the axis of beam motion in the one-wave approximation has the form [3]:

$$U(x,y,z,t) = \frac{U}{2}\left[A_{01}(x^2-y^2) + A_{10}I_0\left(k\sqrt{x^2+y^2}\right) \cdot \sin(kz)\right]\cos(\omega t), \qquad (2)$$

where $U$ – voltage between electrodes;
$k$ – wave number;
ω – RF field frequency;
$I_0$ – modified Bessel function;
$A_{01}$ и $A_{10}$ – focusing and accelerating parameters respectively.

ISBN: 978-3-95450-240-0 ISSN: 2673-5539 doi:10.18429/JACoW-RuPAC2021-TUPSB13

# CHARGED PARTICLE DYNAMICS OPTIMIZATION IN DISCRETE SYSTEMS

E. D. Kotina†, D. A. Ovsyannikov, St. Petersburg State University, St. Petersburg, Russia

*Abstract*

Discrete optimization methods of dynamic systems are widely presented in the scientific literature. However, to solve various problems of beam dynamics optimization, it is necessary to create special optimization models that would take into account specifics of the problems under study. The paper proposes a new mathematical model that includes joint optimization of a selected (calculated) motion and an ensemble of perturbed motions. Functionals of a general form are considered, which make it possible to estimate various characteristics of a charged particle beam and the dynamics of the calculated trajectory. The optimization of a bundle of smooth and nonsmooth functionals is investigated. These functionals estimate both integral characteristics of the beam as a whole and various maximum deviations of the parameters of the particle beam. The variation of a bundle of functionals is given in an analytical form, that allows us to construct directed optimization methods. The selected trajectory can be taken, for example, as the trajectory of a synchronous particle or the center of gravity of a beam (closed orbit). We come to discrete models when we consider the dynamics of particles using transfer matrices or transfer maps. Optimization problems can be of orbit correction, dynamic aperture optimization, and many other optimization problems in both cyclic and linear accelerators of charged particle beams.

## INTRODUCTION

Discrete systems are becoming increasingly important in theory and practical application in optimal control and optimization problems [1-5]. This is due to the fact that many problems are described by discrete equations, since in practice information about the state of the process comes discretely, and control of the dynamic process is implemented most often at discrete moments of time. The standard approach to the design of various control systems involves the initial calculation of the selected motion and the subsequent study of perturbed motions using equations in deviations. This approach, however, does not always lead to the desired results. When analyzing perturbed motions, it turns out that their dynamic characteristics are not always satisfactory from one point of view or another. This is a consequence of the significant dependence of the perturbed motions on the selected motion. In this paper, a mathematical model is proposed that allows simultaneous optimization of the selected motion and the ensemble of perturbed motions in discrete systems. In this case, the simultaneous optimization of smooth and nonsmooth functionals is considered.

† e.kotina@spbu.ru

The classical formulations of optimal control problems in discrete systems are quite well known and studied [1]. These problems can be considered as tasks of single trajectories control. Along with them, non-standard problems of the theory of optimal control are being developed. In particular, the control problems of ensembles of trajectories (beams) were considered under various cost functionals in continuous and discrete-time systems [2]. Further, non-standard problems of joint optimization of program motion and perturbed motions in continuous systems [6, 7], as well as in discrete ones [3-5] were developed. The problems of simultaneous optimization of smooth and nonsmooth functionals defined on a program motion and a beam of perturbed trajectories in continuous and discrete systems were further developed [8-10].

This article is devoted to the construction of new methods for optimizing the bundle of smooth and nonsmooth functionals in discrete systems.

## PROBLEM STATEMENT

In this paper a dynamic system is described by the discrete equations of the following type

$$x(k+1) = f\big(k, x(k), u(k)\big), \quad (1)$$

$$y(k+1) = F\big(k, x(k), y(k), u(k)\big), \quad (2)$$

$$k = 0, \dots, N-1,$$

where $x(k) - n-$ dimensional phase vector, characterizing the state of the system, $y(k) - m-$ dimensional phase vector, $u(k) - r-$ dimensional vector, $f(k) = f\big(k, x(k), u(k)\big)$ is $n-$dimensional vector function, $F(k) = F\big(k, x(k), y(k), u(k)\big) - m-$ dimensional vector function. We suppose that $f(k)$ is defined and continuous in $\Omega_x \times U(k)$ by the arguments $\big(x(k), u(k)\big)$ for $k = \overline{1, N}$ along with their partial derivatives. We also assume that $F(k)$ is defined and continuous in $\Omega_x \times \Omega_y \times U(k)$ by the arguments $\big(x(k), y(k), u(k)\big)$ for $k = \overline{1, N}$ along with their first and second partial derivatives. Here $\Omega_x \subset R^n$, $\Omega_y \subset R^m$, $U(k)$ – a compact set in $R^r$, $k = \overline{1, N}$. We suppose that for a given vector $u(k)$, the vector $x(k)$ and the vector $y(k)$ uniquely determine the phase state $y(k+1)$ of the perturbed particle at the $k-$th step and vice versa, by $y(k+1) -$ the state of the perturbed particle at the previous step.

Equation (1) describes the dynamics of the selected motion. Equation (2) describes the perturbed motion.

We assume, that $x(0) = x_0$, $(x_0 \in \Omega_x \subset R^n)$ and the initial state of the system (2) is described by set $M_0 -$ a compact set of nonzero measure in $R^m$, the sequence of vectors $\{u(0), u(1), \dots, u(N-1)\}$ we will call control and denote $u$ for brevity, $x = \{x(0), x(1), \dots, x(N)\} =$

ISBN: 978-3-95450-240-0 ISSN: 2673-5539 doi:10.18429/JACoW-RuPAC2021-TUPSB16

# CALCULATION AND OPTIMIZATION OF HIGH-ENERGY BEAM TRANSFER LINES BY THE MONTE CARLO METHOD

D.A. Amerkanov†, E.M. Ivanov, G.A. Riabov, V.A. Tonkikh, NRC "Kurchatov Institute" - PNPI, Gatchina, Leningrad district, 188300, Russia

*Abstract*

The calculation of high-energy beam lines consists of tracing of the proton beam trajectories along the transport channel from the source. The PROTON_MK program code was developed to carry out such calculations using the Monte Carlo method. The beam from the accelerator is introduced in the form of a multivariate Gaussian distribution in x,x', z,z', dp/p phase space. In the case when an absorber (absorber, air section, window in the channel, etc.) is installed in the transport channel the beam parameters after the absorber are calculated using the GEANT4. The output file of this code can be used as input for the program. The program allows calculation of any beam parameters - intensity, spatial or phase density, energy distribution, etc. The program includes a block for the optimization of beam parameters presented in a functional form. Random search method with learning for search correction based on analysis of intermediate results (so-called statistical gradient method) is used for obtaining the global maximum of a function of many variables. The program has been tested in calculations of the beam transport lines for IC-80 cyclotron and for the development of the beam line for ophthalmology.

## INTRODUCTION

There is a many of programs in the world for calculating the optics of high-energy beams [1, 2]. In most of them, the ion source is represented in the phase space in the form of a multidimensional ellipsoid, inside which particles and their initial parameters are uniformly distributed while there are no particles outside. Moreover, it is assumed that the beam emittance is conserved during the transport of the beam along the channel, which means that there are no beam losses in the channel. In particular, it is not possible to compute the effect of collimators on the intensity and other parameters of the beam. These assumptions greatly facilitate the mathematical formulation of the problem, but they do not quite reflect the experimental situation. In this work, a more adequate representation of the ion source is proposed.

## REPRESENTATION OF SOURCES

In the experiment, the beam profile i.e. the distribution of the beam intensity over the transverse coordinates is well approximated by the Gaussian distribution, and the beam spot, i.e. intensity distribution in x, z-plane is an ellipse. This situation is typical for a multivariate Gaussian distribution, where any marginal or partial distribution along any axis is also described by a Gaussian distribution. Let's assume that the beam in the ion source can be described by a five-dimensional normal distribution with a distribution function in space $(x, x', z, z', \delta)$:

$$f(X,Z,s,\delta)=\frac{1}{(2\pi)^{5/2}|\Sigma|^{1/2}}\exp\left\{-\frac{1}{2}\begin{pmatrix}X\\Z\\\delta\end{pmatrix}^{T}\Sigma^{-1}\begin{pmatrix}X\\Z\\\delta\end{pmatrix}\right\}$$

where $\sum$ is a 5x5 symmetric matrix, which is the covariance matrix of the adopted distribution, i.e. the mathematical expectation of the distribution and its elements are of interest, X is a vector (x, x '), Z is a vector (z, z'). The components of the matrix Σ have the form where $\sigma_{k\ell} = \langle y_k \cdot y_e \rangle$ $y_k$, $y_e$ are the components of the random vector $(x, x', z, z', \delta)$.

In most cases, the movements along x and z are independent and then $\sum_{xz}$=0.In the case when the magnetic analysis takes place only in the x-plane $\sum_{zp}$=0.Based on the general properties of the multivariate normal distribution, it is possible to write the bivariate Gauss distribution in x, x' space in the form:

$$f(X)=\frac{1}{(2\pi)\left|\sum_{xx'}\right|^{1/2}}\exp\left\{-\frac{1}{2}X^{T}\sum_{xx'}^{-1}X\right\}$$

The elements of the correlation matrix $\Sigma_{xx}$ are the mathematical expectations of the vector ($x_i$ $x_j$') i.e. M ($x_i$ $x_j$), where i, j = 1, 2 and $x_1$ = x, $x_2$ = x'. The matrix $\Sigma_{xx}$ has the form:

$$\sum_{xx'}=\begin{pmatrix}M(x^2) & M(xx')\\ M(xx') & M(x'^2)\end{pmatrix}=\begin{pmatrix}\sigma_x^2 & \rho\sigma_x\sigma_{x'}\\ \rho\sigma_x\sigma_{x'} & \sigma_{x'}^2\end{pmatrix}$$

where M (x, x') = $\rho\sigma_x\sigma_{x'}$ by definition of the correlation coefficient ρ.

Then the bivariate Gaussian distribution on the plane takes the form:

$$f(x,x')=\frac{1}{2\pi\sqrt{1-\rho^2}\,\sigma_x\sigma_{x'}}\exp\left\{-\frac{1}{2\left(1-\rho^2\right)}\lambda^2\right\}$$

where $\sigma_x$ $\sigma_{x'}$ are the standard deviations and ρ is the correlation coefficient. From the general form of the probability density of two random variables, it follows that the probability density is constant in all points of the xx' plane at which

$$\lambda^2=\left(\frac{x^2}{\sigma_x^2}-2\,\rho\,\frac{xx'}{\sigma_x\sigma_{x'}}+\frac{x'^2}{\sigma_{x'^2}}\right)$$

where λ is an arbitrary value.

The curve on the xx' plane, defined by the equations above, is the so-called ellipse of equal probabilities. In the case of a Gaussian distribution, instead of one ellipse, there is a set of concentric ellipses each of which corre-

† amerkanov_da@pnpi.nrcki.ru

ISBN: 978-3-95450-240-0 ISSN: 2673-5539 doi:10.18429/JACoW-RuPAC2021-TUPSB17

# INVESTIGATIONS OF CHARGE PARTICLE DYNAMICS IN SPACE CHARGE FIELDS

A.S. Chikhachev[1], All-Russian Electrotechnical Institute, 111250, Moscow, Russia

*Abstract*

The paper studies the nonstationary dynamics of single-component systems. The problem of the dynamics of a plane layer is considered. The classical collisionless system described by the "Meshchersky integral" and the "conjugate" integral of motion is considered. States characterized by a constant charge in nonstationary coordinates are obtained.

## INTRODUCTION

The study of non-stationary systems that intensively interact with their own field is of great interest from both experimental and theoretical points of view. In this paper, we will use the nonstationary Hamiltonian, which follows from Meshchersky's work [1]. A similar Hamiltonian was used in [2,3,4], in which, apparently, the problem of exact accounting for the eigenfield was solved for the first time. It should be noted that the model Hamiltonian of a nonstationary system can be used both for a quantum mechanical system and for a classical one. In this paper, the classical system is considered.

## CLASSIC COLLISIONLESS SYSTEM

Let us first consider a one-dimensional system of charged particles described by a collisionless kinetic equation. Let x be the coordinate and t be the time. A one-dimensional system can be described by the following nonstationary Hamiltonian:

$$H=\frac{p^2}{2m}+\frac{1}{\xi^2(t)}U\left(\frac{x}{\xi(t)}\right) \tag{1}$$

Where $p=m\dot{x}$, $\xi(t)$ - the characteristic function that satisfies the equation $\ddot{\xi}=\frac{\lambda}{\xi^3(t)}$, Where $\lambda$ - constant.

If, next, enter new variables $x_*=\frac{x}{\xi(t)}$, $\tau=\int\frac{dt'}{\xi^2(t')}$, then from (1.1) we can obtain an expression for the integra of motion:

$$I=\frac{m}{2}\left(\frac{dx_*}{d\tau}\right)^2+\frac{m\lambda}{2}x_*^2+U(x_*). \tag{2}$$

Potential function $U(x_*)=q\xi^2\Phi\left(\frac{x}{\xi}\right)$, where is the elementary charge , is the electrostatic potential. In variables, the expression (2) is essentially the Hamiltonian of a stationary (i.e., independent of ) systems, and the role of the potential is played by the expression $\frac{m\lambda x_*^2}{2}+U(x_*)$.

In addition to (2), there is a conjugate integral:

$$J_I^{\pm}=\pm\int_0^{x_*}\frac{dx_*'\sigma\left(\frac{2}{m}(I-U(x_*'))-\lambda x_*'^2\right)}{\sqrt{\left(\frac{2}{m}(I-U(x_*'))-\lambda x_*'^2\right)}}-\tau,$$

here $\sigma$ is the Heaviside function. The velocity of a particle can be represented as the sum of the portable (or nasal) velocity - this is the magnitude $x\frac{\dot{\xi}}{\xi}$ and relative-

$$\upsilon_x'=\pm\sqrt{\frac{2}{m}(I-U(x_*))+\frac{x_*^2}{4\tau_0^2}}.$$

In this case, the relative movement in the positive and negative directions of the axis is possible $x$. Consider the case of relative forward motion: $\upsilon_x'>0$, then

$$J_I^{=}=\int_0^{x_*}\frac{dx_*'\sigma\left(\frac{2}{m}(I-U(x_*'))-\lambda x_*'^2\right)}{\sqrt{\left(\frac{2}{m}(I-U(x_*'))-\lambda x_*'^2\right)}}-\tau.$$

Performing equality $\frac{dJ_I^+}{d\tau}\equiv 0$ is trivial.

Previously, conjugate integrals of motion, apparently for the first time, were considered in [2].

There are, further, two possibilities: to study the dynamics of a clot with an increasing and decreasing function $\xi(t)$. Let us first consider the case of a decreasing $\xi(t)=\sqrt{\xi_0^2-\frac{t}{\tau_0}}$. In this case,

[1]churchev@mail.ru

ISBN: 978-3-95450-240-0 ISSN: 2673-5539 doi:10.18429/JACoW-RuPAC2021-TUPSB20

# SELECTION OF A SYSTEM FOR CORRECTING THE ENERGY SPREAD OF RELATIVISTIC ELECTRON BUNCHES FOR A FREE ELECTRON LASER

A. M. Altmark†, N. A. Lesiv, K. Mukhamedgaliev, Saint-Petersburg Electrotechnical University "LETI", Saint-Petersburg, Russia

*Abstract*

The object of this work is a device called dechirper, which is used to decrease energy spread in relativistic electron bunch for free electron laser application. This system is based on cylindrical dielectric waveguide with vacuum channel needed for electron bunch passing. The Vavilov-Cherenkov radiation excited in waveguide is used to profile electromagnetic field inside the bunch and therefore to achieve the required energy distribution. The work includes numerical modeling of the electron beam passage through a waveguide structure, the generation of wake radiation and the interaction of this radiation with an electron bunch. We made original code to carry out numerical modeling, where the method of macroparticles and the method of Green's function are implemented. The dependences of the energy compression coefficient and the length at which the maximum energy compression coefficient is achieved on various parameters of the dielectric waveguide structure and the physical parameters of electron bunches were identified. Various recommendations were also made on the choice of a waveguide used as a dechirper.

## INTRODUCTION

The use of undulators for the generation of monochromatic laser radiation is related with energy spread reducing inside electron bunch, implemented with the help of dechirpers. The main advantage of plasma-based dechirpers [1] is the high values of the generated fields, but the realization of such a scheme is associated with high cost of technical implementation and plasma nonstability. Widespread dechirpers based on rectangular dielectric waveguide [2] due to simplicity manufacturing technology of waveguide as well as possibility of adjustment distances between plates. Dielectric rectangular structures are used in STFC Daresbury Laboratory developing Free Electron Laser (FEL) CLARA [3]. Th structure consisting of pairs of flat, metallic, corrugated plates is used in SLAC [4] which, despite its simplicity, has a significant limitation in the form of a low breakdown voltage. This work is concentrated on reducing of energy spread of bunch in cylindrical dielectric waveguide, as it becomes possible to generate higher fields compared to rectangular structure with the same charge and bunch length. In addition, in this case, there are no problems of instability of the structure that accompanies the plasma waveguide.

† aaltmark@mail.ru

## INITIAL PARAMETERS

Dechirper is a part of a FEL that serves for energy spectrum correction of relativistic electron bunch, Fig. 1.

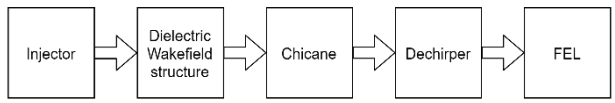


Figure 1: Beam preparation scheme for FEL.

After being generated in the injector, the bunch enters in the wakefield dielectric structure where it is placed in field of another bunch, called "driver". The bunch is placed at a point in the field to create an energy distribution along the bunch when the energy of "head" is less than the energy of the "tail", Fig. 2. This energy distribution is needed for chicane (system of dipole magnets), where it is compressed and then enters in the dechirper. Last one is represented by cylindrical dielectric waveguide (CDW), Fig.2, where the bunch creates a wakefield within itself to profile the energy with minimum spread. There is a clear dependence of its radiation spectrum on the energy distribution along the bunch length. A higher monochromaticity of FEL radiation is observed with a more uniform distribution of energy.

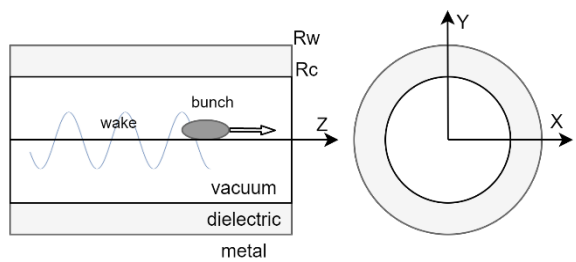


Figure 2: Dechirper based on cylindrical dielectric waveguide.

This paper considers a problem in which a relativistic electron bunch with a given energy distribution along the length enters in CDW(*Rc* – inner radius, *Rw* – external radius, ε – dielectric constant), Fig.2, with dielectric filling and physical parameters of the bunch: *Q* – charge of bunch; *W* – bunch energy; Δ*W* – the spread of the energy; *offset_x* – dismission of the bunch along the *X*-axis, $\sigma_x$, $\sigma_y$, $\sigma_z$ is the standard deviation of Gaussian bunch along the corresponding direction.

The monoenergetic coefficient *C* is obtained from the ratio of the maximum energy difference of the particles in the bunch ($\Delta W_{max}$) and the average energy of the bunch *W*. The energy compression coefficient (ECC) *D* is obtained from the ratio of $C_0$ in start of calculation and $C_f$ at

ISBN: 978-3-95450-240-0 ISSN: 2673-5539 doi:10.18429/JACoW-RuPAC2021-TUPSB21

# SYSTEM FOR CORRECTING THE LONGITUDINAL LENGTH OF ELECTRON BUNCHES FOR GENERATION A FREE ELECTRON LASER

A. M. Altmark†, N. A. Lesiv, K. Mukhamedgaliev, Saint-Petersburg Electrotechnical University "LETI,", Saint-Petersburg, Russia

*Abstract*

The chicane is device for longitudinal compression of electron bunch for generation of coherent radiation in free electron laser. It is present a numerical simulation of beam dynamics passing through system which consist dielectric waveguide and four dipole magnets. The simulations made with use the modified Euler method based on Green-function knowledge for electromagnetic field. We researched influence of various physical parameters of the electron bunch, as well as the chicane parameters on the change in the longitudinal bunch length. The optimal parameters of the focusing system were proposed for a relativistic particle beam with given initial bunch parameters. Recommendations for the selection of chicane parameters are also presented.

## INTRODUCTION

The beam compression is necessary for a variety of applications, such as, for example, the generation of short X-ray pulses [1]. To implement the compression of beams can, for example, using Laser Wake Field Accelerator (LWFA), which forms the necessary energy profile for the further use of this beam in a free electron laser (FEL) [2,3]. Also, for profiling of beam energy it is used Plasma Wake Field Accelerator (PWFA) [4]. The scientists of Argonne Wakefield Accelerator (AWA) employees are developing a compression system to generate a sequence of beams [5], which can then be used to produce THz radiation. The problem of generating a short beam in Stanford Linear Accelerator (SLAC) is solved using a periodic structure [6], where the wakefield creates a profile of the beam energy necessary to create the Linac Coherent Light Source (LCLS), which is part of FEL project. The purpose of this work is to obtain the recommended parameters of the chicane, based on bunch dimensions and the distribution of energy inside the bunch.

## INITIAL PARAMETERS

A relativistic bunch of charged particles with a given linear distribution of energy and bunch length flies through chicane – a system consisting of four two-half magnets.

Simple scheme of chicane illustrated on Fig.1 and consists of four dipole magnets. The high-energy particles located in the "tail" of the bunch move along a short path and catch up with low-energy particles located in the "head" of the bunch, which move along a longer path, thus compressing the bunch.

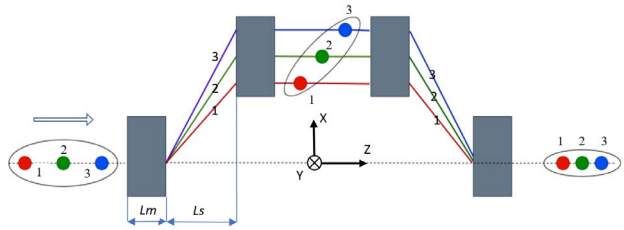


Figure 1: Schematic representation of a chicane consisting of four two-way magnets (1 – "tail" head of bunch and 3 – "head" of bunch).

It is necessary to determine the final length of the bunch, after the flight of the chicane, as well as to consider the influence of the bunch parameters and the parameters of the magnetic system on it. We use a qualitative characteristic of bunch, which is called a compression coefficient along the bunch length $A$. It is defined as:

$$A = \frac{l_0 - l_f}{l_0} 100\%,$$

where $l_0$ is initial bunch length, $l_f$ is final bunch length.

It is also important to note that the height of the magnetic sections is infinite during chicane modeling. Therefore, we exclude in our numerical modeling the situation when particles do not fall into dipole magnets.

In this paper, to calculate the beam dynamics in chicane, two numerical based on macroparticle method [7] and the Euler method. According to macroparticle method the bunch is represented by number of interacting identical particles. This way allows significantly increase the speed of calculations. This method is quite simple to implement and less expensive compared to other methods of calculation. Also, we used modified Euler method was chosen to the simulation.

We choose initial data for numerical simulations: a magnetic system consisting of four dipole magnets arranged symmetrically with a magnetic field $B$ = 1 T, length of magnetic section $Lm$ = 2 cm, the distance between the magnetic sections $Ls$ = 2 cm, the charge of the bunch $Q$ = 0.16 fC, transverse dimensions ($\sigma_x$ and $\sigma_y$) = 0.01 mm, longitudinal size of the bunch (standard deviation) $\sigma_z$ = 0.1 mm, radial displacements along the axes $X$ and $Y$ (*offset_x*, *offset_y*) = 0 cm, bunch energy $W$ = 1000 MeV, relative energy spread $\varkappa$ = 5 %.

It has been shown that the modified Euler method is stable with a sufficiently large number of particles, so it can be used for numerical modeling. Minimum number of *Nopt* lies in the range of 1000 or more particles. For present experiments, this number of particles will be used.

The first experiment is made to identify the dependence

† aaltmark@mail.ru

ISBN: 978-3-95450-240-0 ISSN: 2673-5539 doi:10.18429/JACoW-RuPAC2021-TUPSB22

# WAKEFIELD UNDULATOR BASED ON A SINUSOIDAL DIELECTRIC WAVEGUIDE*

I. L. Sheinman†, O. S. Alekseeva, Saint-Petersburg Electrotechnical University "LETI", Saint-Petersburg, Russia

*Abstract*

The idea of creating an undulator based on the wake principle by passing a beam through a sinusoidal dielectric waveguide is proposed. A numerical analysis of the dynamics of a short electron beam in a wake undulator on a bending wave of a waveguide with a dielectric filling is carried out. The possibility of reducing the instability of the beam by choosing the initial phase of the flexural wave and the initial transverse positioning of the beam is considered.

## INTRODUCTION

Undulators are key elements of free electron lasers [1]. They are devices in which the electron beam in the process of movement experiences the action of transverse periodic force. The oscillations of particles arising under the force in the transverse direction are accompanied by accelerated motion of the particles, which, in turn, generates electromagnetic radiation in the direction of the beam movement. To create a transverse force, electromagnetic fields created by periodically located dipole magnets are used. Undulator radiation also arises when particles move through a periodic lattice of crystals, where the local fields of atoms play the role of deflecting fields.

Undulators have a number of features that make them attractive for creating free electron lasers: a large beam aperture; short undulator period, the ability to generate waves of both circular and plane polarization, dynamic control of the wavelength and undulator coefficient.

Linear charged particle accelerators are used as sources of electron bunch sequences for free electron lasers. An intensively developing direction in recent years is the use of linear wakefield accelerating structures with dielectric filling. They are based on the principle of excitation of Cherenkov radiation in dielectric waveguides by a high-current relativistic electron beam.

The leading bunch (driver) with a large charge, moving along the axis of the vacuum channel of the dielectric waveguide, generates behind itself a wake electromagnetic wave of Cherenkov radiation, the phase velocity of which is equal to the speed of the driver. This wave has a longitudinal field component, which is used to accelerate the witness bunch.

A significant drawback of this approach is the exponentially increasing displacement of the beam relative to the waveguide axis, associated with the interaction of the beam with the wakefield generated by it itself, as a result of which the particles are attracted to the waveguide wall, and at high energy they can destroy its integrity.

In [2-5], it was proposed to use the parasitic effect of beam deflection from the waveguide axis in a wakefield accelerating structure to create a wakefield undulator. The use of the bunch-generated intrinsic transverse fields in a microwave cavity to create an undulator effect was proposed in [2]. In [3], it was proposed to create an alternating transverse electromagnetic field for the generation of undulator radiation with the oncoming motion of the generator and undulator bunches. However, due to significant deflecting fields acting on the generator bunch, the range of its flight turned out to be limited [4], which reduced the effectiveness of the method.

An alternative idea is to use a sinusoidal bent waveguide to create transverse beam oscillations [5]. In such a waveguide, the tail of the main beam or the secondary beam of charged particles, being attracted either to one wall or to the other, will vibrate in the transverse direction (Fig. 1). Due to such oscillations, the beam electrons will move with transverse acceleration and generate electromagnetic waves, which is a necessary condition for creating a free electron laser.

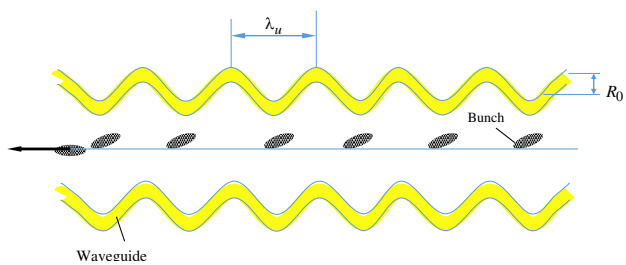


Figure 1: Wakefield undulator.

Modern undulators based on an alternating magnetic field are very expensive and require precise tuning. The proposed approach assumes the use of a bent waveguide with correctly selected parameters as a terminal device for an accelerator for a free electron laser, which will significantly reduce the cost of creating undulators.

## BEAM DYNAMICS IN A WAKEFIELD WAVEGUIDE

To describe the beam dynamics with deviations from the waveguide axis not exceeding $R_c/2$, it is possible with a good degree of accuracy to take into account only the first transverse mode of the wake waveguide with a linear dependence of the transverse force on the distance from the particle generating the force to the waveguide axis.

Let us first consider a filamentary electron bunch (beam) with a longitudinal charge profile $f(\zeta)$ moving

* Work supported by Baltic Science Network powerhouse.
† ishejnman@yandex.ru

ISBN: 978-3-95450-240-0 ISSN: 2673-5539 doi:10.18429/JACoW-RuPAC2021-TUPSB25

# STORAGE RING DESIGN AND BEAM INSTABILITIES INVESTIGATION FOR MEPhI's PHOTON SOURCE*

V. S. Dyubkov†, S. M. Polozov, National Research Nuclear University MEPhI, Moscow, Russia

*Abstract*

There is a design of a compact photon source based on inverse Compton scattering at NRNU MEPhI. Updated synchrotron lattice, electron dynamics simulation and beam instabilities studies are presented.

## INTRODUCTION

Photons of 5-30 keV and flux of about $10^{10}$-$10^{12}$ γ/s are used for materials science, research of nano - and biosystems, medicine and pharmacology, physics and chemistry of fast-flowing processes. There are a few ways of 5-30 keV photon production. This project aims to development of a compact system for generating radiation in a next-generation light undulator in the photon energy range of 5-30 keV for ring and linear sources based on inverse Compton scattering.

A number of facilities based on inverse Compton scattering effect are under design or operation today: MuCLS [1], LyCLS [2], ThomX [3], ODU CLS [4], SLEGS [5], SPARC_LAB [6], LUCX [7], LESR [8], Daresbury Compton Backscattering X-ray Source [9]. Compton light source is supposed to be built on the NRNU MEPhI site. Two operating modes of the compact light source are possible: the storage ring Compton source design and the linac-based Compact-XFEL.

## STORAGE RING

In order to generate 5-30 keV X-rays in light ondulator it is suggested that compact storage synchrotron will be used with top-up injection from normal conducting S-band linac with tuneable energy in the range of 20-60 MeV.

The use of a storage ring provides the following advantages: high intensity of the generated photon flux, high brightness, electron beam energy tuning in a wide range, high degree of monochromaticity and coherence of the generated photons.

In order to get horizontal rms beam size at interaction point (IP) with laser photons of 30 μm for electron horizontal emittance $\varepsilon_{x,\mathrm{rms}}$ of 100 nm the horizontal beta-function value should be equal to 30 cm in accordance with

$$\beta_x = \sigma^2_{x,\mathrm{rms}} \big/ \varepsilon_{x,\mathrm{rms}}.$$

The same value should have the vertical beta-function at IP. Dispersion function $D_x$ should have a zero value at IP to minimize e-bunch size because

$$\sigma^2_{x,\mathrm{rms}} = \beta_x \varepsilon_{x,\mathrm{rms}} + D_x^2 \left[ (p - p_0)/p_0 \right],$$

where $\sigma_{x,\mathrm{rms}}$ – horizontal rms beam size, $\beta_x$ – horizontal beta-function, $p$ – momentum of electron, $p_0$ – equilibrium momentum.

Furthermore, the length of storage ring straight section should be of 1.5 m to increase interaction efficiency between electron bunch and laser photons head-on collision as well as feasibility of laser positioning. The updated version of synchrotron magnetic lattice is presented in Fig. 1. Storage ring circumference is 10.661 m. The quadrupole gradients were calculated numerically by means of AT [10] to satisfy requirements above. Figure 2 shows obtained optic functions. From Fig. 2 it is seen that $\beta_x$ is 24.12 cm and $\beta_y$ is 14.62 cm at IP. Momentum compactification factor is equal to 0.0645 at 60 MeV, betatron horizontal and vertical tunes are 3.762 and 2.794 correspondingly. Also it was estimated dynamic aperture (DA) (Fig. 3). DA is equal to ±4.3 mm which is sufficient value for 30 μm beam-size.

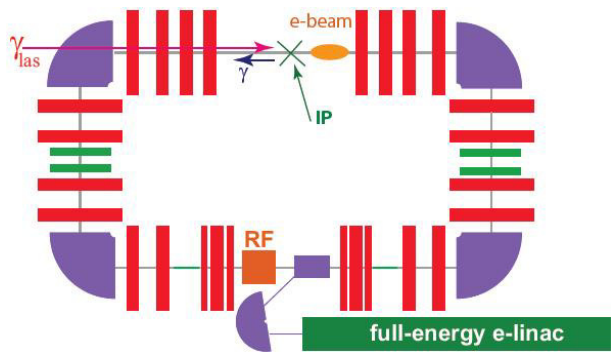


Figure 1: Basic magnet lattice of storage ring.

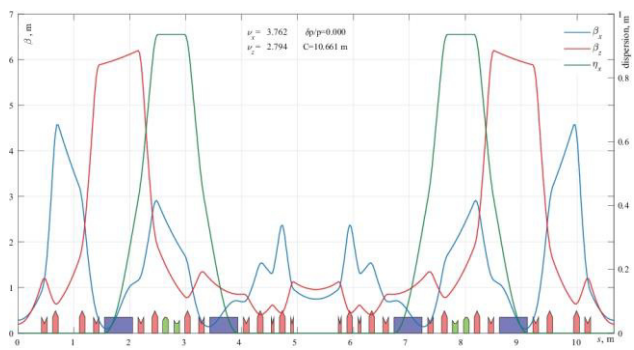

Figure 2: Twiss functions and dispersion.

Two families of sextupoles were arranged in the dispersion function maximum to correct chromaticities.

* Work supported by Russian Foundation for Basic Research, grant no. 19-29-12036
† vsdyubkov@mephi.ru

ISBN: 978-3-95450-240-0 ISSN: 2673-5539 doi:10.18429/JACoW-RuPAC2021-TUPSB26

# LATTICE OPTIONS WITH REVERSE BENDING MAGNETS FOR USSR HMBA STORAGE RING

V. S. Dyubkov[1†], E. D. Tsyplakov[2], T. V. Kulevoy[2], National Research Center "Kurchatov Institute", Moscow, Russia
[1]also at National Research Nuclear University MEPhI, Moscow, Russia
[2]also at ITEP-NRC Kurchatov institute, Moscow, Russia

*Abstract*

The 4th generation light source, the Ultimate Source of Synchrotron Radiation (USSR4) is under design, to be built in Moscow region (Russia). It will be a 6 GeV and about 1100 m circumference storage ring synchrotron [1-3]. Baseline lattice of the USSR4 for now is a scaled version of the ESRF-EBS Hybrid Multi-Bend Achromat (HMBA) lattice that was successfully commissioned in 2020 [4-7]. Its natural horizontal electron beam emittance is about 70 pm·rad. Further reduction of beam emittance can be achieved with the use of reverse bending magnets. The evolution of the envisaged lattices for the USSR4 storage ring, including options with reverse bends is presented.

## INTRODUCTION

Today third- and fourth-generation synchrotron radiation (SR) sources and X-ray free-electron lasers (FEL's) have many different applications in materials science, molecular biology and biochemistry, biomedical studies, crystallography, spectroscopy, studies of fast processes and other fields of scientific and applied research. For such applications the main problem is reaching the diffraction limit for a given beam energy of 3-6 GeV: thereby, an object can be imaged with high contrast and sharpness once its size is comparable to the wavelength of the synchrotron or undulator radiation. It was assumed that transverse emittance value below 100 pm·rad is necessary for the fourth generation light source to reach new horizons in the research by using SR. For a long time it was assumed that such values of the emittance could be reached only with FEL's driven by high-brightness electron linacs. A few years ago, it was demonstrated that low horizontal emittances can be achieved in storage synchrotrons as well and first beams with emittances about 100 pm·rad were generated at MAX-IV (Sweden) [8] and ESRF-EBS (France) [7] synchrotron light sources. Several similar facilities are under design and construction stages [9, 10] but today's trend is the existing SR sources upgrade to the fourth generation.

It is proposed that USSR4 facility will include both the 6 GeV storage synchrotron and FEL(s). The choice of this layout leads to the complication of injection system based on the full-energy linear accelerator. This linac will be used both for top-up injection into storage ring and for a generation of the high-brightness drive bunches for FEL.

## SYNCHROTRON RING LATTICE

Baseline lattice of the USSR4 for now is a scaled version of the ESRF-EBS 40-fold symmetry HMBA lattice that consists of 7 bends for each cell, 4 of them being the so-called LGB magnets, 2 are combined-function magnets (DQ) and "triplet of the magnets" at the centers of the 38 standard cells (Fig. 1). The main difference of this lattice from ESRF-EBS one is the presence of 5 cm long short bend (SB) with high field (~0.86 T) at the cell center. This lattice ensures the designed horizontal emittance 70 pm·rad together with Touschek lifetime (TLT) is equal to 28.9 h for zero current approximation, momentum acceptance (MA) is equal to ±6% at the center of the straight section and sufficient off-momentum dynamic aperture (DA) for off-axis injection schemes (± 1 cm in horizontal plane and about 3 mm in the vertical one) [2]. An advantage of that lattice is the scaling of the commissioned ESRF-EBS storage ring synchrotron and needs minimal changes of components (magnets, chambers) to start its construction in a short time.

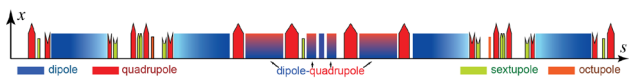


Figure 1: Layout of baseline lattice.

However, equilibrium electron beam horizontal emittance $\varepsilon_x$ already now in 1.5-2 times lower than 70 pm for the similar projects [9, 10] in view of energy and circumference of SR sources. It is well known that the next step towards lower $\varepsilon_x$ values is anti-bends (reverse bends) implementation [11-13] together with mentioned LGB magnets under constant beam energy. So, the expected $\varepsilon_x$ value is about 45 pm for 1104 m long 6 GeV APS-U project [10]. The APS-U lattice is the scaled and modified ESRF-EBS HMBA lattice with six reverse bend (RB) gradient dipoles.

Firstly, an attempt was made by authors to re-optimize USSR baseline lattice by means of re-tune magnets parameters to reduce $\varepsilon_x$ value up to 50 pm. The problem could not be solved without significant modification of the baseline lattice or RB introduction.

The next step toward the solution of the mentioned problem was the considering of RB introducing into baseline lattice by corresponding shifts of the existing quadrupoles in the horizontal plane from the closed orbit. An example of USSR4 lattice with reverse bends is presented in Fig. 2 (we considered lattice without SB at the cell center and with one DQ there).

The main tasks for the lattice optimization were:

1. $\varepsilon_x$ value is about 50 pm or lower.

† Dyubkov_VS@rrcki.ru

ISBN: 978-3-95450-240-0 ISSN: 2673-5539 doi:10.18429/JACoW-RuPAC2021-TUPSB28

# X-RAY THOMSON INVERSE SCATTERING FROM PERIODICALLY MODULATED LASER PULSES*

D. Yu. Sergeeva†, A. A. Tishchenko, National Research Nuclear University MEPhI, 115409 Moscow, Russia
also at National Research Center "Kurchatov Institute", 123098 Moscow, Russia
also at Belgorod National Research University, 308015 Belgorod, Russia

*Abstract*

Being a compact source of x-rays based on the Thomson backscattering, Thomson source has potential to be used in medicine and biology and in other areas where narrow band x-ray beams are essential. We propose and investigate theoretically the idea to use laser pulses modulated with a short period in Thomson backscattering. The coherent radiation is obtained with intensity proportional to the squared number of micro-pulses in the whole laser pulse.

## INTRODUCTION

Thomson (or Compton) backscattering happens when a laser pulse scatters off with a counter propagating relativistic free electron. Thomson backscattering underlies a bright and compact X-ray source. The sizes of such source are much smaller, than synchrotron's sizes, while the brightness is comparable with that. The general layout of this process is shown in Fig. 1.

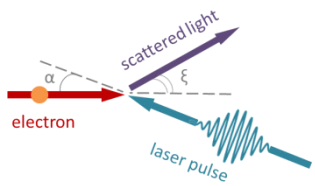


Figure 1: Layout of Thomson backscattering: laser pulse scattering on a moving relativistic electron.

The frequency of the scattered light is defined as without recoil effect:

$$\omega = \omega_0 \frac{1+\beta\cos\alpha}{1-\beta\cos\xi}, \tag{1}$$

where $\omega_0$ is the frequency of incident laser pulse, $\beta = v/c$ with $c$ being the speed of light in vacuum and $v$ being the initial speed of the electron, $\alpha$ is an angle of interaction, $\xi$ is the angle between the electron's trajectory and the propagation direction of the initial laser pulse.

The number of X-ray photons depends on the number of oscillations of electrons in the external field, i.e. the laser pulse duration $T$:

$$N_{\text{ph}} = f\left(N_{\text{oscillations}}\right) \propto T. \tag{2}$$

Increasing T leads to incoherent enhancement of radiation. It is similar to incoherent radiation from a long electron beam [1]:

$$I = I_0\left(N + N^2 F\right). \tag{3}$$

Here the first summand describes incoherent radiation, while the second one describes the coherent radiation. In order to switch on coherence effects we propose to use the laser with periodical longitudinal profile, the layout see in Fig. 2.

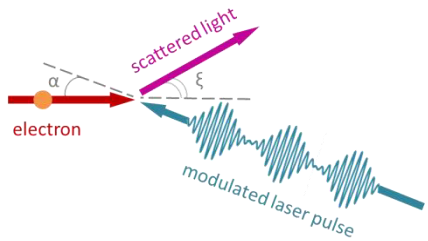


Figure 2: Periodically modulated laser pulse is scattered on a relativistic electron beams, giving rise to the radiation with frequency higher than initial laser.

As the first approximation the laser wave can be considered as a plane wave:

$$\mathbf{E}^{\text{ext}}\left(\mathbf{r},t\right) = \mathbf{E}_0\cos\left(\omega t - \mathbf{kr} + \varphi_0\right), \tag{4}$$

where $\omega$ is the laser frequency, $\mathbf{k}$ is its wave-vector, $\mathbf{E}_0$ is the laser amplitude, $\varphi_0$ is the initial phase. The modulated laser pulse can be described by [2]:

$$\mathbf{E}^{\text{ext}}\left(\mathbf{r},t\right) = \mathbf{E}_0\left(t\right)\cos\left(\omega t - \mathbf{kr} + \varphi_0\right). \tag{5}$$

For periodically modulated beam $\mathbf{E}_0\left(t+t_0\right) = \mathbf{E}_0\left(t\right)$. It means that instead of wave with a modulated profile we can use the set of $N$ short laser pulses each of which is described by the field of a plane wave, see Fig. 3.

* This work was supported by the RFBR grant 19-29-12036
† dysergeyeva@mephi.ru

ISBN: 978-3-95450-240-0 ISSN: 2673-5539 doi:10.18429/JACoW-RuPAC2021-TUPSB29

# GEANT4 FOR INVERSE COMPTON RADIATION SOURCE SIMULATIONS*

A. A. Savchenko†, A. A. Tishchenko, D. Yu. Sergeeva, National Research Nuclear University MEPhI, 115409 Moscow, Russia
also at National Research Center "Kurchatov Institute", 123098 Moscow, Russia
also at Belgorod National Research University, 308015 Belgorod, Russia

*Abstract*

In this paper, creation and implementation of the Compton backscattering module into the Geant4 package are under consideration. Created module of Compton backscattering has been implemented as a discrete physical process and operates with a fixed light target (a virtual volume with the properties of a laser beam), with which a beam of charged particles interacts producing x-rays. Such a description allows user to flexibly change necessary parameters depending on the problem being solved, which opens up new possibilities for using Geant4 in the studied area.

## INTRODUCTION

Compton backscattering or inverse Compton scattering (ICS) [1, 2] is a promising mechanism for engineering of a bright, compact and versatile X-ray source: with dimensions being significantly smaller, the brightness of this source is comparable with that of synchrotron radiation. Nowadays, active researches are underway on various aspects of this phenomenon [3, 4] aiming at increasing of radiation intensity and quality. In modern science, such kind of research is necessarily accompanied by the computer simulations. In this paper, we are discussing creation and implementation of the Compton backscattering module into the Geant4 package [5-7], which is the leading simulation toolkit in high-energy physics [8], accelerator physics [9], medical physics [10], and space studies [11]. This paper is organized as follow. First, we show brief theoretical description of the ICS process, and then some issues of ICS implementation into Geant4 are considered. We finish with Geant4 simulation results and conclusion.

## BRIEF THEORETICAL DESCRIPTION

Let us adduce theoretical description of scattering process shown in Fig. 1. We consider here collision of electron and laser beams under arbitrary angle $\alpha$. In this case ICS photon spectral-angular distribution reads

$$\frac{d^2N(\mathbf{n},\omega)}{d(\hbar\omega)d\theta}=\frac{\sin(\theta)d\phi}{137}\frac{\omega}{4\hbar\pi^2c^2}\times \times\left|\sum_{s=1}^{\omega/\omega_0}\frac{\sin\left((A-s\eta)NT/2\right)}{(A-s\eta)/2}\frac{J_s(B)}{(-1)^{-s}}\left\{\mathbf{H}-s\frac{\mathbf{K}}{B}\right\}\right|^2, \quad (1)$$

where

$$A=\omega-\frac{\omega}{c}\left[n_x\left(v_{0x}+\frac{a_0c}{\gamma}\right)+n_yv_{0y}+ +n_z\left(v_{0z}+\frac{a_0v_{0x}}{\gamma(1-\beta_{0z})}\right)\right], \quad (2)$$

$$B=\frac{\omega}{c}\left[n_x\frac{a_0c}{\omega_0\gamma(1+\beta_{0z})}+n_z\left(\frac{a_0v_{0x}}{\omega_0\gamma(1-\beta_{0z}^2)}\right)\right], \quad (3)$$

$$T_{\text{int}}=NT=N\frac{2\pi}{\omega_0(1+\beta_{0z})}, \quad (4)$$

$$\mathbf{H}=(\mathbf{e}_xn_y-\mathbf{e}_yn_x)\left(v_{0z}+\frac{a_0v_{0x}}{\gamma(1-\beta_{0z})}\right)+ +(\mathbf{e}_yn_z-\mathbf{e}_zn_y)\left(v_{0x}+\frac{a_0c}{\gamma}\right)+(\mathbf{e}_zn_x-\mathbf{e}_xn_z)v_{0y}, \quad (5)$$

$$\mathbf{K}=(\mathbf{e}_xn_y-\mathbf{e}_yn_x)\left(-\frac{a_0v_{0x}}{\gamma(1-\beta_{0z})}\right)+ +(\mathbf{e}_yn_z-\mathbf{e}_zn_y)\left(-\frac{a_0c}{\gamma}\right), \quad (6)$$

$$\eta=\omega_0+\frac{k_{0z}z}{t}\simeq\omega_0(1+\beta_{0z}), \quad (7)$$

$$n_x=\sin\theta\cos\varphi,\ n_y=\sin\theta\sin\varphi,\ n_z=\cos\theta. \quad (8)$$

Here $\omega$ is the frequency of the scattered photon, $\omega_0$ is the laser frequency, $\gamma$ is the electron Lorentz factor (here we consider moderately relativistic electrons), $c$ is the speed of light, $\beta_{0z}=v_{oz}/c$ is longitudinal component of the reduced speed of electron, with $v_{0x},v_{0y},v_{0z}$ being electron velocity projections; $\mathbf{e}_x,\mathbf{e}_y,\mathbf{e}_z$ are unit axes, $\theta$ is the polar angle of observation, $\varphi$ – is the azimuthal angle of observation, $\hbar$ is the Planck constant, $N$ is the number of electron oscillations in the laser field, $T$ – is the laser wave period, $a_0$ is the nonlinearity parameter of laser beam. In this paper we consider only linear scattering i.e. $a_0\to 0$.

The frequency of a scattered photon (in a head-on collision of laser and electron beams) is determined by the relation

* This work was supported by the RFBR grant 19-29-12036
† aasavchenko1@mephi.ru

ISBN: 978-3-95450-240-0 ISSN: 2673-5539 doi:10.18429/JACoW-RuPAC2021-TUPSB32

# EMISSION OF PHOTONS AT THE INTERACTION OF A HIGH ENERGY POSITRON BEAM WITH A PERIODICALLY DEFORMED CRYSTAL*

A. A. Yanovich†, A. G. Afonin, G. I. Britvich, A. A. Durum, M. Yu. Kostin, I. S. Lobanov, V. I. Pitalev, I. V. Poluektov, Yu. E. Sandomirsky, M. Yu. Chesnokov, Yu. A. Chesnokov, NRC "Kurchatov Institute" – IHEP, 142281 Protvino, Russia

*Abstract*

Periodically deformed crystals have long attracted attention as "crystalline undulators" [1-8]. In the experiment carried out at the U-70 accelerator, the radiation of positrons moving in a periodically deformed crystal was observed. Experimental evidence has been obtained for an undulator peak in a radiation spectrum, which is qualitatively consistent with calculations. It is shown that most of the emitted energy is due to hard photons with energies of tens of MeV as a result of channeling and reflection of particles, whose spectral density is several times higher than the radiation in an amorphous target.

## INTRODUCTION

Intense X-rays are currently used for research in biology, medicine, materials science, and many other areas of science and technology. The traditional way to obtain such beams (with energies of several keV and higher) is the use of special magnets - undulators at accelerators [9]. The energy of the photons generated in the undulator is proportional to the square of the Lorentz factor of the gamma particle and inversely to the period of the undulator L.

Unlike conventional undulators with a period of several centimeters, "crystal undulators" have a period of the submillimeter range and are capable of generating photons hundreds of times harder. In [10], a crystalline undulator was created for the first time, and in [11], an indication was obtained of the existence of an undulator peak in radiation. At the same time, background radiation from channeled particles with higher radiation energies was observed. Later it was shown that unchanneled above-barrier particles emit strongly on trajectory segments that are close to tangents to curved crystallographic planes (as a result of the "volume reflection" process [12-14]). In this work, we tried to measure the emission spectrum in a wide range of energies and to understand what proportion of this spectrum is undulator radiation. Figure 1 shows the difference between the trajectories of channeled particles in a crystalline undulator and trajectories in a conventional undulator. In a crystal, the sinusoidal motion of particles with a period of the deformation of the planes (~ 100 μm) is modulated by frequent oscillations (with a period ~ 1 μm) during channeling between curved crystallographic planes. The radiation due to channeling with frequent oscillations is many times tougher, but its spectral density is lower than undulator radiation due to the deformation of the planes.

* Work supported by Russian Science Foundation (grant 17-12-01532).
† yanovich@ihep.ru

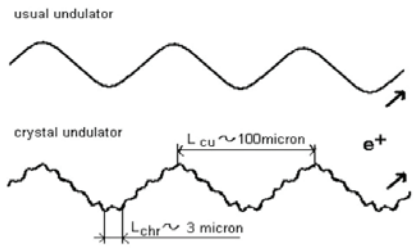


Figure 1: Particle trajectories in a conventional undulator (top) and in a crystalline undulator (bottom).

In addition, as noted above, the above-barrier particles, when their trajectories reach tangents to curved planes, perform aperiodic oscillations (Fig. 2) and also radiate strongly [12]. The techniques described below were used to measure the emission energy spectrum in a wide range.

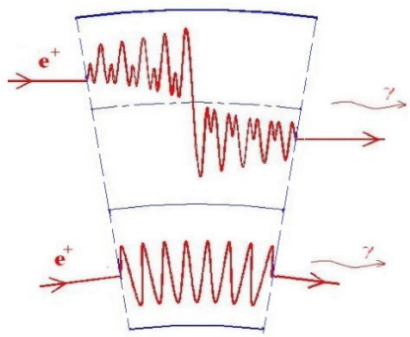


Figure 2: Trajectories of above-barrier particles near the tangent to curved planes (top); the trajectories of channeled particles in the same section are shown below.

## CRYSTALLINE TARGET

In [10], the possibility of creating a crystalline undulator — a periodically bent crystal — by double-sided application of mechanical grooves was shown for the first time. A schematic of an undulator with applied grooves, developed at IHEP according to this principle, is shown in Fig. 3. The period of double-sided application of grooves d must be no less than the thickness of the crystal plate h so that sinusoidal deformations penetrate in deep into the entire thickness of the crystal, according to the Saint-Venant principle, known from the theory of elasticity [15]. The first data on radiation with a crystal undulator were obtained with a positron beam with an energy of 10 GeV at IHEP [11]. However, most electron accelerators, where crystal undulators can be used, operate at energies below 6 GeV.

ISBN: 978-3-95450-240-0 ISSN: 2673-5539 doi:10.18429/JACoW-RuPAC2021-TUPSB33

# 2.5 GeV BOOSTER SYNCHROTRON FOR A NEW KURCHATOV SYNCHROTRON RADIATION SOURCE

A.S. Smygacheva, V.N. Korchuganov, Ye.A. Fomin, V.A. Ushakov, A.G. Valentinov
NRC «Kurchatov Institute», Moscow, Russia

*Abstract*

The Project of complete modernization of the current accelerator complex is in progress in the NRC «Kurchatov Institute». A new booster synchrotron is a part of the injection complex for a new 3-d generation synchrotron light source. The booster has to ensure reliable and stable operation of the upgraded main storage ring. The paper presents the final design of the new booster synchrotron and its main parameters.

## INTRODUCTION

The Kurchatov synchrotron radiation source consists of the 2.5 GeV main storage ring, the 450 MeV booster synchrotron and the 80 MeV linac [1]. The current main ring is the second generation light source with electron beam emittance of 98 nm×rad. The accelerator complex has been in operation for over 20 years in its current configuration. Improvement of the qualities of synchrotron radiation beams is associated with the modernization of the entire accelerator complex and the replacement of the main ring with the 3-d generation source [2].

The need to increase the spectral flux and brightness of a light source demands the creation of a new structure with low electron beam emittance (~1–10 nm×rad) for the main ring. A feature of a low-emittance structure is a high natural chromaticity and a small dynamic aperture. A small aperture can lead to a significant decrease in the efficiency of the electron beam injection from the current booster synchrotron with the high-emittance structure into the new main ring. The need to ensure long-term spatial and temporal stability of photon beams dictates high requirements for temperature stabilization of the main ring (±0.1°C). These requirements can be achieved with constant currents in the magnets and the accelerating RF structure, i.e. when the storage ring is operating at the same energy. In addition, with the possibility of injection at full energy and periodic sub-accumulation of electrons from the booster synchrotron, it becomes possible to carry out experiments on synchrotron radiation without interruptions for re-accumulation of electrons and energy rise in the main storage ring. These conditions do not allow using the current booster synchrotron with electron beam emittance of 800 nm×rad and energy of 450 MeV as an injector for the new low-emittance main ring.

The new booster synchrotron must have a symmetrical structure with a periodicity equal to or multiples of the main ring structure. The length of the main drift spaces must be about 2 m to accommodate the magnets of the beam transport channels and the RF cavity. The booster lattice must have relatively small values of Twiss parameters along a beam orbit and the natural emittance from 40 to 60 nm×rad at the energy of 2.5 GeV.

## BOOSTER LATTICE

The booster magnet lattice is based on the modified DBA structure with 12 cells. The total number of magnets is the 24 dipoles, the 60 quadrupoles, the 48 sextupoles and the 24 correctors. The booster synchrotron will be located in the same tunnel with the main storage ring. The main lattice parameters are given in Table 1. The optics functions are shown in Fig. 1.

Table 1: The Booster Lattice Parameters

| | |
|---|---|
| Energy, GeV | 0.2 – 2.5 |
| Circumference, m | 110.9 |
| Operating frequency, Hz | 1 |
| RF-frequency, MHz | 181.168 |
| Harmonic number | 67 |
| Beam current, mA | 10 – 15 |
| Tunes x/y | 7.178/4.367 |
| Nat. Chromaticity x/y | -9.0/-8.6 |
| Nat. emittance at 2.5 GeV, nm×rad | 43.4 |
| Momentum compaction factor | 0.01 |
| Energy spread at 2.5 GeV | $8.4\times10^{-4}$ |
| Energy loss per turn at 2.5 GeV, keV | 539 |
| Damping time x/y/s at 2.5 GeV, msec | 3.5/3.4/1.7 |

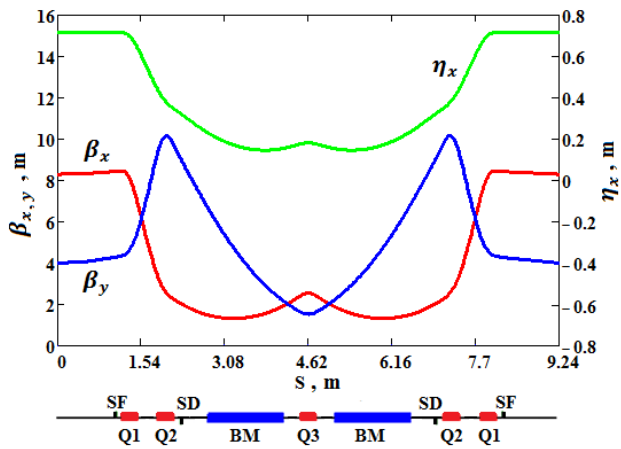


Figure 1: Twiss parameters for one booster cell.

The booster lattice provides the natural emittance of 43.4 nm×rad at the energy of 2.5 GeV. The horizontal and vertical tunes are located far from structure resonances. The dynamic aperture, taking into account chromaticity corrections, is in horizontal from -93 to +129 mm and in vertical of ±105 mm at the center of the main drift. It's

ISBN: 978-3-95450-240-0 ISSN: 2673-5539 doi:10.18429/JACoW-RuPAC2021-TUPSB34

# NEW LATTICE DESIGN FOR KURCHATOV SYNCHROTRON RADIATION SOURCE

Ye. Fomin†, V. Korchuganov, NRC "Kurchatov Institute", Moscow, Russia

*Abstract*

Nowadays the upgrade project of the 2nd generation synchrotron radiation source operating at NRC "Kurchatov Institute" has been ongoing. The main aim of the project is to create a new synchrotron radiation source with the same 124 m circumference and providing synchrotron radiation properties inherent to the 3rd generation sources (emittance ~3 nm·rad). The new machine will consist of a new storage ring with 2.5 GeV electron energy, full energy booster synchrotron, and 0.2 GeV linac. The mandatory requirement for the project is to keep all currently operating beamlines.

In this article, we present the design challenges and approaches for this machine, the conceptual design, and the baseline lattice.

## INTRODUCTION

Kurchatov synchrotron radiation source is a 2nd generation source with 2.5 GeV electron beam energy and 98 nm·rad emittance. The circumference of the main storage ring is 124.13 m. The main storage ring lattice is based on a modified DBA type lattice and consists of 6 cells, each of which contains two 3 m straight sections [1].

Currently, 13 beamlines operate regularly and 4 more are under construction. The main source of synchrotron radiation is bending magnets with 1.7 T magnetic fields. The characteristic photon energy is 7 keV and the full spectral range of synchrotron radiation is 0.1 – 2000 Å. To expand the facility's experimental opportunities 3 superconductive wiggles were installed in the straight sections of the main storage ring (one with 7.5 T and two with 3 T maximum fields).

Improving qualities of photon beams primarily associated with an increase in their intensity and brightness requires the upgrade of the facility completely. So, after such upgrade, the facility must have an electron beam emittance less than 5 nm·rad and provide synchrotron radiation beams with properties close to properties of the beams generated by the 3rd generation sources. For this apart from the development of a new main storage ring, it is necessary to develop a new full energy booster synchrotron and a new linac. Moreover, a mandatory requirement for the upgrade project is the preservation of all currently operating beamlines.

## MAIN REQUIREMENTS

DBA type lattice was designed in the mid-1970s by R. Chasman and G. Green and formed the basis of the 2nd and 3rd generation synchrotron radiation sources [2]. The development of technologies for creating magnet, RF, vacuum systems, software, and hardware for 3D simulations have created opportunities for the construction of new synchrotron radiation sources based on MBA lattice. The use of complex and high-precision magnet elements in MBA lattice makes it possible to reduce electron beam emittance up to 2 orders and even more than in DBA lattice. While the circumferences of both storage rings are about the same. The first successfully commissioned such projects are MAX-IV [3] and ESRF upgrade project – ESRF EBS [4]. Also, deserve attention projects such as the SLS-2 project [5] and one of the most ambitious to date – the PETRA-IV project [6].

Based on the last progress in accelerator physics and technologies and on world scientific community experience in an upgrade of working synchrotron radiation sources we have formulated the main requirements for the new Kurchatov synchrotron radiation lattice:

- Preservation all currently operated beamlines.
- Achievement the electron beam emittance less than 5 nm·rad.
- Preservation spectral range of synchrotron radiation.
- Preservation ring symmetry and zero-dispersion straight sections.
- Providing the possibility of electron beam injection and storing.
- Beam lifetime more than 10 hours.
- Preservation of the main storage ring circumference.
- Compliance with technological limitations.

## NEW LATTICE

Kurchatov synchrotron radiation source is one of the compact sources in the world. The small circumference of the main storage ring is achieved through the use of bending magnets with a high magnetic field (1.7 T). This imposes very strict limitations from the technologies side.

To reduce electron beam emittance and simultaneously minimize a storage ring circumference, it is advisable to use special magnets with combined functions (like sandwich type magnets) and antibend magnets [7, 8]. Based on the results of the conducted research the modified 3BA type lattice is optimal for the new Kurchatov synchrotron radiation source. This half of lattice formed from 3 bending magnets with 2.0 T magnetic field, 4 combined functions magnets, 4 magnets with antibend, 2 doublets of quadrupole lenses, 6 chromatic and 1 harmonic sexupoles. In the new lattice, there are no octupoles. A comparison of current and new lattices of the Kurchatov synchrotron radiation source is illustrated in Fig. 1.

† yafomin@gmail.com

ISBN: 978-3-95450-240-0 ISSN: 2673-5539 doi:10.18429/JACoW-RuPAC2021-TUPSB35

# 3D SIMULATION STUDY AND OPTIMIZATION OF MAGNETIC SYSTEM OF DECRIS ION SOURCE WITH THE PUMPING FREQUENCY 28 GHz

V. Amoskov†, E. Gapionok, V. Kukhtin, A. Labusov, E. Lamzin, A. Makarov, I. Rodin, A. Safonov, N. Shatil, D. Stepanov, E. Zapretilina, JSC NIIEFA, St. Petersburg, Russia
S. Bogomolov, A. Efremov, JINR, Dubna, Russia
S. Sytchevsky, Saint Petersburg State University, Russia

*Abstract*

A superconducting magnet system for a 28 GHz ECR ion source (DECRIS) was studied in order to select its parameters and optimize performance.

Parametric magnetic models were performed for two design configurations, conventional ("sextupole-in-solenoid") and reversed ("solenoid-in-sextupole"). For both configurations, the magnetic effect of the booster and the steel poles on the magnet performance was investigated from the point of view of critical parameters of the system – currents, fields, and forces.

Results of the parametric computations were used to optimize the geometry and sizes of the magnet as well as the magnetic shield, the booster, and the poles.

A comparison of the obtained parameters was used to select the candidate magnet configuration for further design and manufacture.

## INTRODUCTION

A 28 GHz ECR ion source DECRIS will be used for the Superheavy Elements Factory (SHE) at JINR, Dubna, which allows to ensure desired mass and energy ranges and the beam intensity in accelerators.

Operation at the 28 GHz demands efficient magnetic configuration capable to provide the axial field as high as 4 T at the injection side in the plasma region.

In order to generate high confining fields DECRIS utilizes a superconducting magnetic system. Efremov Institute is responsible for the magnetic system (MS) design and optimization. Key parameters of the magnetic system are listed in Table 1.

Table 1: Key Parameters of the Magnet System

| | |
|---|---|
| Warm bore diameter | 142 mm |
| Plasma chamber internal diameter | 125 mm |
| Field peak-to-peak axial distance | 420 mm |
| $B_{inj}$ on axis | 4 T |
| $B_{extr}$ on axis | 2÷2.5 T |
| Minimal axial field $B_{min}$ | 0.5÷0.8 T |
| Field module $\|\mathbf{B}\|$ at $R$ = 62 mm | 2.02 T |

The magnet system consists of two groups of coils capable to generate min-B confining fields in the plasma region. The axial mirror field is produced by a segmented solenoid. The radial field is generated by a sextupole formed with six racetrack coils assembled in a circle so that their poles alternate.

## RESULTS FOR TWO MODELS

Two principal coil layouts are briefly discussed focusing on optimal magnetic performance: a *conventional* ("sextupole-in-solenoid") configuration and a *reversed* ("solenoid-in-sextupole") option. In the "sextupole-in-solenoid" design racetrack coils of the sextupole are located inside the solenoid (Fig. 1a). In the "solenoid-in-sextupole" design the coils arrangement is reversed (Fig. 2a). Both configurations have been well proven in existing ECR sources. Particularly, VENUS for the Facility for Rare Isotope Beams at LBNL utilizes "sextupole-in-solenoid" magnets [1]. An example of the "sextupole-in-solenoid" magnet design is SECRAL-II for the Heavy Ion Facility in Lanzhou, China [2].

Figures 1b-2b show similar models with iron. The racetrack coils contain steel poles. All the coils are enveloped with a steel booster. All steel components are saturated during operation.

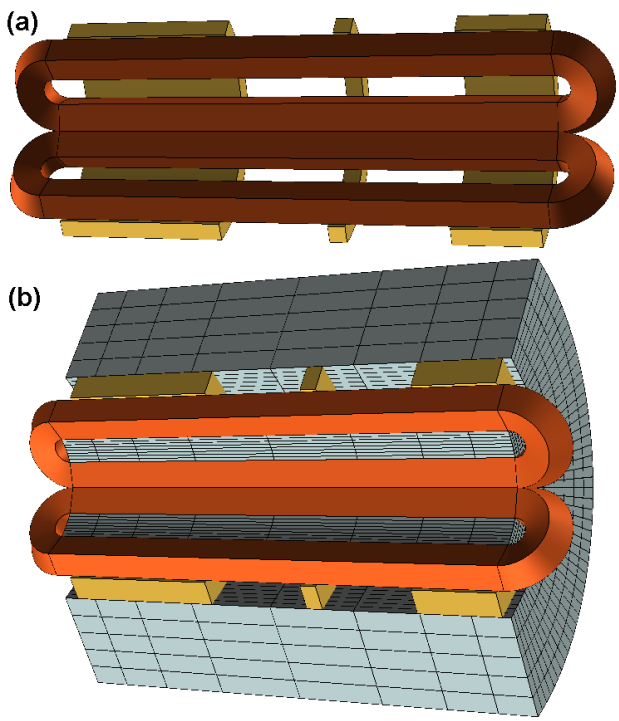


Figure 1: Conventional (sextupole-in-solenoid) magnetic system. Model without (a) and with (b) iron.

† avm@sintez.niiefa.spb.su

ISBN: 978-3-95450-240-0 ISSN: 2673-5539 doi:10.18429/JACoW-RuPAC2021-TUPSB36

# HIGH INTENSITY CALCIUM, CHROMIUM AND TITANIUM ION BEAMS FROM THE PERMANENT MAGNET ECR ION SOURCE DECRIS-PM

D.K. Pugachev†, S.L. Bogomolov, V.E. Mironov, A.A. Efremov, V.N. Loginov, A.N. Lebedev, A.E. Bondarchenko, K.I. Kuzmenkov, K.B. Gikal, A.A. Protasov, Flerov Laboratory of Nuclear Reactions, Joint Institute for Nuclear Research, Dubna, Russia

*Abstract*

The first experiment on synthesis at the Superheavy Elements Factory (SHE) was launched at the end of 2020. The result of the experiment with a calcium ion beam and an Americium target is more than 100 events of the synthesis of Moscovium. Two years of operation have shown good capabilities of the Factory. These results allow to start preparing for the synthesis of SHE with atomic number >118. For these experiments we have to use heavier ion beams, such as titanium and chromium. The article describes the method, technique, and last experimental results on the production of metal ion beams such as $^{48}$Ca, $^{48}$Ti, $^{52}$Cr, and $^{54}$Cr ion beams from the DECRIS-PM ion source at the DC-280 cyclotron.

## INTRODUCTION

For many years, one of the main scientific directions of the FLNR JINR has been the synthesis and study of the properties of superheavy elements. In recent years, almost all the last discovered elements of the Periodic Table have been synthesized using the $^{48}$Ca at the U-400 cyclotron in our laboratory.

Further research into the field of superheavy elements requires a new approach and equipment. For these purposes, SHE was built in the FLNR in 2019. Factory is equipped with cyclotron DC-280 (Fig. 1), the main parameters are shown in the Table 1. The main goals of the SHE Factory are experiments at the extremely low cross sections, such as synthesis of new SHE, new isotopes of SHE and study of decay properties of SHE. In addition, experiments requiring high statistics will be conducted, such as nuclear spectroscopy and the study of the chemical properties of SHE [1].

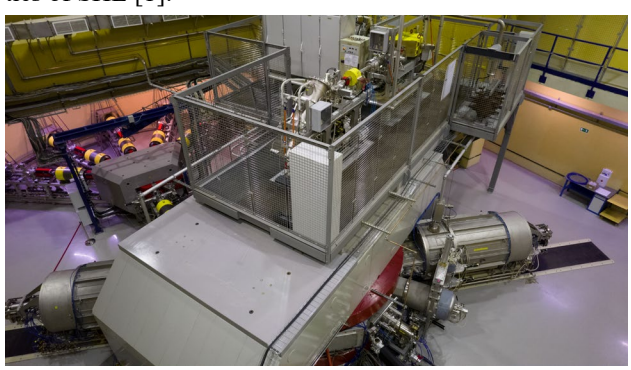

Figure 1: The DC-280 cyclotron.

Table 1: The Main Parameters of DC-280

| | |
|---|---|
| Ion sources | DECRIS-PM - 14 GHz |
| Injection energy | Up to 80 keV/Z |
| A/Z range | 4÷7.5 |
| Energy | 4÷8 MeV/n |
| Magnetic field level | 0.6÷1.3 T |
| K factor | 280 |
| Magnet weight | 1000 t |
| Magnet power | 300 kW |
| Dee voltage | 2x130 kV |
| RF power consumption | 2x30 kW |
| Flat-top dee voltage | 2x14 kV |
| Deflector voltage | Up to 90 kV |

The first experiments at the SHE factory will be performed using $^{48}$Ca+$^{242,\,244}$Pu and the $^{48}$Ca+$^{243}$Am reactions. After completion of these experiments, it is planned to start the synthesis of new superheavy elements in reactions of $^{50}$Ti and $^{54}$Cr ions with $^{248}$Cm, $^{249}$Bk and $^{249\text{-}251}$Cf isotopes.

## DECRIS-PM ION SOURCE

The injector of the cyclotron includes a high-voltage platform to increase the injection energy and thus to reduce the influence of the space charge of the beam. To reduce the power consumption of HV-platform we developed all-permanent magnet ion source DECRIS-PM. The requirements for the ion source are the production of ions with low and medium masses (from He to Kr). The ion source and the high-voltage platform are shown on Fig. 2.

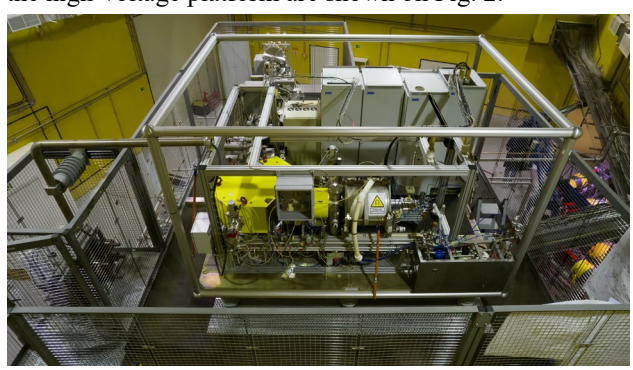

Figure 2: The DECRIS-PM on the high-voltage platform of the DC-280 cyclotron.

The magnetic field of the source is a superposition of an axial magnetic field and a radial magnetic field formed by

† pugachev@jinr.ru

ISBN: 978-3-95450-240-0 ISSN: 2673-5539 doi:10.18429/JACoW-RuPAC2021-TUPSB37

# MODERNIZATION OF THE ECR ION SOURCE DECRIS-2M. RESULTS OF THE FIRST TESTS

A.E. Bondarchenko†, S. Bogomolov, A. Efremov, V. Loginov, A. Lebedev, V. Mironov, D. Pugachev, Joint Institute for Nuclear Research, FLNR, Dubna, Russia

*Abstract*

The article describes the design of the modernized ECR ion source DECRIS-2M. The upgrade consists in increasing the magnetic field to improve plasma confinement and enhance the source performance. The modernization also made it possible to increase the inner diameter of the plasma chamber and replace the coaxial microwave power input by a waveguide. Redesigned injection chamber significantly expands the possibilities of production ions of solids using different methods.

The article also presents the first results of experiments production of Ar, Xe and Bi ion beams from a modernized ion source. The results demonstrate substantial increase of the ion beams intensity, especially in the case of high charge states.

## INTRODUCTION

The ECR ion source DECRIS-2m [1] was developed at FLNR JINR in 2001 and is a CAPRICE-type source with a coaxial microwave input of 14 GHz power. The magnetic structure of this source consists of two independent windings with an iron yoke to form an axial field; the radial magnetic field is created by a hexapole (permanent NdFeB magnet with "Halbach structure"). The main parameters of the ECR ion source DECRIS-2m are presented in Table 1.

Table 1: Main Parameters of the ECR Ion Source DECRIS-2m

| | |
|---|---|
| Frequency (GHz) | 14 |
| Magnetic field in the inj. region $B_{inj}$ (T) | 1.25 |
| Magnetic field in the extr. region $B_{extr}$ (T) | 1.05 |
| Plasma chamber diameter (mm) | 64 |
| Number of coils | 2 |
| $I_{max}$ (A) | 1300 |
| **Hexapole parameters** | |
| Material | NdFeB |
| Inner diameter (mm) | 70 |
| Rad. field on the plasma chamber wall (T) | >1.0 |

The source allows one to produce beams of ions of gaseous and solid substances with medium charges and moderate intensities up to Xe. The disadvantages of the source design include the following:

- in the microwave power input system, a transition from a rectangular waveguide to a coaxial line is used, which leads to losses of microwave power, causing uncontrolled gas desorption in the injection region. This method of microwave power input also requires the use of a special tuning mechanism;
- the size of the evaporator for producing solid ions is limited by the diameter of the inner conductor of the coaxial line;
- there is no room to install additional elements in the plasma chamber, because the injection part of the chamber is used as a coaxial waveguide.

## UPGRADED ECR SOURCE DECRIS-2M

During the development of the project, the experience of the mVINIS ECR source modernization was used [2]. The main goal of the modernization was to replace the coaxial input of microwave power with a standard rectangular waveguide. For this, the outer diameter of the plasma chamber was increased from 64 to 74 mm. This entailed changes in the magnetic system of the source, in particular, a new hexapole with an inner diameter of 80 mm was made, and the configuration of the magnetic inserts in the injection region was changed. The new hexapole consists of 24 identical trapezoidal sectors with the corresponding direction of magnetization. Each sector is made from a single piece of magnetic material, thus avoiding magnetic field irregularity along the hexapole poles.

The design of the injection chamber was changed, which made it possible to significantly expand the possibilities for placing devices for supplying solids (evaporators, sputtering electrodes) in the ionization chamber.

In Fig. 1 a cross-section of the upgraded source is shown.

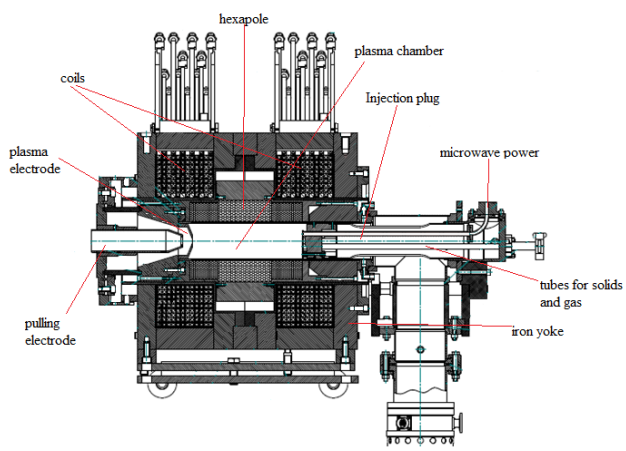


Figure 1: Upgraded DECRIS-2M.

† bondarchenko@jinr.ru

ISBN: 978-3-95450-240-0 ISSN: 2673-5539 doi:10.18429/JACoW-RuPAC2021-TUPSB38

# MAGNETIC SYSTEM WITH VARIABLE CHARACTERISTICS FOR A 2.45 GHz ECRIS

M. S. Dmitriyev†, M. I. Zhigaylova, K. G. Artamonov, O. A. Ivanov National Research Nuclear University MEPhI (Moscow Engineering Physics Institute), Moscow, Russia

*Abstract*

The study considers the development of the magnetic system of the 2.45 GHz ECRIS for the production of protons and double-charged helium ions. The magnetic field configuration is shown to be based on permanent magnets. The results of the simulation made by the Finite Element Method have been performed. To adjust the axial magnetic field profile the configuration with the alternating position of the ring magnets was analyzed. The double series construction of the bar magnets provides the adjustment of the radial magnetic field $B_{rad}$ at the chamber wall. Additional solenoids were introduced to the system for a corrective tuning of the$B_{inj}$ and $B_{ext}$ parameters and the axial profile minimum $B_{min}$ of the magnetic field distribution. Thus, the magnetic system is appeared to provide the mode switching between the ECR and the microwave operating modes.

## INTRODUCTION

A new ECR ion source for the light ion linac is under development at MEPHi. It is designed for the generation of both protons and double charged helium ions. The choice of the operating frequency of 2.45 GHz is specified by several factors: the wide range of elements available at the microwave wavelength, working experience in this frequency range, the compactness of the magnetic system as well as the adjustment ability of the magnetic field distribution inside the plasma chamber.

In order to obtain the required proton intensity and ensure the helium production at the frequency of 2.45 GHz, two types of microwave plasma ion sources were considered as a fundamental base for the development of a new 2.45 GHz ion source with variable characteristics of the magnetic system.

Depending on the ion parameters required, ion sources based on the electron-cyclotron resonance (ECR) or the microwave discharge can be used. The ECR ion sourceprovides the interaction between electromagnetic field and plasma at the frequency of electron-cyclotron resonance and under the vacuum conditions.Unlike the first type, the microwave source does not require the resonance conditions to provide the field-plasma interaction; moreover, gas pressure inside the plasma chamber is several times higher than for the first type. According to the factors of plasma generation ion beam parameters can differ for these two types. ECR ion sources produce multiply charged ions with lower beam currentsin comparison with microwave sources, which provide high beam currents of protons.

The aim of this research is to design a new ECRIS for producing double-charged ions of helium and protons. This aim will be accomplished by meeting the following objectives: developing a magnetic system and calculating the magnetic field parameters to determine the most feasible configuration of the source in order to provide the operation in both ECR and microwave modes.

## BASIC PARAMETERSOFECR AND MICROWAVE ION SOURCES

Microwave discharge sources are usually feasible for generating the single-charged ion beams or proton beams with the current up to 100 mA and low emittance in both pulse and continuous-wave operation mode. High magnetic fields are used to increase the ion density.

This type of a source can be distinguished by the frequency that is higher than for the ECR type. In contrast to the magnetic system of the ECR type, the microwave source configuration does not include hexapole magnets to confine plasma in the ECR region.

The magnetic field profile is important for the plasma generation as well as for the operation stability of the application. The magnetic field for this configuration is usually generated by two solenoids with variable currents.

To accomplish the ion parameters required microwave plasma sources were considered according to the following advantages: stability, long lifetime, high ion concentration, small energy spread in the beam, low emittance, compactness and ease of operation.

As compared to the microwave source magnetic system, the ECR source configuration is usually based on permanent magnets instead of solenoids. Sources with the stepped ionization are needed to generate the multiple-charged ion beams. Electrons are gradually knocked out from the external shell of the ionized atoms by electrons accelerated in an alternating field. Along with that, relatively slow ions continue to lose electrons because of the ionization, caused by the second time accelerated electrons. Slow electrons are confined by the magnetic field of the source.

The efficiency of the RF power transmission into the plasma chamber depends on the magnetic plasma density distribution inside the chamber, which affects the dielectric parameters of the chamber space and consequently the effectiveness of the field-plasma interaction. This research is based on the most optimal configuration principles known as the “ECRIS Standard Model”.

† msdmitriyev@mephi.ru.

ISBN: 978-3-95450-240-0 ISSN: 2673-5539 doi:10.18429/JACoW-RuPAC2021-TUPSB39

# STUDY OF SPACE CHARGE COMPENSATION PROCESS OF A 400 KeV PULSED HYDROGEN ION BEAM

A. S. Belov, S. A. Gavrilov, O. T. Frolov, L. P. Netchaeva, A. V. Turbabin, V. N. Zubets,
Institute for Nuclear Research of the Russian Academy of Sciences, Moscow, Russia

*Abstract*

A three grid energy analyzer of slow secondary ions with a twin analyzing grid is described. The analyzer has cylindrical geometry and π angle for recording of the slow ions. The analyzer has been used for measurements of degree of space charge compensation (SCC) of a pulsed hydrogen ion beam with energy of 400 keV and peak beam current of 60 mA. Results of the measurements are presented and compared with theoretical estimations based on model in which the SCC degree is limited by heating of electrons in collisions with fast ions of the beam.

## INTRODUCTION

Transport of high intensity ion beams in low energy beam transport (LEBT) for injection into linear accelerators is usually space charge dominated. The space charge field can be reduced by process of gaseous SCC. The SCC process consists in the fact that the ions of the beam ionize the residual gas, and the electrons that arise during the ionization of gas molecules compensate the space charge of the beam of positive ions. The slow ions arising due to gas molecules ionization are accelerated in radial direction and acquire energy that determined by the space charge electric field of the ion beam. The degree of SCC can be determined by measurement of the energy distribution of slow ions produced in the beam region.

Electrostatic ion energy analyzers are used to measure slow ions energy spectra [1, 2]. A three grid electrostatic energy analyzer (TGA) has been used to measure SCC of hydrogen ion beam produced by a proton injector of Moscow INR linac [3, 4]. The hydrogen ion beam has peak current of up to 70 mA, energy of 400 keV, pulse duration of 200 μs and repetition rate of 50 Hz. The beam consists mainly from protons (~80%) and $H_2^+$ ions.

In this paper the TGA improvement and calibration is described, and results of study of the SCC process for different ion beam density are presented.

## THE TGA DESCRIPTION

The TGA cross section view is shown schematically in Fig. 1. The analyzer has cylindrical geometry and π angle for recording of the slow ions. The TGA consists of three grids, a collector and a heater. First grid of the TGA is grounded to eliminate influence of electric fields on the ion beam. Second grid is analyzing one. The second grid is twin to decrease effect of electric field penetration through the grid cells. It is under positive potential relative the ground. Retarding field between the first and second grids leads to deceleration of slow ions and to partial decrease or to complete stopping of the slow ion current to the collector in accordance with the slow ions energy spectra.

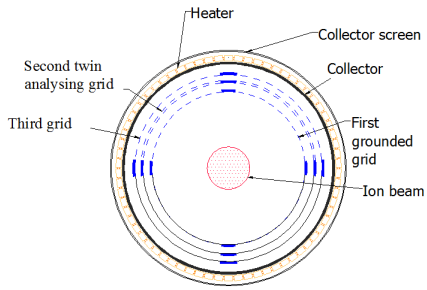


Figure 1: Schematic drawing of the TGA cross-section.

Third grid is under a negative potential (typically -300 V). It is necessary for suppression of secondary electrons from the collector and electrons from the ion beam. The grids have rectangular cells of 0. 5 x 0. 5 mm.

Heating of the TGA is necessary to eliminate systematic error connected with shifting of the TGA characteristics due to charging of the surface layers of the TGA electrodes by the slow ions [2].

Residual gas pressure in vacuum chamber (mainly hydrogen and water vapor) with the TGA was $1.1 \cdot 10^{-5}$ mbar.

Electric field of the TGA as well as ion transport from ion beam to the collector was simulated with COMSOL MP. Figure 2 shows electric field map near the TGA analyzing grid.

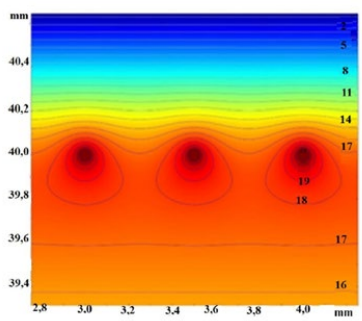


Figure 2: Electric field map of the TGA region near the analyzing grid. Ug2 = 20 V. Ug3 = -300 V.

TheTGA energy resolution is reduced due to the effect of field penetration through the grids and, as the simulation shows, is about 2 eV.

ISBN: 978-3-95450-240-0 ISSN: 2673-5539 doi:10.18429/JACoW-RuPAC2021-TUPSB40

# $He^+$ ION SOURCE FOR THE NICA INJECTION COMPLEX

A.M. Bazanov, A.S. Bogatov, B.V. Golovenskiy*, D.E. Donets, K.A. Levterov, D.S. Letkin, D.O. Leushin, A.V. Mialkovsky, V.A. Monchinskiy, D.O. Ponkin, I.V. Shirikov,
Joint Institute for Nuclear Research, Dubna, Russia

*Abstract*

A mono-ion source of single-charged helium of high intensity has been created to confirm the declared parameters of Heavy Ion Linear Accelerator (HILAC) [1, 2] and for the injection into superconducting synchrotron (SC) Booster during the first run.

The paper presents the design of the $He^+$ ion source, test bench for the TOF measurements and acceleration beam developed at VBLHEP, JINR. The results of the tests of the source are presented. During the tests the intense beams of ions 50 mA of $He^+$ were produced.

## HELIUM ION SOURCE

For designing helium ion source the proton ion sources described in [3, 4] were taken as a prototype. Ion source with cold magnetron cathode and magnetic plasma compression consists of the two basic parts: plasma generator, system of ions extraction and beam formation. There are three basic space may be attributed to plasma generator: space of auxiliary discharge between magnetron cathode and magnetron anode, space of the main discharge between magnetron cathode and anode, and area of plasma expansion (see Fig. 1).

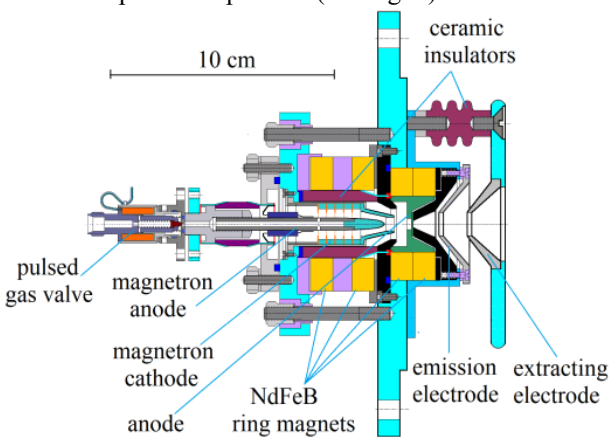


Figure 1: Helium ion source design.

The entire cathode block is placed in a longitudinal magnetic field (see Fig. 2). The magnetic field is organized using four ring neodymium magnets. Two of them with consistent polarity form a longitudinal field in the region of the magnetron cathode. The next two magnets with opposite polarity create a strong non-uniform magnetic field that compresses the plasma into a 1 mm emission hole.

From the region of magnetic compression, the plasma enters the expander and expands in it. A concave plasma boundary (meniscus) is formed, which forms an ejected beam. Extraction of ions from the plasma is carried out by applying a pulsed voltage of up to -40 kV to the extracting electrode.

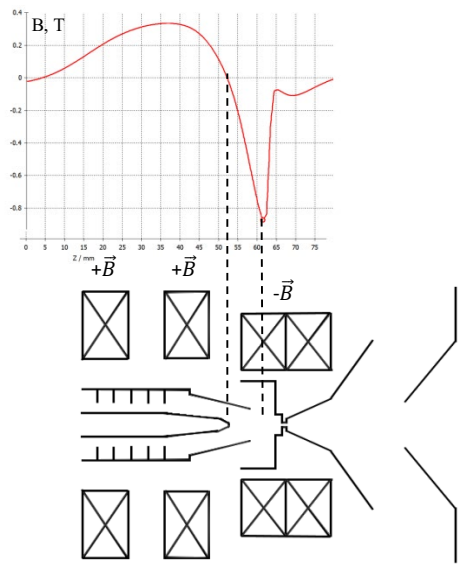


Figure 2: Equivalent diagram and graph of the magnetic field distribution along the axis.

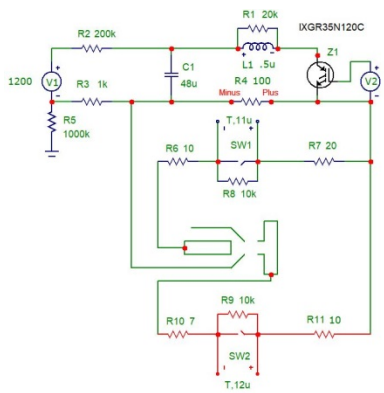


Figure 3: Scheme discharge modulator.

Gas system provides pulsed gas injection into space of magnetron discharge. Pulsed voltage up to 1 kV in the gaps between magnetron anode and magnetron cathode,

* golovenskiy@jinr.ru

ISBN: 978-3-95450-240-0 ISSN: 2673-5539 doi:10.18429/JACoW-RuPAC2021-TUPSB43

# OPTIMAL RF-PHOTOGUN PARAMETERS FOR THE NEW INJECTION LINAC FOR USSR PROJECT

Yu. D. Kliuchevskaia, S. M. Polozov[1]
National Research Nuclear University Moscow Engineering Physics Institute, Moscow, Russia
[1]also at NRC "Kurchatov Institute", Moscow, Russia

*Abstract*

The beam dynamics analysis of the RF-gun with photocathode for Russian 4th generation light source Ultimate Source of Synchrotron Radiation (USSR-4) was done to chose the optimal length of the section and cell's number and also to define optimal accelerating gradient and injection phase. The simulation of electrodynamics characteristics and fields distribution in the RF-gun based on 3.5-, 5.5- and 7.5-cell π-mode standing wave accelerating structure at operating frequency 2800 MHz was done. The influence of the beam loading effect on the field amplitude and beam dynamics was the main purposes of study also. The beam dynamics simulation results will present in the report and optimal RF-gun parameters will discuss.

## INTRODUCTION

The scheme of the proposed linear electron accelerator which will be used as an injector to the main ring (top-up injection) is similar to the structure of the injector for the CERN FCC-ee: two RF-guns (with a photocathode and a thermionic cathode) and several tens of identical regular sections (see Fig. 1) [1-2]. The development was carried out within the design framework of the 4th generation Ultimate Source of Synchrotron Radiation (USSR-4) for the National Research Center "Kurchatov Institute". In this paper beam dynamics simulation results in RF-gun with photocathode are presented. The beam dynamics analysis in the accelerator was done by using of BEAMDULAC-BL code [3]. The program allows to take into account the beam loading effect and quasi-static components of the beam self-coulomb-field.

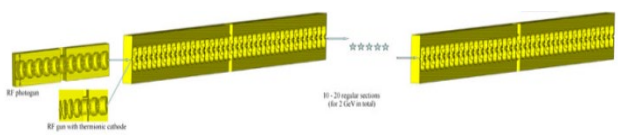

Figure 1: Possible scheme layout of linear accelerator-injector.

## BEAM DYNAMICS SIMULATION IN RF-PHOTOGUN

Beam dynamics simulation in RF-gun with photocathode with intensity of 250 pC per bunch for duration of 10 ps was carried out. To achieve the minimum energy spectrum, the parameters of several versions of the photogun (3.5-, 5.5- and 7.5-cell) were optimized (see Fig. 2). Simulation results depending on the field amplitudes in the cells ($E_1$ – $E_4$, kV/cm) are presented in Table 1, and taking into account the beam loading in Table 2.

Table 1: Simulation Results Depending on the Field Amplitudes in the Cells

| $E_1$, kV/cm | $E_2$, kV/cm | $E_3$, kV/cm | $E_4$, kV/cm | $\frac{\delta W}{W}$, % | Max $E_{out}$, MeV |
|---|---|---|---|---|---|
| 1000 | 1000 | 1000 | 1000 | 2.5 | 9.439 |
| **900** | **1000** | **1000** | **1000** | **1.7** | **9.438** |
| 800 | 1000 | 1000 | 1000 | 2.2 | 8.678 |
| 750 | 1000 | 1000 | 1000 | 2.2 | 8.437 |
| 700 | 1000 | 1000 | 1000 | 2.2 | 8.181 |
| 900 | 900 | 1000 | 1000 | 3.0 | 8.390 |
| **800** | **900** | **1000** | **1000** | **2.0** | **8.808** |

According to results the 5.5-cell photogun provides the required minimum value of the energy spectrum for bunches with a charge of 250 pC per bunch and duration of 10 fs.

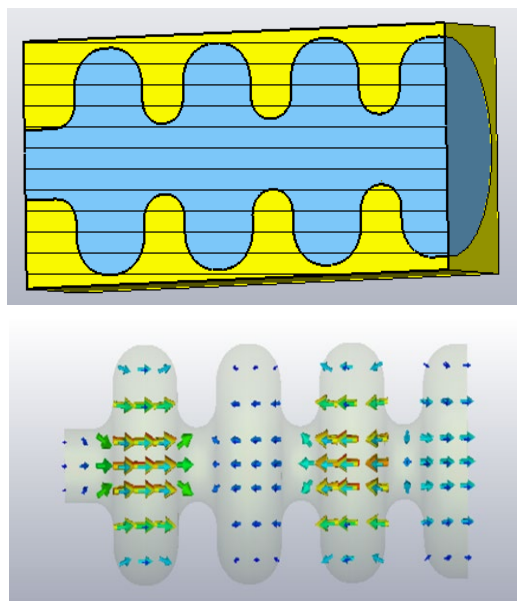

Figure 2: 3.5-cell RF-gun view and electrical field distribution.

The output beam spectrum at different electric field amplitudes (700-1000 kV/cm) in the cells of RF-photogun are shown in Fig. 3. Output longitudinal emittance and beam cross section are shown on Figs. 4 and 5.

ISBN: 978-3-95450-240-0 ISSN: 2673-5539 doi:10.18429/JACoW-RuPAC2021-TUPSB44

# DESIGN AND SIMULATION OF AN S-BAND RF PHOTOGUN FOR A NEW INJECTOR OF THE ACCELERATOR LINAC-200 AT JINR

Y.A. Samofalova, M.A. Nozdrin, V.V. Kobets, A.S. Zhemchugov, JINR, Dubna, Russia
A.M. Barnyakov, BINP, Novosibirsk, Russia

## *Abstract*

A new 1.5-cell 2.856 GHz S-band RF photogun is simulated for the generation of ultrashort electron beams at the Linac-200 accelerator at JINR. The beam parameters at the photogun output are determined to meet the requirements of the Linac-200 injection. The general design of the photogun is presented. The electrodynamic parameters are determined and the accelerating field distribution is calculated. The particle dynamics is simulated and analysed to obtain the required beam properties.

## *Introduction*

Commissioning of a new electron test beam facility Linac-200 [1] comes to the end at JINR (Dubna, Russia). The facility is based on the MEA accelerator that was transferred from NIKHEF to JINR at the beginning of the 2000s. Linac-200 provides electron beams with energy up to 200 MeV, beam current as much as 40 mA. The principal purpose of the facility is providing test beams for particle detector R&D, studies of novel approaches to the beam diagnostics, and training and education of students. Increasing the charge in the bunch from replacement the injector will give the opportunity to use the accelerator as a driver for a source of terahertz, synchrotron, and transition radiation in the soft X-ray range and to study the characteristics of image detectors, drastically expanding the range of available applied.

## *RF Photogun Concept*

The design of the electron injector of the accelerator Linac-200 includes such elements as a triode type DC electron gun with a thermionic cathode, a chopper, a prebancher and a buncher, which is a short section of the accelerating structure designed for bunching a beam. The parameters of the gun and injector of the Linac-200 accelerator are presented in Table 1. The beam charge is 120nC in a 3 us pulse.

Table 1: Linac-200 Accelerator Injector Parameters

| Parameter name | Injector | Electron gun |
|---|---|---|
| Pulse current, mA | 60 | 200 |
| Output energy, MeV | 6 | 400 |

It is proposed to replace the existing injector with a 1.5-cells RF photogun with a cathode integrated into the end wall of the RF cavity. Significant advantages of the photogun include minimization of the emittance growth due to nonlinear components of the transverse electric and magnetic fields owing to the choice of optimal geometry of the accelerating structure.

The design is based on a 1.5-cell RF S-band photogun, similar to the design of the Budker Institute gun [2]. The gun is simulated for the existing laser (Fig. 1) developed by IAP RAS [3], the impulse characteristics are shown in Table 2.

Table 2: IAP RAS Laser Parameters

| Parameter name | Value |
|---|---|
| Wavelength, nm | 262 |
| Bunch train repetition rate, Hz | 10 |
| Bunch train duration, us | 800 |
| Bunches in train | 8000 |
| Bunch duration, ps | 10 |
| Bunch energy, uJ | 1.5 |

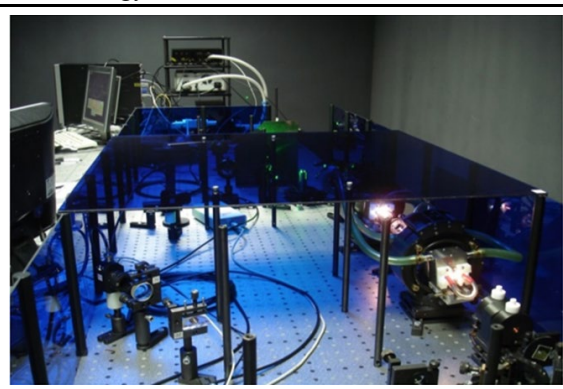

Figure 1: External view of the IAP RAS laser.

One can expect to obtain up to 960 nC in a 3 us pulse using this laser and assuming 10% quantum efficiency of a photocathode.

## *Simulation of a High Frequency Photogun*

The simulation of the RF photogun design model is realized by the software CST Studio Suite 2021 [4] (hereinafter the software). In this work the calculations of the electric and magnetic fields, photoelectron emission and the dynamics of high-frequency ultrashort beams of the photogun were performed using the software. The design model of the RF photogun is 1.5 accelerating cells operating at a 2856 MHz frequency with a π mode oscillation. Microwave power is injected into the cavity by means of a rectangular waveguide and a coaxial line. The calculated standing wave factor is $\rho = 1.1$, the $Q$-factor is 15000. The estimated output beam energy reaches the set value (Fig. 2) and can regulated by the input power, which indicates the correct operation of the calculation model. Figure 3 shows the layout of the simulation model of the photogun and the simulation results with the electric field distribution along the axis of the cavities.

ISBN: 978-3-95450-240-0 ISSN: 2673-5539 doi:10.18429/JACoW-RuPAC2021-TUPSB47

# STABILITY CONDITIONS FOR A PENNING TRAP WITH ROTATING QUADRUPOLE OR DIPOLE ELECTRIC FIELDS

A. D. Ovsyannikov†, Saint-Petersburg State University, Saint-Petersburg, Russia

*Abstract*

The dynamics of particles in a Penning-Malmberg-Surko trap with Rotating Wall (rotating quadrupole and/or dipole electric field) and a buffer gas is considered. Electromagnetic traps are widely used for the accumulation and confinement of charged particles during various experiments in nuclear and accelerator physics, mass spectroscopy, and other fields. Traps are the main element of sources of charged particles in accelerators. An especially important role is played by traps with efficient accumulation during operation (in a cyclic mode) of ion synchrotrons and colliders with short-lived isotopes. The purpose of this work was to develop algorithms for constructing regions of stability (according to Lyapunov) in the space of parameters describing additional rotating electric fields, and to determine the analytical conditions that must be satisfied by the trap parameters to achieve a given degree of stability. The influence of the space charge of a beam of accumulated particles on the stability of the system is also investigated. The calculation results and the proposed models can be used in the selection and adjustment of the main parameters of the designed traps of the considered type.

## INTRODUCTION

Electromagnetic traps are used to accumulate charged particles for various purposes in accelerator physics, mass spectroscopy, nuclear physics, and some other areas of scientific research. Traps are especially important part of charged particles sources in synchrotrons and colliders with short-lived isotopes. The essence of their action is the localization of charged particles in a limited area of space for a sufficiently long time. For this, special combinations of electromagnetic fields are formed that provide the required behaviour of charged particles inside the trap. The most famous traps of the Paul and Penning type, as well as their various modifications. A detailed review of the main known types of traps and the principles of their action is presented in [1].

In this paper, we consider the dynamics of charged particles in a Penning trap with additional rotating dipole electric field (so called Rotating Wall — RW) and a buffer gas or rotating quadrupole electric field without buffer gas, studied earlier in [2-5]. Note also that the investigated model of motion can be used in the analysis of the Penning-Malmberg-Surko trap - an open cylindrical trap and its modifications [1]. The results of the analysis of the influence of the rotating field, obtained earlier, were either insufficiently rigorous from the mathematical point of view [3, 5], or were insufficiently complete [4]. In [6-9], general approaches were proposed that are applicable to the analysis of stability and the construction of numerical-analytical solutions of the equations of motion of the system under study for arbitrary values of its parameters. Examples of such an analysis were given in the works [10, 11]. In this paper the model of dynamics includes also influence of the space charge of a beam of accumulated particles and combination of dipole and quadrupole rotating electric field.

It should be noted that the work investigates the motion of single particles in ideal (linear) fields. Interest in this formulation of the problem arises from attempts [1, 3] to explain the observed in experiments [2] effect of compression of a bunch of accumulated particles by a rotating field at extremely low concentrations of accumulated particles. In this case, the focusing effect should follow from the analysis of the solution of the equations of motion of single particles in the fields of forces acting in the trap [1].

## EQUATIONS OF MOTION

The dynamics of charged particles in a Penning trap with an additional rotating electric field is considered. Charged particle dynamics is considered in the field of the potentials and homogeneous longitudinal magnetic field:

$$\Phi(r,\theta,z) = \frac{m}{q}\left(\frac{\omega_z^2}{2}\left(z^2 - \frac{r^2}{2}\right) - \frac{(q_r r^2 + q_z z^2)}{2} + azr\cos(\theta + t\omega_r) + b\frac{r^2}{2}\cos 2(\theta + t\omega_r + \theta_0)\right),$$

$$\vec{B} = \vec{e}_z B.$$

Here m and $q$ are the mass and the charge of the particle, $\omega_z$ is the frequency of the particle longitudinal oscillations in the axially symmetric electric field of the trap electrodes; $a$, $b$ and $\omega_r$ are amplitude related parameters and the frequency of the rotating electric dipole and quadrupole fields, $\theta_0$ is initial phase parameter of rotating quadrupole field; $q_r$ and $q_z$ are the parameters associated with the space charge, which determine the linear part of the potential of the axially symmetric accumulated beam; $z$, $r$ and $\theta$ are the axial, radial and angular coordinates with the axis coinciding with symmetry axis of the trap electrodes.

The charged particle motion in these fields is described by the following systems of equations correspondingly:

$$\ddot{x} = \left(\frac{\omega_z^2}{2} + q_r\right)x + \Omega_c\dot{y} - k\dot{x} - az\cos(t\omega_r) - b(x\cos 2(t\omega_r + \theta_0) - y\sin 2(t\omega_r + \theta_0)),$$

$$\ddot{y} = \left(\frac{\omega_z^2}{2} + q_r\right)y - \Omega_c\dot{x} - k\dot{y} + az\sin(t\omega_r) + b(y\cos 2(t\omega_r + \theta_0) + x\sin 2(t\omega_r + \theta_0)),$$

$$\ddot{z} = (q_z - \omega_z^2)z - k\dot{z} - a(x\cos(t\omega_r) - y\sin(t\omega_r)).$$

† ovs74@mail.ru, a.ovsyannikov@spbu.ru

ISBN: 978-3-95450-240-0 ISSN: 2673-5539 doi:10.18429/JACoW-RuPAC2021-TUPSB48

# OPTIMIZATION OF THE MASTER OSCILLATOR LASER BEAM PARAMETERS IN THE MULTI–PASS AMPLIFIER

T. V. Kulevoy*, A. N. Balabaev, I. A. Khrisanov, A. A. Losev, V. K. Roerich, Yu. A. Satov, A. V. Shumshurov, A. A. Vasilyev, NRC «Kurchatov Institute» – ITEP, 117218, Moscow, Russia

*Abstract*

Some results devoted to development of the ITEP laser–plasma ion source for a charged particle accelerator are presented. In our case, the laser radiation source is a high-power repetition rate $CO_2$ laser system based on the nonlinear interaction of a light with a multi-pass amplifier medium. The laser chain consists of a master oscillator [1], gas absorber cell, and a four–pass amplifier.

The efficiency of the laser ion source depends on by the output power of laser setup. The output power of such a laser setup is determined by the efficiency of energy extraction from the amplifying medium.

The spatial parameters of a laser beam at the amplifier input are optimized by numerical simulation. The results obtained for fixed master oscillator pulse and amplifying medium parameters. The maximum output energy is achieved with certain laser beam profile at the amplifier input. For this purpose, only central part of the beam with a Gaussian spatial profile, which is close to uniform in intensity, is injected into the telescopic amplifier. The optimal choice of beam diameter ensures the maximum laser efficiency.

## INTRODUCTION

A laser-plasma generator of multiply charged ions based on a $CO_2$ laser is useful for a wide range of practical applications, including as a source for an particle accelerator. A such repetitive rate laser has a relatively low cost and is capable of emitting a pulses with a power of over 5 GW and an energy of over 100 J. A low operating costs, a relatively weak requirements for cleanliness degree, thermal stabilization and dust–free premises is a undeniable advantage of a such laser.

The laser–plasma generator based on a $CO_2$ laser was developed for the lead ion source for the CERN accelerator [2] and for the ITEP–TWAC facility [3]. In the above examples, a laser–optical scheme based on nonlinear effects during propagation of radiation pulses in absorbing and amplifying resonant media [4] was used.

## EXPERIMENTAL SETUP

The optical scheme of the experimental setup is in the Fig. 1. The master oscillator (1) is based on a self-sustained discharge module at atmospheric pressure with UV preionization. The hybrid generation scheme of the generator is required to form single–frequency laser pulses with a smooth temporal shape and an FWHM pulse duration of 80 ns and energy up to 200 mJ for the P(20) line in the 10-$\mu$metre band. The sectioned absorber gas cell (2) [5] of 90 cm length is filled with a mixture of $SF_6/N_2$ and is used to modify the master oscillator pulse front edge. The grating (3) separates the master oscillator and the amplifier medium for the entire spectral range except the desired spectral line.

The spatial parameters of the laser beam are defined by a spatial filter that consists of a pair of confocal mirrors (4, 6) and diaphragm (5). The laser beam formed by the filter is close to a Gaussian beam. In the laser setup a four–pass amplification chain is applied. It is arranged with flat mirrors and a pair of mirrors (8, 10) of a Cassegrain off–axis telescope with multiplication $M = 5.5$.

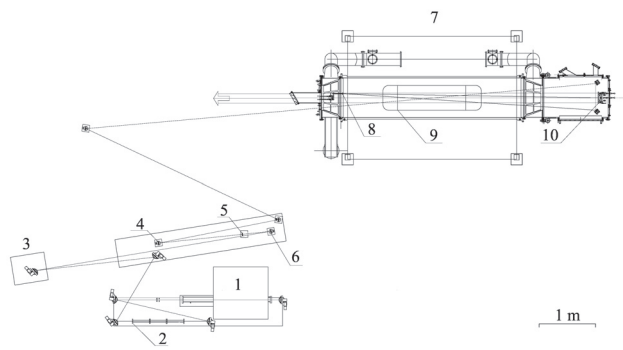


Figure 1: Experimental setup. 1 — master oscillator; 2 — absorbing cell; 3 — diffraction grating; 4 — short–focus mirror of the spatial filter; 5 — spatial filter diaphragm; 6 — long–focus mirror of the spatial filter; 7 — wide-aperture four–pass amplifying module; 8 — small telescope mirror; 9 — active medium; 10 — large telescope mirror.

## SPATIAL PARAMETERS OF THE LASER BEAM CALCULATION

The computer program FOCUSD [2] for analysis of the laser beam spatial distribution in the laser beam shaping scheme describes the distribution of the light energy density in the 1D diffraction approximation in the case of cylindrical symmetry and integrally over time. Active medium gain is uniformly $g_0 = 2.5 \times 10^{-2}\,\mathrm{cm}^{-1}$. An absorbing cell influence is described according to the previously developed phenomenological model of an absorbing medium [6].

* kulevoy@itep.ru

ISBN: 978-3-95450-240-0 ISSN: 2673-5539 doi:10.18429/JACoW-RuPAC2021-TUPSB51

# MEASUREMENT OF NEUTRON FIELD FUNCTIONALS AROUND A NEUTRON CONVERTER OF 50 GeV PROTONS

Ya. N. Rascvetalov†, Yu. V. Beletskaya, A. G. Denisov, A. A. Durum, V. L. Ilyukin, A. M. Mamaev, V. N. Peleshko, I. N. Piryazev, E. N. Savitskaya, M. M. Sukharev, S. E. Sukhikh, A. A. Yanovich, NRC "Kurchatov Institute" - IHEP, 142281 Protvino, Russia

*Abstract*

The experiment was performed on a pulsed neutron source of the "Neutron" research bench, being created at the U-70 accelerator at National Research Center "Kurchatov Institute" - IHEP, Protvino. Neutrons were generated by the 50 GeV proton beam in the special converter.

As a measurement method, neutron activation analysis was used with a set of threshold activation detectors made of C, Al, Nb, In, Bi materials. The neutron energy thresholds of these detectors are in the range from 1 MeV to 75 MeV. The aluminium activation foils were used to calculate the absolute values of the proton quantities in the exposures.

The results of measurements and calculations are presented in the form of the following functionals: nuclides activity of threshold reactions in detectors at the end of the exposure; reaction rate; neutron fluences with energies greater than the threshold. To estimate these values, the spectra of neutrons, protons and pions were calculated using the particle transport codes MARS and HADRON with the FAN15 as a low-energy block. It was found that neutrons dominate up to 100 MeV, and the charged hadrons contribution to the total reaction rate for a particular nuclide formation can range from 4% to 46%.

## INTRODUCTION

Pulsed neutron sources based on high-energy proton beams have a wide range of applications – from transmutation of long-lived radioactive elements to neutronographic studies of materials and rapid processes kinetics. Information of the parameters of the neutron field around the proton converter is necessary for these tasks. Similar problems were studied at IHEP (1999 - 2000) with proton beam energy of 1 and 70 GeV [1]. A special research bench "Neutron" was created in 2019 for the extracted 50 GeV proton beam.

The measurements were performed in the field of secondary hadrons, emitted from the side surface of the converter of the bench "Neutron". The converter consists of a lead core 50 × 50 × 300 mm$^3$ and 40 mm thick polyethylene block surround of the sides. A proton beam with transverse size of 8 mm horizontally and 14 mm vertically dropped on the end face of the lead core along the longitudinal axis. But the beam impact point was shifted horizontally from core center to the right by ~ 8 mm. The intensity of the beam was 1 - 2 bunches per 8.7 s accelerator cycle ($3 \cdot 10^{11}$ protons are in each bunch). As a measurement method, neutron activation analysis was used with a set of threshold activation detectors made of C, Al, Nb, In, Bi materials. The characteristics of the detectors, the threshold reactions, and the identified lines of gamma quanta are fully described in [1].

The aluminium activation foils were used to calculate the number of protons in the exposures. The experiment was performed for three U-70 accelerator runs in the period 2019 - 2021.

## RESULTS

The detectors were irradiated in a series of exposures at the points 1, 2, 3 on the thin aluminium substrate placed on the upper converter surface as shown in Fig. 1. The substrate was cut along the beam axis into 12 rectangles (50 × 65 × 0.2 mm$^3$). The activity $A_0$ of the $^{22}$Na nuclide in these samples at the end of irradiation (a total of $1.3 \cdot 10^{13}$ protons onto converter) is shown in Fig. 2.

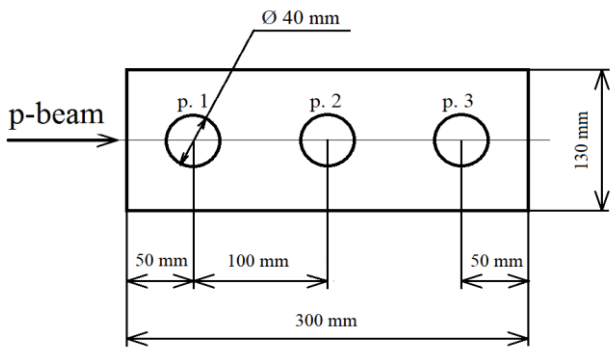


Figure 1: Detectors placement points (p. 1, p. 2, p. 3) on the thin Al substrate.

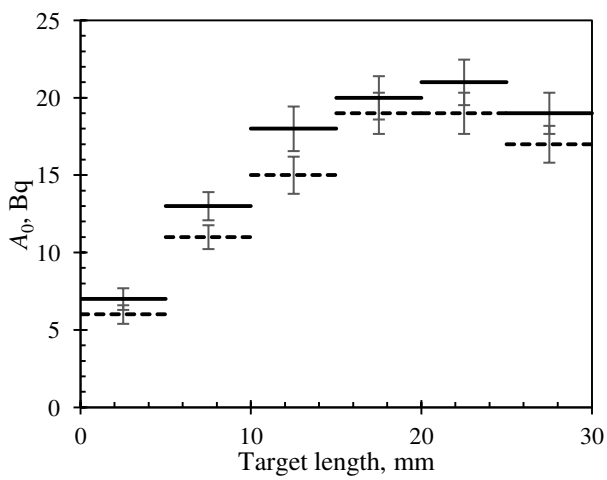


Figure 2: The activities of Na22 in the substrate.

† Jaroslav.Rascvetalov@ihep.ru

ISBN: 978-3-95450-240-0 ISSN: 2673-5539 doi:10.18429/JACoW-RuPAC2021-TUPSB52

# MEASUREMENT OF THE ARGON IONS CURRENT ACCOMPAYNING AT THE ACCELERATING SOURCE OF EPITHERMAL NEUTRONS*

I. A. Kolesnikov†, Yu. M. Ostreinov, P. D. Ponomarev, S. S. Savinov, I. M. Shchudlo, S. Yu. Taskaev
Budker Institute of Nuclear Physics, 630090 Novosibirsk, Russia
Novosibirsk State University, Novosibirsk, Russia

*Abstract*

For the development of a promising method for the treatment of malignant tumors - boron neutron capture therapy - the accelerator-based epithermal neutrons source has been proposed and created in the Budker Institute of Nuclear Physics. Argon ions formed during stripping of a beam of negative hydrogen ions to protons are accelerated and, in parallel with the proton beam, are transported along the high-energy path of the facility. Depending on the relative number of argon ions, their effect can be from negligible to significant, requiring their suppression. In this work, the current of argon ions reaching the beam receiver in the horizontal channel of the setup was measured. It was determined that the argon beam current accompanying the proton beam is 2000 times less than the proton beam current. This makes it possible not to apply the proposed methods of its suppression.

## INTRODUCTION

Charged particle accelerators are widely used in scientific research, medicine, and other applications. Tandem accelerators are high-voltage electrostatic accelerators in which the high-voltage potential is used twice: first to accelerate negative ions, and then, after changing the polarity of their charge in the high-voltage terminal, to accelerate positive ions. Thin foils are used for the conversion of the ion charge, or, at a higher ion current, gas stripping targets similar to the argon target in the tandem accelerator of the Budker Institute of Nuclear Physics of the Siberian Branch of the Russian Academy of Sciences. The stripping gas target provides effective stripping of the negative ion beam; however, its use leads to the formation of an undesirable beam of argon ions, which are formed in the stripping target as a result of argon ionization by the ion beam and penetrate into the accelerating channel. The aim of this work was to measure the current of an argon ion beam in a tandem accelerator with vacuum insulation.

## THE EXPERIMENTAL SCHEME

The studies were carried out at the accelerator neutron source of the Budker Institute of Nuclear Physics (Novosibirsk, Russia). The source diagram is shown in Fig. 1 and its detailed description was given in [1]. A tandem accelerator with vacuum insulation was used to obtain a stationary proton beam with an energy of 0.6 to 2.3 MeV and a current of 0.3 to 10 mA, that is, a tandem accelerator of charged particles with an original design of electrodes. In it, unlike traditional accelerators, there are no accelerating tubes; the high-voltage electrode and electrodes with an intermediate potential are embedded in each other and fixed on a single feedthrough insulator, as shown in Fig. 1. This configuration of the accelerator made it possible to improve the high-voltage strength of the accelerating gaps and, as a consequence, to increase the proton current. One of the main elements of the tandem accelerator is the stripping target 4 placed inside the high-voltage terminal. It provides the conversion of negative hydrogen ions to protons with a high efficiency, usually at the level of 95%. The target is a 400-mm long cooled cylindrical copper tube with an inner hole diameter of 16 mm [1]. The interaction of a hydrogen ion beam with a gas target leads to its partial ionization, and a weakly ionized plasma is formed inside the stripping tube. Since electrons are more mobile than argon ions, the plasma assumes a positive potential to maintain quasineutrality.

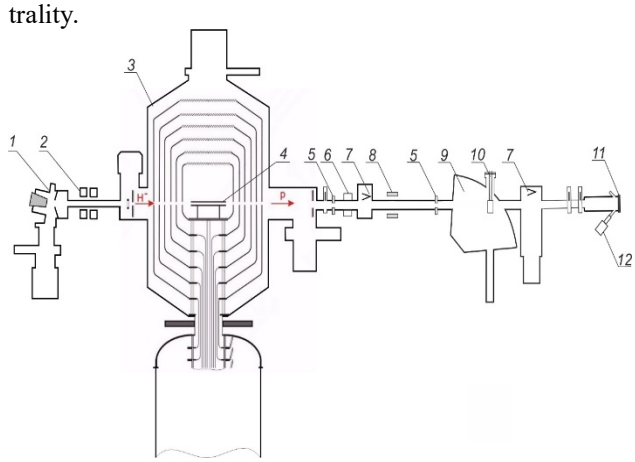


Figure 1: A diagram of an accelerator based source of epithermal neutrons. 1 - a source of negative hydrogen ions; 2 - magnetic lens, 3 - vacuum-insulated tandem accelerator; 4 - gas stripping target; 5 - cooled diaphragm; 6 - contactless current sensor Bergoz (France); 7 - Faraday cups; 8 - corrector; 9 - bending magnet; 10 - cooled beam receiver with a diaphragm; 11 - lithium target; 12 - Hikvision video camera (China).

Under the action of the positive potential, part of the argon ions leaves the stripping tube, enters the accelerating channel, and forms a beam of argon ions. Simple estimates of the argon ion current give values from commensurate to negligible in comparison with the proton

* Work supported by the Russian Foundation for Basic Research, project no. 19-32-90118.
† Ya.A.Kolesnikov@inp.nsk.su

ISBN: 978-3-95450-240-0 ISSN: 2673-5539 doi:10.18429/JACoW-RuPAC2021-TUPSB53

# MEASUREMENT OF PARAMETERS OF NEUTRON RADIATION ON THE ACCELERATOR-BASED EPITHERMAL NEUTRON SOURCE*

M. I. Bikchurina, T. A. Bykov, D. A. Kasatov, Ia. A. Kolesnikov, I. M. Shchudlo, S. Yu. Taskaev,
BINP and Novosibirsk State University, Novosibirsk, Russia
K. A. Martianov, LLC "BINP-Plasma", Novosibirsk, Russia

*Abstract*

Treatment of oncological diseases using Boron Neutron Capture Therapy (BNCT) is an important issue of our time. Cancer cells accumulate a boron-containing drug, after which they are irradiated with a beam of epithermal neutrons, a nuclear reaction $^{10}B(n,\alpha)^{7}Li$ occurs, and the products of a nuclear reaction destroy these cells. In BNCT, it is generally accepted that the total dose of ionizing radiation consists of four components: boron dose, dose from fast neutrons, dose from thermal neutrons, and dose of gamma radiation. Dose values and their ratio strongly depend on the neutron flux; therefore, the measurement of the neutron flux (yield) is an urgent task. In this work, the neutron yield was measured by the activation of the target with the radioactive isotope beryllium-7, which is formed in the reaction of neutron generation $^{7}Li(p,n)^{7}Be$. It was found that the neutron yield from a specifically manufactured lithium target is in good agreement with the calculated one, which is important for planning therapy.

## INTRODUCTION

An accelerator based epithermal neutron source for the development of boron neutron capture therapy (BNCT), a promising method for the treatment of malignant tumors, is proposed, created and is functioning at the Budker Institute of Nuclear Physics [1,2]. The neutron source consists of a tandem accelerator of charged particles of an original design, a lithium neutron-generating target, for generating neutrons as a result of the $^{7}Li(p,n)^{7}Be$ reaction, and a system for forming a therapeutic beam of epithermal neutrons. The total dose of ionizing radiation consists of four components: boron dose, dose from fast neutrons, dose from thermal neutrons, and dose of gamma radiation. Dose values and their ratio strongly depend on the spectrum and neutron flux.

## DESIGN OF THE ACCELERATOR

The neutron source consists of a tandem accelerator of charged particles of an original design, a lithium neutron-generating target and a system for forming a therapeutic beam of epithermal neutrons, Fig. 1.

In a tandem accelerator, a surface plasma source using a Penning discharge with hollow cathodes is used to generate negative hydrogen ions. A beam of negative hydrogen ions with an energy of 20-23 keV and a current of up to 10 mA is focused with magnetic lenses and injected into a tandem electrostatic accelerator. In an accelerator, negative hydrogen ions are accelerated by a voltage applied across six high-voltage electrodes. In a gas stripping target made in the form of a cooled tube with argon inlet in the middle and installed inside a high-voltage electrode, negative ions lose electrons and turn into protons, which are accelerated to an energy equal to twice the potential. Then the proton beam is delivered to the lithium target for neutron generation as a result of the threshold nuclear reaction $^{7}Li(p,n)^{7}Be$.

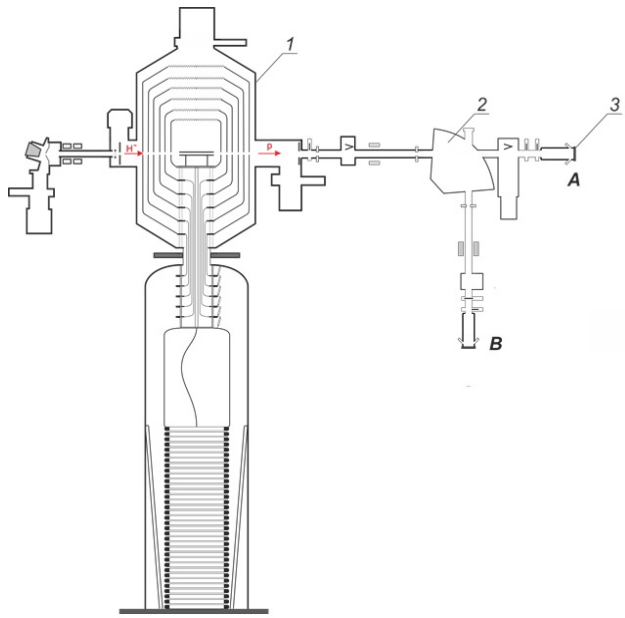


Figure 1: Tandem accelerator with vacuum insulation: 1 – accelerator, 2 – bending magnet, 3 – lithium neutron generating target. The lithium target is placed in the horizontal proton beam transport path (position A) or in the vertical (position B).

## EXPERIMENTAL RESULTS

A total of 15 sessions of neutron generation were carried out; used 13 lithium targets. In the manufacture of all 13 targets, only a new copper substrate was used and a new lithium layer was always deposited.

Since the products of the $^{7}Li(p,n)^{7}Be$ reaction are not only a neutron, but also a radioactive atomic nucleus beryllium-7, measuring the number of $^{7}Be$ nuclei makes it possible to unambiguously determine the number of generated neutrons.

The radioactive atomic nucleus $^{7}Be$, as a result of electron capture, is converted back to lithium-7 with a half-life of 53.22 days. In 10.3% of cases, decay is accompanied

*Work supported by grant from the Russian Science Foundation (grant no. 19-72-30005), the Budker Institute of Nuclear Physics and the Novosibirsk State University

ISBN: 978-3-95450-240-0 ISSN: 2673-5539 doi:10.18429/JACoW-RuPAC2021-WEPSC01

# UNIT FOR MATCHING A DRIVING WAVEGUIDE WITH A CAVITY

V.V. Paramonov†, Institute for Nuclear Research of the RAS, 117312, Moscow, Russia

*Abstract*

To match the driving WaveGuide (WG), usually operating in the fundamental TE10 wave, with the accelerating structure, a device is required that performs the function of a wave-type transformer. In the microwave region, transforming devices with matching windows are usually used, the field distribution in which can also be described as TE-type. At the ends of the window from the side of the structure, regions with an increased density of Surface Currents (SC) inevitably arise, leading to an increase in the surface temperature in a place that is difficult to access for cooling. There are various solutions for matching windows, in order to reduce the maximum SC from the side of the structure, briefly mentioned in the report. A solution based on the dispersion properties of the TE10 wave, providing a significant additional decrease in the SC density, is considered. This solution can be implemented for C-band and lower frequency ranges.

## INTRODUCTION

To transmit RF power from RF source to a cavity at frequencies > 300 MHz rectangular WG's, operating with TE10 wave, are usually used. Reasons are in the higher RF power capability and lower attenuation. The simplest solution for appropriate matching of a cavity with waveguide schematically is shown in Fig. 1. Also may be modifications in waveguide dimensions near matching slot, slot shape an so on. A solution, based on dispersion properties of TE10 wave in driving WG is considered below.

## MOTIVATION

We can consider cavity excitation by tangential electric field $E\tau s$ of the matching slot [1], and expand cavity field in the set over own modes $Ecn$ :

$$\vec{E}_c = \sum_n e_{cn}\vec{E}_{cn}, \mathrm{e}_{cn} = i\frac{\omega_{cn}}{\omega^2-\omega_{cn}^2}\frac{\int_{Ss}\left[\vec{E}_{\tau s}\overrightarrow{H_{cn}}\right]d\vec{S}}{\mu_0\int_{Vc}\vec{H}_{cn}\vec{H}^*_{cn}dV}, \quad (1)$$

where $\omega cn$ are frequencies of own cavity modes. Here and below subscripts *c,s,w* are connected to the cavity, slot and WG respectively. In the same style we can consider excitation of the slot by tangential magnetic fields of the cavity $H\tau c$ and WG $H\tau w$:

$$\vec{E}_s = \sum_m u_{sm}\vec{E}_{sm},$$

$$\mathrm{u}_{sm} = i\frac{\omega}{\omega^2-\omega_{sm}^2}\frac{\int_{Ssd}\left[\vec{E}^*_{sm}\overrightarrow{H_{\tau c}}\right]d\vec{S}+\int_{Sst}\left[\vec{E}^*_{sm}\overrightarrow{H_{\tau w}}\right]d\vec{S}}{\varepsilon_0\int_{Vs}\vec{E}_{sm}\vec{E}^*_{sm}dV} \quad (2)$$

For the field in the slot is known the model of shortened transmission line [2].

† email address paramono@inr.ru

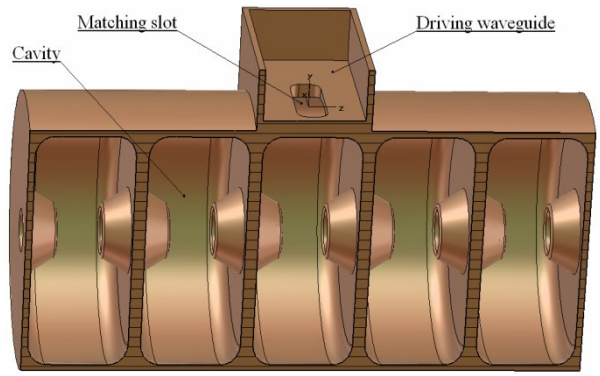


Figure 1: Schematic drawing of the cavity – slot – WG system to be matched.

More descriptive is the slot model, proposed in [3]. The slot is considered as the cavity, bounded by 'magnetic wall' boundary conditions from sides of cavity and WG, Fig. 2.

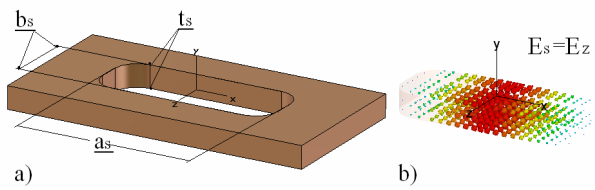


Figure 2: The slot model with dimensions definition, (a), and electric field of fundamental TE10 mode, (b).

In this approximation the field and frequency for fundamental TE10 in the slot are:

$$\vec{E}_{s1} \approx \mathrm{E}_{z0}\cos(\frac{\pi x}{a_s}), \omega_{s1} \approx \frac{\pi c}{a_s} >> \omega, \mathrm{E}_{z0} = 2\sqrt{\frac{W_0}{\varepsilon_0 a_s b_s t_s}}, \quad (3)$$

Supposing fields of own modes in the cavity *Enc* and in the slot *Esm* to be normalized to stored energy *W0=const*, single mode (n=1, m=1), lossless approximations for cavity and slot, after transformation, from Eq. (1) – Eq. (3) one gets:

$$E_{c1} \approx \frac{4\omega_{c1}\omega a_s^2 b_s H_{c\tau}}{W_0(\omega^2-\omega_{c1}^2)\pi^4 c^2\varepsilon_0 t_s}(H_{c\tau}+BH_{w\tau}),$$

$$B = \frac{2}{\pi}\left(\frac{\sin(\frac{\pi}{2}(1+\frac{a_s}{a_w}))}{(1+\frac{a_s}{a_w})}+\frac{\sin(\frac{\pi}{2}(1-\frac{a_s}{a_w}))}{(1-\frac{a_s}{a_w})}\right) \approx \frac{2}{\pi}. \quad (4)$$

Relations in Eq. (4) approximately describe well known correlations and effects. For effective matching the slot should be posted in the region with strong magnetic field of the cavity. The first term in the right hand side of Eq. 4 reflects inevitable reduction of cavity frequency with slot opening.

ISBN: 978-3-95450-240-0 ISSN: 2673-5539 doi:10.18429/JACoW-RuPAC2021-WEPSC03

# MULTIPACTOR DISCHARGE IN SHORT 5-GAP 80 MHz IH STRUCTURES

M. M. Bulgacheva†, M. Gusarova, M. Lalayan, MEPhI, National Research Nuclear University, 115409 Moscow, Russia

*Abstract*

The results of numerical simulations of multipacting discharge in accelerating Interdigital H-type (IH) cavities are presented in this paper. Optimal design parameters were selected to reduce the number of multipactor electrons. The localization of multipactor trajectories in the short 5-gap 80 MHz IH cavities at various levels of accelerating voltage is considered.

## INTRODUCTION

The multipactor effect[1-4] is a phenomenon in radio frequency devices, where secondary electron emission in resonance with an alternating electric field leads to exponential electron multiplication, possibly damaging and even destroying the RF device.

Figure 1 shows the 3D models of the considered 5-gap Interdigital H-type cavities: β=0.06 (a) and β=0.1 (b). This paper investigates the location and possible expansion of the multipactor discharge at different voltage levels.

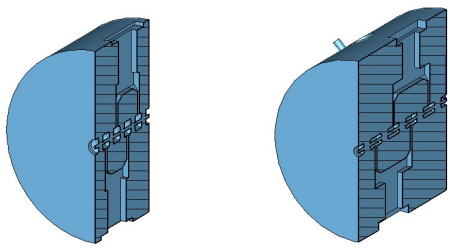

(a) (b)

Figure 1: 3D models of the 80 MHz IH cavities.

In this structure, there are two main areas where a multipactor discharge can occur (see Fig. 2): the gap region at low voltages (up to 10 kV), and the region of the external surface of the resonator and the side walls – at high voltages (up to 4 MV)[5].

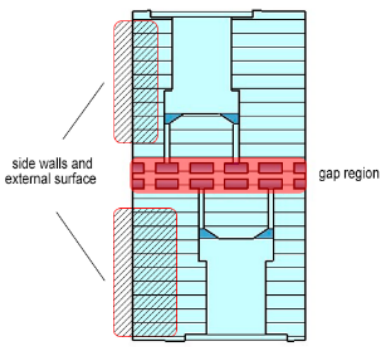


Figure 2: Dangerous areas.

† margaritabulgacheva@gmail.com

## GEOMETRICAL MODIFICATION

To decrease the number of multipactor trajectories, the geometry of the drift tube has been modified. The straight angled tubes were replaced with the drift tubes with a bevel (see Fig. 3).

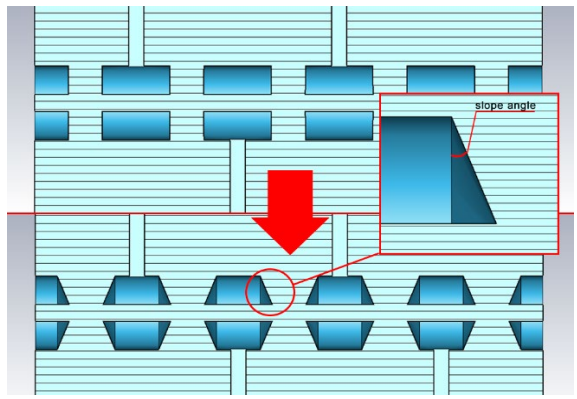


Figure 3: Geometrical modification of the drift tube.

The value of the slope angle of the bevel was selected considering the shunt impedance graph (see Fig. 4).

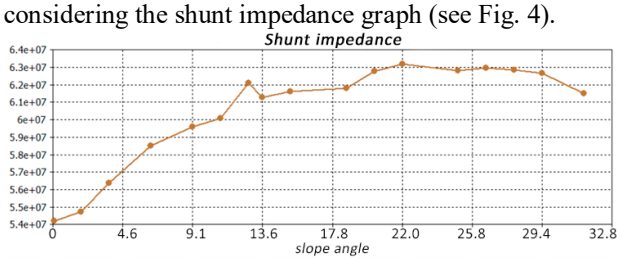


Figure 4: Shunt impedance dependence of the slope angle.

The maximum value of the shunt impedance corresponds to the slope angle of 22°.

## THRESHOLD VOLTAGE

The gap voltage [6] at which two-point multipacting of order n can occur can be calculated using expression (1).

$$V = Ed = \frac{d^2(2\pi f)^2 m}{(2n-1)\pi e}. \quad (1)$$

The results of the theoretical calculation of threshold voltage are summarized in Table 1.

Table 1: The Results of Theoretical Calculation of Threshold Voltage Levels

| | Short gap | Long gap |
|---|---|---|
| Working voltage, MV | 1.5 | 3.5 |
| Threshold voltage (structures without bevel), kV | 1.5 | 5.1 |
| Threshold voltage (structures with bevel), kV | 2.3 | 7.0 |

ISBN: 978-3-95450-240-0 ISSN: 2673-5539 doi:10.18429/JACoW-RuPAC2021-WEPSC04

# ACCELERATING STRUCTURE OF 8 MeV ELECTRON LINAC

A.N. Shein, A.V. Telnov, I.V. Shorikov, RFNC-VNIIEF, Sarov, Russia

*Abstract*

The paper presents results of three-dimensional electrodynamic calculations of an accelerating section of a resonance electron linear accelerator and input and output matching devices (couplers), as well as its electron dynamics calculation.

## INTRODUCTION

Since 1994 a linear electron resonance accelerator LU-10-20 [1], meant for radiation materials processing and radiation processes study has been functioning in RFNC-VNIIEF. Accelerated electron energy – up to 10 MeV, beam average power – up to 12 kW. This accelerator has demonstrated its urgency when conducting radiation studies and tests.

Today modernization of LU-10-20 accelerator, involving an accelerating section and RF power systems, is being conducted. An accelerating section is meant for electron beam acceleration up to nominal energy and represents a complex resonance traveling wave RF structure, consisting of a disk-loaded waveguide and input and output couplers.

## ACCELERATING STRUCTURE TYPE

A basic element for any accelerator is a microwave oscillator. To modernize LU-10-20, MI-470 pulsed magnetron manufactured by corporation Scientific Production Enterprise «Toriy» (Moscow) was chosen. Magnetron MI-470 supplies output pulsed power 10 MW with pulse duration from 3 up to 10 μs. Magnetron operation frequency range – (1883÷1889) MHz.

As an accelerating section for LU-10-20 modernization there was chosen structure based on disk-loaded waveguide (DLW) with variable geometry, operating on the traveling wave with mode 2π/3, similar to LU-10-20 current section. Operating frequency of accelerating structure at mode 2π/3 – 1886 MHz. Main arguments for selecting such a structure is experience availability for development and operation of linear accelerators with DLW, simplicity and cheapness of manufacture, availability of aperture for electron beam of larger diameter and simpler feed circuit as compared to structures on standing wave. Using reference data [2] there was determined preliminary geometry of the given accelerating structure, consisting of 10 cells buncher and 32 regular accelerating cells, and electron dynamics calculations were performed in one-particle approximation [3].

## CELL GEOMETRY OPTIMIZATION

A purely experimental way for size fitting of accelerating cells from initial approximation to more precise ones represents a long process and is rather a labor-intensive occupation. At that during adjustment each cell undergoes processing on the turner not less than 3..5 times, what inevitably results in degradation of accelerating cell pure working surface. In order to reduce the number of adjustment cycle or to exclude process at all, the accelerating cells preliminary geometry was refined in resonance mock-up model.

To determine resonance frequencies, corresponding to definite oscillation modes, and the following calculated cells geometry adjustment to working frequency, the resonance mock-up electrodynamic model (Fig. 1) was developed. The resonance mock-up uses a property of periodic structures – availability of reflection symmetry planes, perpendicular to translation axis. For the disk-loaded waveguide one of reflection symmetry planes is placed symmetrically to adjacent diaphragms.

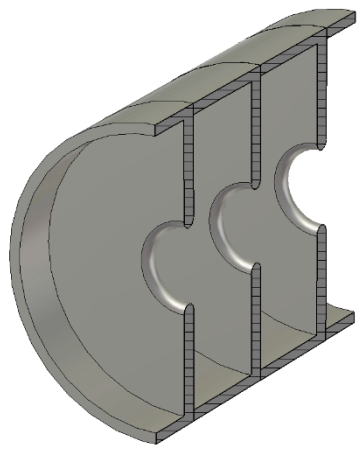

Figure 1: Resonance mock-up model.

In the resonator like that in Fig. 1, consisting of 4 cells, 4 modes become excited. Resonance frequency of the given model on 2π/3 mode was adjusted to the operating frequency 1886 MHz in the frequency band ±40 kHz by changing cell inner diameters (diameter change by 0.01 mm brings to frequency change by 52 kHz). After satisfactory result was achieved one of cells was replaced, and cell adjustments was not continued till all 42 cells were adjusted. Geometry optimization results are given in Fig.2.

ISBN: 978-3-95450-240-0 ISSN: 2673-5539 doi:10.18429/JACoW-RuPAC2021-WEPSC05

# MODELING OF THE ENERGY COMPRESSION SYSTEM SLED FOR THE LINAC-200 ACCELERATOR

K. Yunenko, M. Gostkin, V. Kobets, A. Zhemchugov, JINR, Moscow Region, Dubna, Russia

*Abstract*

This paper is devoted to the research of the possibility of increasing the output energy of an electron beam at the LINAC-200 linear accelerator by using the SLED (Stanford Linac Energy Doubler) [1] energy compression system with constant parameters of the storage cavities [2].

In order to select the necessary parameters and characteristics for the successful creation of this system on the accelerator, the SLED system (Fig. 1) structure simulation and the characteristics of cylindrical hollow resonators [3] calculation were conducted using the CST MICROWAVE STUDIO program [4].

## INTRODUCTION

The LINAC-200 linear electron accelerator operating at a frequency of 2856 MHz can currently increase the energy of particles to 200 MeV. We continue to build up energy by installing accelerating sections, which according to plans can raise energies up to 800 MeV. However, further increasing the size of the accelerator is difficult, so other approaches have been explored.

Figure 1: SLED energy compression system design from IREN (JINR, LNP).

An energy compression system can be used to increase the energy of an electron beam in a linear accelerator without increasing the size of the installation. In our case, the power multiplication system SLED was chosen [2]. This system consists of several components shown in Fig. 2.

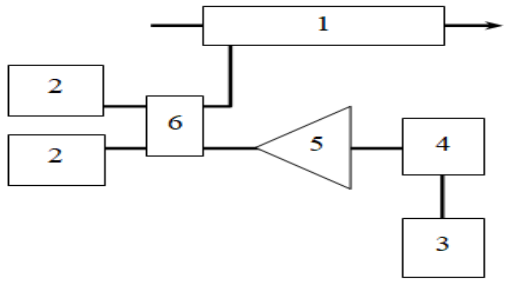


Figure 2: Block diagram of LINAC with an energy compression system SLED (1 - accelerating section, 2 - storage resonators, 3 - master oscillator, 4 - high-speed phase shifter, 5 - power amplifier, 6 - high frequency bridge).

To analyze the structure and obtain results, it is sufficient to consider the process of excitation of a single cavity [1].

## PARAMETER ESTIMATION AND CAVITY MODELING IN THE ENERGY COMPRESSION SYSTEM SLED

Pulsed klystrons of the 10 centimeter range are used as microwave power amplifiers, the operating frequency of which corresponds to 2856 MHz. Information on klystrons is specified in the Table 1.

Table 1: Parameters of Klystrons

| Type | TH 2129 |
|---|---|
| Company manufacturer | TTE (Thomson Tube Electronics) |
| Peak power: | |
| input, W | 100 |
| output, MW | 20 |
| Average power: | |
| input, W | 0.7 |
| output, kW | 20 |
| Pulse duration, μs | 4 |
| Frequency of repetition (max), Hz | 500 |

There are 2 types of accelerating sections: short and long (Fig. 3). They have the characteristics specified in the Table 2.

ISBN: 978-3-95450-240-0 ISSN: 2673-5539 doi:10.18429/JACoW-RuPAC2021-WEPSC06

# ASESS INPUT DATA UNCERTAINTIES IN THERMAL-MECHANICAL CALCULATIONS OF THE OUTLET WINDOW MEMBRANE OF THE LUE-200 ACCELERATOR

I. V. Burkov, A. P. Sumbaev, JINR, Dubna, Russia

*Abstract*

The maximum values of the temperature fields and stress-strain state are calculated for various configurations of the outlet window membrane of the LUE-200 accelerator with assessing uncertainties in input data. The thermo-mechanical parameters are estimated by simulating the electron beam pulsed action mode on the membrane in the computational models based on the mathematical description of the most significant physical processes. The obtained numerical modelling results demonstrated the importance of assessing uncertainties in input data for substantiating the safe operation limits of IREN facility.

## INTRODUCTION

The paper clarifies the previously obtained estimates by reducing the error influence in the calculation results, due to the assumptions and approximations adopted in [1], as well as the uncertainty and formalism when specifying the initial data. A change in the approaches in combination with the development of the initial data processing methods are capable of giving a more detailed description of physical processes and contribute to the further improvement of the membrane assembly design [2, 3].

## MODEL DESCRIPTION

A thermomechanical problem is focused on evaluating the temperatures field and stress-strain state (SSS) arising on the membrane during the installation operation. The solution of a problem was performed by the method of running finite difference equations reduced to the standard three-diagonal form. The mathematical formulation of the heat conduction problem [4, 5] and the elasticity theory [4, 5, 6] have the following form:

$$\rho \cdot c \cdot \frac{\partial T}{\partial t} = LT + E(E_e, r, h) \cdot I(\tau), \quad (1)$$

$$\rho \frac{\partial^2 U}{\partial t^2} = LU + P + \alpha_{ex} \cdot (3k + 2\mu) \cdot grad\ \theta, \quad (2)$$

where: $T$ is the temperature; $U$ is a deformation; $\rho$ is the density; $L$ is a differentiating operator; $E$ is energy deposition; $I$ is beam current; $\tau$ is pulse duration; $k$ and $\mu$ are the Lamé constants; $\alpha_{ex}$ is the coefficient of linear thermal expansion of the medium; $\theta = T\text{-}T_0$ – temperature deviation; $P$ is the applied force.

A. A. Samarskii's discretization scheme [4] is used to solve the heat conduction problem. It is stable and has the total approximation property.

Obtained from the measurements of the Rogowski belt beam current the experimental data ($I(\tau)$ diagrams), the normalized distribution of the energy release in the membrane, taking into account the distribution of the current density over the beam cross section [1], the thermos-physical characteristics of structural materials, and the environmental parameters are used as the initial data for calculating the SSS and temperature fields.

### *Estimation of the Properties*

Based on the calculation model work results an assessment of the impulse characteristics of the thermos-mechanical operating mode of the outlet window membrane became available. Let's consider a mode of operation with a limited power level and carry out the necessary calculations. The current IREN facility parameters by neutron yield determine the average electron beam power $P_{av} \sim 1.1$ kW at a pulse duration of $\tau = 250$ ns, the beam current in the pulse $I = 0.63$ A, the electron energy in the beam at the level of $E = 70$ MeV, and the pulse repetition rate $f = 100$ Hz. Single pulse simulation (Fig. 1) was carried out in order to verify the correct operation and applicability of the developed computational model for assessing the thermal-mechanical characteristics of the membrane in a pulsed mode. In that case, the calculation model of the membrane experiences a single pulse action of an electron beam, described by the course of the averaged interpolated curve. The membrane, being previously in a cold state at room temperature, starts to warm up in proportion to the transmitted by the beam power. The cooling rate of the membrane heated after the pulse depends on the membrane material thermal inertia, which is a function of convective heat transfer and thermal conductivity.

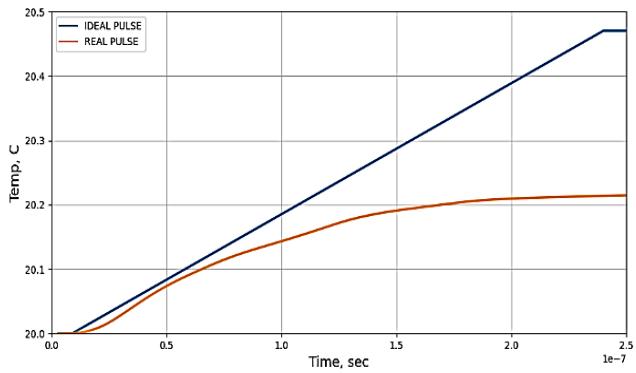


Figure 1: Single pulse.

The subsequent simulation of the installation pulsed operation mode is similar to a single pulse simulation, which is sequentially included in the time series of events $f$ (frequency) times. The steady-state thermo-mechanical characteristics of the membrane for the selected operating mode are shown in Fig. 2 and Fig. 3.

ISBN: 978-3-95450-240-0 ISSN: 2673-5539 doi:10.18429/JACoW-RuPAC2021-WEPSC07

# MEDIUM ENERGY IONS TRANSPORT CHANNEL FOR A PULSED LINEAR ACCELERATOR

V. S. Dyubkov†, National Research Nuclear University MEPhI, Moscow, Russia

*Abstract*

For a transportation and matching proton and light ion beams (the maximal value A/Z is about 3.2) between RFQ and groups of IH-cavities it is suggested medium energy ions transfer line. That line should provide 100% beam transmission under negligible beam envelope increase and small longitudinal beam size growth during particle transport. MEBT consists of two parts. One of them provides ion transfer with energy of 820 keV/u and the second one provides ion transfer with energy of 2.46 MeV/u.

## INTRODUCTION

New linear injector of proton and light ion beams is under design at NRNU MEPhI [1]. This injector will accelerate protons and ions up to oxygen to an energy of 7.5 MeV/nucleon with mass-to charge ratio $A/Z < 3.5$. The main part of linear injector are RFQ linac and two groups of short 5-gaps IH-cavities independently powered. Beams transfer from RFQ linac to the first set of IH-cavities will be done with the help of medium energy beam transport line (MEBT-1). Beams transfer between the first and the second set of IH-cavities will be done by means of MEBT-2. For both transfer lines it is considered to use beam bunchers to control the bunch length and to chop the bunch tails.

## MEBT-1 DESIGN

In order to transfer beams of particles from RFQ linac output to the entrance of the first set of IH-cavities MEBT-1 will be used. The suggested layout of the MEBT-1 is shown in Fig. 1. It consists of two quadruple doublets and two quads [2] and its total length is 3.62 m. *B*-field components at the center of the quadruple lens are shown in Fig. 2. Magnetic field distribution in the cross-section of the quad at its center is presented in Fig. 3. Quad gradients for ion beam with $A/Z = 3.2$ are presented in Table 1.

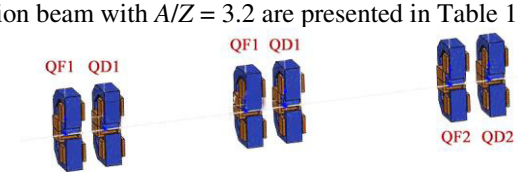


Figure 1: Layout of MEBT-1 line.

Table 1: Quad Parameters

| Name | *G*, T/m | *L*, cm |
|---|---|---|
| QF1 | 7.3 | 10 |
| QD1 | -7.3 | 10 |
| QF2 | 9.0 | 10 |
| QD2 | −11.3 | 10 |

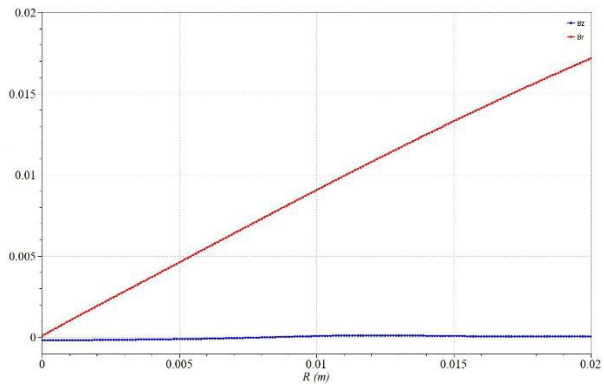


Figure 2: $B_z$ (blue) & $B_r$ (red) field components.

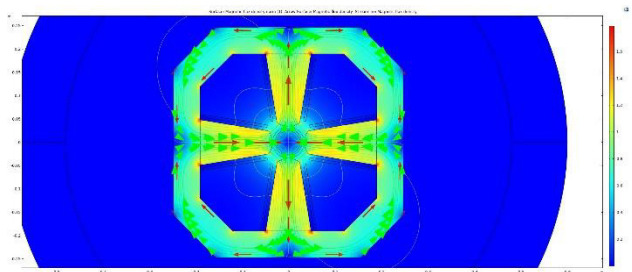

Figure 3: Quad cross-section & B-field distribution. Courtesy to I. Yurin [3].

Also it is supposed that beam buncher will be located in the drift space between doublets. Typical view of that buncher, designed by M. Gusarova, is shown Fig. 4.

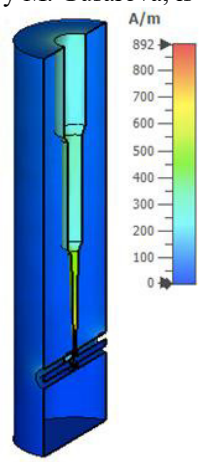


Figure 4: Buncher for MEBT-1.

Self-consistent ion beam dynamics simulation in the calculated 3D fields of MEBT-1 line was carried out by means

† vsdyubkov@mephi.ru

ISBN: 978-3-95450-240-0 ISSN: 2673-5539 doi:10.18429/JACoW-RuPAC2021-WEPSC08

# VACUUM CONDITION SIMULATIONS FOR VACUUM CHAMBERS OF SYNCHROTRON RADIATION SOURCE

S. M. Polozov[1], V. S. Dyubkov[1], V. L. Shatokhin[1], A. S. Panishev, National Research Nuclear University MEPhI (Moscow Engineering Physics Institute), Moscow, Russia
[1]also at National Research Center «Kurchatov Institute», Moscow, Russia

*Abstract*

Analysis of gas loads for the vacuum system chambers of the 6GeV synchrotron radiation (SR) source are carried out. The main source of gas loads is the photostimulated desorption induced by SR. The influence of storage ring lattice, geometric dimensions and beam parameters on the vacuum conditions in SR-source prototype chambers is studied. The geometric model of the storage ring chamber designed for simulation is considered. The simulation of the radiation flux parameters generated by the charged particles passing through the section of the vacuum chamber has been performed. The technique of calculating the parameters of SR and photostimulated desorption by means of Synrad+ and Molflow+ codes is applied.

## MODELING METHODS

During the operation of the SR-source, an intense flux of photon radiation is generated inside the storage ring. Most of this radiation will fall on the inner surface of the vacuum chambers, which leads both to an increase in thermal loads and to the appearance of synchrotron-stimulated desorption. In order to reduce the negative effects of incident radiation, special absorbers are installed in places with a high radiation load. The main part of the heat load is removed with their aid. They are made from a copper alloy (for example CuCrZr) and water cooling is provided in their design. With the change in the parameters and the storage ring geometry, the characteristics of the radiation flux density distribution in separate sections of the vacuum chambers will also change. The parameters of the vacuum system and absorbers must be calculated for these changes.

It is necessary to determine the relationship of changes in SR parameters with new requirements for radiation absorbers. Approaches to determining the characteristics of the radiation flux in the storage ring of the SR-source are considered. For this aim the capabilities of the SynRad + software module and its joint use with the Molflow + package for numerical simulation of accelerator complexes vacuum systems were studied [1].

Synrad+ [2] is a program for determining the parameters of the SR incident on the chambers walls (radiation flux, power, spectrum) by the Monte Carlo method. It calculates the power distribution of the synchrotron radiation incident on the surface. The use of this program in one package with Molflow+ makes it possible to calculate the desorption gas flow from the inner surface of the chambers by SR distribution. Thus, it is possible to determine the effect of changes in the storage ring geometry and optical system parameters on the vacuum level.

## VACUUM SYSTEM

ESRF-EBS research accelerator complex, 4th generation synchrotron radiation source was taken as a prototype of the designed SR-source - Ultimate Source for Synchrotron Radiation (USSR, formerly known as “SSRS-4”).

Improvement of the developed SR source parameters, such as high spatial coherence and brightness, required changes in the magnetic system of the facility. This, in turn, led to a change in the lengths of individual sections of the storage ring and vacuum chambers. The structure of the projected SR-source vacuum system was designed. The storage ring perimeter includes identical standard cell sections with identical vacuum chambers (see Fig. 1).

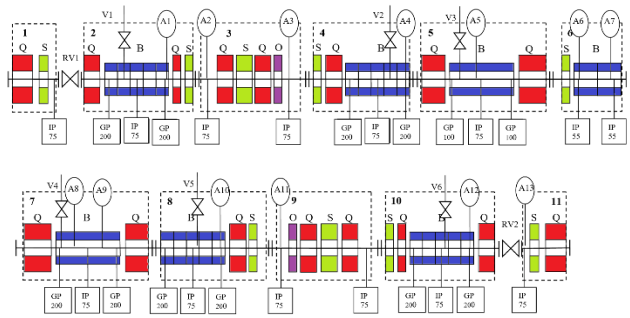

Figure 1: Standard cell: vacuum chambers 1-11, vacuum pumps IP and GP, absorbers A1-13.

Taking into account the change in the geometric parameters of the storage ring, the pressure profiles on the beam axis were modelled (see Fig. 2). There is an insignificant increase in pressure in the region of the chambers length increasing. This is due to an increase in the chambers walls surface area and a slight increase in the total thermal outgassing.

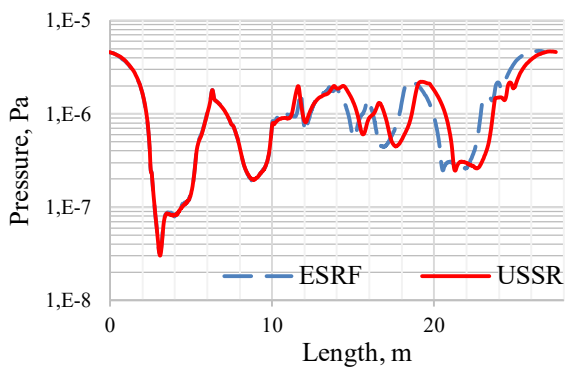


Figure 2: Influence of geometry changes.

ISBN: 978-3-95450-240-0 ISSN: 2673-5539 doi:10.18429/JACoW-RuPAC2021-WEPSC10

# OPTIMIZATION OF ACCELERATORS VACUUM STRUCTURES PUMPING

S. M. Polozov, A. S. Panishev, V. L. Shatokhin, National Research Nuclear University MEPhI (Moscow Engineering Physics Institute), Moscow, Russia

*Abstract*

The pumping features for the complex parts of the accelerator vacuum system are modelled to growth the efficiency of vacuum pumping. The vacuum system of a 7.5 MeV/nucleon proton and light ion (A/Z<3.2) accelerator-injector was considered. The Monte Carlo method is suitable for molecular flow modelling in high vacuum. The Molflow+ program was used for this aim. The pressure distribution simulation over the RFQ, IH resonators chambers volume, connecting vacuum pipes and extended vacuum tracts is carried out. The influence of parameters of individual structural elements changes was investigated to define the vacuum conditions inside the accelerators vacuum chambers. The vacuum system configuration and parameters are selected basing on these results to obtain the required vacuum level.

## VACUUM SYSTEM FEATURES

Molflow+ software package is used to determine the parameters of the linear accelerator vacuum equipment. This is a Monte Carlo simulator intended to calculate pressure profiles and conductance in ultra-high vacuum [1].

To determine the characteristics of the vacuum it is necessary to specify the geometry of the internal vacuum surfaces, gas loads and the parameters of the pumping equipment in the simulation model.

The vacuum requirements are determined by the allowable degree of the beam destruction via capture and loss of electrons, nuclear reactions, Coulomb scattering due to the interaction with residual gas. Based on the loss evaluation the pressure along the channel, providing a stable ion beam passing through the structure should be of the order of $10^{-5}$ Pa. At this pressure the molecules will move independently of each other and the simulation of these conditions by the statistical tests method is possible.

In stationary conditions, the molecules desorption from the vacuum chambers walls is the main source of pumping gas loads. The value of thermal outgassing is chosen $10^{-6}$ Pa·m$^3$/s·m$^2$, which is typical for the initial level of vacuum constructional materials outgassing.

The sections of the linear accelerator structure are independent vacuum systems separated by insulating vacuum gates. This includes ion sources, RFQ section, beam transport sections at low energy LEBT, medium MEBT1, 2 and high HEBT, H-type resonator sections IH1, 2 (see Fig. 1).

## VACUUM PORT

The vacuum pumps are connected to the resonator chambers using vacuum ports (see Fig. 2).

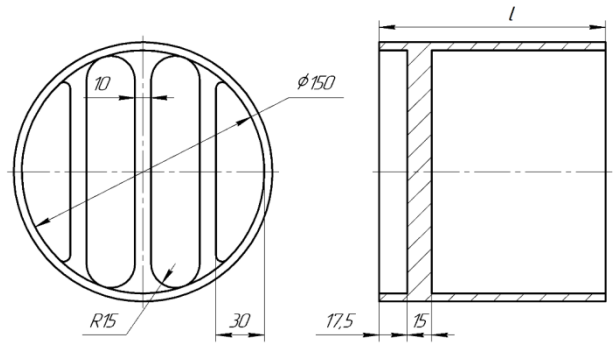


Figure 2: Vacuum port diagram.

Grilles are installed in ports to limit the penetration of microwave power outside the resonator chamber. Vacuum valves are also attached. These construction features affect the vacuum conductivity and reduce the efficient pumping speed. Their conductivity was modelled in the operating mode. The conductivity of the DN 150 port with RF grill according to the simulation results is shown in Table 1.

Table 1: Port conductivity Values

| Port height *l* | Conductivity |
|---|---|
| 55 mm | 1050 l/s |
| 75 mm | 990 l/s |
| 100 mm | 911 l/s |

## RFQ CHAMBER

The model of the RFQ resonator vacuum chamber was used to calculate the pressure distribution along the beam axis and over the volume of the resonator chamber. Vacuum surface model for Molflow+ created from CAD 3D model of the resonator chamber with internal electrodes, plungers, vacuum and RF ports (see Fig. 3).


Figure 1: Block diagram of linear accelerator sections.

ISBN: 978-3-95450-240-0 ISSN: 2673-5539 doi:10.18429/JACoW-RuPAC2021-WEPSC12

# PRELIMINARY CALCULATION OF THE POWER COUPLER FOR THE SYLA STORAGE RING RF CAVITY

S. V. Matsievskiy*, M. A. Gusarova, M. V. Lalayan, Ya. V. Shashkov
NRNU MEPhI, Moscow, Russia and NRC KI, Moscow, Russia

*Abstract*

Several new accelerator facilities will be built in Russia in the next few years. One of those facilities is a 6 GeV storage ring light source, the Ultimate Source of Synchrotron Radiation to be built in Protvino, near Moscow.

This paper considers storage ring RF cavity power coupler design issues and provides preliminary calculations of the device.

## INTRODUCTION

6 GeV Ultimate Source of Synchrotron Radiation is planned to be built in Protvino, Russia. Storage ring scheme is based on the ESRF-EBS design [1]. Thus, many design patterns are copied from the aforementioned project, including the RF system, consisting of a number of a mono-cell normally conducting HOM-damped cavities (HOM mitigation is discussed in other paper in this conference) [2].

Cavity properties are presented in Table 1. Continuations were carried out for the accelerating voltage value for all cavities $V_{cav\ all} = 3$ MV.

Table 1: RF Cavity Properties

| Property | Value |
|---|---|
| f, MHz | 357 |
| Q, $\times 10^3$ | 41 |
| $R_{sh\ eff}$, MΩ | 10 |
| $W_{rad}$, MeV turn$^{-1}$ | 3 |
| $I_{beam}$, A | 0.25 |

## POWER COUPLER

RF cavity with the attached magnetic loop is presented in Fig. 1.

Calculation of the generator power $P_g$ and coupling coefficient $\beta$ was done by using conventional equations for cavity voltage [3]

$$V_{cav} = \frac{2\sqrt{P_g}\sqrt{R_{sh\ eff}}\sqrt{\beta}\left(-\frac{I_{beam}\sqrt{R_{sh\ eff}}}{2\sqrt{P_g}\sqrt{\beta}}+1\right)}{\beta+1} \quad (1)$$

and optimal coupling [4]

$$\beta = \left(\frac{I_{beam}\sqrt{R_{sh\ eff}}}{2\sqrt{P_g}} + \sqrt{\frac{I_{beam}^2 R_{sh\ eff}}{4P_g}+1}\right)^2. \quad (2)$$

* svmatsiyevskij@mephi.ru

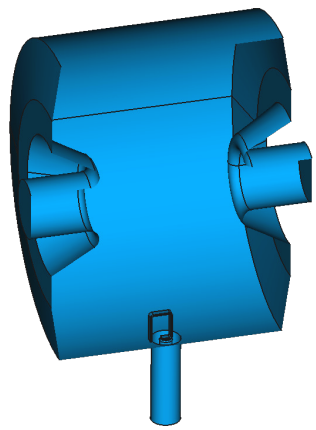

Figure 1: RF cavity with coupling loop.

Substituting Eq. (2) into (1) yields a simple equation for the optimally coupled cavity supply power

$$P_g = \frac{V_{cav}\left(I_{beam}R_{sh\ eff} + V_{cav}\right)}{R_{sh\ eff}}. \quad (3)$$

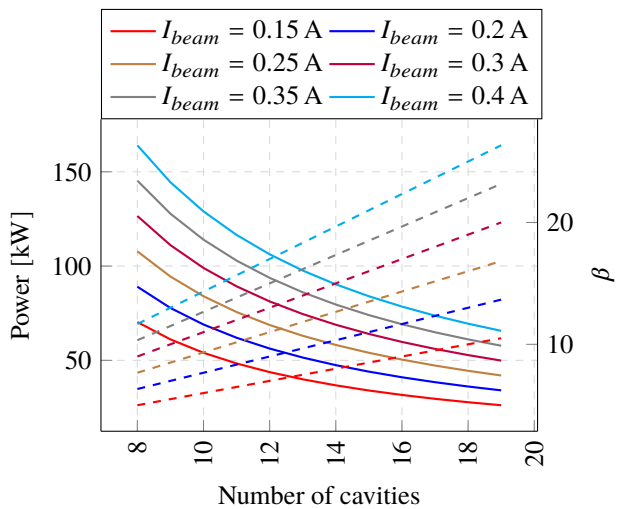


Figure 2: Optimal supply power (solid lines) and coupling coefficient (dashed lines) for different number of cavities.

Equation (3) was used in calculation of Fig. 2. For the operation under 100 kW number of cavities should be greater then 9. Considering a possible cavity failure and operation under higher current a number of cavities in the ring was chosen $N = 14$. Further calculations were done for the constant coupling coefficient value $\beta$ corresponding to the beam current $I_{beam} = 0.25$ A.

ISBN: 978-3-95450-240-0 ISSN: 2673-5539 doi:10.18429/JACoW-RuPAC2021-WEPSC13

# ACCELERATING CAVITIES WITH HOM DAMPING FOR USSR-4 STORAGE RING

N.Yu. Samarokov, Ya.V. Shashkov[1†], M.V. Lalayan[1], M.A. Gusarova[1],
NRNU MEPhI, Moscow, Russia,
[1]also at NRC KI, Moscow, Russia

*Abstract*

Preliminary results on accelerating cavities for USSR-4 facility (also known as SYLA - SYnchrotron and free-electron LAser) project are presented. This facility is under development by collaboration hosted by National Research Center "Kurchatov Institute". SYLA is synchrotron radiation facility based on injector linac and 6 GeV storage ring. Beam energy loss in storage ring is to be compensated by several modified pillbox cavities. Cavity geometry features, its operation frequency choice and induced HOM parameters are discussed. HOM damping technique using corrugated cylindrical waveguides were studied. Longitudinal impedance values of HOM are presented for initial accelerating cavity and structure with waveguides.

## INTRODUCTION

6 GeV Ultimate Source of Synchrotron Radiation is planned to be built in Russia. Storage ring scheme is based on the ESRF-EBS design [1-3]. For sources of synchrotron radiation, large values of beam currents are required. Excitation of Higher order modes (HOM) can lead to multibunch instabilities, emittance growth, beam breakup, etc. [4,5].

The general view of the accelerating cavity with an operating frequency of 357 MHz is shown in Fig. 1.

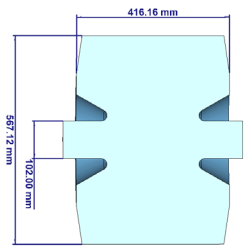


Figure 1: General view of an accelerating cavity at 357 MHz.

For an accelerating cavity the electrodynamic characteristics (EDC) [6] of the fundamental mode (Table 1) and HOM were carried out [7].

Table 1: EDC of Accelerating Cavity

| EDC | Values |
|---|---|
| *f*, MHz | 357 |
| Q, $\times 10^3$ | 41 |
| $R_{sh\ eff}$, MΩ | 10 |

The frequency dependence of the longitudinal shunt impedance for monopole HOMs is shown in Fig. 2.

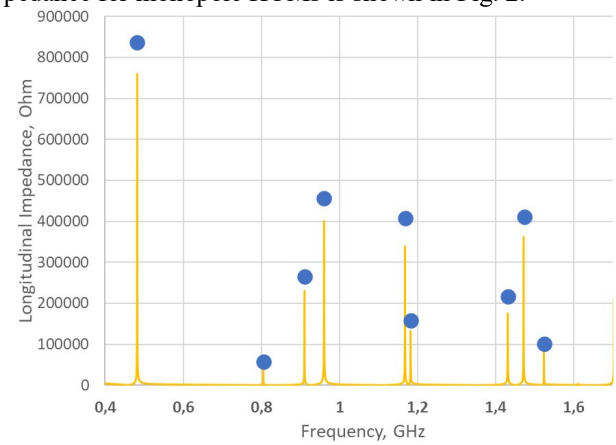


Figure 2: Frequency dependence of the longitudinal shunt impedance for monopole modes for an accelerating cavity at 357 MHz. Graph – result of wakefield simulations, dots – results of eigenmode simulations.

From Fig. 2 one could see that that the shunt impedance of parasitic HOMs accelerating cavity can reach values of up to $10^6$ Ohm.

One of the requirements for EBS-ESRF cavity design was to ensure unconditional beam stability up to currents of 1000 mA. For EBS-ESRF longitudinal coupled bunch instability threshold at 200 mA is $R_{HOM} \cdot f_{HOM} = 16$ kW·GHz (Fig. 3) [4].

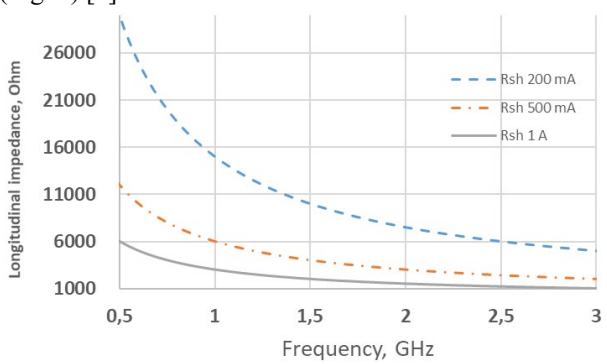


Figure 3: Threshold for longitudinal impedance necessary for unconditional beam stability for 200, 500 and 1000 mA beam current.

From Fig. 2 and 3 we can see that it is necessary to significantly decrease the shunt impedance values of HOMs. To reduce these values, it is proposed to add HOM couplers to the system.

† yvshashkov@mephi.ru

ISBN: 978-3-95450-240-0 ISSN: 2673-5539 doi:10.18429/JACoW-RuPAC2021-WEPSC14

# BOOSTER RF SYSTEM FIRST BEAM TESTS

A.Yu. Grebentsov, O.I. Brovko, A.V. Butenko, V.A. Gerklotts, A.M. Malyshev, V.D. Petrov, O.V. Prozorov, E. Syresin, A.A. Volodin JINR, Dubna, Russia
A.M. Batrakov, S.A. Krutikhin, G.Y. Kurkin, V.M. Petrov, A.M. Pilan[2], E. Rotov[1], A.G. Tribendis[2], Budker INP, Novosibirsk, Russia
G.A. Fatkin[1], Cosylab Siberia, Novosibirsk, Russia
[1]also at Novosibirsk State University, Novosibirsk, Russia
[2]also at Novosibirsk State Technical University, Novosibirsk, Russia

*Abstract*

The project NICA is being constructed in JINR, to provide collisions of heavy ion beams in the energy range from 1 to 4.5 GeV/u at the luminosity level of $1 \cdot 10^{27}$ $cm^{-2} \cdot s^{-1}$.

A key element in the collider injection chain is the Booster a cycling accelerator of ions $^{197}Au^{31+}$. The injection energy of particles is 3.2 MeV/u, extraction energy is 600MeV/u.

Two Booster RF stations provide 10 kV of acceleration voltage. The frequency range from 587 kHz to 2526 kHz at the operation of the stations in the injector chain.

The RF stations were fabricated in the Budker Institute of Nuclear Physics. The main design features and parameters of the first beam tests of the Booster RF system are discussed in this paper.

## RF SYSTEM

The RF System for Booster consists of two resonators, power amplification cascades, and low-voltage electronic, intellectual controller, and tester module. Main parameters of the RF cavity is presented in Table 1.

Acceleration of particles in the Booster will be made in two stages. The operational frequency range corresponds to 0.5 - 2.5 MHz.

The accelerating cavity is formed by two parts of the short-circuited coaxial lines divided by the accelerating gap (Fig. 1). A vacuum-tight ceramic insulator 6 is installed in the gap. Only the stainless-steel beam pipe and the gap ceramic are under vacuum, the remaining cavity is operated in the air [1].

Table 1: Main Parameters of the RF Cavity

| Parameter | Value |
|---|---|
| Frequency range, MHz | 0.5 – 5.5 |
| Gap voltage, kV | 5.0 |
| Beam pipe diameter, mm | 160 |
| Residual gas pressure, Torr | $< 5.5 \cdot 10^{-11}$ |
| Outside station diameter, m | 1.2 |
| Installation length, m | 1.4 |
| Real part of conductance at the cavity gap, Ohm | > 1000 |

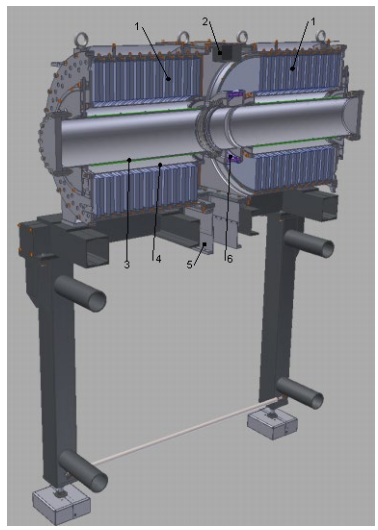


Figure 1: Accelerating cavity of RF station. 1. Amorphous alloy rings, 2. Gap voltage pickup, 3. Beam pipe, 4. Coaxial inner conductor, 5. Connecting nipple, 6. Ceramic insulator.

## RF POWER AMPLIFIER

The output stage of the power amplifier employs two tetrodes GU-36B-1. The tubes are driven in the push-pull mode in the common cathodes schematic. Air-cooling of the tubes is used.

The anodes of tubes are connected directly to an accelerating gap of the cavity through the blocking capacitors $C_b$ (Fig. 2).

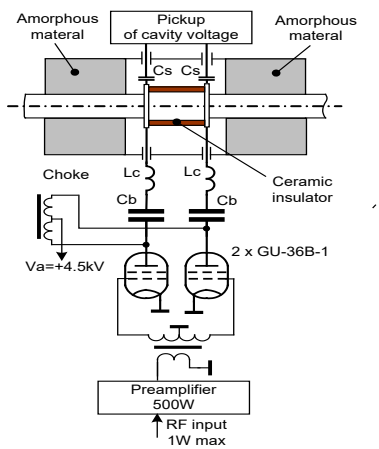


Figure 2: Block diagram of RF power amplifier.

ISBN: 978-3-95450-240-0 ISSN: 2673-5539 doi:10.18429/JACoW-RuPAC2021-WEPSC15

# BARRIER STATION RF1 OF THE NICA COLLIDER. DESIGN FEATURES AND INFLUENCE ON BEAM DYNAMICS

A.M. Malyshev, A.A. Krasnov, Ya.G. Kruchkov, S.A. Krutikhin, G.Y. Kurkin, A.Yu. Martynovsky, N.V. Mityanina[1], S.V. Motygin, A.A. Murasev[1], V.N. Osipov, V.M. Petrov, A.M. Pilan[2], E. Rotov[1], V.V. Tarnetsky[1], A.G. Tribendis[2], I.A. Zapryagaev[1], A.A. Zhukov, Budker INP, Novosibirsk, Russia
O.I. Brovko, I.N. Meshkov[3], E. M. Syresin, JINR, Dubna, Russia
[1]also at Novosibirsk State University, Novosibirsk, Russia
[2]also at Novosibirsk State Technical University, Novosibirsk, Russia
[3]also at Saint-Petersburg State University, Saint-Petersburg, Russia

*Abstract*

This paper reports on the design features and construction progress of the barrier bucket RF systems for the NICA collider being built at JINR, Dubna. Each of two collider rings has three RF systems named RF1 to 3. RF1 is a barrier bucket system used for particles capturing and accumulation during injection, RF2 and 3 are resonant systems operating at 22nd and 66th harmonics of the revolution frequency and used for the 22 bunches formation. The RF systems are designed by Budker INP. Both RF1 stations were manufactured, delivered to JINR and tested at the stand. The test results are presented in the article, as well as some results of calculating the effect of the RF1 system on the beam dynamics.

## INTRODUCTION

The Nuclotron based Ion Collider fAcility (NICA) [1], operating in its heavy ion collision mode is aimed at the experiments with colliding beams of $^{197}Au^{79+}$ ions at energies from 1 to 4.5 GeV/u per beam. Budker Institute of Nuclear Physics contributes to several parts of the project, including its RF systems – barrier bucket and harmonic. Barrier bucket system, RF1, is used to capture the particles injected from the Nuclotron and to accumulate the required number of ions. This is done using moving barriers technique. RF1 also can accelerate the accumulated beam if the injection energy is lower than that of the experiment. Harmonic systems, RF2 and 3, are used to form 22 bunches with required parameters. Each collider ring has one RF1 station, four RF2 and eight RF3 stations.

The RF1 system generates 2 pairs of ±5 kV pulses (accelerating and decelerating in each pair) at the bunch revolution frequency thus forming the two separatrices – injection and stack. A bunch from the Nuclotron is shot into the injection separatrix, moved and added to the stack by switching off the pulses separating the two separatrices and so merging the two bunches. If the combined bunch length exceeds the half-ring perimeter it is compressed by moving the barrier pulses. Ion accumulation process is accomplished by the electron cooling. The accumulated ions trapped between the two barrier pulses may be accelerated, if needed, by ±0.3 kV meander voltage generated by the RF1 as well [2].

## RF1 BARRIER BUCKET SYSTEM – INDUCTION ACCELERATOR

The barrier station is a coaxial line filled with 84XB-M grade amorphous iron rings. Pulse voltages generated by transistors operating in a switching mode are applied to the rings. These voltages are summed up at the accelerating gap of the station.

The station is cooled by water. There are channels for water flow between the rings of amorphous iron. Figure 1 shows the details of the RF1 station.

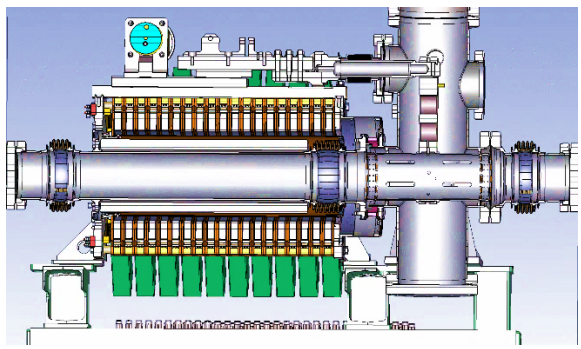

Figure 1: Details of the RF1 station.

To form the barrier voltage, 16 sections 6-20 are used, 3 accelerating sections 5-3, and one damping section.

At the moment when RF1 does not work, the accelerating gap is short-circuited by a contactor.

Figure 2 shows the appearance of the RF1 station.

Figure 2: Appearance of the RF1 station.

† alexmal94@mail.ru

ISBN: 978-3-95450-240-0 ISSN: 2673-5539 doi:10.18429/JACoW-RuPAC2021-WEPSC16

# NUMERICAL RESEARCH OF DESIGN SOLUTIONS FOR THE BENDING MAGNETS OF THE ELECTRON BEAM FACILITY GESA-1M

N. Kazachenko†, E. Gapionok, V. Kukhtin, I. Rodin, K. Tkachenko,
JSC "NIIEFA", St. Petersburg, Russia
D. Ovsyannikov, S. Sytchevsky, St.Petersburg State University, Russia

*Abstract*

Comparative simulations of magnet configurations have been performed searching for the optimum design of bending magnets for the intense pulsed electron beam facility GESA-1M. The beam trajectory through electric and magnetic fields was simulated for three candidate configurations of the bending magnets. A comparison was focused on the expected power density and divergence angle at the target. The most efficient concept was found to be two pairs of coils arranged orthogonally to each other. This configuration produces highly uniform distribution of the current density at the target, the divergence angle being as low as several degrees. An important advantage is that the initial beam power can be intensified by a 20% at the target.

## INTRODUCTION

GESA-1M is used for improvement of material surface properties and is capable to generate a 120 kV, 10 A/cm$^2$, 50 μs electron beam with the diameter of 10 cm. One of specific concerns is to prevent the beam path from micro-contaminations from the irradiated surface. To overcome this problem a system of bending magnets is used to guide and deflect particles. The best efficiency is observed when the electron beam is deposited normally to the surface, and a constant power density is kept across the beam spot. The study has been carried out for three candidate design options illustrated in Fig. 1.

## COMPUTATIONAL PROCEDURE

All electrons in a pulse were assumed to have the same energy of 120 keV. Each electron trajectory was taken tangentially to a field line at the starting point. The starting points were taken on a horizontal plane on the upper surface of the top coil at $Z = 42$ cm. The vertical electron momentum is directed opposite to the axis $Z$.

An electron moves according to the Newtonian equations of motion. Using the Gaussian system of units, the electron motion can be represented in a vector form as

$$\begin{cases} d\vec{p}/ds = \vec{E}'/\beta + [\vec{\beta}, \vec{H}']/\beta \\ d\vec{r}/ds = \vec{p}'/p' \end{cases}$$

Here $\vec{p} = \vec{\beta}/\sqrt{1-\beta^2}$ is the relativistic momentum, $\vec{\beta}$ is the electron velocity, $s$ is the trajectory length, $\vec{r}$ is the position vector, $\vec{E}' = e\vec{E}/E_0$ and $\vec{H}' = e\vec{H}/E_0$ are respective vectors of relative electric and magnetic field strength, $e$ is the electron charge, $E_0$ is the self-energy.

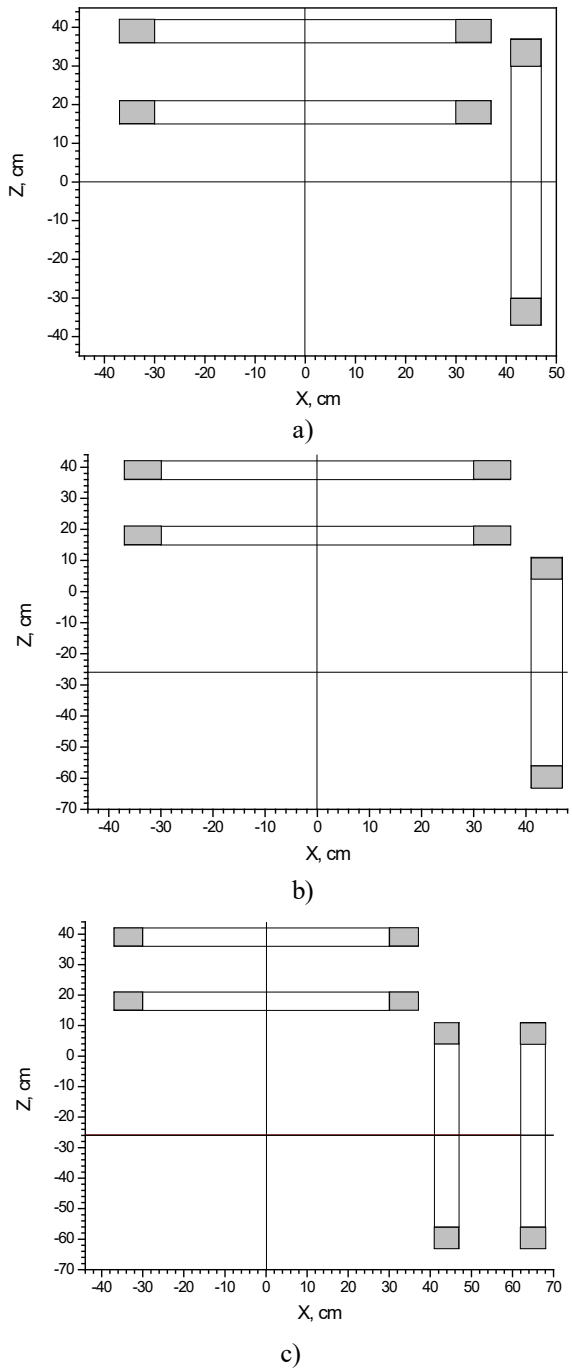


Figure 1: Bending magnet. a) Design option #1, b) Design option #2, c) Design option #3.

A space charge electric field was taken zero assuming magnetic field of the bending magnet is high enough to

† kazachenko-sci@yandex.ru

ISBN: 978-3-95450-240-0 ISSN: 2673-5539 doi:10.18429/JACoW-RuPAC2021-WEPSC17

# VIBRATING WIRE SYSTEM FOR FIDUCIALIZATION NICA BOOSTER SUPERCONDUCTING QUADRUPOLE MAGNETS

T. Parfylo, V. Borisov, M. Kashunin, H. Khodzhibagiyan, B. Kondratiev, S. Kostromin, V. Mykhailenko, M. Shandov
Joint Institute for Nuclear Research, Dubna, Russia

*Abstract*

The NICA (Nuclotron-based Ion Collider fAcility) is a new accelerator complex under construction at the Laboratory of High Energy Physics (LHEP) JINR. The facility includes two injector chains, two existing superconducting synchrotrons Nuclotron and a new Booster, under construction superconducting Collider, consisting of two rings. The lattice of the Booster includes 48 superconducting quadrupole magnets that combined in doublets. Each doublet must be fiducialized to the calculated trajectory of the beam. Alignment of the magnetic axis is necessary for properly install the magnets at the beam trajectory. The vibrating wire technique was applied to obtain the the magnetic axis position of quadrupoles. A new measurement system has been worked out and produced at the LHEP. The magnetic axis positions of the quadrupole doublets are determined at the ambient temperature. The paper describes design of the measurement system, measuring procedure and results of the magnetic axis position measurements.

## INTRODUCTION

The NICA (Nuclotron-based Ion Collider fAcility) is a new accelerator complex under construction at the Laboratory of High Energy Physics (LHEP) JINR [1]. The facility includes two injector chains, two existing superconducting synchrotrons Nuclotron and a new Booster, under construction superconducting Collider consisting of two rings. The Booster have been put into operation at 2020. Main goals of the Booster are accumulation of $2 \times 10^9$ $Au^{31+}$ ions acceleration of the heavy ions up to energy required for effective stripping; forming of the required beam emittance with electron cooling system. It has 210.96 m circumference and includes 48 superconducting quadrupole magnets that combined in doublets. All superconducting magnets for the NICA Booster have been assembled and tested at the test facility at the Laboratory of High Energy Physics. According to the technical specifications [2], the magnetic axis position must be measured with an accuracy less than 0.1 mm.

The vibrating wire technique was applied to achieve the precision of measuring the magnetic axis position. The vibrating wire technique based on Lorentz forces between alternating current flowing through the taut wire and transverse magnetic field excite the mechanical wire vibrations. If the frequency of driving current is close to one of the wire resonance frequencies the effect will be especially strong. The wire position can be obtained by moving the wire across the magnet aperture and measuring the wire vibrating amplitude [3, 4].

## DOUBLET OF QUADRUPOLE MAGNETS

The Booster quadrupole magnets are Nuclotron-type include cold iron yoke with hyperbolic poles, shaped the magnetic field and a coil made of a hollow superconductor. The doublet of quadrupole magnets is a single rigid mechanical construction of about 1.8 m length. It's consists of defocusing and focusing quadrupoles, cylinder for rigid mounting magnets with each other, as well as two beam position monitors within cylinder. The doublet has a removable design that allows splitting it into two parts for assembly-disassembly halves of yoke and coil [5].

The main parameters of the NICA Booster quadrupole magnets are shown in Table 1.

Table 1: The Main Parameters of the NICA Booster quadrupole Magnets

| Parameter | Unit | Value |
|---|---|---|
| Number of magnets | pieces | 48 |
| Maximum field gradient | T/m | 21.5 |
| Effective magnetic length | m | 0.47 |
| Field error at R = 30 mm | | $6 \times 10^{-4}$ |
| Beam pipe aperture (h/v) | mm | 128/65 |
| Pole radius | mm | 47.5 |
| Yoke width/height | m | 0.226 |
| Weight | kg | 110 |

## VIBRATING WIRE SYSTEM

The NICA Booster Vibrating Wire measurement system has been designed, produced and commissioned at the LHEP. The copper-beryllium wire 0.125 mm diameter and length about 5.3 m stretched through the mechanical center of the doublet aperture (see Fig. 1: 2 – defocusing, 3 – focusing magnets) and supported by two stages A and B (4 and 5). Each of them has horizontal and vertical Physik Instrumente linear stages 404.2PD to moving wire (1) across the aperture. The doublet and stages are installed on the balk 6 m along. The geometrical centers of defocusing and focusing magnets are placed at the 3/8 $L_w$ and 5/8 $L_w$, where $L_w$ – wire length. The wire is fixed on stages and stretched by 0.8 kg weight. Digital wave form generator Keithley 6221 was used to drive alternating current through the wire. Two orthogonal Sharp phototransistors GP1S094HCZ0F (6) were used to detect wire vibrations and National Instruments 24-bit PXIe-4464 module for signal registration from them.

ISBN: 978-3-95450-240-0 ISSN: 2673-5539 doi:10.18429/JACoW-RuPAC2021-WEPSC18

# SERIAL MAGNETIC MEASUREMENTS OF THE NICA COLLIDER TWIN-APPERTURE DIPOLES. THE MAIN RESULTS

D. A. Zolotykh†, V. V. Borisov, I. I. Donguzov, O. Golubitsky, H. G. Khodzhibagiyan, B. Kondratiev, S. A. Kostromin, I. Yu. Nikolaichuk, T. Parfylo, M. M. Shandov, A. V. Shemchuk, E. V. Zolotykh,
JINR, Dubna, Moscow Region, Russia

*Abstract*

NICA Collider includes 80 dipole twin-aperture superconducting magnets. Totally 80 main and 6 spare magnets were manufactured and tested by a specially designed magnetic measurement system (MMS). Dipole magnets were tested at the ambient and operating (4.5 K) temperatures. This paper contains the main results of magnetic measurements of the NICA Collider twin-aperture dipoles.

## INTRODUCTION

NICA (Nuclotron-based Ion Collider fAcility) is a new acceleration-storage complex. It is under construction in JINR. Collider includes 80 dipole twin-aperture superconducting magnets [1]. The operating energies for the Collider are 1.0, 3.0, and 4.5 GeV / nucleon, which correspond to the magnetic fields of 0.4, 1.2 and 1.8 T, respectively. Manufacturing of 80 main and 6 spare magnets is finished now. The main parameters of the dipoles were checked:

- Field in the center of the dipole ($B_1(0)$).
- Effective length ($L_{eff}$).

$$L_{eff} = \frac{1}{B_1(0)} \sum_{i=1}^{3} B_{1,i} S_i \quad (1)$$

- Median plane angle.

$$\alpha = -arctg \frac{A_1}{B_1} \quad (2)$$

- Relative harmonics up to $10^{th}$.

Dipoles were tested at the ambient and operating (4.5 K) temperatures. Maximal operating current at operating temperature is 10.44 kA.

## MAGNETIC MEASUREMENTS SYSTEM

Magnetic measurements were completed using the rotating harmonic coil method. Special MMS (see Fig. 1) were designed and manufactured for those tasks. This MMS consists of 3 blocks. Blocks locate in lodgement. Each block (see Fig. 2) includes 3 harmonic coils produced by PCB (printed circuit board) technology. Each coil consists of 400 turns (20 layers of 20 turns) [2,3]. Six MMS were produced and used for the magnetic measurement procedures: 2 for tests at the ambient temperature and 4 for the operating temperature. The basic views (front and rear) of the dipole magnets include MMS are shown in Fig. 3 (before connection with feed box).

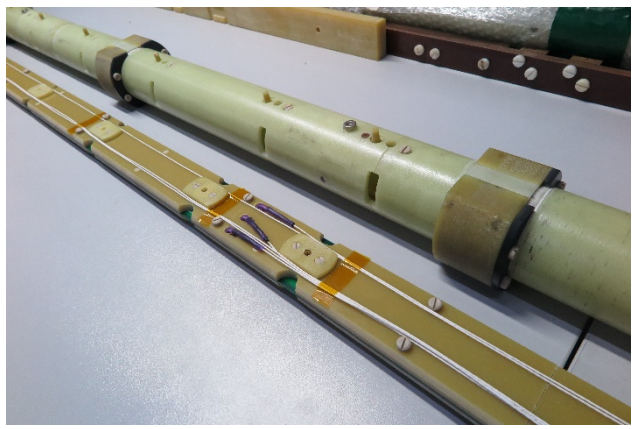

Figure 1: Magnetometer (lodgement and measuring shaft).


Figure 2: Block of the PCB harmonic coils.

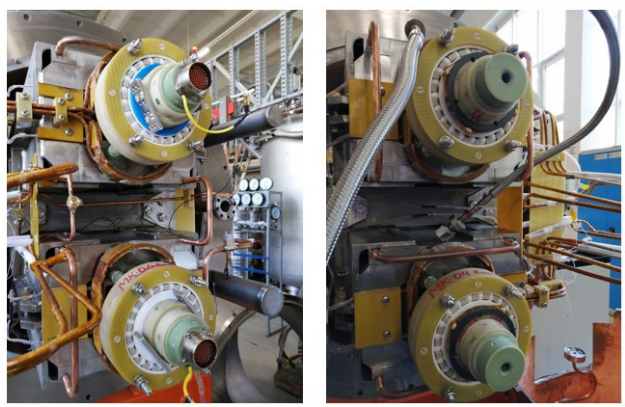

Figure 3: The basic views of dipole magnets.

† zolotykh@jinr.ru

ISBN: 978-3-95450-240-0 ISSN: 2673-5539 doi:10.18429/JACoW-RuPAC2021-WEPSC20

# MAGNETS DESIGN FOR 2.5 GeV BOOSTER SYNCHROTRON

A.S. Smygacheva, V.N. Korchuganov, Ye.A. Fomin
NRC «Kurchatov Institute», Moscow, Russia

*Abstract*

The Project of complete modernization of the current accelerator complex is in progress in the NRC «Kurchatov Institute». The development of a new booster synchrotron as a part of the injection complex for a new 3-d generation synchrotron light source is included in the Project. The booster synchrotron has 24 dipoles, 60 quadrupoles, 48 sextupoles and 24 correctors. In order to obtain the required field quality, 2D- and 3D-simulations of magnets were carried out. The obtained geometry for each of the magnets is presented in the paper.

## INTRODUCTION

The booster synchrotron is based on the modified DBA structure with 12 cells, each with mirror symmetry about the center of the cell [1]. One cell consists of 2 dipoles, 5 quadrupoles, 4 sextupoles and 2 correctors. The booster lattice has a large dynamic aperture with compensated natural chromaticity and low natural emittance (43.4 nm×rad). The structure is stable against various kinds of magnetic field errors within the permissible values.

The sensitivity of the booster lattice to errors and the parameters of the electron beam set the requirements for the quality of the magnetic fields. Optimization of the main characteristics of the field (the integral homogeneity of the field and the effective length) to the required values is carried out by searching the magnet pole geometry in 2D- and 3D-simulations of magnetic fields. The manufacturing technology and the magnetic properties of the steel have to be taken into account during magnet field optimization.

The booster synchrotron will operate in a cyclic mode with a frequency of 1 Hz in the energy range from 200 MeV to 2.5 GeV. The presence of alternating magnetic fields determines the manufacturing technology of the magnets of the booster synchrotron. The yoke of each magnet will be laminated, i.e. will be assembled from 1 mm thick magnetic steel sheets. The steel chosen for the magnet yokes is M940-100A. To ensure high quality of the magnetic field, the profile of each sheet must be made with an accuracy of 10–20 μm. The entire internal geometry of the magnet yoke must be maintained with the same accuracy during assembly.

The paper presents the optimization results of magnetic fields, electrical parameters and geometry of the booster magnets. 2D- and 3D-simulations of magnetic fields were carried out in the CST Studio Suite [2].

## DIPOLES

The dipole magnet is a sector bending magnet. The ends of the magnet are parallel to each other. The main dipole parameters are presented in Table 1. The cross section of the dipole is shown in the Fig. 1.

The dipole magnet has also two additional coils for the field correction. The cross-sectional conductor size is 3.15×3.15 mm$^2$. The maximum current is 10 A in the correction coils.

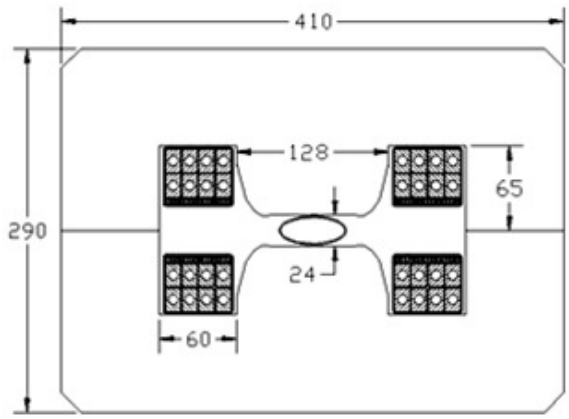


Figure 1: The dipole cross section.

Table 1: Dipole Parameters

| | |
|---|---|
| Number of magnets | 24 |
| Deflection angle, deg | 15 |
| Magnetic field, T | 0.1-1.3 |
| Magnetic length, mm | 1679.363 |
| Yoke length, mm | 1674 |
| Curvature radius, mm | 6415 |
| Gap, mm | ±12 |
| Homogeneity within the GFR | $\leq \pm 2\times10^{-4}$ |
| Number of coils | 2 |
| Number of turns per pole | 8 |
| Conductor cross section/ Inner hole diameter, mm$^2$/mm | 18×12/ 8 |
| Max. current, kA | 1.56 |
| Resistance per magnet, mΩ | 6.47 |
| Inductance per magnet, mH | 2.86 |
| Max. power loss, W | 15.8 |
| Pressure drop, bar | 4 |
| Cooling water flow rate, l/min | 17.3 |
| Temperature rise, °C | 13.1 |
| Magnet weight, kg | 1500 |

The geometry of the pole, obtained in 2D- and 3D-simulations, provides the dipole field homogeneity in the central section of the magnet better than $\pm5\times10^{-5}$ in a good field region (GFR) of 20×40 mm$^2$ (h×w) and the integral homogeneity of $\pm2\times10^{-4}$ (Fig. 2). To reduce the

ISBN: 978-3-95450-240-0 ISSN: 2673-5539 doi:10.18429/JACoW-RuPAC2021-WEPSC21

# MAGNETS FOR LIGHT IONS ACCELERATOR

I. A. Yurin, S. M. Polozov, M. S. Dmitriev, E.N. Indyushnii, National Research Nuclear University MEPhI (Moscow Engineering Physics Institute), Moscow, Russian Federation.

*Abstract*

At the moment, the National Research Nuclear University (MEPhI) is developing an injector for an accelerator of light ions with an energy of 7.5 MeV / nucleon. The injector uses several tens of quadrupole magnets with a magnetic field gradient of 6-18 T / m and several units of dipole magnets. Key requirements for quadrupole magnets include large aperture, compact transverse dimensions, uniform shape and design, ease of fabrication from a manufacturing standpoint, field accuracy within 0.1%, and low power consumption. This article will describe the requirements, simulation results, and preliminary designs for quadrupole and dipole magnets.

## INTRODUCTION

The new project of the injector for the proton and light ion accelerator will have several tens of quadrupole magnets, the range of the magnetic field gradient is 6-18 T / m, the aperture of the transport channel is 66.5 mm, the physical length of the lens is 100 mm, and the pulse repetition rate to 5 Hz. The original concept of a quadrupole magnet was continuous operation, since in any case the inductive component will be large enough and the transient time will not allow reducing the operating time with the power supply turned on. Based on the simulation results, for the maximum value of the magnetic field gradient (18 T / m), the active power of each cooling will be 582 W, and an active liquid system will also be required to maintain an acceptable temperature with a water flow rate of 0.415 liters / minute for each winding. According to the concept, the operating mode of the accelerator system is continuous (24/7), therefore, efficiency in terms of operation is also an important aspect. For example, for 10 quadrupole magnets (with the maximum gradient value), the electricity consumption per week will be $3.9\times10^3$ kW-hr, and the volume of water pumped will be 167 $m^3$. The optimal solution was to switch to a pulsed mode of operation.

## MAGNET DESIGN

When developing the quadrupole, several important points were taken into account: the power source must be made on existing serial electronic components (in particular, IGBT transistors), the cooling system must be passive, the magnet design for all sections of the injector must be unified. The simulation resulted in a quadrupole magnet with the following parameters in Table 1.

Table 1: Quadrupole Specifications

| Parameters | Value | Unit |
|---|---|---|
| Quadrupole gradient | 18.0 | T/m |
| Physical length | 100 | mm |
| Effective length | 128.5 | mm |
| Good field region | ±15 | mm |
| Number of turns per pole | 48 | |
| Conductor dimension | 4×8 | $mm^2$ |
| Weight | 138.25 | kg |
| Steel | 3408 | |
| Operating temperature | 48 | °C |
| Total heat dissipation | 10.55 | W |

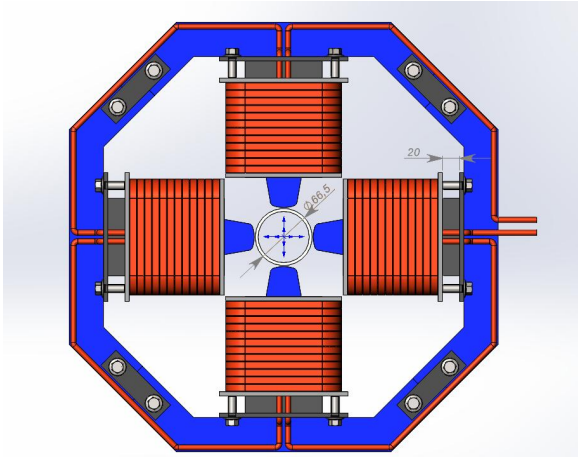


Figure 1: Front view of the pulse quadrupole.

The Pulsed Quadrupole was developed using 3D modeling software. To realize the maximum gradient of 18 T / m, the excitation current must be 180.5 A, the number of turns in coil is 48, the transverse dimensions of the conductor are 4 × 8 $mm^2$. A sketch of the model is shown in Fig. 1. The inductance of each coil is $3.17 \times 10^{-3}$ H. The pole shape is built according to the equation [1]

$$xy = \frac{h^2}{2} \quad (1)$$

The magnet yoke is designed out of silicon steel, since this steel has a narrow hysteresis loop and, unlike low-carbon steel, will reduce the transient time by 5-6 times (for this model), in this case, steel grade 3408 is chosen. The yoke design is 4 connecting elements. The elements are packets of laminated steel with a thickness of 0.35 mm, this thickness is due to the decay time of eddy currents [2]

ISBN: 978-3-95450-240-0 ISSN: 2673-5539 doi:10.18429/JACoW-RuPAC2021-WEPSC28

# OPTICAL DIAGNOSTICS OF 1 MeV PROTON BEAM IN ARGON STRIPPING TARGET OF A TANDEM ACCELERATOR*

A. N. Makarov#, S. S. Savinov, I. M. Shchudlo, S. Yu. Taskaev
Budker Institute of Nuclear Physics, Novosibirsk, Russia
Novosibirsk State University, Novosibirsk, Russia

*Abstract*

A neutron source for boron neutron capture therapy based on a vacuum-insulated tandem accelerator has been developed and operates at Budker Institute of Nuclear Physics. Conducting a ~10 mm proton beam with a power of up to 20 kW through a system of accelerating electrodes and 16 mm argon stripping tube is not an easy task. Any mistake made by operator or a malfunction of the equipment responsible for the correction of the beam position in the ion beam line can lead to permanent damage to the accelerator when a powerful beam hits the surface of the stripping tube or diaphragms of the electrodes. To determine the position of the proton beam inside the argon stripping tube, optical diagnostics have been developed based on the Celestron Ultima 80-45 telescope and a cooled mirror located at an angle of 45° to the beam axis in the straight-through channel of the bending magnet. The cooled mirror, in addition to the optical function, also performs the function of measuring the neutral current due to the electrical isolation of the mirror and the extraction of secondary electrons from its surface. The luminescence of a beam in the optical range, observed with the help of the developed diagnostics, made it possible for the first time to determine beam size and position inside the stripping tube with an accuracy of 1 mm. The light sensitivity of applied optical elements is sufficient for using a shutter speed from 2 to 20 ms to obtain a color image of the beam in real time. This makes it possible to realize a fast interlock on the event of a sudden displacement of the beam.

## INTRODUCTION

Boron neutron capture therapy (BNCT) is currently considered as a promising technique for treatment of malignant tumors [1, 2]. Two clinics using accelerator based BNCT technique began treating patients in 2020 and four more BNCT clinics are ready to start. An accelerator neutron source developed [3] at Budker Institute of Nuclear Physics serves as a prototype for a facility constructed in 2021 for a BNCT clinic in Xiamen (China). It is planned to equip the National Medical Research Center of Oncology (Moscow, Russia) and National Oncological Hadron Therapy Center (Pavia, Italy) with the same vacuum-insulated tandem accelerators (VITA). Safety and durability of the new type of the accelerator are very important in case of 24/7 clinical operation and have not been studied in detail yet. One of the possible reasons that can lead to permanent damage of the accelerator and interrupt normal operation is the situation when a powerful ion beam hits the surface of the stripping tube or diaphragms of the accelerating electrodes. Since 2008, the year we obtained first neutrons at the accelerator [4], the stripping tube and diaphragms were damaged several times by the beam (Fig. 1).

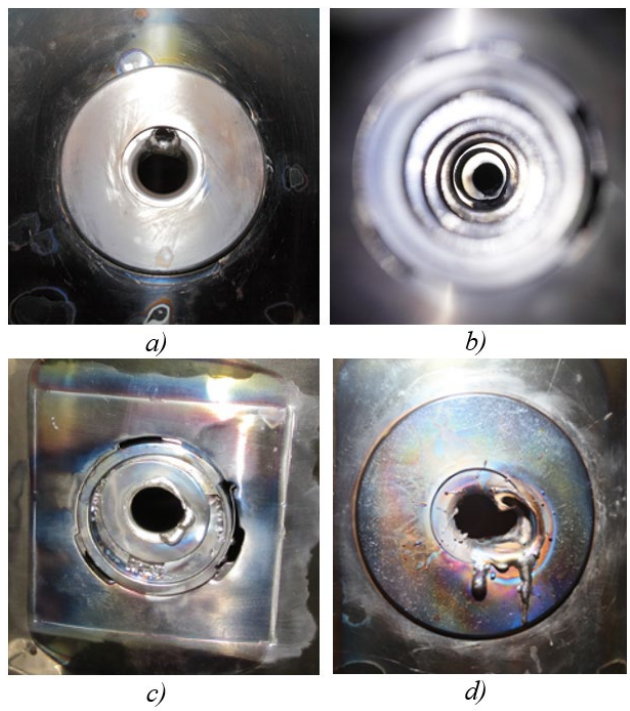


Figure 1: Photos of accelerator diaphragms (diameter is 20 mm) melted by the beam in different times: a) 12.2011, b) 03.2013, c) 03.2015, d) 06.2016.

With a DC current of up to 10 mA and energy of 2 MeV it takes only a few seconds for the beam to melt a diaphragm. In this case, one second of beam displacement will cost 2 weeks of repairing the accelerator. Reasons of sudden beam displacement from the axis can be different: it can be a mistake made by operator, or a malfunction of the equipment responsible for the correction of the beam position, or fast variation in conditions of a gas discharge in the $H^-$ ion source. In this paper we describe an optical diagnostics that is capable to determine the position and size of the proton beam inside the accelerator with an accuracy better than 1 mm in real time. Such diagnostics can improve the reliability of the accelerator in clinical use. Available beam diagnostics, such as optical diagnostics at the entrance to the accelerator [5], calorimetric diagnostics

* This research was supported by Russian Science Foundation, grant No. 19-72-30005
# A.N.Makarov@inp.nsk.su

ISBN: 978-3-95450-240-0 ISSN: 2673-5539 doi:10.18429/JACoW-RuPAC2021-WEPSC29

# DIAGOSTICS OF THE PROTON BEAM POSITION USING THE LUMINESCENCE OF A LITHIUM NEUTRON-GENERATING TARGET*

E.O. Sokolova†, A.N. Makarov, S.Yu. Taskaev,
Budker Institute of Nuclear Physics, Novosibirsk, Russia
Novosibirsk State University, Novosibirsk, Russia

*Abstract*

A compact accelerator-based neutron source [1] has been proposed and created at the Budker Institute of Nuclear Physics in Novosibirsk, Russia. An original design tandem accelerator is used to provide a proton beam. The neutron flux is generated as a result of the $^7$Li (*p, n*) $^7$Be threshold reaction using the solid lithium target. A beam shaping assembly is applied to convert this flux into a beam of epithermal neutrons with characteristics suitable for BNCT (boron neutron capture therapy) [2]. In addition to the main purpose the neutron source is used to measure the content of impurities in ceramic samples developed for ITER [3], for measurement of the cross section of the reaction of inelastic scattering of a proton on a lithium nucleus. The neutron source is planned to be used for radiation testing of optical fibers of the laser calorimeter calibration system of the CMS [4] for the High Luminosity Large Hadron Collider (CERN). The need to provide the long-term stable generation of neutrons requires the development of diagnostic techniques that display relevant information from various subsystems of the neutron source in real time. We have developed and put into operation diagnostics for monitoring the position of the proton beam on a lithium target, which is also resistant to radiation exposure.

## EXPERIMENTAL SETUP

An accelerator-based source of epithermal neutrons (Fig. 1) consists of an ion source *1a*, tandem accelerator with vacuum insulation *1* to obtain a stationary proton beam with an energy of up to 2.3 MeV and a current of up to 9 mA, lithium target *3* to generate neutrons as a result of the $^7$Li (*p, n*) $^7$Be threshold reaction. The lithium target is a copper disk, on which a thin lithium layer (usually 60 μm) is deposited from the side of the proton beam, and spiral channels for water cooling occur on the back side. The lithium targets may be installed in various positions: *A* after the bending magnet, *B* inside the irradiation room, *C* with movable system, *D* along the proton beam, *E* along the proton beam in the separate bunker, inside the beam shaping assembly (optionally).

To develop diagnostics for visual monitoring of the position of the proton beam, a lithium target was placed in the position *C* behind the bending magnet, which in this case was turned off. A Hikvision (China) video camera was installed on one of the branch pipe of the target assembly with barium fluoride glass; on the second branch pipe, with fused quartz glass, a darkened adapter was located, to which a CCS200 Compact Spectrometer (Thorlabs, United States) with the wide range (200–1000 nm) was connected through a multimode 5-m-long quartz fiber, with a core diameter of 200 μm and a numerical aperture of 0.22 NA. The spectrometer and PC were placed in the separate bunker to protect the spectrometer from bremsstrahlung radiation and neutrons.

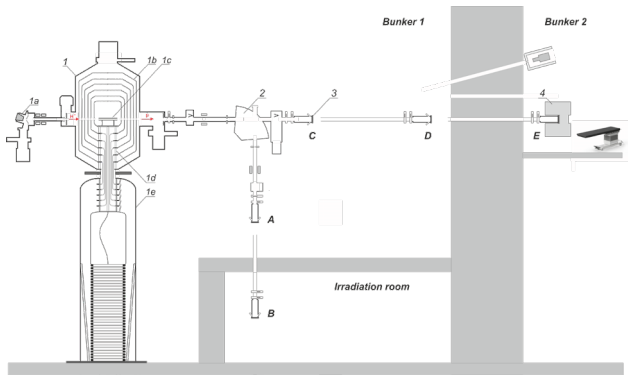


Figure 1: Compact accelerator-based neutron source: *1* – tandem accelerator with vacuum insulation; *2* – bending magnet; *3* – lithium neutron-generating target; *4* – beam shaping assembly.

## RESULTS AND DISCUSSION

The emission spectrum of the lithium target was measured with a spectrometer when it was irradiated with a 2 MeV proton beam (see Fig. 2). The 610.3 ± 0.5 nm emission line corresponds to the $1s^2 3d \rightarrow 1s^2 2p$ electronic transition in the lithium atom, while the 670.7 ± 1 nm line corresponds to the $1s^2 2p \rightarrow 1s^2 2s$ transition in the lithium atom, and the 656.3 ± 1 nm line is the $H_\alpha$ spectral line observed for the hydrogen atom.

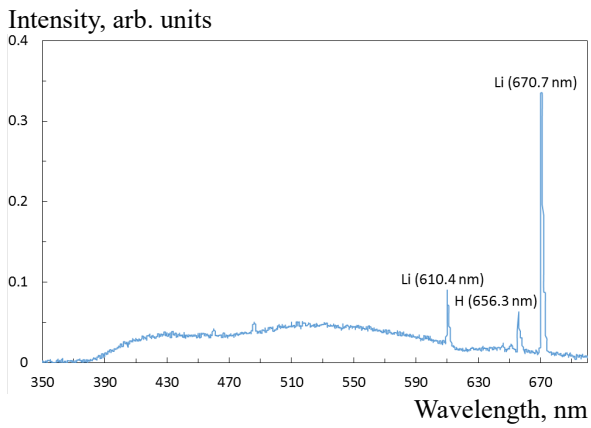


Figure 2: The luminescence spectrum of the lithium target.

* Work supported by supported by the Russian Foundation for Basic Research, project No. 19-32-90119.
† buiya@bk.ru

ISBN: 978-3-95450-240-0 ISSN: 2673-5539 doi:10.18429/JACoW-RuPAC2021-WEPSC30

# MEASUREMENT OF THE PHASE PORTRAIT OF A 2 MeV PROTON BEAM ALONG BEAM TRANSFER LINE*

T. Bykov, Ia. Kolesnikov, S. Savinov, I. Shchudlo, S. Taskaev,
Budker Institute of Nuclear Physics, 11 Lavrentiev ave., 630090 Novosibirsk, Russia

*Abstract*

For the development of a promising technique for the treatment of malignant tumors - boron neutron capture therapy - an accelerator source of epithermal neutrons has been proposed and created at the Budker Institute of Nuclear Physics (Novosibirsk, Russia). For future therapy and radiation testing of materials for ITER and CERN with fast neutrons, it is necessary to ensure the transportation of a proton beam in a high-energy path at a distance of 10 meters.

For this purpose, a phase portrait of the proton beam was measured in the vertical and horizontal high-energy paths using a movable diaphragm with a diameter of 1 mm, mounted on a three-dimensional vacuum driver, and a wire scanner.

The software for remote control of the movable diaphragm and data processing of the wire scanner was developed. An algorithm for processing a series of measurements was also developed to reconstruct the image of the phase portrait of the beam and calculate the emittance. This work describes in detail the features of the measuring devices, control algorithms and data processing.

An experiment was carried out to measure the phase portrait and emittance of a proton beam with an energy of 2 MeV and a current of up to 3 mA. A beam of neutral particles was also measured. The effect of a bending magnet on the focusing and emittance of the beam is studied. The invariant normalized emittances calculated from the measured phase portraits make it possible to claim that the beam can be transported over distances of about 10 meters without changes in the current geometry of the high-energy beam line.

## INTRODUCTION

Epithermal neutrons source based on a vacuum-insulated tandem accelerator [1] with a lithium target and a neutron Beam Shaping Assembly (BSH) [2] is currently the only experimental facility of this class in the world. It is able to generate a stationary beam of protons or deuterons with an energy range of 0.6 to 2.2 MeV and a current range of 1 pA to 10 mA. Such a wide range of parameters opens up a whole range of applications, in addition to clinical trials and therapy.

For future therapy and radiation testing of materials with fast neutrons [3, 4], it is necessary to ensure the transportation of a proton beam in a high-energy path at a distance of 10 meters. For that purposes a beam phase portrait and emittance was measured.

* The study was supported by a grant from the Russian Science Foundation (project No. 19-72-30005) with the support of the Budker Institute of Nuclear Physics SB RAS.

## EXPERIMENTAL SETUP

To measure the phase portrait of the proton beam, the cooled diaphragm and the three-dimensional vacuum driver are placed in the diagnostic chamber in front of the bending magnet, the wire scanner is placed behind the bending magnet, and the luminescence effect of the lithium target is monitored by a video camera (Fig. 1). The wire scanner is placed so that one wire measures the current horizontally and the other vertically.

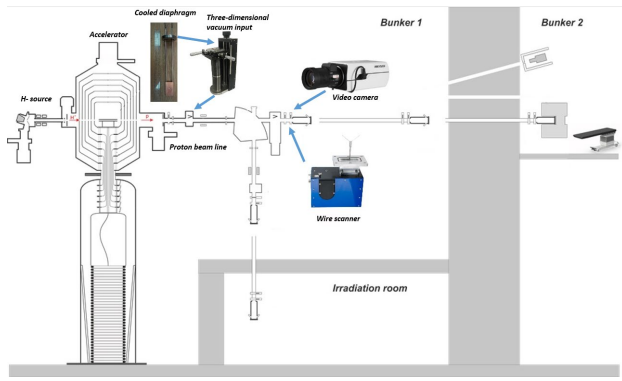


Figure 1: Experimental setup.

First, using a lithium target like a Faraday cup, the center of the beam is found. Further, by entering the motion, one coordinate is left fixed, and the other is moved and the current profile is measured. The same is repeated for the second coordinate.

It should be said that the wire scanner was used not in a standard way. Normally it should be used to measure low-energy charged-particle beam profiles (< 1 MeV) [5]. The use of cooled diaphragm with a hole of 1 mm allows to reduce the heat power generated on the wire probes so that it allows to measure the proton beam current with energy of 2 MeV and current up to 3 mA. During the experiments this constraint were found. A further increasing in current leads to overheating of the tungsten scanner probes and to the ignition of a plasma discharge.

## DATA PROCESSING

An example of a measurements made by wire scanner is shown on Fig. 2. Each graph corresponds to the measurement of the beam at a given position of the cooled diaphragm. In this case it can be seen that the beam distribution is measured along the X axis, and the Y axis is fixed. Then the graphs are shifted taking into account the coordinates of the cooled diaphragm.

ISBN: 978-3-95450-240-0 ISSN: 2673-5539 doi:10.18429/JACoW-RuPAC2021-WEPSC31

# 2D-TOMOGRAPHY OF THE PROTON BEAM IN THE VACUUM INSULATED TANDEM ACCELERATOR*

M .I. Bikchurina†, I A. Kolesnikov, S. S. Savinov, I. M. Shchudlo, S. Yu. Taskaev,
Budker Institute of Nuclear Physics, 630090 Novosibirsk, Russia
Novosibirsk State University, Novosibirsk, Russia

*Abstract*

For the development of a promising method for the treatment of malignant tumors - boron neutron capture therapy - the accelerator-based epithermal neutrons source has been proposed and created in the Budker Institute of Nuclear Physics [1,2]. With different parameters of the proton beam - the energy and current of the beam, the parameters of the ion-optical system, the parameters of the ion source - the conditions for beam transportation change - its size, angular divergence, and position relative to the axis of the accelerator. For optimal conduction of the beam along the path, two-dimensional tomography of the beam can be used - using a cooled diaphragm with a diameter of several millimeters installed on a vacuum three-dimensional motion input, and a Faraday cup, fast chord measurements are carried out, on the basis of which the beam profile is restored. The beam profile obtained in this way is somewhat different from the profile obtained by measuring the phase portrait of the beam using a wire scanner [3]. The advantage of this method is a relatively short time to restore the profile, depending on the diameter of the cooled diaphragm hole.

## INTRODUCTION

Charged particle accelerators are widely used in scientific research, medicine, and other applications. Tandem accelerators are high-voltage electrostatic accelerators in which the high-voltage potential is used twice: first to accelerate negative ions, and then, after changing the polarity of their charge in the high-voltage terminal, to accelerate positive ions. Since power density of the proton beam can reach tens of kW/cm$^2$ there are mechanisms, influencing on the transportation of the beam, such as parameters of the $H^-$ source (accelerating and extracting potentials, voltage of the discharge), focusing and correctors values and energy of the beam there is a need to diagnostic beam with such power and transport it through the high-energy beam line correctly, without heating vacuum chambers. For solve this task it was proposed and realized fast diagnostic of the beam profile, size and destination – two-dimensional tomography.

## THE EXPERIMENTAL SCHEME

The studies were carried out at the accelerator neutron source of the Budker Institute of Nuclear Physics (Novosibirsk, Russia). The source diagram is shown in Fig. 1 and its detailed description was given in [1]. A tandem accelerator with vacuum insulation was used to obtain a stationary proton beam with an energy of 0.6 to 2.3 MeV and a current of 0.3 to 10 mA, that is, a tandem accelerator of charged particles with an original design of electrodes.

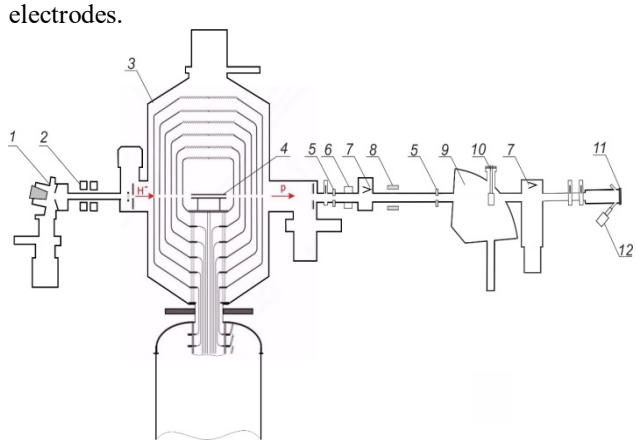


Figure 1: A diagram of an accelerator based source of epithermal neutrons. 1 - $H^-$ source, 2 – magnetic lense, 3 – vacuum-insulated tandem accelerator, 4 – gas stripping target, 5 – cooled diaphragm, 6 –NPCT contactless beam sensor (Bergoz, France), 7 – movable Faraday cup 8 – corrector, 9 – bending magnet, 10 – cooled beam receiver with a diaphragm, 11 – lithium target, 12 – Hikvision video camera.

$H^-$ beam, extracted from $H^-$ source *1*, focusing by a magnetic lense *2* and injected in the accelerator *3*. Inside the accelerator $H^-$ stripping by an argon target *4*, transform into proton with probability 90÷95% [4], and accelerates to the energy equal to the double potential of the accelerator. After the accelerator proton beam goes through cooled diaphragm *5* and its current measuring by a contactless beam sensor *6*. Then proton beam goes through bending magnet *9* and small part of it pass through the cooled diaphragm with aperture of 2 mm *10*, installed on the vacuum three-dimensional motion input. Finally, it comes to the Faraday cup (lithium target *11*, electrically isolated from rest part of the facility). Camera *12* detect luminescence of the lithium target [5], caused by the proton beam bombardment.

Using vacuum three-dimensional vacuum input proton beam current measured and two arrays of the proton currents obtained.

## RESULTS

An example of the image obtained given in the Fig. 2. The easier way to obtain necessary information of the proton beam profile is find peak current, passing through

* Work supported by the RFBR project no. 19-72-30005.
† knkstdor@gmail.com

ISBN: 978-3-95450-240-0 ISSN: 2673-5539 doi:10.18429/JACoW-RuPAC2021-WEPSC32

# PROTON BEAM SIZE DIAGNOSTICS USED IN THE VACUUM INSULATED TANDEM ACCELERATOR*

M .I. Bikchurina, T. A. Bykov, D. A. Kasatov, I A. Kolesnikov†, A. M. Koshkarev, A. N. Makarov, Yu. M. Ostreinov, S. S. Savinov, I. M. Shchudlo, E. O. Sokolova, I. N. Sorokin, S. Yu. Taskaev,
Budker Institute of Nuclear Physics, 630090 Novosibirsk, Russia
Novosibirsk State University, Novosibirsk, Russia

*Abstract*

For the development of a promising method for the treatment of malignant tumors - boron neutron capture therapy - the accelerator-based epithermal neutrons source has been proposed and created in the Budker Institute of Nuclear Physics [1,2]. After the acceleration phase, a proton beam with an energy of up to 2.3 MeV and a current of up to 10 mA is transported in a high-energy path. With a beam size of 1 cm$^2$, its power density can reach tens of kW/cm$^2$. Diagnostics of the size of such a powerful beam is a nontrivial task aimed at increasing the reliability of the accelerator. The paper presents such diagnostics as: 1) the use of the blister formation boundary during the implantation of protons into the metal; 2) the use of thermocouples inserted into the lithium target; 3) the use of the melting boundary of the target lithium layer when it is irradiated with a beam; 4) the use of the activation of the lithium target by protons; 5) the use of video cameras; 6) the use of an infrared camera; 7) the use of the luminescence effect of lithium when it is irradiated with protons; 8) the use of collimators with a small diameter of 1-2 mm; 9) the use of the method of two-dimensional tomography [3].

## INTRODUCTION

Charged particle accelerators are widely used in scientific research, medicine, and other applications. Tandem accelerators are high-voltage electrostatic accelerators in which the high-voltage potential is used twice: first to accelerate negative ions, and then, after changing the polarity of their charge in the high-voltage terminal, to accelerate positive ions. Thin foils are used for the conversion of the ion charge, or, at a higher ion current, gas stripping targets similar to the argon target in the tandem accelerator. After the acceleration phase, a proton beam with an energy of up to 2.3 MeV and a current of up to 10 mA is transported in a high-energy path. With a beam size of 1 cm$^2$, its power density can reach tens of kW/cm$^2$. Diagnostics of the size of such a powerful beam is a nontrivial task aimed at increasing the reliability of the accelerator.

## THE EXPERIMENTAL SCHEME

The studies were carried out at the accelerator neutron source of the Budker Institute of Nuclear Physics (Novosibirsk, Russia). The source diagram is shown in Fig. 1 and its detailed description was given in [1]. A tandem accelerator with vacuum insulation was used to obtain a stationary proton beam with an energy of 0.6 to 2.3 MeV and a current from 1 pA to 10 mA, that is, a tandem accelerator of charged particles with an original design of electrodes.

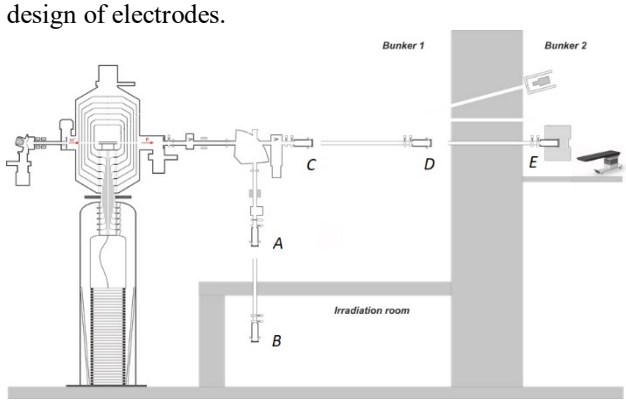


Figure 1: A diagram of an accelerator based source of epithermal neutrons. A-E – sites of the lithium neutron generating target.

## RESULTS AND DISCUSSIONS

Below will be briefly discussed 9 implemented at the vacuum-insulated tandem accelerator diagnostics of the proton beam size with a high power density (up to tens of kW/cm$^2$).

### *Use a Blistering Effect at Proton Implantation in Metal*

Implantation of the protons in the metal cause blistering – deformation of the target surface by the “bubbles” – blisters. Knowing the progress of the blisters appearing we can estimate profile of the proton beam and calculate the proton beam size. Example of this calculations presented in Fig. 2. And details are given in [4]. The effective square of the beam is 0.75±0.07 mm$^2$.

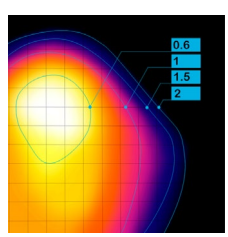


Figure 2: Blistering-covered area of the target versus current fluence (mA·hours).

* Work supported by the Russian Foundation for Basic Research, project no. 19-72-30005.
† Ya.A.Kolesnikov@inp.nsk.su

ISBN: 978-3-95450-240-0 ISSN: 2673-5539 doi:10.18429/JACoW-RuPAC2021-WEPSC33

# INCREASING QUALITY OF EXPERIMENT INTERPRETATION IN REAL-TIME*

A. M. Koshkarev†, T. A. Bykov, Ia. A. Kolesnikov, A. N. Makarov, E. O. Sokolova, S. Yu. Taskaev
Budker Institute of Nuclear Physics, 630090 Novosibirsk, Russia
Novosibirsk State University, Novosibirsk, Russia

*Abstract*

An Epithermal neutron source based on an electrostatic tandem accelerator of a new type – Vacuum Insulation Tandem Accelerator, and a lithium neutron generating target has been proposed and developed at the Budker Institute of Nuclear Physics [1] for the Boron Neutron Capture Therapy [2] – the promising method for treatment of tumours and for other applications. This paper proposes and implements a flexible and customizable method for the operational data processing, allowing an operator and physicists to obtain and analyze the information during the experiment without the need of post-processing data. The application of it accelerates the process of obtaining informative data during the experimental research and automates the analysis process. Also it was proposed and implemented a process of automatic distributed journaling of the results of the experiment. As a result of the implementation of the proposed tools the productivity of the analysis of experimental data and the detailing of the experimental journal was increased the developed and implemented system of real-time data processing has shown its effectiveness and has become an integral part of the control system, data collection and data storage of the epithermal neutron source.

## INTRODUCTION

One of the most important and time consuming parts of researcher's everyday life is the post-processing of experimental data. Sometimes it takes more than 3 hours, but in some experiments physicists need results in real time. For example: visualization of diagnostics, such as beam position by thermocouples or calculation of average beam currents only when the energy is in the nominal range.

## SYSTEM ARCHITECTURE

The developed and implemented accelerator control system consists of many units, such as measurement controllers, server, database, operator's software, software for TVs and physicist-analytics software.

Architecture on Fig. 1. allows collecting data from all units of the accelerator on the server and transfer measurements to clients, that can proceed their own real-time analytics.

Main idea of this architecture is to process data on distributed way on client PC. In this case server only collects data, stores it in database and sends to clients. Also, server checks some low-speed interlocks and calculates some composite diagnostics, like proton fluence or power on the stripping target inside the accelerator.

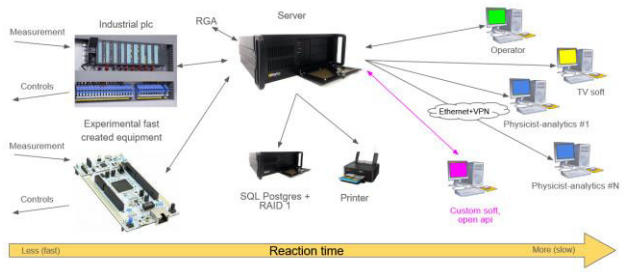


Figure 1: System architecture.

### *Physicist-Analytics Software*

This is a software for physicist-analytics, that allows to proceed a real time analysis, like building a dependence of gamma radiation divided by beam current on the energy (Fig. 2), that was used in the experiment with reactions in lithium targets [3, 4]. Also, this system was used in different experiments [5, 6].

Basic functions are listed below:

1. Plotting the dependences of any measurement channel on another.
2. Time averaging of any channel with displaying "Box plot" on the graph (Fig. 2).
3. Averaging of any channel only by a given condition (example: average if the current is in the selected range).
4. Distribution of the logging status of the experiment with personal notes and an automatic printing at the end of the experiment.
5. Creation of an own channel on the basis of other channels data, for example *(a+b)*c* with all above functions.
6. The program can work from anywhere (via VPN), which can be useful in the case of the new wave of COVID-19.

If this functionality is not enough – programmer can create his own soft, that will process some complex operations and get data with system API.

### *TV Software*

This software is designed to display data on three 50" TVs. During a collaboration experiment with other labs (sometimes international), all physicists who do not have access to the system can see the instantaneous value of the measurements and observe the graph of values.

* Work supported by Russian Science Foundation, grant No. 19-72-30005
† email address: koshi8bit@mail.ru

ISBN: 978-3-95450-240-0 ISSN: 2673-5539 doi:10.18429/JACoW-RuPAC2021-WEPSC34

# TREATMENT OF THE RESULTS MEASUREMENT OF PROFILE BEAM USING WIRE SCANNERS AT ACCELERATOR U-70 IHEP

D. A. Vasiliev †, V. T. Baranov, V. A. Kalinin, O. P. Lebedev, A. V. Louttchev, D. A. Savin, Institute for High Energy Physics in National Research Centre "Kurchatov Institute", 142281 Protvino, Russia

*Abstract*

The IHEP has developed fast wire scanners based on servomotors with a scanning speed of V=16 m/s. For processing of analog signals from detectors, a digital USB oscilloscope NI USB-5133 manufactured by National Instruments has been chosen. The paper describes methods of data processing from a wire scanner using a program developed in the LabVIEW environment and obtaining information about beam parameters as well. To determine the beam revolution frequency, a fast Fourier transform is used. The measured input signal is integrated at a chosed number of turns of the beam. The amplitude, center position, offset, rms deviation of the resulting distribution and beam sizes at the corresponding energy level are calculated using the Gaussian Peak Fit VI library element. The beam profile data in different modes of accelerator operation are presented.

## INTRODUCTION

When setting up and operating the accelerator, it becomes necessary to measure the profile of the circulating beam. At IHEP, a transition was made to modern methods of developing fast wire scanners, taking into account the latest developments in mechatronics and robotics. The choice and justification of this approach were presented in [1]. Some results on the introduction of horizontal and vertical wire scanners U-70 into operation were presented at the RUPAC 2018 conference [2, 3]. This paper presents methods for processing the beam profile data using a program developed in the LabVIEW environment. Also the results of measurements of some parameters of the U-70 accelerator for proton and carbon beams at the speed of the carbon fiber V=16 m/sec are given.

## COMPONENTS OF WIRE SCANNERS FOR THE U-70 ACCELERATOR

Two brushless 4490H024BS (Faulhaber) servo motors with RE-10-1-C64 resolvers (LTN Servotechnik) are controlled by ACJ-055-18R controllers through the Copley Motion Explorer CME2 software shell from Copley Controls. CME2 is installed on a computer under Windows.

The system provides double crossing of the carbon fiber the proton beam per one revolution. The speed of movement is used for processing scintillation detectors signals.

† Dmitry.Vasiliev@ihep.ru

## PROCESSING OF BEAM PROFILE MEASUREMENT DATA

For automated processing of analog signals from wire scanners on the U-70 accelerator, an ADC with an external trigger, a conversion frequency of at least 50 MHz per channel, 8-bit capacity and with a memory of at least 3 MB per channel is required. A digital USB oscilloscope NI USB-5133 from National Instruments is used.

This converter allows to measure and analyze the amplitude and time parameters of the recorded signals. Using the National Instruments LabVIEW2012 development environment, we have created software for working with the NI USB-5133 oscilloscope. The software algorithm is as follows:

Initialization of the device; Selection of the measurement mode (AC, DC); Configuration of the measurement channels (ADC frequency, input signal range, number of measurement points); Selection of the number of measurement channels (1 or 2); Selection of the number of measurements (ADC buffer size); Setting the ADC operation mode by an external sync pulse; Reading the measured data; Saving the array of measured data to a file for subsequent processing.

The time of a half a revolution of the carbon fiber at a constant speed is determined as:

$$T_{1/2} = \frac{\pi \cdot r}{v},$$

where r is the length of the arm of the measuring frame (R-190 mm x 100 mm, Z-150 mm x 150 mm), v is the linear speed of movement (v=16 m/s), $T_{1/2}$=37.3 ms (R-axis), $T_{1/2}$=29.45 ms (Z-axis)

Minimum ADC buffer size for measuring half a revolution

$$N = f_{ADC} \cdot T_{1/2},$$

where $f_{ADC}$ is the conversion frequency. For a conversion frequency of 100 MHz, the minimum buffer size is $3.7\times10^6$ (R axis) and $2.9\times10^6$ (Z axis). To measure the direct passage of the fiber through the beam, the buffer size at the ADC frequency of 100 MHz was set to $2\times10^6$, to measure the forward and reverse passage – $3.5\times10^6$.

The program performs:

ISBN: 978-3-95450-240-0 ISSN: 2673-5539 doi:10.18429/JACoW-RuPAC2021-WEPSC36

# SIMULATION OF THE COHERENT RADIATION INTERFEROMETRY FOR THE BEAM TEMPORAL STRUCTURE DIAGNOSTICS

M. Toktaganova*, D. Shkitov†, M. Shevelev, S. Stuchebrov
Tomsk Polytechnic University, Lenina ave. 2a, 634050 Tomsk, Russia

*Abstract*

We consider a mathematical model and computer simulation results describing the interferometry of both diffraction and transition radiation to develop an electron bunch train structure diagnostic method. The results of the autocorrelation function simulation indicate a possibility of diagnosing the bunch number in the train as well as spacing between them in case of using narrowband or broadband detectors. The suggested method will allow rejecting spectrum reconstruction in favor of extracting information directly from the autocorrelation function.

## INTRODUCTION

Nowadays, free electron lasers and new facilities that are capable of generating sequences of short electron bunches with a high (THz) repetition rate have widely developed [1]. The existing diagnostic methods for such sequences have limitations or are not applicable. Therefore, it is important to develop new approaches to diagnose the temporal structure of such sequences (trains) in modern accelerators. In this report, we describe a model of coherent radiation interferometry. Based on the analysis of interferometer autocorrelation function (ACF), we can derive the information about temporal structure of the trains.

## MODEL DESCRIPTION

In this section, we describe the mathematical model for the ACF simulation underlying the proposed approach. In general case, the intensity of radiation produced by the train registered by the detector after passing through the interferometer is determined by the following expressions:

$$I(\Delta l) = \int_{\nu_1}^{\nu_2} [N + N(N+1)F(\nu)] \frac{d^2W}{d\nu d\Omega} V(\nu)T(\nu)P(\nu)M(\nu)S(\nu),$$

$$F(\nu) = \frac{1}{m^2} e^{-\frac{4\pi^2\nu^2}{c^2}\left(\sigma_x^2 s_x^2 + \sigma_y^2 s_y^2 + \sigma_z^2 s_z^2\right)} \left| \sum_{j=1}^{m} e^{-i\frac{2\pi\nu}{c} l(j-1)s_z} \right|^2,$$

where $\nu$ is the radiation frequency, $c$ is the speed of light in vacuum, $\{\nu_1, \nu_2\}$ is the detector sensitivity range, $N$ is the electron number in the train, $c$ is the speed of light, $\frac{d^2W}{d\nu d\Omega}$ is the spectral-angular distribution of radiation from one electron, $F(\nu)$ is the form-factor of a uniform electron bunch train, $S(\nu)$ is the detector sensitivity function, $M(\nu)$ is the interference multiplier, $T(\nu)$ is the multiplier responsible for transmission properties of the vacuum chamber window, $V(\nu)$ is the multiplier responsible for radiation propagation medium and splitter material in the interferometer, $P(\nu)$ is the multiplier responsible for the polarizer characteristics. In [2–4] you can find more information on how to calculate the bunch form-factor. As seen, the model takes into account the train structure parameters and the detector characteristics. The mechanisms of transition radiation (TR) and diffraction radiation (DR) are selected as the radiation source. Note that TR mechanism is invasive and DR one is noninvasive. The geometries of TR and DR generation are illustrated in Fig. 1. However, other type of radiation could be selected as a source (e.g., synchrotron or Cerenkov radiation).

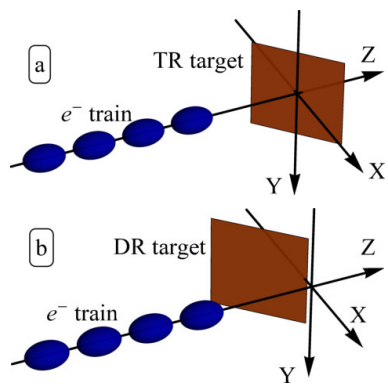


Figure 1: The schematic interaction geometries of the train with the target in cases of TR (a) and DR (b).

In these geometries, only the horizontal component of the radiation polarization is mainly present. It means that $\frac{d^2W}{d\nu d\Omega} \approx \frac{d^2W_z}{d\nu d\Omega}$.

## SIMULATION

The simulation of the TR and DR spectra from single electron, illustrated in Fig. 2, was carried out based on the program written on the *Wolfram Language* code [5], developed earlier [6]. For numerical integration, the default method and the Monte Carlo method [7] was used[1]. In the simulation, the target is flat and has a finite size to be acceptable for use in the accelerator path. The $\theta_0$ is the angle between the normal vector and the particle trajectory. The center of the TR target is located at the coordinate system center. The DR target edge is located at the distance equal to

* mmt8@tpu.ru
† shkitovda@tpu.ru

[1] {Automatic, "SymbolicProcessing"->False} and {"MonteCarlo", "MaxPoints"->$10^8$, Method->{"MonteCarloRule", "AxisSelector"->Random, "Points"->$5 * 10^6$}, "SymbolicProcessing"->False}

ISBN: 978-3-95450-240-0 ISSN: 2673-5539 doi:10.18429/JACoW-RuPAC2021-WEPSC39

# DATA COLLECTION, ARCHIVING AND MONITORING SYSTEM FOR U70 SYNCHROTRON

V. A. Kalinin†, N. A. Oreshkova, NRC "Kurchatov Institute" - IHEP
(Institute for High Energy Physics), Protvino, Moscow region, Russia

*Abstract*

This paper describes a data collection, archiving and monitoring system for U70 synchrotron. The system is designed to monitor the operation of the U-70 accelerator and is responsible for the collection of low-frequency (less than 2 kHz) analog signals from the U-70 technological systems, their processing and subsequent sending to the database using the Data Socket technology. The developed complex block diagram is presented. The hardware and its characteristics (number of channels, resolution, bandwidth) and the interface and functionality of the software are described. The results of using this system at the U-70 accelerator complex are presented.

## INTRODUCTION

U-70 personnel need to control a large number (more than 100) parameters when controlling the accelerator complex, most of which are represented in the form of low-frequency (frequencies less than 2 kHz) analog signals. To quickly identify malfunctions and improve the efficiency of the accelerator complex, it was decided to create a system for monitoring and archiving low-frequency signals.

## HARDWARE

The block diagram of the data collection, archiving and monitoring system for U70 synchrotron is shown in Fig. 1. It includes analog-to-digital converters (ADC), local servers and a database server.

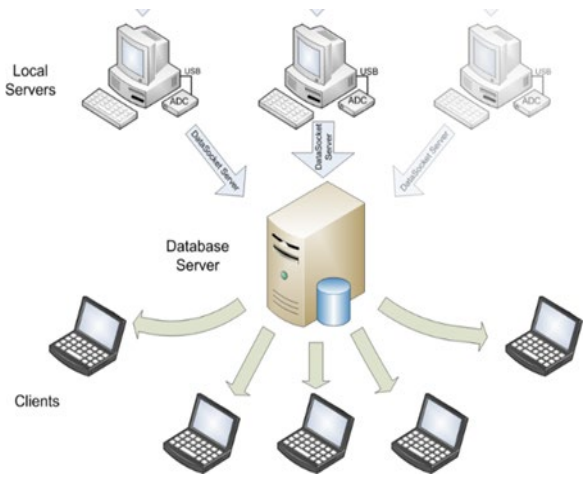


Figure 1: The block diagram of the data collection, archiving and monitoring system for U70 synchrotron.

An analog-to-digital converter (ADC) E-14-140-M is used to digitize the signals. Its characteristics are presented in Table 1. The ADC is connected to the Local server (a PC running the WINDOWS 7 32bit operating system) by a USB cable. The HP proliant dl160 running the Debian 8 operating system is used as a database server (Database server).

Table 1: Characteristics of the ADC E-14-140-M

| | |
|---|---|
| Number of channels | 32 with "common ground" |
| Resolution | 14 bits |
| Input signal range | ±10 V |
| Conversion frequency | 100 kHz |

Each ADC operates in the mode of 32 analog channels and 8 digital channels.

The analog inputs of the ADC are supplied with 31 signals from the control outputs of various sources (induction sensor, total voltage of the electric field RF, magnetic field corrections, etc.) (Data Sources) and one synchronization signal (common for all ADCs). The synchronization signal represents two pulses of different amplitudes (8V and 3V). The pulses are linked to the supercycle of the U-70 accelerator with a duration of 8-10s.

The digital channels receive the following signals from the synchronization system [1]:

- NC (start of the accelerating cycle);
- B1 (technological pulse generated on the falling part of the magnetic field of the previous magnetic cycle);
- B2 (the beginning of magnetic field booster plateau stabilization pulse);
- KS1 (end of the booster plateau);
- T0 (the beginning of magnetic field main plateau stabilization pulse);
- KS2 (end of the main magnetic field plateau);
- Reset (service pulse delayed in time relative to the NC pulse);
- Two backup channels of the U-70 timer system.

The parameters of the magnetic cycle are monitored using digital signals.

## SOFTWARE

The software is created in LABVIEW and consists of the server and client parts.

†vakalinin@ihep.ru

ISBN: 978-3-95450-240-0 ISSN: 2673-5539 doi:10.18429/JACoW-RuPAC2021-WEPSC40

# DETECTION OF ANOMALIES IN BPM SIGNALS AT THE VEPP-4M

I.A. Morozov*, P.A. Piminov, BINP SB RAS, Novosibirsk, Russia

*Abstract*

Beam position monitors (BPMs) are widely used for beam diagnostics in particle accelerators. Turn-by-turn (TbT) beam centroid data provide a means to estimate performance-critical accelerator parameters, like betatron frequency and optical functions. Parameter estimation accuracy is heavily related to TbT data quality. BPM faults might lead to erroneous estimation of accelerator parameters and should be accounted for achieving accurate and reliable results. Several anomaly detection methods for TbT data cleaning are considered. Derived features of BPM signals along with their robust dispersion estimation are used to flag faulty BPM signals. Estimated contamination factor is used with unsupervised learning methods (Local Outlier Factor and Isolation Forest). Application of anomaly detection methods for the VEPP-4M experimental TbT data is reported.

## INTRODUCTION

The VEPP-4M storage ring [1] is equipped with 54 dual-plane BPMs [2]. The system can provide TbT data with resolution close to 20 µm. TbT data is acquired by excitation of the circulating beam with impulse kickers. To improve the reliability of optics inference, detection of anomalies in BPM signals is required.

Anomaly detection is widely used for TbT data quality control [3, 4]. Anomalies caused by BPM electronics failures might deteriorate the measurements quality of accelerator parameters. To mitigate the effects of anomalies, robust parameter estimators should be used. Flagged BPMs should be excluded at the optics inference stage where it's possible.

Previously BPM signal quality was judged only based on the frequency spread across BPMs during single data acquisition. In this paper extended procedure of anomaly detection at the VEPP-4M is described. This procedure was tested on a large set of measurements and found to be reliable. Results of anomaly detection and classification at the VEPP-4M are reported.

## ANOMALY DETECTION LOOP

A schematic view of the anomaly detection loop is shown in Fig. 1. Usable signal length is limited by decoherence. For frequency measurement, 1024 turns are used and 128 turns are used for amplitude and phase computation.

Each signal is split into several overlapping samples of short lengths. This allows generating large data set. Several different features are computed for each normalized sample. These features are used as a measure of samples similarity. Close samples are assumed to have close set of features. Thus, signals with samples containing large deviations of features can be flagged as anomaly candidates. In our case,

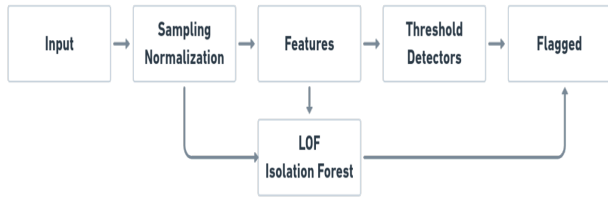


Figure 1: Anomaly detection loop at the VEPP-4M.

eight different derived features were tested. Each feature is also processed separately with a threshold detector. This allows defining anomaly score for each signal as the number of samples from a given signal with a feature value above the defined threshold. Anomaly scores across different features are combined to flag anomaly candidates and to estimate the contamination rate of a given measurement. A combination of threshold detectors performs well for anomaly detection in both simulations and experimental data. Robust estimation of feature spread allows to minimize the number of false positive cases.

For known contamination rate, several unsupervised machine learning (ML) methods can be applied. Local Outlier Factor [5] and Isolation Forest [6] techniques are used as a second layer in anomaly detection. These methods are applied directly to samples and in the feature space. Local Outlier Factor was found to perform well in both cases, while Isolation Forest worked better in feature space.

## DERIVED FEATURES GENERATION

For normalized samples, several derived features can be computed. These features are obtained directly from a sample or from a full sample matrix.

Maximum absolute amplitude value in a sample is computed. This feature performs well for identification of spikes in TbT signals. For each sample, the frequency of the largest spectrum peak is computed. Significant frequency deviation across samples might indicate an anomaly and is sensitive to large spikes and noise. Fourier spectrum floor level in a given range of frequencies is used as a next feature. Samples with large noise should have a large spectrum floor level. A selected range of frequencies is assumed to contain no large peaks. Quasiperiodic decomposition reconstruction error is used as a measure of how well a given sample is approximated by several harmonics. From the SVD decomposition of the full sample matrix, the maximum absolute values of SVD space modes are used. Sample noise is also estimated using optimal SVD truncation [7]. Samples with anomalies are assumed to have larger noise estimations. Hankel filter [8] is applied to each sample and a feature is generated as a norm of the difference between filtered and original sample. Robust PCA [9] is used on the full sample matrix.

* I.A.Morozov@inp.nsk.su

ISBN: 978-3-95450-240-0 ISSN: 2673-5539 doi:10.18429/JACoW-RuPAC2021-WEPSC42

# RF CAVITY BASED CHARGE DETECTOR FOR A LOW CHARGE ULTRA SORT SINGE ELECTRON BUNCH MEASUREMENT

K.V. Gubin, ILP SB RAS, Novosibirsk, Russia
A.M. Barnyakov, S.L. Samoylov, D.P. Sukhanov[1], BINP SB RAS, Novosibirsk, Russia
[1]also at Novosibirsk State University, Novosibirsk, Russia and Novosibirsk State Technical University, Novosibirsk, Russia

*Abstract*

Nowadays the project of laser-driven Compton light source started in ILP SB RAS in collaboration with BINP SB RAS. It was expected the production of 1-10 pC electron beams sub-ps time range duration with energies up to 100÷150 MeV as a result of the first stage of the project. It is necessary to have the non-destructive charge detector for on line measurements during experiments. We proposed the detector based on reentrant RF resonator technology. Single circular cylinder geometry of measuring RF cavity is insensitive to electron beam position and size as well as time structure of bunch (on the assumption of sufficiently short bunch). Base data of cavity are close to acceleration section elements of VEPP-5 linac.The prototype of the detector was successfully tested at VEPP-5 electron linac. Measured charge of single bunch reaches down to 1 pC and less. This paper presents the results of development and testing of diagnostics.

## INTRODUCTION

At the present time, the impressive progress in laser wakefield acceleration (LWFA) of charged particles gives grounds to consider LWFA as a perspective method of electron beam production in the GeV energy range.

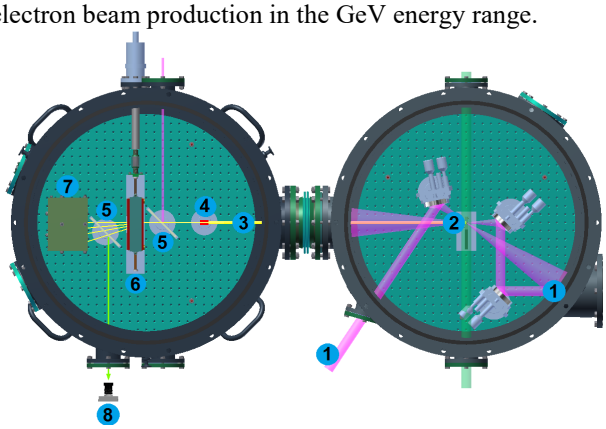


Figure 1: Experimental vacuum chamber. (1) Laser beams, (2) supersonic gas jet, (3) electronic beam, (4) RF beam charge detector, (5) screens, (6) magnet spectrometer, (7) faraday cap, (8) CCD.

The project of laser-driven Compton light source started in ILP SB RAS in collaboration with BINP SB RAS. The first stage of the project is to create a stand for obtaining and studying LWFA-accelerated electron beam inside the supersonic gas jet with energy as high as 100 MeV. At the next stage, it is planned to obtain a high-energy gamma-ray beam by means of Compton backscattering of a probe light beam on LWFA-accelerated electrons [1] (see Fig.1). Expected parameters of the electron beam are: up to 50-100 MeV of energy, 1-10 pC of charge, 1-10 mrad of angular divergence, ≤ 0.1 ps of beam duration.

## DETECTOR PURPOSE, DESIGN AND PARAMETERS

Non-destructive beam current measurement is a necessary constituent of any accelerator facility. In our case we propose to use the wide-used diagnostics based on reentrant RF resonator. This kind of detector was realized, for example, [2] as a beam current monitor or beam position monitor [3, 4].

The development of beam charge detector is constrained by the following general demands:

- Compact size (full dimensions not more than ~10 cm) because the device will be placed inside limited volume of experimental vacuum chamber (Fig. 1) with diameter 70 cm and height 50 cm.
- Detector will operate with single bunch condition. Storage methods of measurements are unacceptable because of the electron beam has repetition rate not more 1 Hz. Moreover, expected beam parameters (as charge as beam size and position) will be very unstable between charge pulses.
- Maximum unification of detector parameters with parameters of VEPP-5 RF elements [5].
- Beam charge range is from 100÷500 fC (tuning regime of LWFA experiment) to 1÷5 nC (RF-photogun experiments).
- In any case beam structure can has as one bunch as bunch train structure. But the bunch duration inside the train will be more or less uniform.

According to the fundamental properties of beam loading we can estimate analytically induced wakefield in the cavities of the millimeterwave structure [6, 7]. A pointlike beam induces a voltage (and, therefore, signal amplitude from pickup antenna) linearly depended on beam charge

$$U_p = 2kq \tag{1}$$

For the $TM_{010}$ mode in the cylindrical waveguide with radius R and length L final expression of the loss parameter is

$$k = \frac{LT^2}{2\varepsilon_0 R^2 J_1^2(\nu_{01})} \tag{2}$$

ISBN: 978-3-95450-240-0 ISSN: 2673-5539 doi:10.18429/JACoW-RuPAC2021-WEPSC44

# BEAM LOSS MONITORING SYSTEM FOR THE SKIF SYNCHROTRON LIGHT SOURCE

Yu. I. Maltseva*[1], S. V. Ivanenko, A. Khilchenko, X. C. Ma, O. I. Meshkov[1], A. Morsina[2], E. A. Puryga
Budker Institute of Nuclear Physics SB RAS, Novosibirsk, Russia
[1]also at Novosibirsk State University, Novosibirsk, Russia
[2]also at Novosibirsk State Technical University, Novosibirsk, Russia

*Abstract*

The Siberian ring source of photons (SKIF) is a new 3 GeV fourth-generation synchrotron light source being developed by the Budker Institute of Nuclear Physics (BINP). In order to ensure its reliable operation, beam loss diagnostics system is required. Two types of beam loss monitors will be installed at the SKIF: 5 fiber-based Cherenkov Beam Loss Monitors (CBLM) for the linac and transfer lines and 128 Scintillator-based Beam Loss Monitors (SBLM) for the storage ring. Sophisticated electronic equipment are employed to use these monitors at different SKIF operating modes. The article describes the design of the SKIF beam loss diagnostics system based on numerical simulations and experimental studies.

## INTRODUCTION

The SKIF is the 4th generation synchrotron light source with 3 GeV energy and emittance of 75 pm rad, that is under construction in Novosibirsk, Russia [1]. The SKIF consists of 200 MeV electron linac, linac-to-booster transfer line (LBT), booster synchrotron with maximum energy of 3 GeV and circumference of 158.7 m, booster-to-storage ring transfer line (BST) and storage ring with 16-fold symmetry and 476 m circumference. The storage ring is designed to operate at top-up injection with up to 400 mA beam current. Current stability of 1% is required. The layout of the SKIF accelerator facility is shown in Fig. 1.

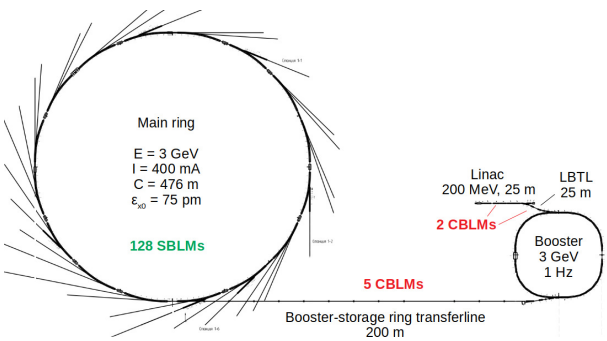


Figure 1: The SKIF layout.

The SKIF is aimed to provide users with syncrotron radiation (SR) almost in 24/7 operation. Therefore, strict requirements on the electron beam stability are imposed. In order to achieve effective SKIF commissioning in the future and its reliable operation and performance in various modes, beam loss diagnostics system is required. This system is an essential tool for real time monitoring of beam losses usually caused by misaligned beam during the machine commissioning or faulty condition of accelerator subsystems or related with beam lifetime [2].

For the linac, LBT and BST where single-bunch mode is available, we proposed to use the CBLMs. For the storage ring in order to control beam losses during machine tuning and operation at top-up mode, the SBLMs were proposed.

## CHERENKOV BEAM LOSS MONITOR

The operation principle of the CBLM is based on the registration of the Cherenkov radiation generated by secondary charged particles in the optical fiber attached to the vacuum pipe [3]. The Cherenkov light propagates upstream and downstream along the optical fiber and can be detected usually by a photomultiplier (PMT) at either one or both ends of the fiber. Timing of the PMT signal gives the location of the beam loss and signal intensity is proportional to the number of lost particles.

### *Simulations and Experimental Studies*

The CBLM prototype tests were performed at the operating BINP accelerator [4] with beam parameters similar to the SKIF. As an optimal fiber type in terms of sensitivity, radiation hardness and cost effectiveness, multimode silica fiber with step-index profile FG550UEC by Thorlabs was selected. It has 550 $\mu$m core diameter, high OH–, F-doped silica cladding. Measured light dispersion was obtained to be 0.17±0.01 ns/m. In order to achieve desired CBLM spatial resolution of 1 m due to the SKIF magnet spacing, maximum fiber length should be about 40 m.

As a photodetector microchannel plate PMT (MCP-PMT) was selected, with gain over $10^6$, dark current less than 1 nA, front rise time of 0.5 ns and the duration (FWHM) of the anode current pulse of at least 1.5 ns. It allows detecting beam losses of ~1 pC corresponding to 1% of the total bunch charge.

The experimental results of 500 MeV beam loss distribution at the downstream and upstream fiber ends are shown in Fig. 2. The upstream signal has 4.2 times better spatial resolution than the downstream one. Taking into account the difference in PMT gains, the downstream signal sensitivity

* yu.i.maltseva@inp.nsk.su

ISBN: 978-3-95450-240-0 ISSN: 2673-5539 doi:10.18429/JACoW-RuPAC2021-WEPSC45

# MEASUREMENT OF THE ELECTRON BEAM SPECTRUM BY THE ABSORBING FILTERS METHOD DURING A SINGLE PULSE

A. Drozdovsky, A.Bogdanov, S. Drozdovsky, A.Kantsyrev, A.Khurchiev, V. Panyushkin, S.Savin, A.Skobliakov, S.Visotski, V.Volkov
NRC «Kurchatov Institute» - Institute of theoretical and experimental physics, Moscow, Russia

*Abstract*

Equipment for measuring the spectrum of an electron beam during a single pulse has been developed and manufactured. We developed a method of processing experimental data and present the obtained results.

## INTRODUCTION

The interest in measuring the energy spectrum of electron beams by the method of absorbing filters is due to the technical availability in comparison with magnetic spectrometry. Moreover, the measuring unit is compact, efficient and suitable for various research facilities.

## EXPERIMENTAL FACILITY

The task of our work was to determine the spectrum of an electron beam with a maximum energy up to 300 keV during one pulse. We applied elements of the technique by [1] to obtain the spectrum from the absorption curves of the beam. The beam passed through a sequence of metal plates of same thickness located perpendicular to the beam axis at fixed interval, while the charge *Qi* absorbed in each plate is measured for each pulse. The measurement scheme is shown in Fig. 1.

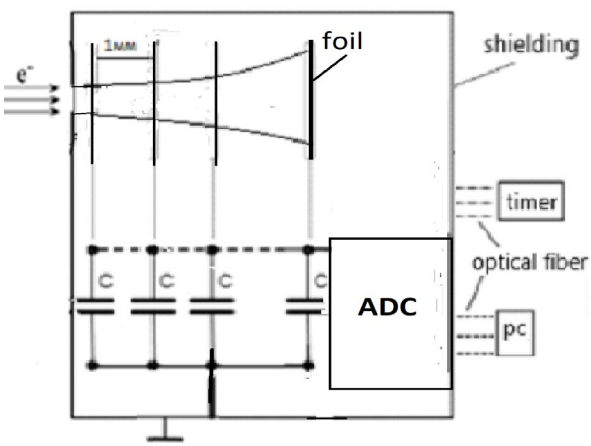


Figure 1: The measurement scheme.

Beams of energy up to 300 keV were emitted from an electron gun [2]. The current collector package consists of 16 insulated identical aluminum foils with the gap of 1 mm between. The thickness of the foils varies from 10 to 25 microns depending on the maximum electron energy. The charge of the foils after passing the beam was measured by an ADC. The charge absorbed by the nth foil $Q_n = V_n C_n$. Each foil is connected to a capacity $C_n$ = 7 nF. The distribution of voltage $V_n$ over the foils of thickness 16 microns after passing an electron beam through at different charging voltages is shown in Fig. 2.

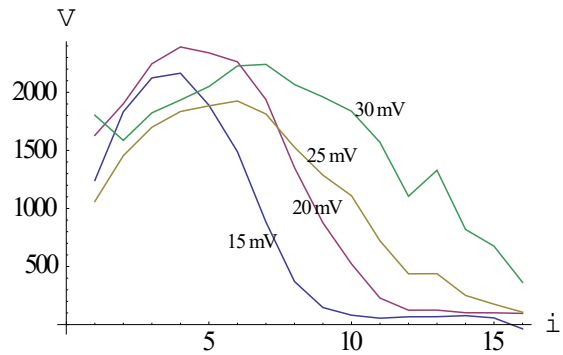


Figure 2: Distribution of voltage $V_n$ over foils at different voltages of the pulse generator of the gun.

Measurements with foils of thickness 16 microns are suitable for the correct determination of the spectrum at charging voltages up to 25 kV. For high voltages the data is incomplete as can be seen from the absorption curves.

## METHOD OF SPECTRUM RESTORING

The measurement process is related to the following system of integral equations:

$$\int_{E_{min}}^{E_{max}} K_i(\varepsilon)\, q(\varepsilon)\, d\varepsilon = Q_i\,, \quad i = 1, \ldots, n\,, \qquad (1)$$

where $Q_i$ is the experimentally obtained charge absorbed by the plate number $i$, $q(\varepsilon)$ is the charge density with respect to the energy (the energy spectrum of the beam), $K_i(\varepsilon)$ is the kernel of the integral transform, with a physical meaning of the probability for a particle with the energy $\varepsilon$ to be absorbed in the plate $i$. The integration is bounded by the interval $\{E_{min}, E_{max}\}$, which limits the range of particle energies in the beam. Our task is to restore $q(\varepsilon)$ from $Q_i$ by solving this system of integral equations. After approximation $q(\varepsilon)$ and $K_i(\varepsilon)$ by step functions, piecewise constant on the intervals $\{\varepsilon_j - \Delta\varepsilon/2, \varepsilon_j + \Delta\varepsilon/2\}$, $\varepsilon_{j+1} - \varepsilon_j = \Delta\varepsilon$, the system (1) takes the discrete form:

* Work supported by R&D Project between NRC "Kurchatov Institute" - ITEP and TRINITI

ISBN: 978-3-95450-240-0 ISSN: 2673-5539 doi:10.18429/JACoW-RuPAC2021-WEPSC50

# ENHANCEMENT OF TRANSVERSE BEAM PHASE SPACE ANALYSIS BY TOMOGRAPHY METHOD AT INR LINAC

A. I. Titov[1†], S. A. Gavrilov[1], S. E. Bragin, O. M. Volodkevich,
Institute for Nuclear Research of the Russian Academy of Sciences, Moscow, Russia
[1]also at Moscow Institute of Physics and Technology (State University), Moscow, Russia

*Abstract*

The investigation of transverse beam phase space parameters behavior along the accelerator is important for proper accelerator tuning. At INR RAS linac transverse emittance and Twiss parameters are reconstructed from beam profile measurements with quadrupole scan technique at several measurement points along the accelerator. Profile treatment is performed with ordinary transverse profiles method and tomographic reconstruction method. Various experimental data is presented. The comparison of the results obtained by the two methods is done. Features of beam dynamics simulation based on the data from these methods are discussed.

## INTRODUCTION

The investigation of transverse beam phase space parameters behavior along the accelerator is important for proper accelerator tuning and beam transport simulation. For low-energy beams direct measurements can be done with slit-grid or pepper pot devices. For high-energy beams direct measurements are impossible and reconstruction method is applied – a quadrupole scan technique (QST). A typical layout of components, required for QST measurements, is presented in Fig. 1.

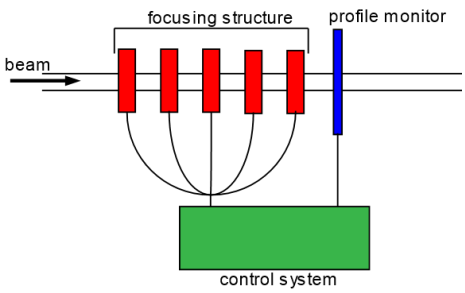


Figure 1: Typical layout of components required for quadrupole scan technique measurements.

QST is a group of methods that in general provides information only about phase ellipse parameters. That is enough for the majority of the beam transfer codes that are used for dynamics simulation. However, if accelerator is not tuned properly, particles distribution in transverse phase space can be non-elliptical. In that case inaccuracy of methods, which reconstruct phase ellipse, grows and so does inaccuracy of the simulation.

One of the methods of beam transverse phase portrait parameters measurements, which can be attributed to QST, is a tomographic reconstruction. It can reconstruct internal structure of the phase space distribution and is applicable for all possible particle distributions in phase space.

† aleksandr.titov@phystech.edu

Beam transfer simulation at INR linac is performed with TRACE 3D code and the main method for phase ellipse parameters measurements at INR linac is a typical QST realization – transverse profiles method (TPM). Also a tomographic reconstruction was implemented as an alternative and enhancement to the TPM.

## TRANSVERSE PROFILES METHOD

Transverse profiles method requires rms beam size and beam centre measured for its operation. These values are represented as vertical lines in corresponding phase plane. The disposition of these lines can be transferred to arbitrary point of measuring area by transfer matrix method. Results of the measurement represent a set of lines. The phase ellipse is inscribed in these lines with the iteration algorithm (Fig. 2). Twiss parameters and rms emittance values are then obtained. In more detail TPM is described in [1].

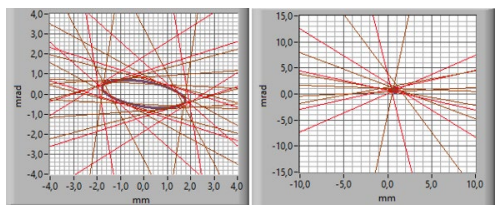


Figure 2: Results of TPM reconstruction. Phase ellipse (on the left) and phase ellipse center (on the right).

## TOMOGRAPHIC RECONSTRUCTION

Tomographic reconstruction requires all information about beam profiles for its operation. Obtained profiles are transformed with use of the transfer matrices and converted into a sinogram. The rotation angles in phase space are also obtained from transfer matrices. The sinogram and rotation angles are then transmitted to tomography kernel. The kernel is based on the Simultaneous algebraic reconstruction technique (SART). Result of the tomography is post-processed so it can be used for beam dynamics simulation (Fig. 3). In more detail tomographic reconstruction kernel and post-processing of the results is described in [2].

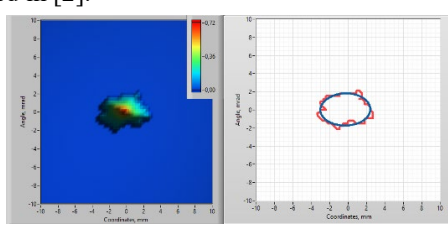

Figure 3: Results of the tomographic reconstruction. On the left – phase portrait. On the right – phase portrait envelope (red) and phase ellipse (blue).

ISBN: 978-3-95450-240-0 ISSN: 2673-5539 doi:10.18429/JACoW-RuPAC2021-WEPSC51

# CONCEPT OF DECISION SUPPORT SYSTEM FOR INR RAS LINAC BEAM TUNING

A. I. Titov†, S. A. Gavrilov,
Institute for Nuclear Research of the Russian Academy of Sciences, Moscow, Russia and
Moscow Institute of Physics and Technology (State University), Moscow, Russia

*Abstract*

During the last decade instruments of machine learning are gaining popularity in accelerator control systems. One of these instruments is decision support system (DSS) that is already successfully used in other fields of science. In this article a motivation for implementation of such system for INR RAS linac tuning is discussed. Concept of developed DSS is presented. Changes in INR RAS linac data acquisition system essential for future DSS operation are proposed.

## INTRODUCTION

Machine learning (ML) techniques are widespread in modern science, industry and everyday life. ML popularity is explained in its ability to surpass human in such tasks as forecasting based on analysis of huge amount of data, online recommendation based on personal preferences or object recognition, like faces or voices.

Majority of these tasks can be applicated to accelerator physics. For example, now ML algorithms are used to detect faulty BPMs and make orbit correction of the beam at LHC [1] or to determine critical situation at the neutrino beam facility at J-PARC [2].

One of the ML instruments is a decision support system (DSS). These are systems that support decision making activities. DSSs are already successfully used in medicine and help doctors make a diagnosis considering patient's medical history and many other factors.

In theory DSS could be used to help beam operators during accelerator run. However, this system is not used for accelerators. The reason is that new accelerator complexes have precise computer models of the beamline and other ML instruments are used like already mentioned orbit correction system at LHC.

At INR RAS linac the issue of personnel is acute. For the last decade amount of beam operators reduced by half and training of new operators can take years. Moreover, INR linac was constructed almost 30 years ago and does not have a precise model.

In that case DSS, which can help beam operator to analyze the current situation and make decisions to solve problems that arise during accelerator run, is a suitable system that would be extremely helpful for routine operation. Such system would decrease problem solving time and prevent personnel from making wrong decisions during accelerator tuning.

## INR LINAC DSS CONCEPT

INR linac DSS is designed as a Bayesian network. It is based on the Bayes' theorem and can be presented as a directed acyclic graph. Its advantage is ability to insert knowledge in it by designing its structure and to determine probabilistic transition values based on the knowledge base. This type of networks is already used for accelerator tuning at LCLS [3].

Input to the DSS will be problems that arise during accelerator operation and output will be ranged list of the most probable solutions for the problems. System has 6 layers. With the increase of a layer number operator need to provide more information about the problem. To work with outer layers information to the inner layer should also be provided. Layered structure of the DSS allows its step-by-step realization. Connection between layers is shown in Fig. 1. Concept scheme of the DSS is shown in Fig. 2.

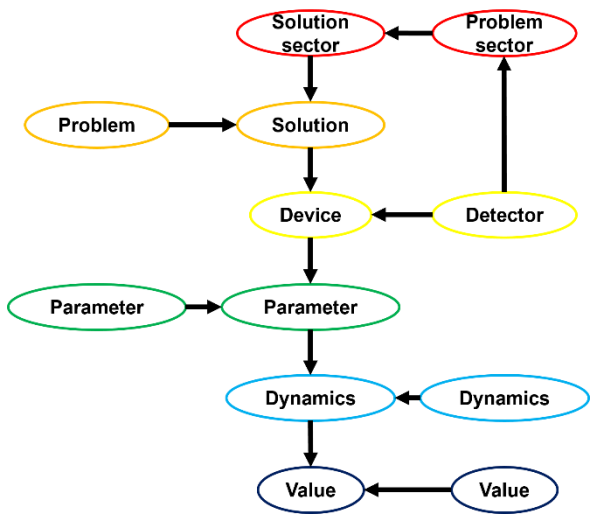


Figure 1: INR linac DSS connections scheme.

Layer 1 is a sector-sector layer. INR linac is divided into 5 sectors and multipurpose research complex (MPC), which is counted as sixth sector. and problem can be attributed to the sector where it occurred. Output of this layer is a sector number where problem solution is located. If problem occurs simultaneously at several sectors DSS should at first provide solution to the sector with the least number.

Layer 2 is a parameter-system layer. Input of this layer is a beam parameter which value is unsatisfactory. As an output DSS should provide type of the linac system, which parameters should be changed to solve the problem. If there are several problems at once, system should solve them in a prescribed way.

† aleksandr.titov@phystech.edu

ISBN: 978-3-95450-240-0 ISSN: 2673-5539 doi:10.18429/JACoW-RuPAC2021-WEPSC55

# DEVELOPMENT OF THE LOW INTENSITY EXTRACTION BEAM CONTROL SYSTEM AT PROTOM SYNCHROTRON FOR PROTON RADIOGRAPHY IMPLEMENTATION

A. A. Pryanichnikov†[1,2], P. B. Zhogolev[1], A. E. Shemyakov[1], M. A. Belikhin[1,2],
Lebedev Physical Institute RAS, Physical-Technical Center, Protvino, Russian Federation
A. P. Chernyaev, Lomonosov Moscow State University,
Accelerator Physics and Radiation Medicine Department, Moscow, Russian Federation
V. Rykalin, ProtonVDA, Naperville, USA
[1]also at Protom Ltd., Protvino, Russian Federation
[2]also at Lomonosov Moscow State University,
Accelerator Physics and Radiation Medicine Department, Moscow, Russian Federation

*Abstract*

Currently, the calculation of the proton range in patients receiving proton therapy is based on the conversion of Hounsfield CT units of the patient's tissues into the relative stopping power of protons. Proton radiography is able to reduce these uncertainties by directly measuring proton stopping power. However, proton imaging systems cannot handle the proton beam intensities used in standard proton therapy. This means that for implementation of proton radiography it is necessary to reduce the intensity of the protons significantly.

This study demonstrates the current version of the new beam control system for low proton intensity extraction. The system is based on automatic removable unit with special luminescence film and sensitive photoreceptor. Using of the removable module allows us to save initial parameters of the therapy beam. Remote automatic control of this unit will provide switch therapy and imaging modes between synchrotron cycles. The work describes algorithms of low flux beam control, calibration procedures and experimental measurements. Measurements and calibration procedures were performed with certified Protom Faraday Cup, PTW Bragg Peak Chamber and specially designed experimental external detector.

The development can be implemented in any proton therapy complexes based on the Protom synchrotron. This allow us to use initial synchrotron beam as a tool for patient verification and to eliminate proton range uncertainties.

## INTRODUCTION

Proton therapy is rapidly spreading throughout the world [1]. At present, the calculation of the proton range in patients receiving proton therapy is based on the conversion of Hounsfield CT units of the patient's tissues into the relative stopping power of protons. Uncertainties in this conversion necessitate larger proximal and distal planned target volume margins [2]. These larger margins increase the dose to nearby healthy tissues, causing unwanted and avoidable toxicities [3]. Proton radiography avoids these uncertainties by directly measuring the stopping power of protons, and this can significantly reduce the planned target volume, which directly reduces toxicity [4]. It has the ability to accurately target the patient to the proton beam and quantify anatomical consistency and proton range in the treatment position immediately prior to treatment, resulting in more consistent target coverage, leading to improved patient outcomes [5].

Figure 1: Protom synchrotron-based accelerator complex.

Protom Synchrotron [6-8] is a medical accelerator specially designed for proton therapy. The accelerator complex based on the Protom synchrotron is shown in Fig. 1.

The synchrotron is able to accelerate protons up to 330 MeV. This fact makes proton imaging of the entire human body available without any restrictions. The use of proton imaging will allow us to avoid the uncertainty of the proton range in the patient's body and will make the treatment process more accurate. Moreover, proton radiography can be used as a tool for verification of patient position instead of standard cone beam computed tomography systems. The proton imaging system has a lower equivalent dose to the patient than comparable X-ray imaging systems. However, proton imaging systems cannot handle the proton beam intensities used in standard proton therapy. This means that for implementation of proton radiography it is necessary to reduce the intensity of the protons significantly.

## REQUIREMENTS FOR BEAM EXTRACTION MODE

This work was focused on a proton detector prototype being developed by ProtonVDA [9-10]. ProtonVDA has developed a highly efficient and inexpensive proton radiography system based on solid state photomultipliers and fiber detectors. A key feature of this detector is its operation

ISBN: 978-3-95450-240-0 ISSN: 2673-5539 doi:10.18429/JACoW-RuPAC2021-WEPSC56

# BEAM PARAMETERS MEASUREMENT AND CONTROL SOFTWARE TOOLS FOR VEPP-5 INJECTION COMPLEX DAMPING RING

V. V. Balakin*[1], F. A. Emanov[2], D. E. Berkaev, Budker INP, Novosibirsk, Russia
[1]also at Novosibirsk State Technical University, Novosibirsk, Russia
[2]also at Novosibirsk State University, Novosibirsk, Russia

*Abstract*

Beam parameters control and operation software tools for BINP VEPP-5 injection complex damping ring consisting of two parts were developed. Beam parameters control includes processing of measured turn-by-turn beam coordinates from all damping ring beam position monitors and displaying such features as tunes and beam position into vacuum chamber. This part gives an opportunity to measure damping ring response matrices and carry out its processing too. Beam parameters operation is based on knobs creating. Knob is combination of accelerator control elements, which performs an isolated shift of one selected parameter, e.g. only vertical betatron tune. This part is devoted to their creation and application on VEPP-5 injection complex. This paper presents review of developed software tools and their application result on VEPP-5 injection complex: beam position adjustment via response matrix measurements and quantification the amount of damping ring captured particles during the injection process depending on beam tunes.

## VEPP-5 INJECTION COMPLEX

Injection complex VEPP-5 (IC) is a part of VEPP-4 - VEPP-2000 electron-positron colliders complex. It intended for high-energy, nuclear physics and synchrotron radiation experiments conducting. IC (Fig. 1) constists of electron gun, 2 linear accelerators, $e^- \rightarrow e^+$ conversion system, damping ring and transport channels K-500 [1].

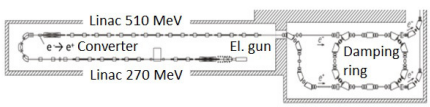


Figure 1: VEPP-5 injection complex scheme.

## SOFTWARE TOOLS DESCRIPTION

Beam position monitors (BPM) data processing is a key weapon for obtaining information about beam parameters and their response on accelerator magnetic system changes. Software tools, which includes data obtaining, processing, displaying and keeping, was developed to take advantage of the BPM potential. Software tools are consist from 3 parts:

- Daemons:
  - BPM data processing - *orbitd*
  - knobs service - *knobd*
- GUI-applications for operational staff:
  - damping ring beam positions displaying and keeping in different IC modes - *orbit*
  - turn-by-turn measurements displaying - *turns*
  - tunes displaying and keeping - *tunes*
- GUI-applications for administration:
  - damping ring response matrix collecting - *rmc*
  - magnetization of magnetic system elements - *magn*
  - user application for knob creating and using - *knob*
  - measurement of injected particles number into damping ring vs. tunes - *inj_resp*
  - collected response matrix processing and based on them knob creating - *rmc_proc*

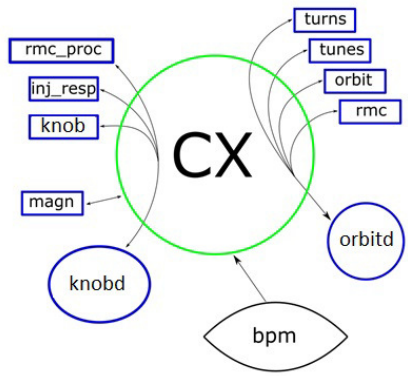


Figure 2: Software tools principal scheme.

Software tools principal scheme is presented on Fig. 2. Black arrows show links between different parts of software, which communicate each other throw CX-server [2].

Program separation into daemons and GUI-applications are conditioned by the need to separate direct processing of data from the display and use of the results of this processing. On the one hand, this gives an opportunity to independenly change each component (logic or visualization) without affecting another part, from other hand, running multiple copies of displaying application requred only one copy of daemon with data processing.

## SOFTWARE TOOLS USAGE ON INJECTION COMPLEX

### *Lattice*

Damping ring has 28 quadropole lenses, which means that detecting the tunes shift from varying the current of qudrupole corrector of each lens allows us to measure aver-

* vit.v.balakin@inp.nsk.su

ISBN: 978-3-95450-240-0 ISSN: 2673-5539 doi:10.18429/JACoW-RuPAC2021-WEPSC57



# ONLINE MONITORING SYSTEM OF ACCELERATOR ELECTRON BEAM ENERGY

N.N. Kurapov, Ya.V. Bodryashkin, A.V. Tel'nov, A.S. Cherkasov, I.V. Shorikov, RFNC-VNIIEF, Sarov, Russia

*Abstract*

A necessity for online measurement of the output electron energy arises during start-up, adjustment or operation of an accelerator. For this purpose, there has been developed a system, allowing an online monitoring of energy spectrum accelerated electrons simultaneously with measuring of average beam current. This system is meant for reconstruction of the accelerated electron energy spectrum in the energy range from 1 to 10 MeV at the average beam current from 20 to 150 μA.

The system is based on an absorbing filter method and consists of an assembly, absorbing the accelerated electron beam, and a measuring system.

The developed system tests on the electron accelerator have proved the possibility for its application to monitor electron beam energy in real time.

## INTRODUCTION

A number of linear resonance electron accelerators functions in RFNC-VNIIEF. Among these are such accelerators as LU 10 20 [1] and LU-7-2 [2]. These accelerators are meant for generation of intense electron beams and bremsstrahlung and research the radiation hardness of instruments and materials by the means of generating such radiation.

Measurement of the output electron energy is required both during start-up, adjustment or study of accelerator properties, as well as during physical experiments, requiring precise testing of output beam energy. To supply operability and universality (including a capability for application in different accelerators), it was decided to use an absorbing filter method for measurement of the beam energy. As a result, there has been developed a system for measuring beam parameters, consisting of a measuring assembly and a monitoring system. The developed system is portable, compact, and it helps to organize online measurements of accelerated electron beam spectral response inany accelerator with the energy from 1 to 10 MeV in the shortest time

## OUTPUT BEAM ENERGY MEASUREMENT USING ABSORBING FILTER METHOD

The simplest way to resolve the problem of measuring the beam energy is to use a method of electron absorption in matter. For aluminum the energy dependence on free path Is of the form [3]:

$$R = 0.412 \cdot W_k^n, \quad \text{for } 0.01 \le W_k \le 3\ МэВ \quad (1)$$

$$R = 0.53 \cdot W_k - 0.106, \text{ for } 3 \le W_k \le 10\ МэВ$$

Where R – free path of electrons in aluminum, g/cm$^2$;
$W_k$ – kinetic energy, MeV;

$$n = 1.265 - 0.0954 \cdot \ln W_k.$$

One can obtain a full energy response of an accelerated electron beam by restoring energy electron spectrum from current distributions, measured in absorbing assembly plates. A measuring absorbing assembly was developed for this purpose. It represents a set of 20 insulated from each other current-conducting plates of size 100x100 mm and thickness from 0.15 to 1 mm with air gap between plates 2 mm. Appearance of the assembly is shown in Fig. 1.

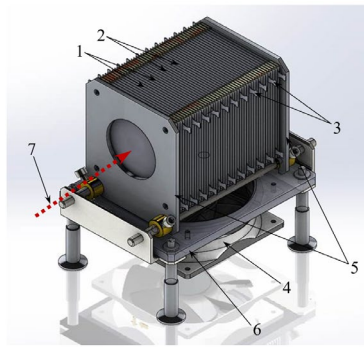


Figure 1: Measuring assembly, 1 - Aluminum plates; 2 - insulation between plates; 3 - leads for current measurement; 4 - fan; 5 - strengthening flanges; 6 - supporting frame; 7 - beam axis direction.

Spectral response of the assembly was calculated in the program C-007 [4] by Monte-Carlo method in the energy range from 1 to 10 MeV in increments of 0.5 MeV. Calculation results are given in Fig. 2.

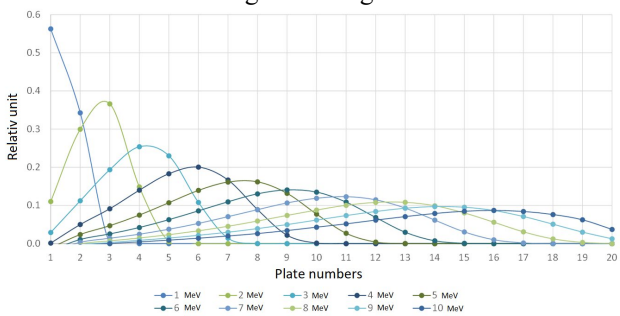


Figure 2: Spectral response of 20 plates assembly.

## ENERGY SPECTRUM RECONSTRUCTION PROGRAM REVIEW

To reconstruct the accelerated electron beam spectrum from current distributions over measuring assembly plates, one should solve the system of 20 equations (number of plates) with 19 variables (values of plate current intensities at different beam energies – 1, 1.5, 2, …, 10 MeV). The system in a matrix notation is of the form:

$$\boldsymbol{A} \cdot \boldsymbol{X} = \boldsymbol{B}, \quad (2)$$